NOVEL LIPIDOMIC APPROACHES TO ANALYSE GLYCEROPHOSPHOLIPIDS AND SPHINGOLIPIDS IN COMPLEX MIXTURES USING MASS SPECTROMETRY

GUAN XUE LI

NATIONAL UNIVERSITY OF SINGAPORE

2008

NOVEL LIPIDOMIC APPROACHES TO ANALYSE GLYCEROPHOSPHOLIPIDS AND SPHINGOLIPIDS IN COMPLEX MIXTURES USING MASS SPECTROMETRY

GUAN XUE LI

(B.Sc. (Hons.), National University of Singapore)

A THESIS SUBMITTED FOR THE DEGREE OF

DOCTOR OF PHILOSOPHY

DEPARTMENT OF BIOCHEMISTRY

NATIONAL UNIVERSITY OF SINGAPORE

2008

Acknowledgements

Very sincerely,

I thank my supervisor, Markus R. Wenk, for being a mentor with a very unique style and for paving the way and filling it with immense support, unceasing patience, many deep insights and stimulating ideas. And with utmost appreciation, thank you very much for firmly believing in me.

I thank Howard Riezman, not only for his contribution to a major focus in my thesis, and the opportunity to work in his laboratory, but his unceasing enthusiasm and engagement in science is inspirational. And for making a difference during this journey, to both Howard and Isabelle Riezman, I express my heartfelt gratitude.

To Shui Guanghou, Anne K. Bendt, Chua Gek Huey and Aaron Fernandis, thank you for the encouragement, the stimulation to find a better person in me, the knowledge shared, the support during those dark moments, for everything.

To Sashi Kesavapany and Maxey Chung, thank you for being in my thesis committee and providing all the constructive feedback.

To Lim Tit Meng, thank you for all the support through these years.

To Gisou van der Goot, thank you for the helpful discussions, and the enthusiasm and immense support, particularly for the Swiss exchange which had been an invaluable experience.

To Ernst Hafen and his group members, Katja Kohler and Irena Jevtov, thank you for collaborating and the helpful discussions on fly biology.

To Marcos Gonzalez, thank you for being an enthusiastic partner for fly lipidomics.

To Ong Wei Yi and his then PhD student, He Xin, thank you for collaborating and the expertise in animal work.

To all my other collaborators, thank you for the interest, the enthusiasm, and the opportunities to learn about many amazing things beyond the scope of my thesis work.

To all past and present members of the Wenk and neighbouring laboratories, thank you for providing a pleasant scientific as well as non-scientific environment. And also to members of the Riezman laboratory, thank you for the hospitality during the exchange. Cleiton Martins de Souza, then Howard Riezman's PhD student, is acknowledged for his enthusiasm and help throughout the collaboration.

To my friends outside the laboratory, Heiny, Petrina Fan, Goh Shu Shang and Tan Yong Wah, thank you for always being there and for whom I can turn to especially when I need a break from those greasy works.

And to my family, thank you very much for the unconditional and silent support. And for providing a place to fall back on when all else fail, thank you.

I would also like to acknowledge the European Molecular Biology Organization (EMBO) for its generous funding of a short term fellowship (ATSF 07-2008) for a two-month exchange to Howard Riezman's laboratory in University of Geneva in 2008, the Yong Loo Lin School of Medicine for the research scholarship during my PhD candidature, the Pediatric Dengue Vaccine Initiative (PDVI) for a travel award for the 3rd Asian Regional Dengue Research Network Meeting in 2007 and the National University of Singapore for the prestigious President's Graduate Fellowship in 2006/2007.

Table of Contents

Summary

Lipids are rapidly moving to center stage in many fields of biological sciences and technological advancements in lipid analysis is a major driving force for the emergence of lipidomics, the systems-level scale analysis of lipids and their interacting factors. In this thesis, I describe the development of a novel mass spectrometry-based approach for comprehensive profiling of glycerophospholipids and sphingolipids in complex lipid mixtures. The first step includes semi-quantitative surveys of lipids in an untargeted fashion, termed 'differential profiling', and is particularly powerful for detection of changes during a cellular perturbation which cannot easily be anticipated. This leads to the identification of ions with increased or decreased signal intensity. Subsequent targeted analysis using tandem mass spectrometry and collision-induced dissociation allows for quantification of glycerophospholipids and sphingolipids. The method was validated in experimental models based on mammalian tissues/ cells and the eukaryotic model organisms, *Saccharomyces cerevisiae* and *Drosophila melanogaster*. The methodology detailed the comprehensive characterisation of major glycerophospholipids and sphingolipids in these organisms, which is currently lacking in the field particularly for the non-mammalian species. Given the high degree of conservation in pathways of lipid metabolism between different organisms, it can be expected that this method will lead to the discovery of novel enzymatic activities and modulators of known enzymes, in particular when used in combination with genetic and chemogenetic libraries and screens.

One of the greatest challenges in biology is to understand how the intricate balance of composition, distribution and interactions of lipids in a cell is regulated. Sterols and sphingolipids are mainly limited to eukaryotic cells and their interaction has been proposed to be central for formation of lipid microdomains. While there is abundant biophysical evidence demonstrating the interactions of different classes of lipids in artificial systems *in vitro*, little evidence of how lipids function together in cells exist. These issues were addressed through an interdisciplinary approach, based on lipidomics, genetics and cell biology. The analytical approach described in this thesis was applied to survey glycerophospholipids and sphingolipids in yeast single deletion mutants in sterol metabolism. It was demonstrated that cells adjust their membrane lipid composition in response to mutant sterol structures mainly by changing their sphingolipid composition. The interactions between sterols and sphingolipids were further probed genetically by combining mutations in sterol biosynthesis with mutants in sphingolipid hydroxylation and headgroup turnover. This resulted in a large number of synthetic and suppression phenotypes, demonstrating that the two classes of lipids function together to carry out a wide variety of processes. Our data revealed that cells have a mechanism to sense their membrane sterol composition and proteins might recognize sterol-sphingolipid complexes, which is critical for their localisation and function. Furthermore, the observations also led us to hypothesize the co-evolution of sterols and sphingolipids.

List of Tables

List of Figures

List of Abbreviations

3-KDS	3-ketodihydrosphingosine
ABC	ATP binding cassette
APCI	Atmospheric pressure chemical ionisation
ATP	Adenosine triphosphate
°C	Degree Celsius
C. elegans	*Caenorhabditis elegans*
Cer	Ceramide
CERT	Ceramide transport protein
CFP	Cerulean fluorescent protein
CID	Collision-induced dissociation
CoA	Coenzyme A
COW	Correlation Optimised Warping
D. melanogaster	*Drosophila melanogaster*
DAG	Diacylglycerol
DESI	Desorption electrospray ionisation
DNA	Deoxyribonucleic acid
DHS	Dihydrosphingosine
EGTA	Ethylene glycol tetraacetic acid
ESI	Electrospray ionisation
FA	Fatty acyl
FDA	Fluorescein diacetate
FT-ICR	Fourier transform ion cyclotron
GC-MS	Gas chromatography mass spectrometry
GC	Glucosylceramide
GFP	Green fluorescent protein
GPA	Phosphatidic acid
GPCho	Glycerophosphocholine
GPEtn	Glycerophosphoethanolamine
GPGro	Glycerophosphoglycerol
GPIns	Glycerophosphoinositol
GPInsP	Glycerophosphoinositol phosphate
GPInsP2	Glycerophosphoinositol bisphosphate
GPInsP3	Glycerophosphoinositol triphosphate
GPL	Glycerophospholipid
GPSer	Glycerophosphoserine
H. sapiens	*Homo sapiens*
HygB	Hygromycin B
IPC	Inositolphosphorylceramide
IS	Internal standard
iTRAQ	Isobaric tag for relative and absolute quantification
kV	kilovolt
LC	Liquid chromatography
LCB	Long chain base
LC-MS	Liquid chromatography mass spectrometry

log	Logarithmic
M	Molar
M(IP)2C	Mannosyl diinositolphosphorylceramide
m/z	mass-to-charge ratio
MALDI	Matrix-assisted laser desorption ionisation
mg	Milligram
min(s)	Minute(s)
MIPC	Mannosyl inositolphosphorylceramide
mL	Millilitre
mM	Millimolar
MRM	Multiple-reaction monitoring
MS	Mass spectrometry
MS/MS	Tandem mass spectrometry
MS^3	MS/MS/MS
NL	Neutral loss
nm	Nanometer
OD	Optical density
OD600	Optical density at 600nm
PCA	Principal components analysis
PCR	Polymerase chain reaction
PE-ceramide	Phosphorylethanolamine ceramide
PHS	Phytosphingosine
PIs	Phosphoinositides
pmole	Picomole
PREIS	Precursor ion scan
PUFA	Polyunsaturated fatty acid
Q-ToF	Quadrupole-Time of Flight
s	Seconds
S. cerevisiae	*Saccharomyces cerevisiae*
S. pombe	*Schizosaccharomyces pombe*
SDS	Sodium dodecyl sulfate
SELDI	Surface-enhanced laser desorption/ionisation
SEM	Standard error of the mean
SM	Sphingomyelin
sn	Stereospecific numbering
SPL	Sphingolipid
SREBP	Sterol regulatory element binding protein
TLC	Thin layer chromatography
ToF	Time of Flight
ToF-SIM	Time-of-flight secondary ion mass spectrometry
TOR	Target of Rapamycin
TORC	Target of Rapamycin Complex
μg	Microgram
μL	Microlitre
V	Volt
v/v	Volume to volume

WT	Wild type

All glycerophospholipids cited in this work are based on the nomenclature x:y Z, where x denotes the length of the fatty acid chain, y, the number of double bonds and Z the lipid specie based on its backbone and headgroup moiety. For instance, a 18:1 GPIns is a glycerophosphoinositol (Z) with a 18-carbon (x) fatty acid chain containing 1 (y) double bond.

All sphingolipids are represented with the nomenclature d/t x_1:y_1/x_2:y_2 Z, where d and t denotes the number of hydroxyl groups on the sphingoid base (d, di; t, tri), x_1 and x_2, the length of the sphingoid base and fatty acyl chain respectively, y_1 and y_2, the number of double bonds on the sphingoid base and fatty acyl chain respectively, and Z the lipid specie based on its backbone and headgroup moiety. For instance, d18:1/19:0 Cer is a ceramide (Z) with a 18-carbon (x_1) sphingosine (d, dihydroxy; y_1, one double bond) and a 19-carbon acyl chain (x_2) without any double bond (y_2).

For sphingolipids found in *S. cerevisiae*, the suffix ‘A’, ‘B’, ‘C’ and ‘D’ is used to indicate the degree and site of hydroxylation. For instance, phytoceramide-A is a dihydroceramide with two hydroxyl groups on the sphingoid base; -B, is a phytoceramide with three hydroxyl groups on the sphingoid base; -C, is a phytoceramide with an additional hydroxyl group on its fatty acyl chain; and -D, is a phytoceramide with two hydroxyl groups on its fatty acyl chain.

List of Publications

1) Damm E, Stergiou L, Snijder B, **Guan XL**, Wenk MR, Pelkmans L. Focal adhesion kinase establishes lipid rafts on the cell surface by controlling transcription of the cholesterol transporter ABCA1. *Submitted.*

2) Gebert N, Joshi AS, Kutik S, Becker T, McKenzie M, **Guan XL**, Wenk MR, Rehling P, Meisinger C, Ryan MT, Wiedemann N, Greenberg ML, Pfanner N. Mitochondrial cardiolipin involved in outer membrane protein biogenesis: implications for Barth syndrome. *Submitted.*

3) **Guan XL**, Riezman I, Wenk MR, Riezman H. Yeast Lipid Analysis and Quantitation by Mass Spectrometry in **Methods in Enzymology**. *Submitted.*

4) Kohler K, Brunner E, **Guan XL,** Boucke K, Greber UF, Mohanty S, Barth J, Wenk MR and Hafen E. A combined proteomic and genetic analysis identifies a role for the lipid desaturase Desat1 in starvation induced autophagy in Drosophila. **Autophagy** *(Under Revision).*

5) **Guan XL**, Souza CM, Pichler H, Dewhurst G, Schaad O, Kajiwara K, Wakabayashi H, Ivanova T, Castillon GA, Piccolis M, Abe F, Loewith R, Funato K, Wenk MR and Riezman H. Functional interactions between sphingolipids and sterols regulating cell physiology. **Mol. Biol. Cell.** 20(7):2083-95.

6) Kutik S, Rissler M, **Guan XL**, Guiard B, Shui G, Gebert N, Heacock P, Rehling P, Dowhan W, Wenk MR, Pfanner N and Wiedemann N (2008). The translocator maintenance protein Tam41 is required for mitochondrial cardiolipin biosynthesis. **Journal of Cell Biology.** 183(7): 1213-21.

7) Mousley CJ, Tyeryar K, He KE, Schaaf G, Brost R, Boone C, **Guan XL**, Wenk MR and Bankaitis VA (2008). Coordinate defects in Sec14 and Tlg2-dependent trans-Golgi and endosome dynamics derange ceramide homeostasis and compromise the unfolded protein response. **Mol. Biol. Cell.** 19(11): 4785-803.

8) **Guan XL** and Wenk MR (2008). Biochemistry of inositol lipids. **Frontiers in Bioscience.** 13: 3239-3251.

9) He X, **Guan XL**, Ong WY, Farooqui AA and Wenk MR (2007). Expression, activity, and role of serine palmitoyltransferase in the rat hippocampus after kainate injury. **J Neurosci Res.** 85(2): 423-32.

10) **Guan XL**, He X, Ong WY, Yeo WK, Shui G and Wenk MR (2006). Non-targeted profiling of lipids during kainate induced neuronal injury. **FASEB J.** 20(8): 1152-61.

11) **Guan XL** and Wenk MR (2006). High resolution and targeted profiling of phospholipids and sphingolipids in extracts from *Saccharomyces cerevisiae*. **Yeast**. 23(6): 465-77.

12) Chee JL, **Guan XL**, Lee JY, Dong B, Leong SM, Ong EH, Liou AK and Lim TM (2005). Compensatory caspase activation in MPP+-induced cell death in dopaminergic neurons. **Cell Mol Life Sci.** 62(2): 227-38.

13) Fernandis AZ, Kothandaraman N, Chua GH, **Guan XL**, Shui G, Choolani M and Wenk MR. Plasma lipid profiling as a diagnostic tool for detection of ovarian tumor. *In preparation.*

14) Souza CM, Pichler H, Leitner E, **Guan XL**, Wenk MR, Jeannerat D, Tornare I and Riezman H. Cholesterol can replace ergosterol for tryptophan uptake, but not weak organic acid resistance in yeast. *In preparation.*

15) Shui G, Jenner A, Chan R, **Guan XL**, Pan N, Tan BKH, Halliwell B, Wenk MR. Desferal selectively normalizes levels of membrane raft lipids in liver of rabbits challenged with high cholesterol diet. *In preparation.*

16) Shui G, Gopalakrishnan P, **Guan XL**, Goh JSY, Xue Y, Yang H, Wenk MR. Characterization of substrate preference for *Slc1* and *Cst26* using sensitive fatty acyl-based multiple reaction monitoring approach. *In preparation*.

17) Shui G, **Guan XL**, Low CP, Chua GH, Goh JSY, Yang H, Wenk MR. Towards one step analysis of major cellular lipidome using liquid chromatography coupled to mass spectrometry. *In preparation*.

18) Bendt AK, Shui G, Tan BH, Fernandis AZ, **Guan XL**, Dick T, Pethe K, Wenk MR. Lipid profiling of Mycobacterium during hypoxic dormancy. *In preparation.*

Abstracts Presented at Conferences

1. "A combined genetics and lipidomics approach to explore metabolism and functions of membrane lipids". **Frontier Lipidology: Lipidomics in Health and Disease**, Gothenburg, Sweden, May 2009. Abstract Speaker.

2. "Functional interactions between sphingolipids and sterols in biological membranes". **Keystone Symposium – Complex Lipids in Biology: Signaling, Compartmentalization and Disease**, California, US, April 2009. Poster.

3. "Lipidomics of dengue virus replication". **1st Singapore MIT Alliance Research and Technology (SMART) Retreat, Bintan, Indonesia**, July 2008. Poster.

4. "Functional interactions between sphingolipids and sterols in biological membranes". **5th Lipid Maps Annual Meeting**, California, US, May 2008. Poster.

5. "Functional interactions between sphingolipids and sterols in biological membranes". **2nd Singapore Lipid Symposium**, Singapore, March 2008. Poster.

6. "Functional interactions between sphingolipids and sterols in biological membranes". **EMBO-FEBS Workshop on Endocytic Systems**, Villars-sur-ollon, Switzerland, September 2007. Poster.

7. "Lipidomics of dengue virus replication". **3rd Asian Regional Dengue Research Network Meeting**, Taipei, Taiwan, August 2007. Poster.

8. **"**High resolution and targeted profiling of phospholipids and sphingolipids in Saccharomyces cerevisiae". **47th International Conference on the Bioscience of Lipids (ICBL)**, Pecs, Hungary, September 2006. Poster.

9. "Non-targeted profiling of lipids during kainate induced neuronal injury". **7th Biennial Meeting of the Asian-Pacific Society for Neurochemistry (APSN)**, Singapore, July 2006. Poster.

10. "High resolution and targeted profiling of phospholipids and sphingolipids in Saccharomyces cerevisiae". **1st Singapore Lipid Symposium**, Singapore, February 2006. Poster.

Patents

Wenk MR, Fernandis AZ, Chua GH, **Guan XL.** System Level Scale Analysis of Lipids as a Diagnostic Tool. Patent filed through NUS with the Intellectual Property office of Singapore (Ref: 2008007734/080205/TMFMK/1436).

Chapter 1. Introduction

The definition of lipids has undergone dramatic changes with the constant revelation of novel structures (Ito *et al.*, 2008;Korekane *et al.*, 2007) and discovery of the functions of these compounds. With the burgeoning appreciation of the critical functions of lipids in biological processes, and aided by advances in technologies that afford an '-omic-centric' view of the lipid inventory of biological systems, the field of lipidomics, which is the systems-level analysis of lipids and their interacting partners, has emerged in recent years (Wenk, 2005). Although lipidomics has lagged in comparison to the development of genomics and proteomics, numerous analytical and information technology tools have been put in place over the last five to ten years by various international initiatives such as the LIPID MAPS consortium in the US, the European Lipidomics Initiative (ELIfe), the LipidX initiative in Switzerland, as well as other research groups, to better understand the lipidome of various biological systems. The field of lipidomics is advancing, and has indeed made important contributions to our understanding of lipids in various pathobiological phenomena. The impact of lipidomics (integrated with other 'omics' fields) on biology, drug discovery and developments and personalized medicine is immense. However, this emerging field is facing many issues which need to be overcome in order for its full potential to be realized. The achievements in the fields of genomics and proteomics has taught us an important lesson – development of sophisticated instrumentation is desired to advance the field of lipidomics, but just as important is a good understanding of the capability of available technologies and developing sensible lipidomic strategies. Here I will review some of the recent strategies in analysis of lipids based on mass spectrometry (MS) without attempting exhaustive descriptions of lipid functions and analytical technologies as excellent reviews on these

aspects are widely available (Maxfield and Tabas, 2005;Liscovitch and Cantley, 1994;Merrill *et al.*, 1997;Serhan *et al.*, 2008;Escriba *et al.*, 2008;Di Paolo and De Camilli, 2006;Vance, 2008;Balazy, 2004;Hou *et al.*, 2008;Isaac *et al.*, 2007;Zehethofer and Pinto, 2008;Schiller *et al.*, 2007;Han and Gross, 2003;Merrill, Jr. *et al.*, 2005). In addition, due to the diverse nature of the systems involved in this study, a separate introduction will be included in each chapter to provide an overview to the biology/chemistry under investigation.

1.1 Membrane Lipids

1.1.1 Structural diversity

While it is increasingly appreciated that lipids have diverse biological functions, it is not well understood why nature has created such an immense combinatorial and structural heterogeneity among lipids (Fig.1.1). William Christie restricts the use of 'lipids' to "fatty acids, their naturally-occurring derivatives (esters or amides), and substances related biosynthetically or functionally to these compounds" (refer to http://www.lipidlibrary.co.uk/Lipids/whatlip/index.htm), which is probably one of the most widely accepted definitions for lipids. The estimation of the number of lipids that exist is a daunting task, because lipids are not genetically encoded and are instead the products of enzymatic and chemical reactions (e.g. oxidation, Schiff base formation, etc). A conservative theoretical estimation of the number of lipids covering major lipid classes is close to 180 000 molecular species (Yetukuri *et al.*, 2008) and this might still be an underestimate because even with completely sequenced genomes, annotation of genes and functions is still on its way and many enzymes, regulators of lipid metabolism and novel lipids remained to be discovered. The construction of databases and information

exchange between various users of this diverse range of metabolites is a great challenge and a unifying nomenclature, built on a scalable structure with eight categories was recently proposed by Fahy and co-workers to facilitate communication within the lipid community (Fahy *et al.*, 2005).

Glycerophospholipids, sphingolipids and sterols are the three major classes of lipids that make up the bulk of eukaryotic cell membranes. Table 1.1 summarizes the different classes of membrane lipids found in various model organisms. The structural information of lipids serve as an important starting point for their analysis, and a review of mass spectrometry-based analytics will be incomplete without first introducing lipids and their structures, which entail the inherent ionisation property of a lipid.

Table 1.1 Membrane lipids of various organisms.

	Mycobacterium tuberculosis	*Escherichia coli*	*Saccharomyces cerevisiae*	*Caenorhabditis elegans**	*Drosophila melanogaster**	*Homo sapiens*
Glycero-phospholipids						
GPA	+	+	+	+	+	+
GPGro	+	+	+	+	+	+
GPEtn	+	+	+	+	+	+
GPCho			+	+	+	+
GPSer		+	+	+	+	+
GPIns	+		+	+	+	+
Sterols						
ergosterol			+		+	
cholesterol				+	+	+
Sphingolipids			+	+	+	+

*** sterols auxotrophs**

The general structure of a simple glycerophospholipid consists of a polar headgroup with a phosphate moiety, a fatty acyl, alkyl or alkenyl group at the stereospecifc numbering (sn) position 1 (sn-1) and a fatty acyl group at the sn-2 position of a glycerol backbone (Fig. 1.1A). Common head group substitutions include choline,

ethanolamine, inositol, serine, glycerol or hydrogen, which may not be found in all organisms (Table 1.1 and Fig. 1.1D). Additional structural diversity of this class of lipid exists in the chemical moiety present at the sn-1 and sn-2 positions, which vary in carbon chain length and degree of unsaturation, and often undergo extensive enzyme-mediated remodeling (Fig. 1.2). Variations from the 'classical' glycerophospholipids are minor, but structurally more complex lysobisphosphatidic acid, cardiolipins, and N-acylated glycerophospholipids.

The backbone of sphingolipids comprises of a long-chain amino alcohol (also known as a sphingoid base or long chain base) to which a fatty acid can be covalently linked to form ceramide (Fig. 1.1B). Again, structural variants arise from head group substitutions as well as chain length differences and hydroxylation in the sphingoid base and fatty acyl chains (Fig. 1.1D and Fig. 1.2). Naturally occurring sphingoid bases alone are now known to encompass hundreds of compounds (Pruett *et al.*, 2008). Although sphingolipids have a 'two-tailed' nature like the major glycerophospholipids, there are many more restrictions to the chain length and degree of saturation. An interesting phenomenon in sphingolipid biology is the structural uniqueness of phosphosphingolipids between various eukaryotic model organisms. Unlike glycerophospholipids, which comprise of a variety of headgroups, the unique substitutions for phosphosphingolipids are inositol, ethanolamine and choline, forming inositolphosphorylceramide (IPC), phosphorylethanolamine ceramide (PE-ceramide) and sphingomyelin (SM) in yeast, fruit fly and mammals respectively (Fig. 1.1D). Note however that in mammals, glycerophosphoethanolamine:ceramide-ethanolaminephosphotransferase activity is

present as an alternative pathway for sphingomyelin biosynthesis but the precise function of PE-ceramide in mammals is unknown (Maurice and Malgat, 1990;Nikolova-Karakashian, 2000). Sphingolipids in higher eukaryotes can be further decorated with highly complex glycoconjugates, introducing yet another level of diversity to the structures of sphingolipids (Merrill, Jr. *et al.*, 2007).

Sterols are a subgroup of steroids and are derivatives of cyclopentanopherhydrophenanthrene, with a C3 hydroxyl (-OH) group and a branched aliphatic side chain of 8 to 10 carbon atoms at the C17 position. Most vertebrate cells contain cholesterol, while ergosterol is the main yeast sterol (Fig. 1.1C). Humans derive their cholesterol from two sources, *de novo* synthesis and diet, while other organisms may favour either source as the predominant supply. *Saccharomyces cerevisiae*, for instance, relies on *de novo* sterol biosynthesis under aerobic growth conditions, while *Drosophila melanogaster* and *Caenorhabditis elegans* are sterol auxotrophs. Sterols can be found as free sterols, acylated (sterol esters), alkylated, sulfated, or linked to a glycoside moiety, which can be itself acylated.

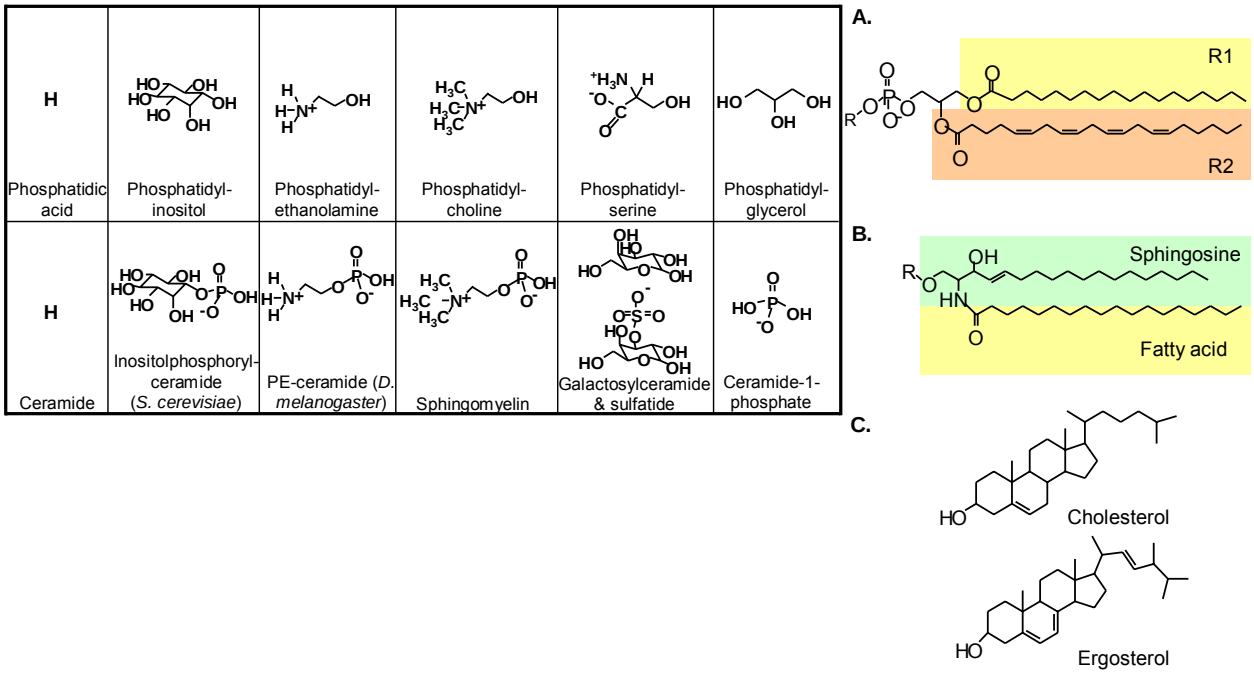

Figure 1.1 Structural diversity of membrane lipids.
(A) Glycerophospholipids. (B) Sphingolipids and possible headgroup modifications (R). Stereospecific numbering positions 1 and 2 (sn-1 and sn-2): acyl, alkyl or alkenyl substitutions: (C) Major sterols found in eukaryotic cells. For shorthand purposes, a nomenclature for sphingoid base similar to fatty acid can be used: the chain length and number of double bonds are denoted in the same manner with the prefix 'd' or 't' to designate di- and trihydroxy bases, respectively. In this case, (B) represents a sphingosine, which is denoted as d18:1.

1.1.2 Biological functions of lipids

The organisation and diversity of the lipid inventory of different organisms (Table 1.1), cell types, organelles, and even between the lipid bilayer of biological membranes is impressive. Even the simplest life forms, viruses, require a high level of organisation of lipids for their propagation and survival (Campbell *et al.*, 2002;Chan *et al.*, 2008;Ye, 2007). Unlike proteins which possess localisation signals, the intracellular organisation of lipids is attributed to the localisation of the biosynthetic and remodeling machineries, transport mechanisms as well as the interactions with other lipids and proteins. In fact, the tight regulation of lipid metabolism and localisation are essential, and mutations in genes, and deficiencies and defects in proteins mediating these processes have been

implicated, directly or as a predisposition factor, in many human diseases (Goker-Alpan *et al.*, 2008;Guldberg *et al.*, 1997;Puri *et al.*, 1999;Akiyama, 2006;Allikmets *et al.*, 1997).

Lipids were once thought to be merely structural components of biological membranes defining permeability barriers of cells and organelles and providing great flexibility and stability as membranes constantly undergo morphological changes and fusogenic processes. As lipid research progresses, our knowledge on the functions of lipids are constantly evolving. Each unique structural entity is believed to encode for specific, but not necessarily exclusive, cellular function. Metabolic (and non-enzymatic) conversion of membrane lipids produce a wide range of bioactive mediators, including eicosanoids (Balazy, 2004), endocannabinoids (Devane *et al.*, 1992) and oxidized glycerophospholipids (Subbanagounder *et al.*, 2000), and signalling molecules such as platelet activating factors (Benveniste *et al.*, 1977), the phosphorylated derivatives of glycerophosphoinositol (phosphoinositides) (Hokin and Hokin, 1955) and sphingolipids (Ghosh *et al.*, 1990). In addition, membrane lipids are critical for cellular functions through their regulatory role on proteins via various mechanisms, including post translational modifications, regulation of the location and activity, and defining membrane microdomains that serve as spatio-temporal platforms for interacting signalling proteins.

Functions of lipids are not only defined by their structural and elemental composition, but are also dependent on the specific metabolic source (e.g. *de novo* synthesis versus breakdown), their sub-cellular localisation, and their environment (van

Meer *et al.*, 2008). A classical example is the phosphoinositides (PIs), phosphorylated derivatives of GPIns, which are are optimal mediators of signalling events in cellular compartments due to the differential intracellular distribution and their high metabolic turnover. An important feature of these lipids is the inositol headgroup which can be reversibly phosphorylated by kinases and phosphatases (Vanhaesebroeck *et al.*, 2001). Seven naturally occurring phosphoinositides, which differ in their position and degree of phosphorylation, are known to date in eukaryotes. The functions of PIs are mediated by (i) interactions between the phosphorylated headgroups and effector molecules bearing specific phosphoinositide binding domains (e.g. PH, PX, FYVE, ENTH, etc) (Lemmon, 2003), (ii) soluble metabolites (inositol phosphates and diacylglycerols) which are generated through the action of phospholipases, and (iii) fatty acyl derivatives which originate from the membrane bound portion of the lipid molecule. Thus, the PIs can be considered "high-power" signalling entities. Sphingolipids are also emerging as key cellular mediators which share similar features as PIs in terms of their 'elasticity' in their metabolism, structures and functions. For instance, ceramide and sphingosine 1-phosphate are antagonistic in their functions in apoptosis and their metabolic juxtaposition constitute a rheostat system that determines cellular life and death (Taha *et al.*, 2006).

Another prominent lipid which exhibits spatio-dependence for its function is glycerophosphoserine (GPSer), which in normal resting cells are found in the inner leaflet of the lipid bilayer. Exposure of GPSer on the outer leaflet of plasma membrane is a hallmark of apoptosis and serves as a signal to allow the safe clearance of apoptotic

waste by phagosomes without triggering inflammatory response (Fadok *et al.*, 1992). Interestingly and probably coincidentally, the enrichment of GPSer on vaccinia virus envelope adopts the process for successful cellular entry (Mercer and Helenius, 2008). Many lipids in fact have been identified as potent ligands mediating a wide range of cellular processes.

An additional level of complexity of membrane lipid functions lies in the metabolic and/or regulatory relationship between lipid classes. Ceramide transport protein (CERT) mediates the transport of ceramide from the endoplasmic reticulum to the Golgi apparatus where it is converted to sphingomyelin. Targeting of CERT to the Golgi and its activation are dependent on phosphoinositides and sterols, respectively (Hanada *et al.*, 2003;Perry and Ridgway, 2006). Furthermore, while many studies have reported the individual functions of lipids on a particular cellular process, the molecular links between distinct classes of lipids are recently beginning to be revealed. Mutants of enzymes involved in phospholipid metabolism have been isolated in various genetic screens in *S. cerevisiae* for suppressors of sphingolipid defects, suggesting that these classes of lipids may function together (Beeler *et al.*, 1998;Nagiec *et al.*, 1993). Tabuchi and Kobayashi and their co-workers had independently reported a molecular link between phosphoinositides and sphingolipid signalling in the regulation of actin cytoskeleton organisation and cell viability (Tabuchi *et al.*, 2006;Kobayashi *et al.*, 2005). These examples clearly illustrate the interactions and dependence of different classes of lipids in regulating lipid metabolism, transport and function, even though the existence of such highly complex regulatory mechanisms remains poorly understood.

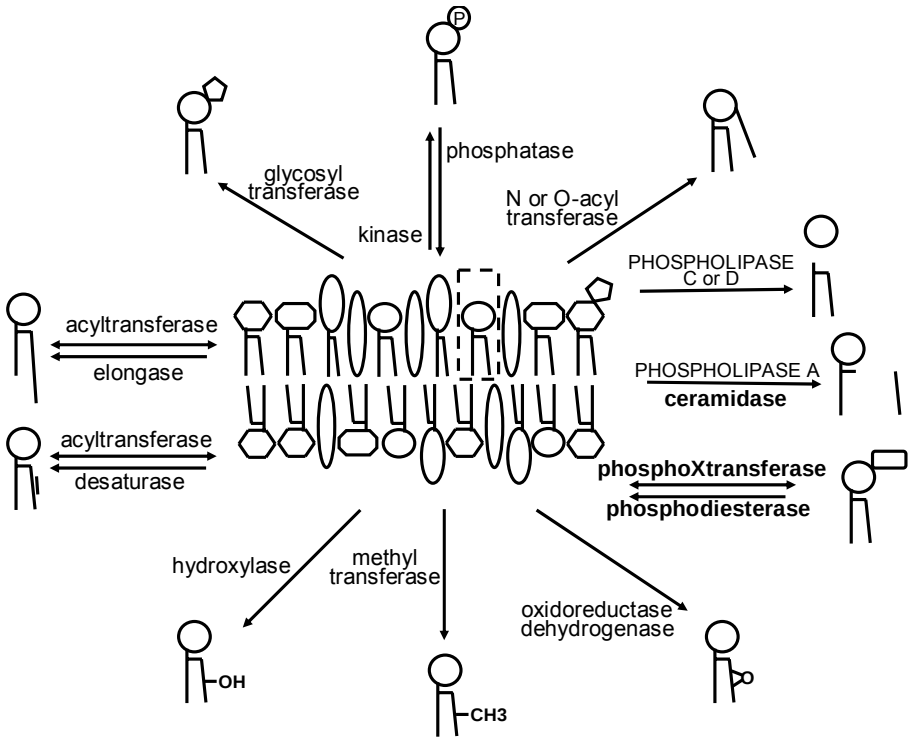

Figure 1.2 The complex life of a membrane glycerophospho- or sphingo-lipid.
Lipid undergoes extensive enzymatic as well as non-enzymatic modifications, which changes their properties and functions. General enzyme classes are indicated. CAPS: glycerophospholipid-specific. Bold: sphingolipid-specific. X- choline, ethanolamine or inositiol.

Why does nature need to invest on a bioenergetically expensive process to create and organise such an impressive catalogue of lipids that defines distinct life forms? An obvious reason for the structural diversity is complementation of cellular function. Apparently, there is a 'redundancy' of lipids under 'normal' growth condition evidenced by the 'knocking out' of certain lipids which do not cause lethality (Kawai *et al.*, 1998;Takamiya *et al.*, 1996;Choi *et al.*, 2004). However, the maintenance of lipid diversity will be appreciated when allostatic forces are applied to a system. Organisms in fact exploit lipid-remodeling mechanisms to recreate structural diversity that allow them to adapt to their environments. Membrane remodeling during temperature acclimation

has been well documented (Overgaard *et al.*, 2008;Polozov *et al.*, 2008;Bhattathiry, 1971;Goldman, 1975). In addition, although sphingolipid biosynthesis is required for growth in eukaryotes, a mutant strain of *S. cerevisiae* lacking sphingolipids, which compensates for the defect by synthesis of a set of novel GPIns (Lester *et al.*, 1993), has been isolated. Clearly, lipids have evolved functionally to allow the survival, proving the worth of the system which cells have paid a high price for.

In the past, lipid research had been relatively focused on a specific lipid (class) of interest and neglected the natural environment of lipids and the important fact that lipids often do not function as a standalone entity. For instance, sphingolipids are structural components of eukaryotic cell membranes, often described in context with sterols to form specialized functional microdomains, commonly known as lipid rafts (Simons and Ikonen, 1997). As discussed, perturbation of membrane lipids often result in extensive remodeling, suggesting the intimate interactions between the various membrane components. Interest towards the understanding how lipids and their interacting partners function in such a systems context is immense and the definition of lipidomics to include both lipids and their interacting partners and the advances in analytics that allow a global snapshot of cellular lipidome cannot be more appropriate and timely. From a translational viewpoint, the influence of lipids on protein functions and biological processes and sometimes, the high specificity of function of a unique chemical entity, offers the possibility to modulate these metabolites as an alternative therapeutic approach, which has been termed membrane-lipid therapy (Escriba *et al.*, 2008). In fact, our knowledge

about the many aspects of lipid function and regulation is still very limited and the road ahead for lipid research is definitely long but exciting.

1.2 Biochemical analysis of lipids

Unlike proteins or genes, which are made up of a limited number of monomeric units, lipids comprise of a structurally diverse collection of molecules that vary in physicochemical properties and dynamic range, which poses a huge technical challenge to analysts. Biochemical analytics of lipids have made enormous progress in the past ten to twenty years. Although the term lipidomics was coined to define the global study of the lipid components of cells, tissues or organisms, it is a far-fetched dream to be able to capture the entire lipidome in a single analysis, a reality that even the advanced field of proteomics faces. The field definitely needs further technological breakthroughs but adopting combinatorial strategies based on currently available methodologies/technologies may be the way to circumvent the problem. In this section, I limit my discussion to the isolation, and mass spectrometry-based detection, characterisation and quantification of major membrane lipids (Fig. 1.3). However, it is important to acknowledge the contribution of conventional methods, such as metabolic labelling and thin layer chromatography, as well as more advanced technologies such as nuclear magnetic resonance, and imaging using lipid-based optical probes, which had greatly complemented and advanced lipid research.

1.2.1 Isolation and purification of membrane lipids

The structural diversity found in lipids challenges common textbook definitions of lipids as molecules that are highly soluble in organic solvents. Polarity differs depending

on the lipid backbone as well as the headgroup modification (Fig. 1.1) (Guan and Wenk, 2008). Sugar modification and phosphorylation render some of these lipids highly polar, and thus they may escape into the aqueous milieu during isolation. For instance, phosphoinositides, due to their polar nature and low abundance, are poorly recovered using conventional Bligh and Dyer or Folch methods of extraction, which is commonly used for bulk membrane lipids including sterols, ceramides, sphingomyelin and major glycerophospholipids. Modifications such as acidification or use of ion pair agents to aid in solubility, and therefore recovery, of this important class of bioactive lipids in organic solvents, have been reported (Gray *et al.*, 2003;Pettitt *et al.*, 2006;Wenk *et al.*, 2003). Often, a compromise has to be made when isolating lipids, for instance, alkaline hydrolysis enriches for sphingolipids, at the expense of the removal of the bulk cellular glycerolipids (Jiang *et al.*, 2007). This may itself be an added advantage, as selective enrichment of lipids is a way to overcome the dynamic range of current instruments. Chemoselective probes for the capture and enrichment of metabolites (Carlson and Cravatt, 2007) which are typically of low abundance, or easily lost during generic extraction, offers the possibility to explore the deep end of the lipidome. In general, the choice of extraction protocol depends on the nature of the biological sample (e.g. tissue, cells or fluids) and the chemistry of the lipid of interest, and ultimately, quantitative isolation of lipids with maximal recovery and purity is desired.

Isolation of lipids, although dating back to the 1800's, has not made significant advances in terms of throughput and automation. Lipids of all major classes can be recovered via chloroform/methanol extraction, typically according to Folch and co-

workers (Folch *et al.*, 1957) or Bligh and Dyer (Bligh and Dyer, 1959), in which they are mostly enriched in the chloroform phase. Because of the higher density of chloroform compared with a water/methanol mixture, it forms the lower phase of the two-phase partitioning system, and tends to be a rate-limiting step and a technical challenge for automation of the extraction procedure. Replacement of chloroform by methyl-*tert*-butyl ether is suited for automation because the low density, lipid-containing organic phase forms the upper layer during phase separation (Matyash *et al.*, 2008). Monophasic extraction followed by separation such as the increasingly common solid phase extraction is amenable to medium to high throughput developments (Jemal *et al.*, 1999). Furthermore, direct analysis of tissue and even intact single cell by mass spectrometry (MS) is possible (Altelaar *et al.*, 2007), and incremental technological advances have been made for lipidomic applications.

1.2.2 Mass spectrometry

The precipitous advances in mass spectrometry (MS), particularly the development of soft ionisation methods, electrospray ionisation (ESI) and matrix-assisted laser, desorption/ionisation (MALDI) mass spectrometry, has led to the realisation of a new level of sensitivity, resolution and throughput for simultaneous analysis of multi-component lipid mixtures (Brunelle and Laprevote, 2008;Han and Gross, 2005a;Isaac *et al.*, 2007;Pulfer and Murphy, 2003;Schiller *et al.*, 2007;Zehethofer and Pinto, 2008). Han and co-workers demonstrated the differential ionisation efficiency of lipid classes based on their inherent electrical propensities (Fig. 1.3A) and termed this separation and/or selective ionisation of different lipids as ‘intrasource separation’ (Han and Gross, 2005a). Enhanced sensitivity of microfluidics-based ionisation (Han *et al.*, 2008) and ultra high

resolution MS such as Fourier Transform Ion Cyclotron (FT-ICR) MS (Schwudke *et al.*, 2007) have tremendously improved the separation of lipids, providing an unparalleled platform for MS-based profiling to provide a global and high density fingerprint of the cellular lipidome. Information of the fine details of molecular species is indicated by the mass-to-charge ratio (m/z) and the ion intensity correlates to quantity (Zacarias *et al.*, 2002) (Fig. 1.3A). The convenience of direct analysis of lipid mixture with minimal sample processing by mass spectrometry is confounded by suppression of ionisation due to competition with other ions within the complex environment for charge during the ionisation process. For quantitative purposes, a suitable cocktail of internal standards that has the same ionisation properties as the analyte(s) of interest needs to be spiked into the mixture, which however is an issue due to the choice and availability of relevant standards. Upfront chromatographic separation of mixtures reduces suppression effects and resolves isobaric complications, therefore allowing the sensitive profiling of extracts harbouring lipids of considerable chemical complexity (Shui *et al.*, 2007).

The ideal of capturing the entire lipidome is challenged by the diverse chemistries, the wide dynamic range of the abundance of the heterogeneous catalogue of lipids as well as their rapid turnover. For instance, cholesterol is highly abundant in the mammalian brain but due to its poor ionisation efficiency in the negative ion mode, is not represented in the profile shown in Figure 1.3A. The use of additives to promote ionisation, alternative ionisation polarities and sources such as Atmospheric Pressure Chemical Ionisation (APCI) which is more suitable for less polar lipids such as cholesterol, and/or coupling to liquid chromatography (LC) represent solutions to improve the range of lipids

to be measured. Clearly, there is no one single method available to probe the entire cellular lipidome.

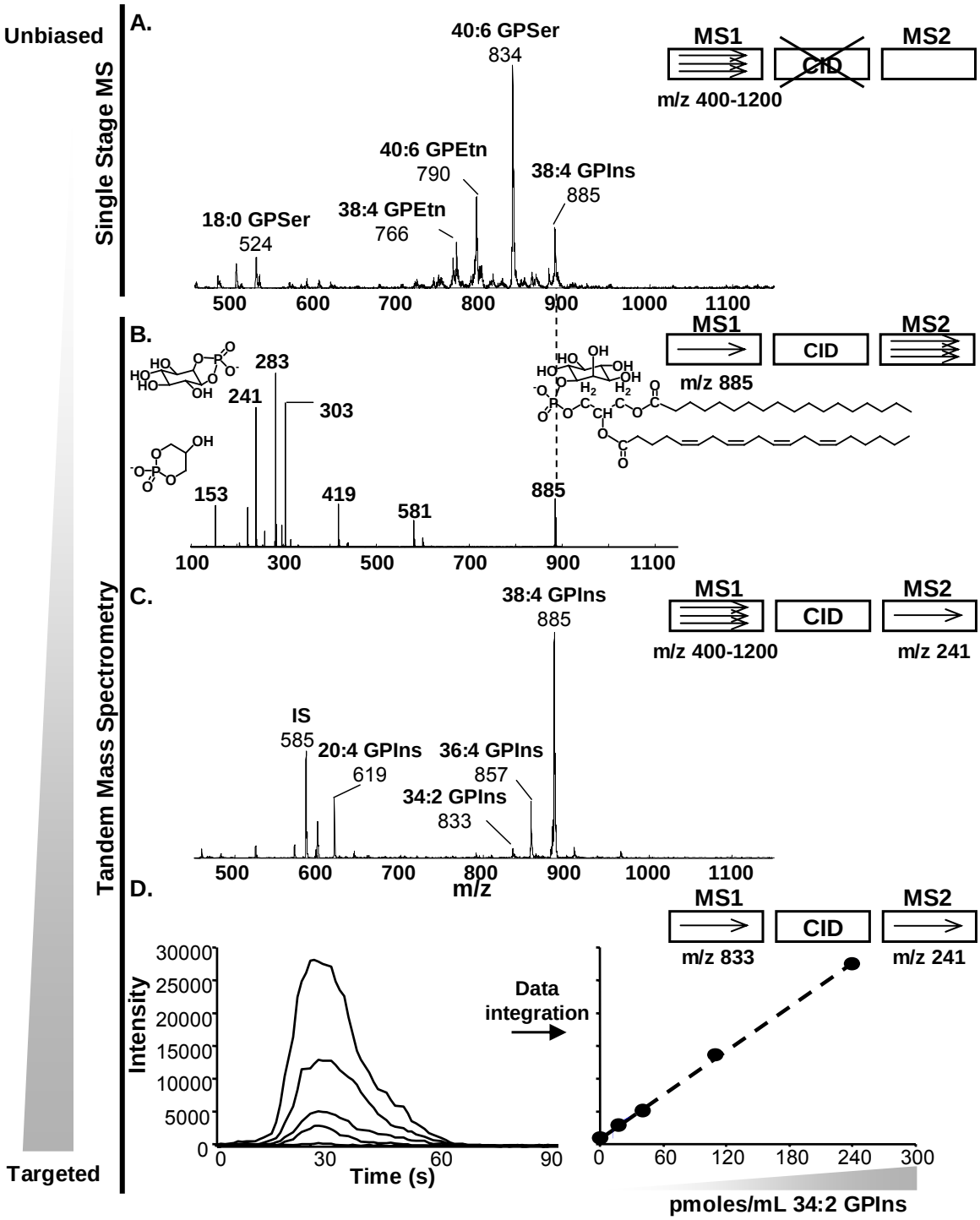

Figure 1.3 Analysis of brain lipids by negative ion mode ESI-MS.
(A) Single stage electrospray ionisation mass spectrum (ESI-MS) in the negative ion mode. The majority of phospho- and sphingo-lipids are detected in the mass range of 400-1200. The ions can be tentatively assigned by their mass-to-charge (m/z) ratio. Characterisation of ions can be achieved by collision-induced dissociation (CID) and tandem mass spectrometry (MS/MS). (B) MS/MS spectra of ions with m/z 885. An ion of interest can be selected in the first mass analyser (MS1) and after CID, the fragment ions are analysed in the second mass analyser (MS2). The product ions of the parent with m/z 885 (38:4 GPIns) includes m/z 153, 241, 283 and 303, which correspond to ions arising from the glycerol phosphate backbone, inositol phosphate headgroup and fatty acyls, respectively. Such information on a common fragment ion that is characteristic and specific for a class of lipids can be used for other MS experiments, such as multiple-reaction monitoring (MRM) and precursor ion scans. (C) Precursor ion scans for lipids containing inositol phosphate headgroup (m/z 241). The second mass analyser is fixed at m/z 241 and the first analyser scans the mass range of interest. Consequently, ions with the propensity to form fragment ions with m/z 241 is selectively detected. Samples can be spiked with internal standards (IS), which is typically not found naturally in the samples under investigation, to allow for semi-quantitative profiling. (D) Overlay of chromatogram (left panel) and standard curve (right panel) obtained from quantification of varying concentrations of a commercially available 34:2 GPIns by MRM. The first and second mass analysers are fixed at the parent ion of interest and its unique fragment ion respectively and selective quantification can be attained with a reasonably good linearity. Note that 34:2 GPIns is a minor ion in the complex lipid mixture and MRM offers a selective and sensitive method for quantification.

The term ‘shotgun lipidomics’ was first coined and refers to the direct analysis of individual lipid molecular species from a crude lipid extract, but it quickly evolved and is inseparable from multi-dimensional ESI-MS (Ekroos *et al.*, 2002;Han and Gross, 2003;Han *et al.*, 2004). For long, tandem mass spectrometry has aided in characterisation and identification of lipids (Fig. 1.3B). An ‘-omic-centric’ view of a sublipidome can be acquired by experimentally filtering for specific classes of lipids using precursor (PREIS) or neutral-loss (NL) scanning (also known as focused lipidomics) (Fig. 1.3C) (Taguchi *et al.*, 2005). These methods are based on selective monitoring of common fragment ions and can be conveniently achieved with triple quadrupole instruments. The fragmentation pattern and structure has to be pre-determined as it is prudent to find a product ion that is unique to the structure. This, however, is not an issue for well-characterised lipids such as major glycerophospholipids, sphingolipids and sterols (Table 1.3). For instance, multiple precursor ion scans of the inositol phosphate headgroup and fatty acyl fragments (Fig. 1.3B) can be used to selectively and unambiguously measure glycerophosphoinositol in

complex lipid mixtures (Fig. 1.3C). This method has been more commonly applied than global analysis to fingerprint cellular lipidome (Ekroos *et al.*, 2002), partly because of enhanced selectivity and sensitivity (Taguchi *et al.*, 2005;Han *et al.*, 2004). With the information of parent and fragment ions, the mass spectrometer can be set to selectively quantify a compound of interest in a mixture when used with pertinent internal standards, a method known as multiple-reaction monitoring (MRM) (Fig. 1.3D), which is highly selective and sensitive. Combining the collection of dataset from sublipidome analyses will eventually lead to extensive lipidome maps of the various samples and species types.

Table 1.2 Sublipidome analysis by tandem mass spectrometry (MS/MS) – list of precursor ions for selective detection of major mammalian membrane lipids.

Lipid	Precursor ion	MS/MS Modes	Fragment	Reference
Sterol				
Cholesterol	[M+NH4]+	PREIS 369	Cholestane cation	(Liebisch *et al.*, 2006)
Cholesterol ester	[M+NH4]+	PREIS 369	Cholestane cation	(Han and Gross, 2005a;Liebisch *et al.*, 2006;Hutchins *et al.*, 2008)
Glycero-phospholipid				
GPA	[M-H]-	PREIS 153	Glycerophosphate derivative	(Han and Gross, 2005a)
GPGro	[M-H]-	PREIS 153	Glycerophosphate derivative	(Han and Gross, 2005a)
	[M+NH4]+	NL 189	Phosphoglycerol	(Taguchi *et al.*, 2005)
GPCho	[M+H]+	PREIS 184	Phosphocholine	(Brugger *et al.*, 1997;DeLong *et al.*, 2001;Han and Gross, 2005a)
GPEtn	[M-H]-	PREIS 196	Glycerophosphoethanolamine derivative	(Brugger *et al.*, 1997;Han and Gross, 2005a)
	[M+H]+	NL 141	Phosphoethanolamine	(Taguchi *et al.*, 2005;DeLong *et al.*, 2001;Brugger *et al.*, 1997)
GPSer	[M-H]-	NL 87	Serine	(Brugger *et al.*, 1997;Han and Gross, 2005a)
	[M-H]-	PREIS 153	Glycerophosphate derivative	(Brugger *et al.*, 1997;Han and Gross, 2005a)
	[M+H]+	NL 185	Phosphoserine	(Brugger *et al.*, 1997;Taguchi *et al.*, 2005)
GPIns	[M-H]-	PREIS 241	Cyclic inositol phosphate	(Brugger *et al.*, 1997;Han and Gross, 2005a)
	[M-H]-	PREIS 153	Glycerophosphate derivative	(Brugger *et al.*, 1997;Han and Gross, 2005a)
	[M+NH4]+	NL 277	Phosphoinositol	(Taguchi *et al.*, 2005)
GPInsP	[M-H]-	PREIS 321	Phosphoinositol phosphate	(Han and Gross, 2005a;Wenk *et al.*, 2003)
GPInsP2	[M-H]-	PREIS 401	Diphosphoinositol phosphate	(Han and Gross, 2005a;Wenk *et al.*, 2003)
GPInsP3	[M-H]-	PREIS 481	Triphosphoinositol phosphate	(Milne *et al.*, 2005)
Sphingolipid				
Ceramide	[M-H]-	NL 256	Sphingosine derivatives	(Hsu and Turk, 2002;Han, 2002)
	[M-H]-	NL 327	Sphingosine derivatives	(Hsu and Turk, 2002;Han, 2002)
	[M-H]-	NL 240	Loss of 2-trans-palmitoyleyl alcohol (for d18 sphingoid base)	(Han, 2002)
	[M+H]+	PREIS 264	Double dehydration product of d18:1 sphingoid base	(Liebisch *et al.*, 1999;Sullards and Merrill, Jr., 2001)
Sphingomyelin	[M-CH3]-	PREIS 168	Dimethyl-ethanolaminephosphate	(Brugger *et al.*, 1997)
	[M+H]+	PREIS 184	Phosphocholine	(Han and Gross, 2005a)
Ganglioside	[M-H]-	PREIS 290	N-acetylneuraminic acid derivative	(Tsui *et al.*, 2005)
Sulfatide	[M-H]-	NL 97	Sulfuric acid	(Hsu *et al.*, 1998;Whitfield *et al.*, 2001)
	[M+H]+	PREIS 264	Double dehydration product of d18:1 sphingoid base	(Hsu *et al.*, 1998;Whitfield *et al.*, 2001)
Mono- and di-glycosylated ceramides	[M+H]+	PREIS 264	Double dehydration product of d18:1 sphingoid base	(Sullards and Merrill, Jr., 2001)

Abbreviations: PREIS, Precursor ion scan; NL, Neutral loss scan.

Technology is constantly improving to overcome many of these present issues, which include the development of hybrid instruments, interchangeable ionisation source, and rapid polarity switch of quadrupole instruments, the latter of which allows acquisition in both the positive and negative ion modes within a single analytical run (Hou *et al.*, 2008;Zehethofer and Pinto, 2008). An exciting technology in the field is the possibility to perform imaging MS, most commonly enabled by MALDI, desorption electrospray ionisation (DESI), surface-enhanced laser desorption/ionisation (SELDI) MS and time-of-flight secondary ion mass spectrometry (ToF-SIMS), which will add a new dimension, particularly spatial information, to lipid analysis. In addition, with the possibility to laterally resolve lipid location in model membrane systems (McQuaw *et al.*, 2007), it will be highly attractive such resolution can be applied to intact cells as many fundamental questions regarding membrane organisation remain to be unraveled.

The volume of data generated by mass spectrometry is immense and interpretation of data was hampered during the dawn of lipidomics when there was a virtual absence of comprehensive and integrated reference databases which can aid in the annotation of known lipid metabolites and the identification of novel lipid metabolites, for instance. Nonetheless, the landscape is rapidly changing. Several public databases (Table 1.3) and open source as well as proprietory software tools for lipid MS data analysis (Table 1.4) now exist. As a refinement of Fahy and co-workers' classification system to improve computational queries, Baker and co-workers recently proposed structural definitions for different classes of lipids and presented an ontology-driven lipid bibliosphere navigation infrastructure (Baker *et al.*, 2008). Automated MS analysis and data processing has set

the stage for high comprehensive and high throughput profiling of cellular sublipidomes (Ejsing *et al.*, 2006a). It should be acknowledged that the advancement of the field is not solely attributed by state-of-the-art instrumentation, but can only be achieved with complementation by bioinformatics and data processing tools (Yetukuri *et al.*, 2008).

Table 1.3 List of lipid-related databases

Database	Content	URL
LIPID MAPS	Largest curated lipid database containing i) mass spectra; (ii) classifications; (iii) protocols of 10,000 lipid species.	http://www.lipidmaps.org/
LMSAD (Lipid Mass Spectrum Analysis Database)	Subset of LIPID MAPS database, encompassing structures and annotations of biologically relevant lipids. Structures of lipids in the database come from four sources: (i) LIPID MAPS Consortium's core laboratories and partners; (ii) lipids identified by LIPID MAPS experiments; (iii) computationally generated structures for appropriate lipid classes; (iv) biologically relevant lipids manually curated from LipidBank LIPIDAT and other public sources. (Sud *et al.*, 2007)	http://www.lipidmaps.org/data/structure/index.html
LipidBank	A Japanese library containing > 7000 lipid species, partly with experimental information including MS data and references. (Taguchi *et al.*, 2007)	http://lipidbank.jp/
MassBank	A database of comprehensive high-resolution mass spectra of metabolites. (Taguchi *et al.*, 2007)	http://www.massbank.jp/index-e.html
LIPIDAG	A relational database of lipid miscibility and associated information. LIPIDAG includes references to almost 1600 phase.	http://www.lipidag.ul.ie/
LIPIDAT	A central depository for information on lipid mesomorphic and polymorphic transitions and miscibility. (Caffrey and Hogan, 1992)	http://www.lipidat.ul.ie/
SphingoMap	A curation of pathway map for sphingolipid biosynthesis that includes many of the known sphingolipids and glycosphingolipids arranged according to their biosynthetic origin(s).	http://sphingolab.biology.gatech.edu/
Kyoto Encylopedia of Genes and Genomes, KEGG	A database of biological systems, consisting of genetic building blocks of genes and proteins (KEGG GENES), chemical building blocks of both endogenous and exogenous substances (KEGG LIGAND), molecular wiring diagrams of interaction and reaction networks (KEGG PATHWAY), and hierarchies and relationships of various biological objects (KEGG BRITE).	http://www.genome.jp/kegg/
Lipid Library	A collection of links and information, including lipid biochemistry and analytical techniques, such as mass spectra, NMR techniques, Ag+ chromatography.	http://www.lipidlibrary.co.uk/
CyberLipids	A collection of links and information, including extraction protocols and lipid analytics.	http://www.cyberlipid.org

Table 1.4 List of MS-related softwares for lipidomic analysis

Software	Utility	Source	URL
LipidSearch	A high-throughput and automatic system for glycerophospholipids identification by various types of MS raw data file.	Department of Metabolome, Graduate School of Medicine, the University of Tokyo (Taguchi *et al.*, 2007)	http://lipidsearch.jp/LipidNavigator.htm
LipidMaps MS Tool	Find mass, number of carbons, number of double bonds, abbreviation, MS/MS product ions (neutral loss), formula, and ion based on input criteria, with links to structure and isotopic distribution.	LipidMaps (Fahy *et al.*, 2007)	http://www.lipidmaps.org/tools/index.html
LipidInspector	Lipid profiling and identification by multiple precursor and neutral loss scanning based in specified criteria in a data-dependent fashion.	Scions (Schwudke *et al.*, 2006)	http://www.scionics.de/lipidinspector
Lipid Profiler	Identification and quantification of molecular species of glycerophospholipids by automated interpretation of multiple precursor ion scan spectra.	MDS Sciex (Ejsing *et al.*, 2006a)	Enquiries on software can be made to MDS Sciex http://www.mdssciex.com/
Fatty Acid Analysis Tool, FAAT	Analyse high-resolution mass spectra of lipids obtained with FT-ICR instruments, includes assignment of ions from a user-defined library based on their exact mass, and comparative analysis of monoisotopic ions in complex mixture.	(Leavell and Leary, 2006)	http://pubs.acs.org/doi/suppl/10.1021%2Fac0604179
LIpid Mass Spectrum Analysis, LIMSA	Peak detection and integration tool for identification (based on user defined lists).	Freeware provided by University of Helsinki (Haimi *et al.*, 2006)	http://www.helsinki.fi/science/lipids/software.html
Spectrum Extraction from Chromatographic Data, SECD	For display of LC-MS chromatograms as two-dimensional “maps” for visual inspection and extraction of mass spectra from LC−MS data.	Freeware provided by University of Helsinki (Haimi *et al.*, 2006)	http://www.helsinki.fi/science/lipids/software.html
Lipid Qualitative/ Quantitative Analysis, LipidQA	Automated identification and quantification of complex lipid molecular specis in mixtures. Library of reference spectra is built based on previous fragmentation pattern of known lipid.	Washington University Biomedical Mass Spectrometry Resource (Song *et al.*, 2007)	Access to LipidQA software can be obtained through Haowei Song (hsong@im.wustl.edu), John Turk (jturk@wustl.edu), or the Washington University Biomedical Mass Spectrometry Resource website.

1.3 Lipidomics as a pathway discovery tool

The contributions of lipidomics research is very obvious in a few aspects of science – (i) making advances in analytical and information technology, (ii) understanding the biological roles of lipids, and discovery of novel lipids, genes and proteins functions (van, 2005), (iii) contribution to systems biology through the integration with other – omics fields to systematically study the complex interactions in biological systems, (iv) application of the toolset in health and environmental research and assessment (Wenk, 2005) and (v) therapeutics (Escriba, 2006). Functional lipidomics aims at providing novel insight into lipid functions, and comparative analysis is highly appealing for unravelling previously unknown correlation between lipid metabolism and a perturbation of interest (Fig. 1.4) (Rilfors and Lindblom, 2002;Wenk, 2006;Li and Prestwich, 2005). Changes in lipid species patterns provide a wealth of information for further studies and can potentially have predictive or diagnostic value. Comparative analysis is not new in lipid research as exemplified by previous studies based on metabolic labelling and thin layer chromatography (TLC), which had led to the characterisation of many lipid enzymes (Sawai *et al.*, 2000;Leber *et al.*, 1997), and lipid factors of medical importance, such as microbial lipids (Azad *et al.*, 1997;Robinson *et al.*, 2007).

A.

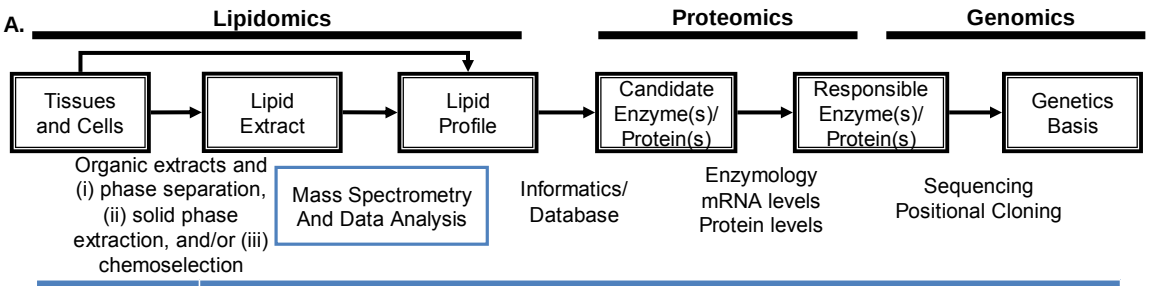

B.

Approach	Non-targeted Analysis		Targeted Analysis
"Biasness"			
MS Method	Single-Stage MS Profiling	Neutral Loss and/or Precursor Ion Scans	Multiple Reaction Monitoring
Advantage	Unbiased, powerful for discovery of novel lipid species and/or novel lipid mediators involved in a biological process	Lipid-Class Selective	Lipid Species Selective
		-Minimize Data Redundancy	
	Prior knowledge of lipids is not required	Quantitative	
		Sensitive	
Disadvantages	Isobaric complications e.g. between GPCho and GPEtn, requires upfront LC separation	Requires prior knowledge of lipids and fragments	
	Requires MS of high mass resolution	Requires reproducible and unique fragments	
	Not suitable for minor lipid species	Consist of an 'inclusive' list and may miss important information on lipids that are not measured	
	Not suitable for comprehensive quantification		

Figure 1.4 Lipidomic strategy for pathway discovery.
(A) Integration of lipidomics, proteomics and genomics tools for systems-level scale analysis of lipids and pathway discovery (Modified from (Wenk, 2005). Lipidomics based on biochemistry is the main focus. In such cases lipids are typically extracted with organic solvents from the source material and are then analysed by chromatography and spectrometry, for example. A lipid profile, which is a biochemical snapshot of the lipid inventory of the cell or tissue under investigation, is generated. Different functional states of the system under investigation can produce differences in such profiles. Based on the aberrations of the lipid metabolites, a hypothesis on the metabolic pathways that might be affected can be formulated. (B) Comparison of non-targeted and targeted analysis by mass spectrometry.

Discovery, based on lipidomics, in general, has taken two approaches (i) non-targeted and (ii) targeted analysis which will be described in this section.

1.3.1 Unbiased discovery lipidomics

The capacity for global profiling has driven biology into a dimension, in which large volumes of complex, but inter-related data can be mined for patterns that will stimulate new hypotheses for experimental validation. Analysis of total lipid extracts by

high resolution mass spectrometry (with or without upfront LC) allows the simultaneous measurement of hundreds of lipids species and represents an attractive top-down approach to study global changes in the lipidome upon perturbation. In this 'brute-force' approach, the instrument is programmed to collect data on whichever ions that are detectable to provide a 'fingerprint' and the ions are surveyed in a non-targeted fashion to determine changes in profiles between experimental conditions. However, the technique of labelling proteins or genes with isotopes or dyes to allow comparative analysis in a multiplex context is not available for lipids, primarily due to a lack of common functional groups between various classes of lipids, which limits the possibility of integrating currently existing platforms for proteomics analysis for lipidomics. Selective labelling of specific classes of lipids for comparative lipidomics, is however possible, for targeted analysis (see Section 1.3.2).

Comparative analysis of high resolution (and high density) profiles can be achieved by specialized softwares (Table 1.4) which include functions such as peak detection and isotopic correction. A list of ions (or identified lipids) and their abundance can be generated for further computation of differences in paired sample sets. Forrester and co-workers described the possibility of identifying more than 450 glycerophospholipids, and used a computational algorithm which performs statistical normalisation to compare the lipid profiles of mast cells during degranulation (Forrester *et al.*, 2004). Quantitative information of individual lipids is however lost in the final lipid array presented. Nonetheless, computational strategies, using mathematical and statistical algorithms, provide a compelling approach for non-targeted analysis of lipid

profiles. Multivariate analyses can serve as exploratory tools for huge data sets such as MS data to uncover unknown trends in a relatively unbiased fashion (Pietilainen *et al.*, 2007;Ding *et al.*, 2008;Schwudke *et al.*, 2007). For instance, Principal Components Analysis (PCA) is a common tool in metabolomic research used to reduce data dimensionality by performing a covariance analysis between factors (lipids) and deriving a small set of variables that can explain the original data set and possibly reveal groupings between data sets. However, PCA is biased against small signals and appropriate scaling is required. Furthermore, statistical testing has to be included to determine the significance of difference in the ions that had the major impact on the data grouping. Pattern and trend recognition of lipid profiles by clustering analysis provide a powerful alternative to survey the high volume of information in a unsupervised fashion that allow associations of lipids to phenotypes. In principle, these data analyses methods can also be applied to datasets derived from targeted lipid analysis (Yetukuri *et al.*, 2007) (See section 1.3.2).

In general, high resolution MS fingerprints of multiple conditions can be compared to 'detect' differences in lipid profiles. Misregulated ions can then be selected for identification and further targeted analysis (Fig. 1.4), thereby bypassing the tedious process of first characterizing the entire spectra of ions. With development of LC/ESI-MS methodology to simultaneously profile lipids of diverse chemistry, including sterols, glycerolipids, glycerophospholipids and sphingolipids (Shui *et al.,* unpublished data), such unbiased method for analysis will allow a more dynamic view of the interactive nature of lipid classes in cellular processes.

An unbiased approach is highly practical at a stage whereby the inventory of the entire cellular lipidome is incomplete. Furthermore, for samples that have not been previously characterised, as long as the lipids ionise and are detected, rapid analysis can be achieved. The likelihood of discovering an unexpected lipid mediator under a given condition and/or a previously uncharacterised lipid moiety makes unbiased profiling highly appealing. However, the likelihood of missing a relevant lipid cannot be ruled out because of the incomplete detection of all lipid species due to the dynamic range and complex chemistries of lipids in a mixture, which is beyond the capacity of existing instrumentations.

1.3.2 Targeted lipidomic analysis

The LIPID MAPS initiative is organised into different cores, based on major lipid categories, to map the lipidome and identify lipid metabolites and pathways in macrophage cells during immunogenic perturbations, reflecting the more common strategy of a targeted lipidomics approach for discovery. The criteria for targeted analysis include (i) defining the target(s) of interest to measure (here a target is defined as a specific lipid class, or a specific lipid species), and often, this is hypothesis-driven and (ii) development of a method by which these target metabolites is selectively measured. Liquid chromatrography-mass spectrometry (LC-MS) operated in selected ion monitoring mode, precursor ion (PREIS) or neutral loss (NL) scan and multiple-reaction monitoring (MRM), with the latter offering the highest sensitivity and selectivity. This approach is highly information-based and is dependent on robust characterisation and selective detection of the class of lipids of interest. The process of target characterisation and measurement is greatly facilitated by automated information-dependent acquisition,

whereby the mass spectrometer is set to run a survey scan and several tandem MS events, which is usually user defined, to identify as many putative compounds as possible in a mixture within a single run (Schwudke *et al.*, 2006).

Precursor and neutral ion scanning provide a fingerprint of a sub-lipidome and it is possible to perform multiplex differential analysis for specific lipid class if the unique functional group of the lipid class of interest can be labelled (Zemski Berry and Murphy, 2006). On the other hand, analysis by MRM with appropriate internal standards, allow for absolute quantification of each metabolite tested. Targeted analysis offers the advantages of enhanced sensitivity and also, the inherent redundancy in data collection and analysis, particularly in applications with a working hypothesis, is eliminated. Furthermore, targeted analysis is the approach of choice when specific lipids, particularly isobaric compounds with different chemistry but exact same mass, have to be unambiguously measured.

Quantification by targeted MS analysis is of high relevance, for instance in diagnostic work. Biochemical diagnosis based on cholesterol and triglycerides levels has a sufficiently long history in clinical applications. Selective monitoring of lipid metabolites by mass spectrometry is increasingly common and have provided robust readouts for a few pathologies with known aberrations in lipid metabolism, including Barth syndrome (cardiolipin) (Kulik *et al.*, 2008), sphingolipidosis (sphingolipids) (Kitagawa *et al.*, 2005;Cui *et al.*, 2008), various cancers (lysoglycerophospholipids) (Sutphen *et al.*, 2004;Zhao *et al.*, 2007;Xiao *et al.*, 2000), as well as detection of foreign

microbial lipids (Hamasur *et al.*, 2001). However, these are relatively straightforward applications of targeted lipid analysis and the real challenge arises at the systems-level scale. In the context of systems biology, it is essential that identical sets of metabolites are precisely quantified in multiple samples, such as those derived from differentially perturbed system, for downstream applications such as modelling and simulations. Considerable knowledge of the biology and information of the lipidome of the system of interest is essential for the success of a targeted approach and its applications in systems biology. A further complication is the diversity and differences in lipid catalogues between various systems. For instance, a list of MRM transitions for quantification of the lipidome of a neuronal cell line may not be fully applicable to a red blood cell, not to mention the transferability of methods between different tissues, organs, and obviously organisms.

Even with the most comprehensive set of target lists, the approach tends to be biased since analytes are pre-determined and discovery rates for novel lipid mediators is compromised. Unbiased and targeted analyses each have their own strengths and weaknesses, but both approaches are highly complementary and their combination is a powerful discovery tool for lipidomics.

1.4 Motivations and aims

Novel analytical approaches, primarily based on liquid chromatography and mass spectrometry, have driven lipid research to a level that allows the systems-level analysis of these metabolites and their interacting partners. However, at its dawn, the field was met with many obstacles, including a lack of robust and versatile platform to quantify the

entire lipidome, computer algorithms for automated data analysis and data integration with other omics, and inadequate database, amongst other issues. In fact, the field of lipidomics is at such a young stage, a complete catalogue of cellular lipidome is not even available, in particular for different biological species.

The aim of this study is to develop a combinatorial approach of both unbiased and targeted lipidomic analyses that can be generally applied to any biological systems of interest. With a time of flight (ToF) instrument, high resolution lipid profiles from a crude lipid extract will be generated and a computational tool will be developed for non-targeted comparative lipidomics, with a focus on glycerophospholipids and sphingolipids. The aim is to develop a rapid method for differential profiling, analogous to other –omics platform such as microarray or isobaric tag for relative and absolute quantification (iTRAQ)-LC-MS for proteomic analysis, but under a label-free constraint. Such a method will allow an unbiased survey of the (sub-)lipidome that is captured by the mass spectrometer and lead to the identification of lipid mediators during a perturbation of interest. The method will first be validated using lipid extracts isolated mammalian tissues and cells, for which the isolation and characterization of the lipids have already been previously described and allow for unambiguous description of the lipids (Brugger *et al.*, 1997;Sullards and Merrill, Jr., 2001). It should be noted that although the focus of this work is on glycerophospholipids and sphingolipids which are a subset of the entire lipidome, the the novel analytical approach developed is also termed 'lipidomic' as a global snapshot of multiple metabolites is captured.

With the successful endeavour of determining the complete genome sequences in many organisms, and annotation of gene products, the creation of genome wide knock out or knock down mutant libraries for various model organisms has been an indispensable tool for research. The wide range of yeast mutants, for instance, offers unparalleled opportunities for genome-wide screens to discover and/ or characterise mutants involved in lipid metabolism, transport and turnover (Daum *et al.*, 1999;Proszynski *et al.*, 2005). I will next develop methods for isolation and analysis of glycerophospholipids and sphingolipids from *S. cerevisiae*. Deletion mutants of known lipid metabolism pathways obtained from publicly available libraries will be selected to validate the analytical approach developed. The availability of these mutants offers the opportunity to characterise lipids that would otherwise be present in low abundance, and will not be detected under 'normal' conditions. In addition, a simple theoretical lipid database that will facilitate the tentative assignment of ions will be built based on arithmetic. Given the relatively simple composition of yeast lipids, I will comprehensively characterise yeast major glycerophospholipids and sphingolipids and establish a more targeted method for relative quantification of individual molecular species.

The intricate balance of composition, distribution and interactions of lipids in a cell is critical for normal function and one of the greatest frontiers in biology is to understand how this is mediated. The appreciation of the fine coordination of lipids and cellular function can be illustrated by the image of the lipid bilayer in eukaryotic cells, which has undergone a distinct change recently. The original fluid-mosaic model predicted free

diffusion of all components within the plane of the membrane, but lately it has been proposed that eukaryotic plasma membranes are composed of micro/nanodomains, commonly called rafts, and it has been shown that proteins and lipids do not freely diffuse over the entire surface of the cell (Simons and Ikonen, 1997;Kusumi *et al.*, 2005;Jacobson *et al.*, 2007). This membrane specialization seems to correlate with the presence of sterols and sphingolipid species, which, in contrast to the glycerophospholipids, are found with few exceptions only in eukaryotic cells. There is now clear biophysical evidence that sterols and sphingolipids can segregate from other lipids in simple artificial membrane systems to form liquid-ordered domains (Ahmed *et al.*, 1997). Some evidence exist, suggesting genetic interactions between mutants in sterol and sphingolipid biosynthesis (Eisenkolb *et al.*, 2002;Baudry *et al.*, 2001;Swain *et al.*, 2002). However, there is little, if any, convincing evidence showing that these two lipid species function together in complex biological membranes of living cells. Genetic manipulation of lipid metabolism in live cells provides an invaluable set of reagents to probe lipid functions and the lipidomic approach described will be applied, in combination with yeast genetics, to study the functional interactions of membrane lipids in cells and how this affects cell physiology.

Finally, the glycerophospholipidome and sphingolipidome of *D. melanogaster* will be characterised. The fruit fly offers an opportunity to study biology from the subcellular to the whole organism level and methods to isolate lipids from different parts of the will be established and comparative lipidomics will be performed to biochemically characterise a mutant deficient in a fatty acid desaturase, Desat1.

In summary, although the use of mass spectrometry to characterise and quantify lipids is not new (Table 1.5), these are often lipid class specific. This thesis presents a novel analytical approach to measure glycerophospholipids and sphingolipids in samples derived from mammalian tissue/cells, yeast and fly in a global fashion and the methods described in this thesis have in fact found wide-spread applications which have contributed to (i) characterisation of various glycerophospholipids and sphingolipids not previously described (Guan and Wenk, 2006); (ii) novel lipid regulators/ enzymes (Kutik *et al.,* in press); (iii) elucidation of lipid interactions and functions (Mousley *et al.*, 2008) (iv) lipid biomarker discovery for disease diagnosis and/or prognosis (Fernandis *et al.*, in preparation).

Table1.5 MS-based analysis of glycerophospholipids (GPL) and sphingolipids (SPL) in mammals, yeast and fly and lipids analysed in this thesis

Application	Glycerophosphospholipid (GPL)#								Sphingolipid (SPL)#			Reference
	PC	PE	PI	PS	PG	PA	CL	others	Cer	Phospho-SPL and/or glyco-SPL	SB	
Mammalian cells/tissues (relatively well-established)												
Profiling, characterisation and quantification of GPL and SPL	**+**	**+**	**+**	**+**	**+**	**+**		**+**	**+**	**+**		**This thesis (Guan *et al.*, 2006)**
S. cerevisiae												
Characterisation of substrate utilisation for phospholipid biosynthetic enzymes	+	+						+				(Boumann *et al.*, 2004a; Boumann *et al.*, 2004b)
Lipid remodeling associated with glycerophosphocholine depletion	+	+										(Boumann *et al.*, 2006)
Biochemical characterisation of glycerophosphocholine deficient strains	+	+										(Choi *et al.*, 2004)
Cardiolipin and Bax-mediated cytochrome c release from mitchondria							+					(Iverson *et al.*, 2004)
Biochemical characterisation of human homologue of gene,TAZ1, causing Barth syndrome							+					(Vaz *et al.*, 2003;Gu *et al.*, 2004)
Identification of a very long chain-substituted glycerophosphoinositol			+									(Schneiter *et al.*, 2004)
Role of glycerophosphoethanolamine in growth and membrane structure	+	+						+				(Storey *et al.*, 2001)
Characterisation of a novel acyl-coenzyme A 1-acylglycerol-3-phosphate O-acyltransferases, Slc1p and Slc4p	+	+	+	+	+							(Benghezal *et al.*, 2007)
Characterisation of a novel O-acyltransferase, Lpt1p	+	+										(Tamaki *et al.*, 2007)
Characterisation of a functional homologue of human seipin, FLD1, with a potential role in GPL metabolism*	+	+	+	+								(Fei *et al.*, 2008)
Characterisation of *Schizosaccharomyces pombe* ceramide desaturase											+	(Garton *et al.*, 2003)
Organisation of membrane lipids	+	+	+	+					+	+		(Schneiter *et al.*, 1999)
Role of acyl coA binding protein, Acb1p, on lipid metabolism, regulation and membrane functions	+	+	+	+					+	+		(Faergeman *et al.*, 2004)
	+	+	+	+	+	+						(Feddersen *et al.*, 2007)
	+	+	+	+		+				+		(Gaigg *et al.*, 2001)
Functional and biochemical characterisation of a mitochondrial translocator, FOMP7**					+	+	+					Kutik *et al.,* in press
Functional substitution of sphingolipids by GPL containing C26 very long chain fatty acids			+							+		(Gaigg *et al.*, 2006)
Regulation of sphingolipid levels in mitochondria									+	+		(Kitagaki *et al.*, 2007)
Structural and functional characterisation of sphingosine phosphate lyase, Dpl1p											+	(Mukhopadhyay *et al.*, 2008)
Fatty acid requirement of yeast sphingolipid			+							+		(Cerantola *et al.*, 2007)
Regulation of ceramide biosynthesis by target of rapacymin complex 2 (TORC2)									+		+	(Aronova *et al.*, 2008)
Membrane dynamics, ceramide homeostasis and cellular signalling**									+	+		(Mousley *et al.*, 2008)
Sec14-dependent secretion and non-dependence on SPL biosynthesis										+		(Stock *et al.*, 1999)
SPL and heat stress									+			(Wells *et al.*, 1998)
Discrimination of yeast strains based on cell surface lipid profiling	+	+	+	+	+		+					(Jungnickel *et al.*, 2005)
Characterisation and quantification of inositol containing SPL										+		(Hechtberger *et al.*, 1994)
Quantitative analysis of phosphoinositides			+					+				(Wenk *et al.*, 2003; Pettitt *et al.*, 2006)
Characterisation of SPL										+		(Ejsing *et al.*, 2006b)
Profiling, characterisation and quantification of GPL and SPL and application to study functional interaction between membrane lipids	**+**	**+**	**+**	**+**		**+**	**+**		**+**	**+**		**This thesis (Guan and Wenk, 2006)**

Application	Glycerophosphospholipid (GPL)#								Sphingolipid (SPL)#			Reference
	PC	PE	PI	PS	PG	PA	CL	others	Cer	Phospho-SPL and/or glyco-SPL	SB	
D. melanogaster												
Modulation of SPL biosynthetic pathway rescues photoreceptor degeneration									+			(Acharya *et al.*, 2003)
Effects of acclimation temperature on thermal tolerance and membrane GPL composition	+	+										(Overgaard *et al.*, 2008)
A screen of 13 non-lepidopteran insects for presence of fatty acid amides								+				(Yoshinaga *et al.*, 2007)
Fast atom bombardment MS/MS analysis of GPL	+	+	+	+								(Gamo *et al.*, 1999)
Zwitterionic and acidic glycosphingolipids of *D. melanogaster* embryo										+		(Seppo *et al.*, 2000)
Characterisation of free endogenous C14 and C16 sphingoid base											+	(Fyrst *et al.*, 2004)
Identification and characterisation by ESI-MS of endogenous sphingadienes									+		+	(Fyrst *et al.*, 2008)
Profiling, characterisation and quantification of GPL and SPL and application to biochemically characterise a *desat1* deficient mutant	**+**	**+**	**+**	**+**		**+**			**+**	**+**		**This thesis [Kohler *et al.*, in preparation]**

Due to space limit, the standard abbreviations for the various sub-classes of sphingolipids (SPL) and glycerophospholipids (GPL) have been replaced in the header of this table by the following: CL, cardiolipin; PA, phosphatidic acid; PC, glycerophosphocholine; PE, glycerophosphoethanolamine; PG, glycerophosphoglycerol; PI, glycerophosphoinositol; PS, glycerophosphoserine. Other abbreviations used in this table include: Cer, ceramide; SB, sphingoid base.

* Method developed in this thesis was adopted by others and cited in their studies.

** Method developed in thesis was applied in these studies during the course of this thesis.

Chapter 2. Novel Analytical Approach to Study Mammalian Glycerophospholipids and Sphingolipids[1]

[1] The work described in this Chapter is part of the following publications:

1) **Guan XL**, He X, Ong WY, Yeo WK, Shui G and Wenk MR (2006). Non-targeted profiling of lipids during kainate induced neuronal injury. **FASEB J.** 20(8): 1152-61.

2) He X, **Guan XL**, Ong WY, Farooqui AA and Wenk MR (2007). Expression, activity, and role of serine palmitoyltransferase in the rat hippocampus after kainate injury. **J Neurosci Res.** 85(2): 423-32.

In addition, a manuscript is currently in preparation, which describes the analysis of human plasma lipidome and the use of multivariate statistics and supervised learning based on support vector machines for the classification of ovarian cancer.

Fernandis AZ, Kothandaraman N, Chua GH, **Guan XL**, Shui G, Choolani M and Wenk MR. Classification of benign and malignant ovarian cancers by multiparametric analysis of lipids in blood plasma. *In preparation.*

2.1 Introduction

In this chapter, a mass spectrometry based method for non-targeted profiling of lipids from mammalian tissue and cell extracts is described. The approach can in principle be used whenever two lipid extracts of similar composition are to be compared. Indeed, this is very often the case in biological applications (Rapaka *et al.*, 2005;Wenk, 2005). This approach was employed to determine the changes of artificially perturbed brain lipid mixture. The application of the methodology was extended to unravel changes in hippocampal lipids during kainate induced neuronal injury, which is the first study that addresses lipid metabolism of neuronal damage in such a non-targeted fashion. In addition, candidate lipid metabolic pathways were identified based on the alterations observed and these pathways were pharmacologically modulated to examine their effects on rescuing cells from neurotoxic insults. These works have been published in 2006 in the FASEB Journal and Journal of Neuroscience Reseach (Guan *et al.*, 2006;He *et al.*, 2006). However, it is not in the context of this thesis to rewrite these findings, but because the approach of 'differential profiling' I have developed can be generally applied to any sytems of interest and is the platform employed in many studies during the course of this thesis, it is thus imperative to describe in detail its development.

2.2 Materials and Methods

2.2.1 Chemicals and reagents

In this study, all reagents were obtained from Sigma Aldrich, USA and organic solvents were obtained from Merck, Germany and are of analytical grade, unless otherwise stated.

2.2.2 Animal handling and collection of brain tissue

Animals were acquired and cared for in accordance with guidelines published in the NIH Guide for the Care and Use of Laboratory Animals. All procedures involving animals were approved by the Animal Care and Use Committee of the National University of Singapore and performed in the laboratory of Dr Ong Wei Yi, the collaborator in this project.

Male wistar rats weighing approximately 200grams were anesthetized deeply by intraperitoneal injection of 1.5mL of 7% chloral hydrate and sacrificed by decapitation. The hippocampi were promptly excised and snap frozen in liquid nitrogen. The right and left hippocampi of each rat were stored in separate tubes and analysed independently to minimize variations. The hippocampal samples were stored at -70°C until required.

2.2.3 Sample preparation and collection of brain tissue

Rat hippocampi were weighed and homogenized in 5 volumes of breaking buffer [500mM potassium chloride (KCl), 10mM magnesium chloride ($MgCl_2$), 250mM sucrose, 25mM Tris, pH 8, 2mM EGTA, pH 8, 1mM dithiothreitol, and protease inhibitor mix] using a small tissue blender. A 150μL aliquot of the homogenate was used for subsequent lipid extraction step and the remaining was used for protein quantification.

2.2.4 Internal standards

Synthetic lipids with fatty acyl compositions that are naturally low abundant were used as internal standards. Phosphatidic acid (GPA) with C17 fatty acyl chains (diheptadecanoyl GPA, di17:0-GPA), C14-glycerophosphoserine (dimyristoyl GPSer,

di14:0-GPSer), C14-phosphatidyglycerol (dimyristoyl GPGro, di14:0-GPGro), C19-ceramide (C19-Cer) and C12 sphingomyelin (C12-SM) were obtained from Avanti Polar Lipids (Alabaster, AL). Glycerophosphoinositol with C8 fatty acyl chains (dioctanoyl GPIns, di8:0-GPIns) was obtained from Echelon Biosciences, Inc (Salt Lake City, UT). The internal standards were solubilised in chloroform at a stock concentration of 10μg/μL.

2.2.5 Lipid extraction

A modified protocol of Bligh & Dyer (Bligh and Dyer, 1959) was used to extract lipids from rat hippocampal tissue. Briefly, 400μL of chloroform-methanol, (1:2, volume-to-volume (v/v) was added to 20mg of tissue homogenate and 5μg of internal standards, di17:0-GPA and di8:0-GPIns were added. After a 10 minute incubation on ice, 300μL of chloroform and 200μL of 1M hydrochloric acid (HCl) were added to the mixture. The mixture was centrifuged at 9000rpm for 2 minutes at 4°C and the lipids were isolated from the lower organic phase. The sample was vacuum dried (Thermo Savant SPD SpeedVac with UVS400A Universal Vacuum System) and the lipid film was resuspended in 2mL of chloroform-methanol (1:1, v/v) for subsequent analysis.

2.2.6 Lipid analysis by electrospray ionisation mass spectrometry (ESI-MS) and tandem mass spectrometry (MS/MS)

Electrospray Ionisation Mass Spectrometry (ESI-MS) was performed on a Waters Micromass quadrupole-Time of Flight (Q-ToF) micro (Waters Corp., Milford, MA) mass spectrometer. Typically, 2μL of sample were injected for analysis. The capillary voltage and sample cone voltage were maintained at 3.0 kilovolts (kV) and 50 volts (V),

respectively. The source temperature was 80°C and the nano-flow gas pressure was 0.7 bar. The mass spectrum was acquired from m/z 400 – 1200 in the negative ion mode with an acquisition time of ten minutes and the scan duration was 1 second (s). The inlet system consisted of a Waters CapLC autosampler and a Waters CapLC pump and chloroform-methanol (1:1, v/v) at a flow rate of 3μL/min was used as the mobile phase. Individual molecular species were identified using tandem mass spectrometry. In general, the collision energy used range from 25 – 80 eV.

Quantification of individual molecular species was performed using multiple-reaction monitoring (MRM) with an Applied Biosystems 4000 Q-Trap mass spectrometer (Applied Biosystems, Foster City, CA). Tandem mass spectrometry (MS/MS) for characterisation/identification as well as quantification of lipid molecular species was performed using precursor ion scanning (PREIS), neutral loss scanning (NL) and multiple-reaction monitoring (MRM) respectively with an Applied Biosystems 4000 Q-Trap mass spectrometer (Applied Biosystems, Foster City, CA) (Fig. 1.3). Based on product ion and precursor ion analysis of head groups and fatty acyls or sphingoid base, comprehensive sets of multiple-reaction monitoring (MRM) transitions were set up for quantitative analysis of various glycerophospholipids and sphingolipid, respectively. In a typical MRM experiment, the first quadrupole, Q1, was set to pass the precursor ion of interest to the collision cell, Q2, where it underwent collision-induced dissociation. The third quadruple, Q3, was set to pass the structure specific product ion characteristic of the precursor lipid of interest (Fig. 1.3D). Each individual ion dissociation pathway was optimised with regard to collision energy to minimize variations in relative ion

abundance due to differences in rates of dissociation (Merrill, Jr. *et al.*, 2005). A high performance liquid chromatography system (Agilent Technologies, Santa Clara, CA) was coupled to the mass spectrometer and samples were introduced into the mass spectrometer by loop injections with chloroform-methanol (1:1, v/v) as a mobile phase at a flow rate of 200μL/min.

2.2.7 Data processing

Data was acquired using MassLynx 4.0 (Waters Corp., Milford, MA). The combined spectra lists were copied with MassLynx and saved as separate tab-delimited plain text files. All programs were coded in MATLAB 7 (The MathWorks Inc., Natick, MA) for Windows operating system (Microsoft Corp., Redmond, WA) and all data analyses were performed on a 1.5GHz Pentium 4 personal computer.

The plain text files obtained from MassLynx were loaded into Matlab for processing (refer to Supplementary material 2.1 for the algorithm in Matlab format). Correlation optimised warping (COW) was used as a pre-processing method in order to obtain precise alignment of the normalized MS data (Nielsen *et al.*, 1998). For averaging of spectra from replicate independent samples the normalized data of each replicate was warped against a reference set. After alignment of the spectra, the intensity values of individual m/z were then averaged to obtain one mean spectrum for each condition (i.e. spiked versus control, also refer to Fig. 2.2A). The mean spectrum for the 'treated' condition was then aligned relative to the mean spectrum for the control condition. After alignment of the mean spectra of the two conditions, relative differences at each data

point can be computed by simple arithmetic division and represented as the ratios, intensity of 'treated'/ intensity of control, converted to a logarithmic scale (log10 ratios) against the m/z axis. In this work, the term 'differential profile' refers to the graphical readout which represents the differences in the MS profiles between two conditions under investigation. It should be noted that these changes are arbitrary in units. A '5-fold' difference in a given peak means the ion response was 5-fold different at that particular m/z. This may, or may not, relate to a 5-fold difference in metabolite levels. In the case of internal glycerophospholipid standards used in this study a good linearity between metabolite concentration in the complex mixture and the ion response was observed however.

Currently, the algorithm is implemented using C programming to increase the processing speed (Chua GH *et al.*, unpublished data) and a Matlab graphical user interface is designed to allow end users to change various parameters including smoothing of spectra and peak detection.

2.3 Results

2.3.1 Profiling of mammalian brain lipids by negative ion ESI-MS

Figure 2.1A shows a typical mass spectrum of a total lipid extract derived from rat hippocampal tissue. In this case, the lipid mixture was infused into a quadrupole-Time of Flight (Q-ToF) mass spectrometer by electrospray ionization (ESI) in negative mode. Ions of many prominent glycerophospholipids can readily be detected and tentatively assigned based on lipid masses (Murphy, 2002). Some of the most prominent ions detected include glycerophosphoethanolamines, GPEtn (18:1 GPEtn, 20:4 GPEtn, 22:6

GPEtn), glycerophosphoserines, GPSer (20:4 GPSer, 38:4 GPSer, 36:1 GPSer, 40:6 GPSer) and glycerophosphoinositol, GPIns (38:4 GPIns) at m/z 478, 500, 524 (GPEtn), 528, 766, 788, 834 (GPSer) and 885 (GPIns) respectively. Glycerophosphocholine (GPCho) as well as sphingolipids ionize well in the positive ionisation mode but considerable signals, for instance m/z 564 is a ceramide, can be detected in the negative ionisation mode. Therefore, single stage ESI-MS provides a considerably comprehensive profile of cellular glycerophospholipids and sphingolipids.

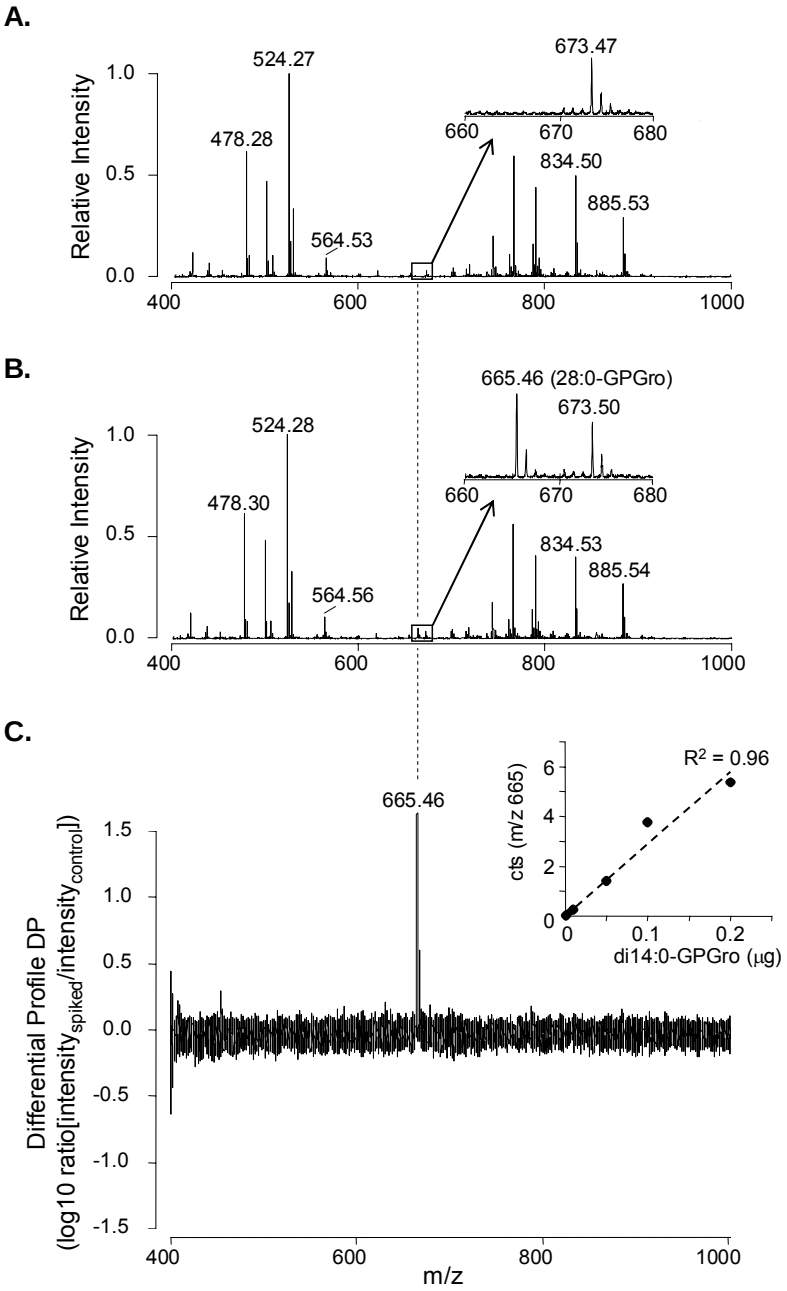

Figure 2.1 Differential lipid profiles of spiked complex lipid mixtures.
Lipids were extracted from rat brain hippocampus using a standard chloroform-methanol protocol and the extracts were analysed using negative-ion mode ESI-MS (A). The same lipid extracts were next spiked with synthetic short chain glycerophosphoglycerol, 0.2μg of di14:0-GPGro, and spectra were recorded again (B). (C) A differential profile to represent difference in lipid composition between control and spiked extract. Lipid profiles of control and spiked extracts were aligned by correlation optimised warping and profiles of the spiked spectrum relative to the control spectrum were calculated and plotted as log10 ratios. The inset shows the response between the difference in ion intensity in m/z 665 for increasing amounts of spiked di14:0-GPGro. Data are presented as means from three independent experiments.

2.3.2 Non-targeted differential profiling based on ESI-MS and chemometry

Figure 2.1B shows replicate analysis of the same extract, which has been spiked with a small amount (0.2μg) of synthetic glycerophosphoglycerol (di14:0-GPGro). Hence, the overall appearance of the mass spectrum is very comparable, yet the exogenously added GPGro leads to a small increase in the ion intensity at m/z 665 (Fig. 2.1B, inset), the expected mass of di14:0-GPGro. Note that ToF analysis yields sharp signals with readily resolved isotopic peaks and high mass accuracy (e.g. Fig. 2.1A & B, inset).

To identify differences in such high resolution mass spectra in a non-targeted fashion, a chemometric approach that allows comparison of differences in ion intensities of all detectable ions between two experimental conditions was developed (Fig. 2.2A). Slight differences in m/z values of ions between experiments are common due to small drifts in experimental conditions such as variations during ToF measurements and are a problem in particular when multiple spectra are to be processed. Note for example the slight differences in m/z values of some of the ions in Figure 2.1A and 2.1B (e.g. 478.30 vs. 478.28, 524.28 vs. 524.27). In order to perform direct analysis of the entire mass spectra, and to utilize all collected data, the mass spectra should be properly aligned. Therefore, a previously developed chemometric method, which is based on correlation optimised warping (COW) (Nielsen *et al.*, 1998), was adopted. COW builds on piecewise stretching and compression of spectra along the m/z axis to correct for drifts (Fig. 2.2B). Importantly, such warping does not affect the peak intensities (Nielsen *et al.*, 1998).

As the total lipid concentration of different samples may vary slightly, it is important to normalize the data so that subsequent comparative studies based on differences in peak intensity is not due to differences in total lipid concentration. A challenge in lipid analysis is that because lipids are metabolites with high turnover, and are highly heterogeneous between biological sources, there is no one 'housekeeping' lipid, unlike proteins and genes, to control for amount of material. Normalisation in this case was performed in two ways – i) the peak intensity at each point (m/z) was first normalised to the sum of peak intensities of all the ions within the scan range or ii) the intensity value of each m/z was normalized to the tissue mass or protein amounts based on the di17:0-GPA internal standard, which was spiked according to the amount of material. Both methods for normalisation produced consistent results. It should however be noted that standardisation of the normalisation protocol is dependent on the nature of the samples.

Using such chemometric warping it is hence possible to almost perfectly align spectra from multiple replicates of experimental condition A (A1…An) and condition B (B1…Bn). Once spectra are aligned they can be further processed arithmetically. A differential profile, DP, which is the ratio of averaged replicate spectra from condition A, <A>, and averaged replicate spectra from condition B, <B>, can be computed as a function of m/z. In the case of the spiking experiment mentioned above, this yields a 'differential profile' which displays a single sharp peak at m/z 665, the expected mass of di14:0-GPGro (Fig. 2.1C). In addition, using a peak detection algorithm, a list of peaks that are differentially regulated is generated and these candidate ions are selected for

identification by MS/MS and quantification by multiple-reaction monitoring (MRM) (Fig. 2.2A).

The ion response of such exogenously added lipids is linear as a function of the amount of spiked material for a variety of different chemistries (e.g. GPGro, GPSer and ceramides, [Fig. 2.1C inset and data not shown]). Thus, for samples of comparable similarity, which typically are at the source in many biological applications, this approach allows for detection of differences in lipid compositions. While this analysis is not as quantitative as for example MRM, it certainly has its advantages. Most importantly, the above method allows for non-targeted screening of multiple lipid species in complex lipid extracts.

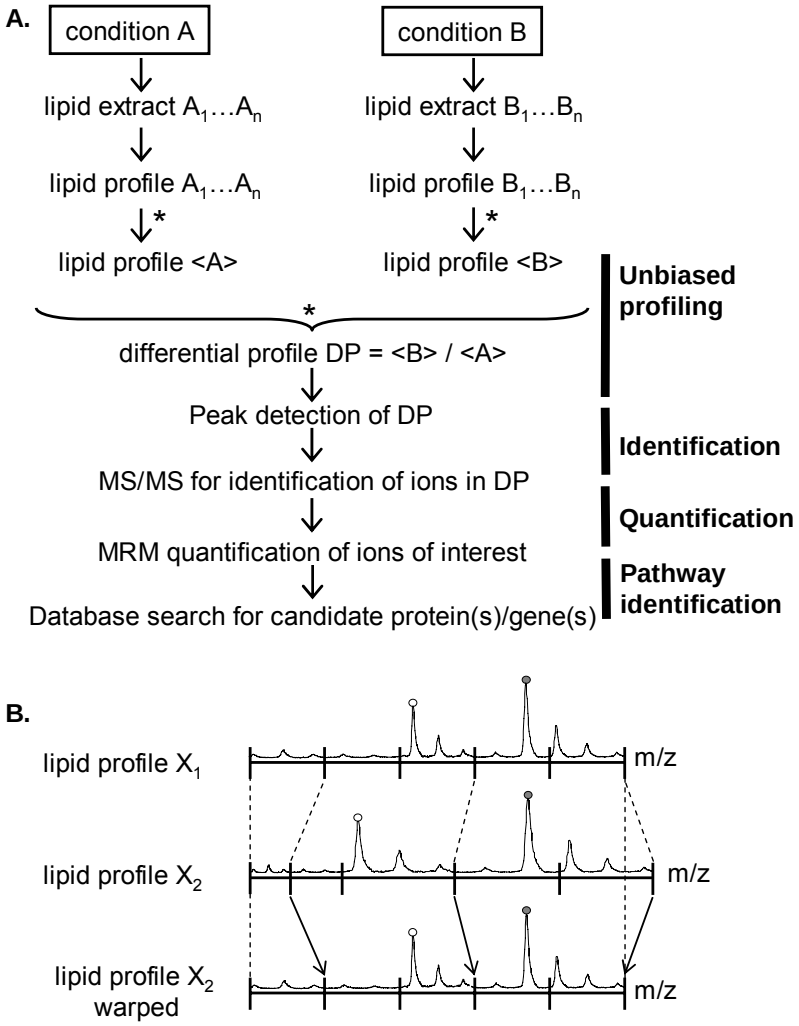

Figure 2.2 Cartoon illustrating the general approach of the method applied here for identification of lipid metabolites that are altered in paired sample systems analysis.
(A) Typically two conditions for which multiple independent replicate samples (e.g. lipid extracts A1…An) are available are at the origin of the approach. Each lipid extract yields a corresponding lipid profile (e.g. lipid profile A1…An, which are single stage mass spectra in this study). These replicate spectra are next aligned using chemometric alignment based on correlation optimised warping (COW, see panel B) and subsequently the ratio of the signal intensities is computed as a function of m/z (DP). (B) Correlation optimised warping of mass spectra. COW was used as a pre-processing method for the mass spectral data. Briefly, a sample mass spectrum profile (X2) is aligned to a reference spectra (X1) by piecewise linear stretching and compression - also known as warping - of the m/z axis of the reference (X1). The asterisk denotes steps which include COW based alignment of spectra.

2.4 Discussion

It is indeed becoming increasingly evident that lipids are important mediators in diverse biological functions, and the dynamics of lipid metabolism and trafficking is critical in these processes. Using lipidomic profiling, it is now becoming possible to determine the levels of many lipids, including membrane constituents (Han *et al.*, 2004;Forrester *et al.*, 2004) as well as soluble lipid mediators (Balazy, 2004;Serhan, 2005), with great sensitivity and selectivity. However, no platform for simultaneous determination in a single experiment was available at the point of this work. Instead existing approaches use highly selective and optimised conditions for the different classes of lipids and required sufficient knowledge on the chemistry of the lipids investigated.

In this work, a unique approach for non-targeted profiling of lipids in complex mixtures is presented. The method does not require any prior knowledge of the identity nor chemical (and fragmentation) property of the lipids in the mixture. It is furthermore particularly sensitive to changes in intensities which arise from ions with low intensity which is very often the case for signalling compounds. Conceptually, the approach follows comparative analysis of paired samples which is reminiscent of other systems level scale methodologies. The results are plotted in 'up-and-down' format and for some lipid chemistries the signal intensities are linearly dependent on ion concentration (Fig. 2.1).

The Q-Tof based metabolite profiling as performed here is considered an excellent initial screening tool. It is particularly powerful when used in combination with alternative analytical methods, such as MS-based targeted analysis by multiple-reaction

monitoring (MRM), or lipid-based imaging, the latter which is able to provide spatial information. Indeed, I have characterised and optimised parameters to selectively quantify mammalian membrane glycerophospholipids and sphingolipids (Supplementary Table 2.1) by MRM (Fig. 1.3) and applied this method to quantify changes associated with (i) excitotoxicity in rat hippocampi, as a validation of our observations based on differential profiling (Guan *et al.*, 2006) and (ii) quantitative analysis of the lipidome of biological fluids as a diagnostic tool for a few human pathologies, including ovarian cancer and Alzheimer's disease (Fernandis *et al.*, in preparation). In addition, elucidation of mechanisms/ enzymes underlying changes observed in lipid profiles to provide greater insights into a biological perturbation of interest can be complemented by proteomics and genomics approach (Fig. 1.4A and 2.2A).

Note that measurement of the levels of other biologically important lipids, such as phosphorylated or breakdown products of glycerophospholipids and sphingolipids for example, was not attempted as these metabolites might have to be extracted with different methods due to their high solubility in aqueous solutions and therefore a tendency to escape during organic extraction. The method works well for lipids with different chemical structures if these lipids can be recovered in the extraction method of choice and ionize efficiently. It will be interesting to extend such metabolite analysis to soluble lipid mediators (e.g. platelet activation factors, anandamides, sphingoid bases etc).

This novel analytical approach should also be applicable to other modes of ionisation (e.g. APCI, MALDI, photoionisation) and mass spectrometric detection. An

important prerequisite is high mass resolution. Indeed, differential profiling of MS/MS scans such as PREIS and NL using high resolution ToF-quadrupole instruments can be achieved. In addition, future applications in combination with ultra-high resolution mass analysis, e.g. FT-ICR mass spectrometry (Schaub *et al.*, 2003), will lead to enhanced mass resolution. This, together with the capabilities of mass spectrometers to allow unambiguous identification of ions based on very accurate mass measurements, makes this method a most promising new tool for lipidomics research. Modifications to the algorithm to process LC-MS data in a three-dimensional space, to include retention time, in addition to the current two-dimensions, m/z and intensity, (Shui *et al.,* unpublished data) have been made and allow for more comprehensive profiling of lipids, with enhanced resolution of isobaric compounds with the same m/z but different chemistries.

Collectively, the current work describes a method for non-targeted profiling of lipids from tissue and cell extracts which is particularly useful for detection of 'large changes on small signals' (signalling lipids).

Chapter 3. High Resolution and Targeted Profiling of Glycerophospholipids and Sphingolipids in Extracts from *Saccharomyces cerevisiae*[2]

[2] The work described in this Chapter has been published in the following publication: **Guan XL**, and Wenk MR (2006). High resolution and targeted profiling of phospholipids and sphingolipids in extracts from *Saccharomyces cerevisiae*. **Yeast**. 23(6): 465-77.

In addition, the application of the approach described in this Chapter has contributed to significant findings in the following publications:

1) Kutik S, Rissler M, **Guan XL**, Guiard B, Shui G, Gebert N, Heacock P, Rehling P, Dowhan W, Wenk MR, Pfanner N and Wiedemann N. The translocator maintenance protein Tam41 is required for mitochondrial cardiolipin biosynthesis. **Journal of Cell Biology.** *In press*.

2) Mousley CJ, Tyeryar K, He KE, Schaaf G, Brost R, Boone C, **Guan XL**, Wenk MR and Bankaitis VA (2008). Coordinate defects in Sec14 and Tlg2-dependent trans-Golgi and endosome dynamics derange ceramide homeostasis and compromise the unfolded protein response. **Mol. Biol. Cell.**

3.1 Introduction

Lipids are small molecules which play important roles in physiology and disease. They are building blocks of cellular membranes, precursors for signalling molecules and they serve as storage of chemical energy in highly reduced form. At the moment, the field of lipid research is undergoing revolutionary developments driven by (i) technological advances for lipid detection, and (ii) insights from recent functional characterisation of lipid enzymes in model systems.

Studies in *S. cerevisiae* have played a particularly crucial role in the advancements of our knowledge of lipid function. As a result, much is known about the pathways, and their regulation, of (glycerophospho)lipid biosynthesis in yeast (Daum *et al.*, 1998;Vance, 2003;Kohlwein *et al.*, 1996;Homann *et al.*, 1987;Carman and Henry, 1989). In addition, and more recently, elegant experiments using combined genetic, biochemical and functional approaches have shed light on the role of phosphoinositides in secretion (Odorizzi *et al.*, 2000;Simonsen *et al.*, 2001;Huijbregts *et al.*, 2000), the role of sterols in endocytic events (D'Hondt *et al.*, 2000;Heese-Peck *et al.*, 2002), and triglyceride synthesis for storage of lipids in intracellular deposits (Mullner and Daum, 2004;Zweytick *et al.*, 2000).

While many of these studies were aimed at investigating physiological processes (such as membrane trafficking) in yeast, it is clear that they also advanced tremendously our understanding of lipid metabolism in other organisms, including mammals. It is important to note that many pathways of lipid biosynthesis and metabolism are well conserved between species ranging from yeast to worm to mouse and human. There are

however also a number of notable differences in yeast lipids compared to mammalian counterparts. For example, *S. cerevisiae* synthesizes ergosterol as its major sterol lipids as opposed to cholesterol in mammalian cells (Munn *et al.*, 1999;Zinser *et al.*, 1993). Yeast sphingolipids contain inositol mannosyl residues rather than glucosyl sugars found in complex glycolipids in Man (Daum *et al.*, 1998).

Traditional lipid analysis, such as thin layer and gas chromatography, is hampered with limited sensitivity, selectivity and resolution. Gas chromatography mass spectrometry (GC-MS), for example, is a powerful method for determination of fatty acyl heterogeneity but it requires derivatisation and pertinent standards. In addition, information on the origin of the fatty acyl moiety is generally lost. Metabolic labelling using lipid precursors (such as radiolabelled inositol, serine or fatty acyls) have been widely used to (selectively) label certain classes of lipids which are then typically separated using thin layer chromatography (TLC) and visualized by autoradiography. While these approaches are generally fairly easy to use and do not require specialized equipment, they do only deliver mass levels of lipids under conditions of steady-state incorporation of the label (which sometimes is difficult to achieve technically). In addition, TLC separation is generally of low resolution.

Electrospray ionisation mass spectrometry (ESI-MS) has been used for analysis of lipids with great success (Wenk, 2005;Forrester *et al.*, 2004;Han and Gross, 2005a). Major advantages of this method is its capability to detect large numbers of individual lipid ions (currently in the order of hundreds to a few thousands), with different

chemistries, in complex mixtures and a single experiment (Han and Gross, 2005a;Hughey *et al.*, 2002;Mougous *et al.*, 2002).

In this Chapter, the MS-based approach described in Chapter 2 is adopted to profile lipids from minimally processed organic extracts of *S. cerevisiae*. The method is based on (i) high resolution analysis for detection of global changes ('non-targeted profiling') followed (ii) by characterisation and quantification of changes of interest using tandem mass spectrometry (MS/MS), MS/MS/MS (MS^3) and multiple-reaction monitoring (MRM). Furthermore, in order to facilitate tentative assignment and identification of ions, this work describes the comprehensive theoretical calculations of molecular masses for yeast glycerophospholipids and sphingolipids, of which a large number can be measured experimentally in a single extract using the present method. Given the high degree of conservation in pathways of lipid metabolism between different organisms it can be expected that this method will lead to the discovery of novel enzymatic activities and modulators of known ones, in particular when used in combination with genetic and chemogenetic libraries and screens. Specifically, mutants from the EUROSCARF library of non-essential deletion mutants to were obtained to validate the analytical approach. Mutants of *SCS7*, a fatty lipid hydroxylase, and *SLC1*, a putative acyl transferase with unknown substrate specificity, were profiled for their glycerophospholipid and sphingolipid content. The observed changes in lipid profiles are consistent with previous observations and extend our knowledge on *in vivo* substrate use under permissive growth conditions.

3.2 Materials and Methods

3.2.1 Strains, media and culture condition

The strains used in this study (Table 3.1) are obtained from the EUROpean *Saccharoymces Cerevisiae* ARchive for Functional analysis (EUROSCARF) library. BY4741 is a wild type strain while *slc1*Δ and *scs7*Δ are deletion mutants for genes encoding a putative acyltransferase (*SLC1*) and sphingolipid alpha-hydroxylase (*SCS7*), respectively. Cells were kept on YPD plates and single colonies were cultured overnight in YPD medium (1% yeast extract, 2% Bacto-peptone and 2% glucose (Difco Laboratories, USA). The cells were then diluted into fresh medium to an optical density (OD) at 600nm (OD600) of 0.075 and grown to an OD600 of ~ 0.65 – 0.85. All steps were carried out at 30°C in a rotary shaker.

Table 3.1 List of *S. cerevisiae* strains used in this study

Strain	Genotype	Source
BY4741 (wild type, WT)	MATa; his3Δ1; leu2Δ0; met15Δ0; ura3Δ0	EUROSCARF
*scs7*Δ	BY4741; Mata; his3Δ1; leu2Δ0; met15Δ0; ura3Δ0; YMR272c::kanMX4	EUROSCARF
*slc1*Δ	BY4741; Mata; his3Δ1; leu2Δ0; met15Δ0; ura3Δ0; YDL052c::kanMX4	EUROSCARF

3.2.2 Lipid standards

Synthetic lipids with fatty acyl compositions that are naturally low abundant in *S. cerevisiae* were used as internal standards. Phosphatidic acid with a C17 chain (di17:0-GPA), C19-ceramide (C19-CER), C8 glucosylceramide (C8-GC) and liver glycerophosphoinositol (GPIns) were obtained from Avanti Polar Lipids (Alabaster, AL). The internal standards were solubilised in chloroform at a stock concentration of 10μg/μL.

3.2.3 Lipid extraction

25 OD600 equivalents of yeast cells were harvested by centrifugation at 4000rpm for 5 minutes and washed twice with deionised water. Lipids were extracted by a method described by Angus and Lester, with slight modifications (Angus and Lester, 1972). Briefly, cells were resuspended in 2mL of 95% ethanol-water-diethyl ether-pyridine-ammonium hydroxide (15:15:5:1:0.018, v/v/v/v/v). 0.1μg of C19-Cer, 0.05μg of C8-GC and 0.25μg di17:0-GPA were added as internal standards. Cells were broken by glass beads vortexing (two times for one minute each) and incubated for 20 minutes at 60°C. Debris was pelleted by centrifugation and the supernatant was transferred to a fresh tube. The pellet was re-extracted once more using the same procedure. The pooled supernatants were divided into three aliquots and dried under a stream of nitrogen. One aliquot was used for total lipid analysis (mainly glycerophospholipids) and the others for sphingolipid analysis (see also Fig. 3.1).

For total lipid extraction, the dried lipid film was desalted by butanol extraction. Briefly, the lipid film was resuspended in 200μL of water-saturated butanol. 100uL of water was added and the mixture was vortexed for one minute, followed by centrifugation at 14 000rpm for two minutes to induce phase separation. The top butanol fraction was collected and the bottom aqueous phase was re-extracted with 200μL of water-saturated butanol. The two butanol fractions were pooled and dried under a stream of nitrogen and this extract constitutes the ‘total lipid extract’.

A fraction enriched in sphingolipids was obtained by mild alkaline hydrolysis which degrades ester linkages found in many glycerophospholipids (Brockerhoff, 1963). To achieve this, the dried lipid films from the ethanol-water-diethyl ether-pyridine-ammonium hydroxide extract were resuspended in 400μL of chloroform-methanol-water (16:16:5, v/v/v). Glycerophospholipids were deacylated by 400μL of 0.2N sodium hydroxide (NaOH) and incubation at 30°C for 45 minutes. 400μL of 0.5M EDTA was added and the samples were neutralized with 1N acetic acid. 400μL of chloroform was added and the mixture was vortexed for one minute, followed by centrifugation at 9000rpm for two minutes at 4°C. The lower organic phase was collected and dried under nitrogen.

3.2.4 Lipid analysis by ESI-MS, MS/MS and MS^3

ESI-MS was performed using a Waters Micromass Q-Tof micro (Waters Corp., Milford, MA) mass spectrometer. Lipid extracts were reconstituted in 2mL of chloroform-methanol (1:1, v/v). Typically, 2μL of sample was injected for mass spectrometry analysis. The capillary voltage and sample cone voltage were maintained at 3.0 kV and 50 V respectively. The source temperature was 80°C and the nano-flow gas pressure was 0.7 bar. The mass spectrum was acquired from m/z 400 – 1400 in the negative ion mode with an acquisition time of three minutes, and the scan duration was 1s. The inlet system, consisting of a Waters CapLC Autosampler and a Waters CapLC Pump, was used to provide the mobile phase and to inject samples. Chloroform-methanol (1:1, v/v) at a flow rate of 15μL/min was used as the mobile phase. Individual molecular

species were identified using tandem mass spectrometry and in general, the collision energy used ranged from 25 – 80 eV (see also Fig. 3.5).

Tandem mass spectrometry for characterisation, identification as well as quantification of lipid molecular species was performed using MS^3, precursor ion (PREIS) and neutral loss (NL) scanning and multiple-reaction monitoring (MRM) respectively with an Applied Biosystems 4000 Q-Trap mass spectrometer (Applied Biosystems, Foster City, CA) (see Section 2.2.6 and also Fig. 3.1 and 3.5). Samples were directly infused using a Harvard syringe pump at a flow rate of 10μL/min. Each individual ion dissociation pathway for the various scan modes was optimised with regard to collision energy to minimize variations in relative ion abundance due to differences in rates of dissociation. In MS^3, the fragment ions themselves obtained from MS/MS are subjected to further fragmentation steps. The additional fragmentation provides more information about the molecular structure of the precursor ion, which is a powerful method for identification of complex molecule. The relative concentration of each lipid species was selectively measured by MRM and calculated by normalizing (dividing) its intensity to the intensity of the relevant internal standards.

3.2.5 Data analysis

Data was acquired using MassLynx 4.0 (Waters Corp., Milford, MA). The plain text files obtained from MassLynx were loaded into Matlab (The MathWorks Inc., Natick, MA) for processing (Guan *et al.*, 2006) (See Chapter 2). Briefly, correlation optimised warping (COW) (Nielsen *et al.*, 1998) was used as a pre-processing method in

order to obtain precise alignment of normalized MS spectra from replicate samples. Individual spectrum was normalized using total ion counts. For averaging of spectra from replicate independent samples the normalized data of each replicate was warped against a reference set. After aligning the peaks, the intensity values of individual m/z were then averaged to obtain one mean spectra representative of the replicates. To compare between different experimental conditions, the mean spectrum for one experimental condition (e.g. mutant) was warped against the mean spectrum for the control condition (wild type). After alignment, relative difference in the lipid compositions of the mixture can be computed by calculating the logarithm (log10) of the ratio of ion intensities relative to control samples and is represented as a 'differential profile'.

3.2.6 Statistical analysis

Comparison of the wild type and mutant strains was performed using the mean of at least 4 independent samples ± standard error of the mean (SEM) from individual samples. Statistical significance between wild type and mutant yeast strains was determined using Student's t-test.

3.3 Results

The main classes of lipids in *S. cerevisiae*, like in most other eukaryotic cells, are glycerophospholipids, sphingolipids, sterols and glycerolipids (such as diacylglycerols and triacylglycerols), with the polar lipids comprising of approximately 40% of total lipids and neutral lipids 60%, respectively (Blagovic *et al.*, 2001). The goal of this study was to establish a simple and rapid method which allows profiling of total polar lipids, containing mainly glycerophospholipids and sphingolipids, and with a focus on

sphingolipids (Fig. 3.1). In order to validate the approach, mutant strains which have previously been implicated with aberrant (sphingo)lipid metabolism were obtained from EUROSCARF, a public collection of non-essential gene deletion mutants.

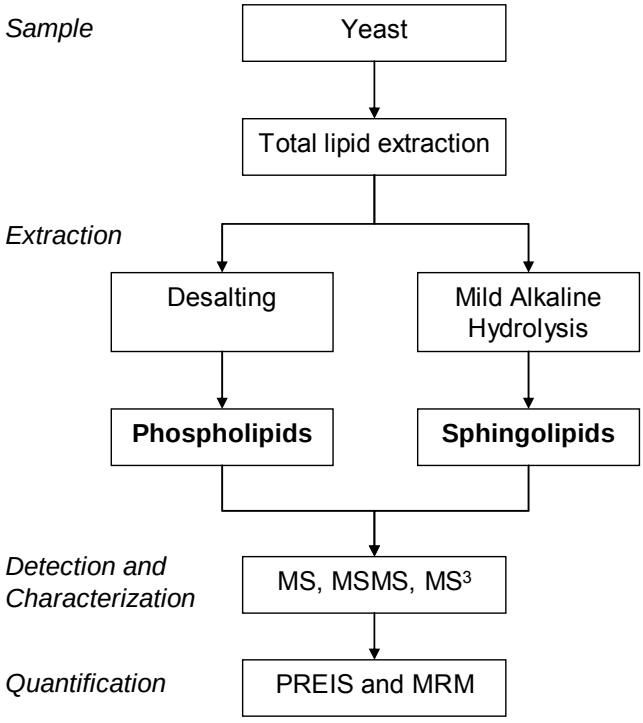

Figure 3.1 Workflow of method.
A cell pellet from 25OD units of yeast is extracted using ethanol-water-diethyl ether-pyridine-ammonium hydroxide ('total lipid extract'). This fraction contains both glycerophospholipids and sphingolipids. The fraction is then split and processed for analysis of major glycerophospholipid (which includes a 'desalting' step) and sphingolipids (which resist 'mild alkaline hydrolysis'). Single stage mass spectrometry (MS) is used to profile the extracts in a non-targeted fashion. Tandem mass spectrometry (MSMS) and MS^3 is employed to further characterise (MSMS, MS^3) and quantify lipids of interest (precursor ion scanning, PREIS and multiple-reaction monitoring, MRM).

3.3.1 Theoretical calculation of the masses of yeast glycerophospholipids and sphingolipid molecular species

Similar to peptides, lipids can be identified through database match based on the mass-to-charge ratio (m/z). Several initiatives, including LIPID MAPS, have embarked on creating databases for lipids, their structures and even fragmentation patterns (Table

1.3). However, these databases were not available at the dawn of lipidomics, and their development is only making advance progress in recent years. Furthermore, the comprehensiveness of such databases is limited to the interest of the research group. For instance, the table of molecular and product ions published by Murphy is restricted to phospholipids (i.e. glycerophospholipids and sphingomyelins) (Murphy, 2002), and these molecular species are well-suited for analysis of samples derived from mammalian tissues or cells but clearly, the lipid inventory varies between organisms. Therefore, a simple database containing theoretical calculations of the m/z of yeast glycerophospholipids and sphingolipids is presented in this work, which will serve as a reference database for annotation of lipid metabolites detected by ESI-MS.

Basically, the building block of a glycerophospholipid molecule comprises of a headgroup, hydrophobic tails (acyl, alkenyl or alkyl), and a glycerol backbone (Fig. 1.1). Sphingolipids, on the other hand, comprise of a sphingoid base, a fatty acyl chain and a headgroup (Fig. 1.1). For these relatively 'simple' and structurally defined lipids, the theoretical mass of each molecular species can be calculated based on the elemental composition and a library of lipids and their corresponding m/z can be built (Supplementary material 3.1). However, with isobaric complications, the assignment of ions of interest based solely on m/z will inevitably lead to a few possibilities and this requires further experimental validation, and confirmation.

3.3.2 Rapid isolation and profiling of polar lipids from *Saccharomyces cerevisiae*

Water-rich, slightly alkaline solvents appear to be more efficient in isolating inositol-containing lipids from *S. cerevisiae* (Angus and Lester, 1972). Figure 3.2A

shows a typical profile of a total lipid extract obtained from a wild type yeast strain (Table 3.1). The most prominent ions represent major glycerophospholipid species which ionize efficiently in negative mode. The major fatty acyls in yeast are C16 and C18 with none, one or two double bonds. Yeast, unlike mammalian cells, does not synthesize polyunsaturated fatty acids (Schneiter *et al.*, 1999;Blagovic *et al.*, 2005). The most prominent inositolphosphorylceramide (IPC) yields a weak signal at m/z 952 under these conditions (Fig. 3.2A, asterisk).

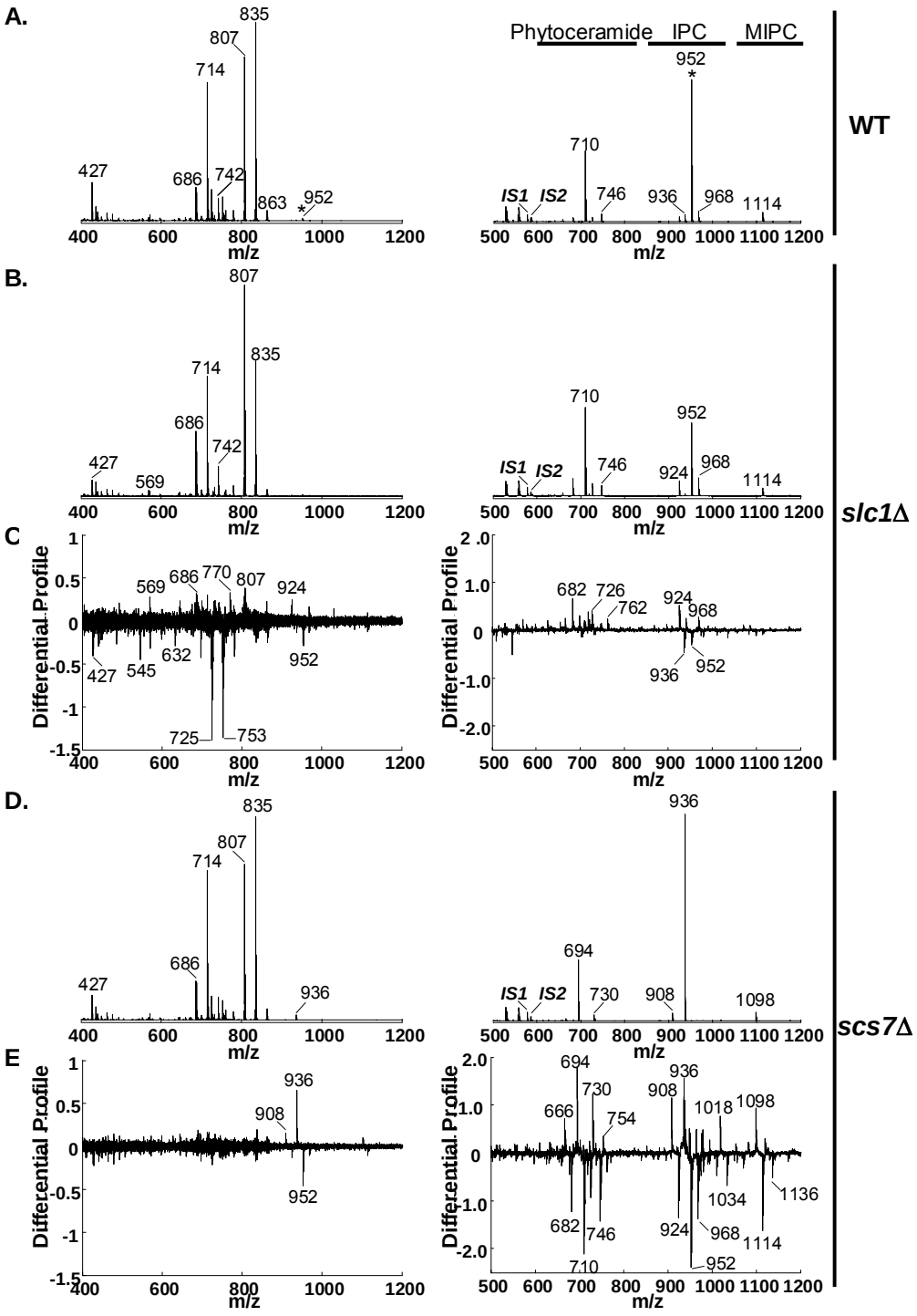
A.
B.
C
D.
E
Phytoceramide
IPC
MIPC
WT
slc1Δ
scs7Δ
IS1
IS2
m/z
Differential Profile

Figure 3.2 (Differential) Profiling of glycerophospholipids and sphingolipids of yeast mutants
Typical glycerophospholipid (left panels) and sphingolipid profiles (right panels) of wild type (WT) yeast (A), and deletion mutants of the *slc1* (B & C) and *scs7* (D & E) genes. Mass spectra from at least 4 independent samples were averaged for each condition (n=4). Differential lipid profile, which are ratios of single stage mass spectrometry scans plotted as log10 ratios, are used to compare differences in glycerophospholipid and sphingolipid composition between *slc1*Δ and WT (C) and *scs7*Δ and WT (E). Note that this approach does not require knowledge of the underlying lipid species for a given ion of interest. Instead, it serves as an 'unbiased' screening tool for discovery of lipids which are present in different amounts between two conditions. Deletion of *slc1*, which encodes a putative acyl transferase, leads to pronounced differences in glycerophospholipid profiles (C, left panel) while sphingolipids are less affected when compared to WT (C, right panel). The opposite is the case for deletion of *scs7*, which encodes a ceramide hydroxylase. *scs7*Δ displays striking differences in the sphingolipids (E, right panel) with only minor alterations in glycerophospholipids (E, left panel).

To improve detection of (other) sphingolipid molecular species, the total lipid extract was subjected to mild alkaline hydrolysis. This treatment hydrolyzes acyl bonds (and hence the majority of glycerophospholipids) but leaves amide linkages largely intact. It has in the past been successfully used for measurement of sphingolipids in mammalian cells and tissues (Merrill, Jr. *et al.*, 2005). Figure 3.2A shows a high resolution Q-ToF scan of such a sphingolipid enriched fraction (right panel).

The profiling of complex lipid mixtures in such a fashion, i.e. using single stage mass spectrometry, serves as a powerful initial screen when different conditions or strains are to be compared.

3.3.3 Pilot screen of yeast mutants deficient in known lipid biosynthetic pathway

The lipids of yeast mutants deficient in known lipid biosynthetic pathway were analysed using the non-targeted differential profiling described in Chapter 2. In addition, major yeast sphingolipids were characterized and MS conditions were optimised for their relative quantification. The rationale behind the use of knockout of lipid metabolic enzymes as a proof of concept is two-prong – 1) changes can be anticipated and 2) these

knockouts will accumulate various metabolic intermediates that normally occur in low abundance, which will be used for precise characterisation, overcoming the problem of a lack of pure lipid standards, particularly for the yeast inositol sphingolipids.

3.3.3.1 Non-targeted profiling and characterization of glycerophospholipids and sphingolipids of slc1Δ by ESI-MS, MS/MS and MS^3

Figure 3.2B and 3.2D show profiles from *slc1* and *scs7* deletion strains (Table 3.1). *SLC1* encodes for a putative acyltransferase which has been implicated in the synthesis of phosphatidic acid from lysophosphatidic acid (Dickson *et al.*, 1990;Athenstaedt and Daum, 1997). It was originally discovered in a screen for bypass mutants that regain the ability to grow in the absence of sphingolipid biosynthesis. Indeed, *slc1-1* is a suppressor of *lcb1*, which catalyzes the committed step of sphingolipid biosynthesis. These original experiments, due to the setup of the genetic screens, were mainly carried out in the absence of long chain bases (LCB) in the growth medium. Under these conditions, *slc1-1* leads to the generation of unusual inositol containing glycerophosphospholipids (Lester *et al.*, 1993).

It is demonstrated that under permissive growth conditions, i.e. complete medium rather than media devoid of LCB, the glycerophospholipids resemble largely those found in the wild type strain (Fig. 3.2B, left panel). A differential profile which displays differences in ion response between the *slc1*Δ and wild type conditions is shown in Figure 3.2C (left panel). The major differences lie in ions at m/z 725 and 753, which, based on the mass, can tentatively be assigned to glycerophosphoinositols (GPIns) with a total fatty acyl carbon number of 26 and 0 double bonds (26:0-GPIns) as well as 28:0-

GPIns, i.e. GPIns species with unusually short and saturated fatty acyls. Indeed, a precursor scan for m/z 241, which is an indicator fragment of inositol-containing lipids, reveals a GPIns profile which is devoid of these short chain species (Fig. 3.3). Interestingly, such short chain GPIns have previously been shown to be enriched at the plasma membrane (Schneiter *et al.*, 1999).

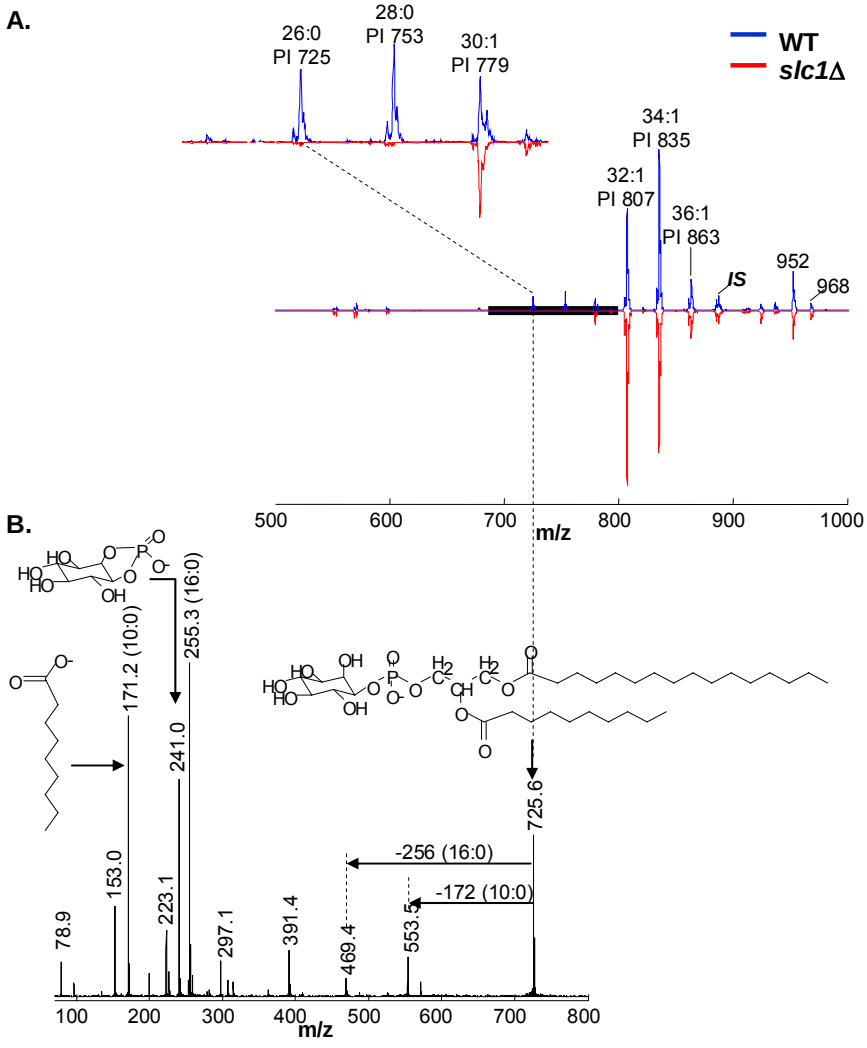

Figure 3.3 Molecular species of glycerophosphoinositol (GPIns) in *slc1*Δ.
(A) Precursor ion scans of m/z 241 (the mass of dehydrated inositol phosphate, see also panel B) were used to selectively measure GPIns species in *slc1*Δ (red downward profiles) and wild type (WT, blue upward profiles). Liver GPIns was spiked into the extracts prior to extraction and used as an internal standard (IS) for quantification. Note the almost complete absence of very short chain GPIns (26:0 GPIns & 28:0 GPIns) in the mutant strains (inset) which is highly selective. GPIns with a total carbon number of 30 and more are present in comparable amounts between *slc1*Δ and WT. (B) Tandem mass spectrometry and collision-induced dissociation (CID) of m/z 725. Based on theoretical calculation of glycerophospholipid and sphingolipid molecular species (see Supplementary material 3.1) this ion can tentatively be assigned to 26:0 GPIns. This is supported by analysis of the fragment ions which have m/z characteristic of an inositol (m/z 241) containing glycerophospholipid (m/z 153) with C10:0 (m/z 171) and C16:0 (m/z 255) as major fatty acyl chains.

The sphingolipids of *slc1*Δ using the alkali-treated fraction were analyzed next. Major ions correspond in m/z to those of the WT, albeit at altered levels. Ions at m/z 682, 924, 936 and 952 correspond to t18:0/24:0 phytoceramide-C, t18:0/24:0 IPC-C, t18:0/26:0 IPC-B and t18:0/26:0 IPC-C, respectively (Figure 3.5 and Supplementary material 3.1). It should be noted that sphingolipids enter the gas phase efficiently in both negative and positive ionisation mode. Tandem mass spectrometry and collision-induced dissociation were used to further characterise and identify changes of interest (Figure 3.4 and data not shown). The mannosyl inositolphosphorylceramides (MIPCs) in yeast are lipids with considerable structural complexity. Figure 3.4A shows the product ion spectra of a positive ion of m/z 1116 in positive mode (equivalent to m/z 1114 in negative ion). Two major fragments were observed with m/z 954 and 694. The daughter ion with m/z 954 corresponds to the m/z of 26:0 inositol phosphoryl ceramide (IPC-C). Furthermore, it is equivalent to a loss of 162 mass units from the parent ion, suggesting a loss of a sugar group from MIPC-C. Tandem mass spectrometry of ceramides, and glycosylated derivatives, yield fragments which have to be further characterised for unambiguous identification. Hyphenated MS is a powerful tool for such analysis and figure 3.4B shows MS/MS/MS (MS^3) of the most prominent product ion, m/z 694, derived from collision-

induced dissociation of ion of m/z 1116. MS^3 of m/z 694 forms dehydration products of phytoceramide as well as (dehydration products) of the t18:0 sphingoid bases thus supporting m/z 1116 to originate from a C26 MIPC-C with a t18:0 sphingoid base (Figure 3.5 and Supplementary material 3.1). In conclusion, these results indicate that disruption of the *SLC1* gene leads to moderate (yet highly specific) changes in molecular species in glycerophospholipids as well as sphingolipids, most notably complete elimination of very short chain GPIns and a concomitant increase in short chain sphingolipids, phytoceramide and IPC.

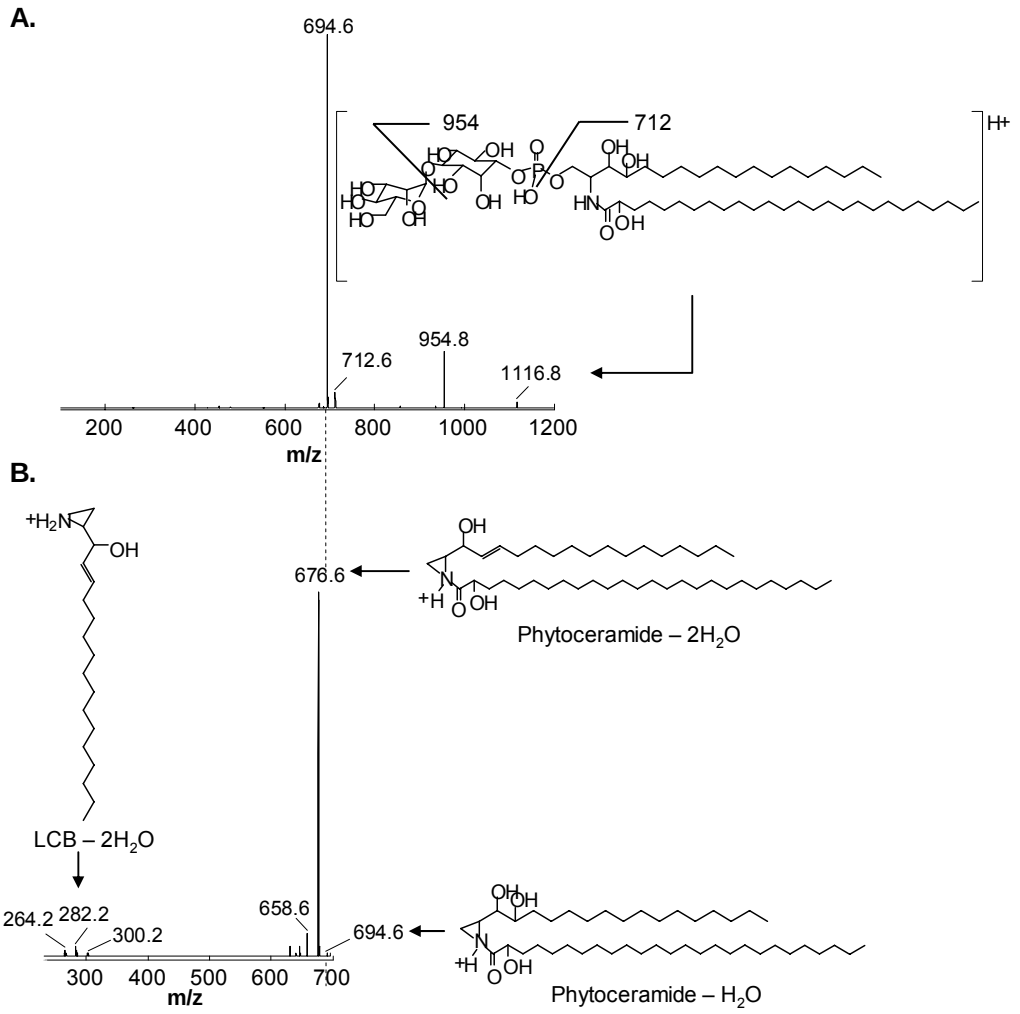

Figure 3.4 Biochemical characterisation of a complex sphingolipid using MSMS and MS^3.
The ion with m/z 1116.8 can be tentatively assigned (based on the mass) to mannosyl inositol-phosphorylceramide (MIPC) of the C-series (t18:0/26:0, see also Figure 3.5 and Supplementary material 3.1). Tandem mass spectrometry (positive mode) of m/z 1116.8 yields a dominant ion at m/z 694.6, the expected mass for the dehydrated phytoceramide backbone of t18:0/26:0 MIPC (A). This is supported experimentally by subsequent MS analysis using MS^3 (on a linear ion trap) of m/z 694.6 (B) which produces the doubly dehydrated phytoceramide (m/z 676.6) and fragments corresponding to the long chain base (LCB) of the ceramides (e.g. m/z 282.2).

3.3.3.2 Non-targeted profiling of glycerophospholipids and sphingolipids of scs7Δ

In contrast, the total lipid profiles of the deletion mutant in the *SCS7* gene displays glycerophospholipids which in their levels are almost identical to wild type conditions (Fig. 3.2D & E, left panels). Ions at m/z 936 and 952, which are shown in the differential profile, stem from abundant sphingolipid species (see also Fig. 3.2D & E,

right panels). *SCS7* encodes for sphingolipid alpha hydroxylase, an enzyme involved in the generation of monohydroxylated inositol ceramides (Dunn *et al.*, 1998;Haak *et al.*, 1997). In case *SCS7* contributes in a major way to sphingolipid hydroxylation one would expect dramatic differences in sphingolipid species. This is indeed revealed experimentally. The levels of hydroxylated ceramides and mannosylated ceramides are drastically reduced in the mutant (Fig. 3.2D & E, right panels). This is mirrored with almost identical concomitant increases in the 'B' series for ceramide species, i.e. those ceramides which do not carry a hydroxyl group on the fatty-acyl chain (Fig. 3.5 & 3.6D).

The above results demonstrate the power of comparative single stage analysis of complex lipid mixtures. The mass of glycerophospholipids and sphingolipids, including their mannosylated derivatives, is calculated based on chemical composition (Section 3.3.1; Supplementary material 3.1) (Wenk and De Camilli, 2005;Marsh, 1990), leading to a large array of theoretical lipid species, of which 5-10% are found in typical yeast extracts. Such a combined experimental and theoretical approach is an excellent tool for discovery of unexpected changes in lipid levels and lipid species. It also sets the ground for subsequent targeted quantification of lipids of interest.

3.3.4 Targeted quantification of yeast sphingolipids by multiple-reaction monitoring

Multiple-reaction monitoring (MRM) is a highly selective and sensitive (though biased) way for quantification of small molecules in complex mixtures. It requires information of specific fragments as well as pertinent internal standards. The method is based on monitoring of specific parent ion/fragment ion pairs which are filtered in the

two quadrupoles of a tandem mass spectrometer. Based on the tandem MS profiles of all major yeast sphingolipids in the positive ion mode, the phytoceramides and the inositol sphingolipids share a common fragment derived from the sphingoid base. Precursor ion or neutral loss scans of sphingoid base fragments were used to obtain information on yeast sphingolipid compositions. Based on this information, a comprehensive list of MRM transitions (parent → sphingoid base fragment transitions) was set up to follow sphingolipid compositions. The signal intensity of each MRM value was normalized to the intensity of the C19 ceramide internal standard, which was spiked according to the starting amount of material, and therefore normalized value represents the relative quantity of each lipid species (note absolute quantity could not be obtained due to a lack of pertinent standards for yeast sphingolipids). Figure 3.5 contains the MRM pairs of yeast sphingolipids which are covered in this study.

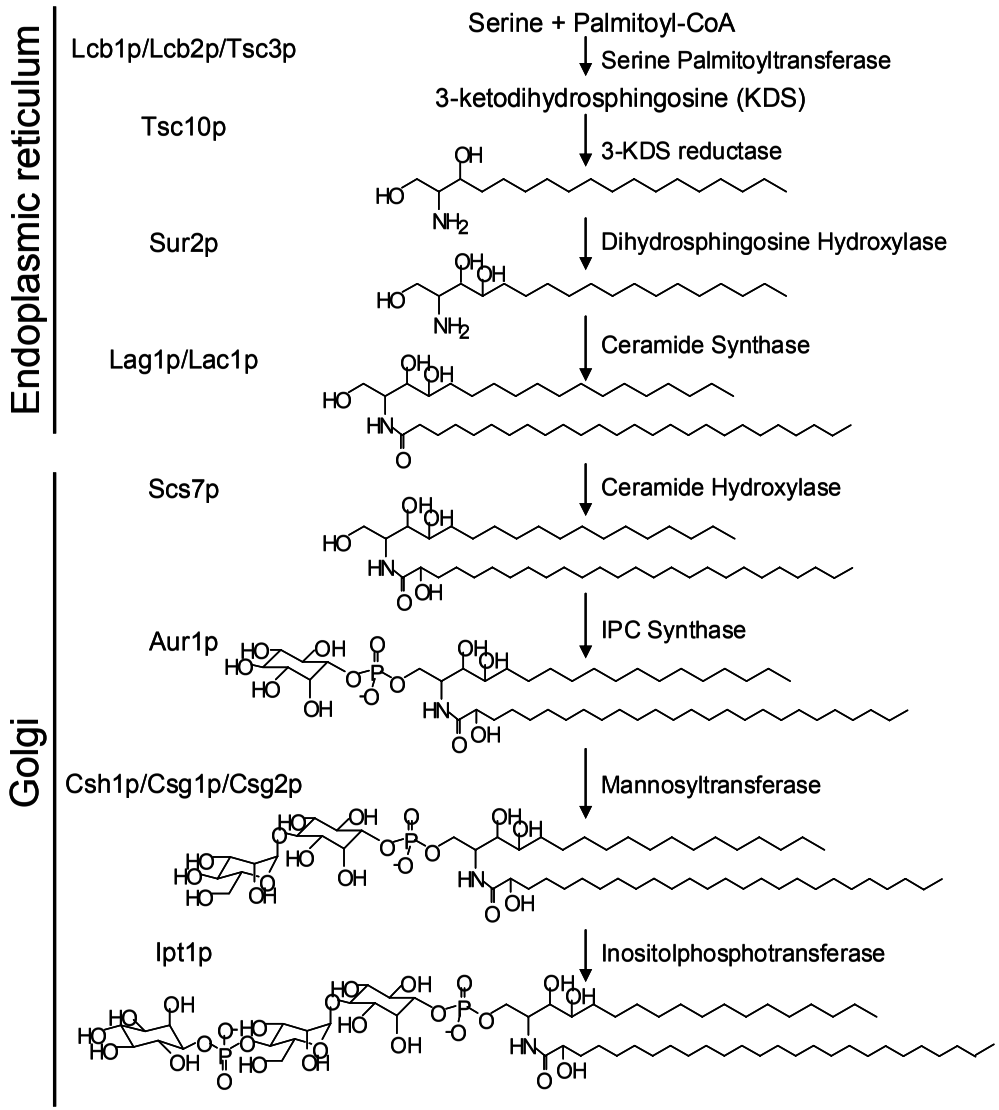

Species	Precursor/ product ion m/z	DP (eV)	CE (eV)
Sphingoid Base			
Dihydrosphingosine			
d18:0	302.2/284.2	70	20
d20:0	330.2/312.3	80	20
Phytosphingosine			
t18:0	318.3/282.3	60	25
t20:0	346.3/310.3	100	25
Phytoceramide (Sphingoid base/Fatty acid-Type)			
d18:0/18:0-A	568.6/284.3	60	40
t18:0/18:0-B	584.6/282.3	80	40
t18:0/24:0-C	684.7/282.3	80	45
t18:0/26:0-B	696.7/282.3	80	45
t18:0/26:0-C	712.7/282.3	80	45
t18:0/26:0-D	728.7/282.3	80	50
t20:0/26:0-B	724.7/310.3	100	45
t20:0/26:0-C	740.8/310.3	100	45
t20:0/26:0-D	756.8/310.3	100	50
Inositol Phosphorylceramide (IPC)			
t18:0/24:0-C	926.7/282.3	80	60
t18:0/26:0-B	938.7/282.3	80	65
t18:0/26:0-C	954.7/282.3	100	65
t18:0/26:0-D	970.7/282.3	100	70
t20:0/26:0-B	966.8/310.3	80	70
t20:0/26:0-C	982.8/310.3	80	70
Mannosyl Inositol Phosphorylceramide (MIPC)			
t18:0/26:0-B	1100.8/282.3	100	75
t18:0/26:0-C	1116.8/282.3	100	80
t20:0/26:0-B	1128.8/310.3	100	80
t20:0/26:0-C	1144.8/310.3	100	80
t20:0/26:0-D	1160.8/310.3	100	80
Mannosyl Diinositol Phosphorylceramide (M(IP)2C)			
t18:0/26:0-B	670.2/241.0	-180	-75
t18:0/26:0-C	678.2/241.0	-180	-75
Internal Standard			
d18:1/19:0 Ceramide	580.6/282.3	45	35
d18:1/8:0 Glucosylceramide	588.6/282.3	45	45

Figure 3.5 Sphingolipid pathway of *S. cerevisiae* and molecular species of lipids covered in this study. The table summarizes the precursor/product pairs, declustering potential (DP) and collision energies (CE) used for multiple-reaction monitoring (MRM) quantification of yeast sphingolipids. Results obtained using this method for two yeast mutants, *slc1*Δ and *scs7*Δ are shown in Figure 3.6.

Multiple-reaction monitoring (MRM) was employed quantify changes in sphingolipids in *slc1*Δ and *scs7*Δ (Fig. 3.6). Although the detection and characterisation of M(IP)2C is reported, its quantification is excluded due to the presence of both a singly and doubly charged ions under the experimental condition used (Guan and Wenk, 2008). In addition, lipid standards with similar chemistry of the analytes are required for absolute quantification. However, there is currently no such standards available for inositol sphingolipids. In this study, a synthetic C19 ceramide standard was used as the reference standard for relative quantification of all sphingolipids measured. Nevertheless, note the generally good agreement between this full quantitative analysis and the semi-quantitative pre-screening shown in Figure 3.2.

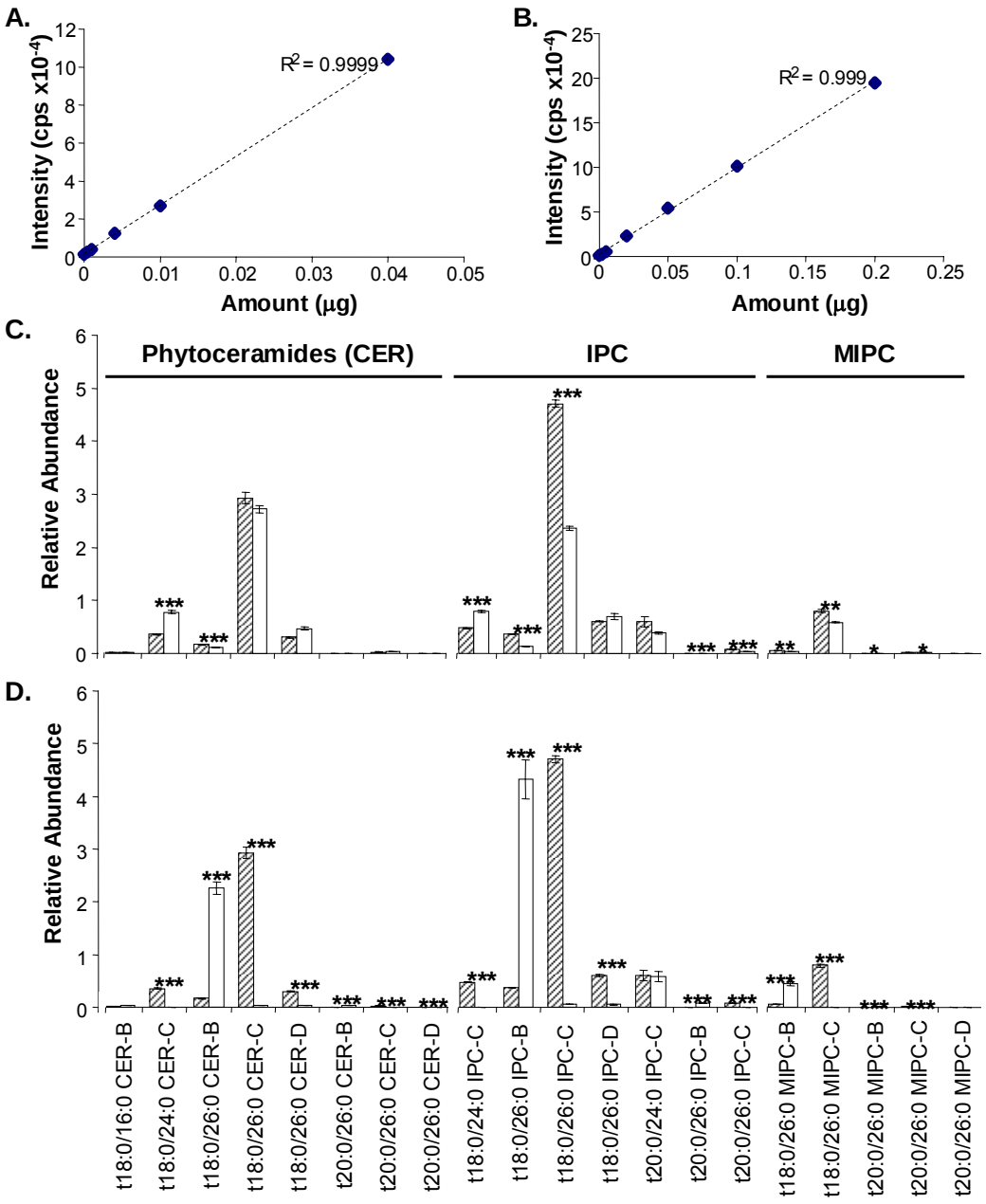

Figure 3.6 Sphingolipid levels *slc1*Δ and *scs7*Δ relative to a wild type strain using MRM quantification.

(A) and (B) show the ion response (in MRM quantification mode, see also Figure 3.5) for increasing amounts of t18:0 phytosphingosine and t18:0/18:0 phytoceramide standards, respectively. Comparison of sphingolipid molecular species in wild type (hatched bars), *slc1*Δ (C, open bars) and *scs7*Δ (D, open bars). Data are presented as means ± SEM of four independent experiments. Statistical significance between wild type and mutant strains was determined using Student's t-test. * $p<0.01$, ** $p<0.005$, *** $p<0.001$.

3.4 Discussion

In this Chapter, I described a novel mass spectrometry-based approach for screening of lipid metabolites in the yeast *S. cerevisia*e, with a focus on glycerophospholipids and sphingolipids. Using a rather simple extraction protocol it is possible to obtain semi-quantitative information of overall changes in lipid levels (Fig. 3.2) as well as fully quantitative levels of a large number of lipids in the sphingolipid pathway, including mannosylated inositol ceramides (Fig. 3.6). While full automation is difficult to achieve for liquid/liquid extraction, it is now feasible to analyse ~100 strains per day of mass spectrometry time. Extraction of yeast cells typically requires 6 hours including incubation and drying steps. It thus will be possible to screen libraries of mutant yeast strains for discovery of mutants with defects in certain aspects of glycerophospholipid and sphingolipid metabolism.

A major advantage of this method is that it is does not require metabolic labelling (e.g. use of radioactive precursors), and sample preparation and cleanup is minimal. The method is robust and directly measures mass levels of these lipids. It can thus be used as a discovery tool in many applications ranging from experiments which address basic molecular mechanisms of membrane traffic (Odorizzi *et al.*, 2000;Simonsen *et al.*, 2001;Huijbregts *et al.*, 2000), to screening of (chemo)genetic libraries (Zewail *et al.*, 2003). In fact, a major motivation for the establishment of conditions which allow parallel determination of glycerophospholipids and sphingolipids in yeast is the aim to screen existing libraries, such as the EUROSCARF collection of (non-essential) deletion strains. It can be anticipated that careful examination of glycerophospholipid and sphingolipid profiles of yeast strains involved in sphingolipid biosynthesis (and

metabolism) will yield new insights into the crosstalk between these two classes of lipids. Indeed, there is a growing body of evidence which suggests that sphingolipid and glycerophosphoinositol lipid metabolism are functionally interconnected (Huijbregts *et al.*, 2000;Kearns *et al.*, 1998;Lester *et al.*, 1993;Dickson *et al.*, 1990;Nagiec *et al.*, 2003). *slc1-1*, in absence of LCB, produces inositol-containing glycerophospholipids which can rescue the growth phenotype otherwise observed (Lester *et al.*, 1993).

An important 'by-product' of the results presented here is a better understanding of possibly non-essential lipids that are able to support growth despite alterations in their levels. The *scs7*Δ deletion strain for example is able to grow (in YPD) yet displays alterations is both glycerophospholipid and sphingolipid levels which range up to two fold. Indeed, deletion of *SCS7* almost completely abolishes the 'C series' of inositol ceramides (Fig. 3.6D). Overlay of genetic libraries with pharmacological treatments offers enormous potential for identification of pathways which are required for a functional condition, such as sensitivity to wortmannin (Zewail *et al.*, 2003), calcium (Ohya *et al.*, 1986), heat shock (Ferguson-Yankey *et al.*, 2002;Jenkins *et al.*, 1997) or control of cell growth (Kunz *et al.*, 1993). It will be interesting for example to use this method to analyse the precise lipid inventory of the strains used in this study when grown under calcium stress and in the absence of LCB precursors, rather than growth under fully permissive conditions (Dunn *et al.*, 1998). This could lead to the discovery of lipid entities which are closely correlated with the calcium phenotype and which would yield important molecular information of mechanisms of action.

Glycerophospholipids and sphingolipids are two major classes of membrane lipids found in yeast. In the future, it will be important to include sterol and non-polar lipids, such as diacylglycerols and triacylglycerols, in screens such as the one presented here. However, this will likely require different modes of ionisation (such as atmospheric chemical pressure ionisation) as well as additional extraction procedures as these lipids are much more non-polar than glycerophospholipids and sphingolipids.

Chapter 4. A Combined Genetics and Biochemical Approach to Explore the Functional Interactions between Sphingolipids and Sterols in Biological Membranes[3]

[3] The work described in this Chapter is presented in the following manuscript :
Guan XL, Souza CM, Pichler H, Dewhurst G, Schaad O, Kajiwara K, Wakabayashi H, Ivanova T, Castillon GA, Piccolis M, Abe F, Loewith R, Funato K, Wenk MR and Riezman H. Functional interactions between sphingolipids and sterols regulating cell physiology. **Mol. Biol. Cell.** 20(7):2083-95.

4.1 Introduction

Sterols are major plasma membrane components of most eukaryotic membranes, although their precise structure differs between the kingdoms; animals contain cholesterol, plants have sitosterol, campesterol and stigmasterol, whereas fungi use mainly ergosterol. The plant and yeast sterols both differ from cholesterol in their side chain and yeast sterols also have an extra double bond in the B ring. As sterols appear only in eukaryotes, it is likely that they confer properties to membranes or provide functions that may not be required in prokaryotes and possibly not even in all eukaryotes (Matyash *et al.*, 2004). Cholesterol has been shown to modulate membrane thickness in artificial membranes and this property has been proposed to play a role in membrane protein localisation *in vivo* (Bretscher and Munro, 1993) although an alternative explanation for the control of membrane thickness has been postulated (Mitra *et al.*, 2004). Recently it has been shown that proteins and lipids do not freely diffuse over the entire surface of the cell and it has been proposed that eukaryotic plasma membranes contain micro/nanodomains (for review see (Jacobson *et al.*, 2007;Kusumi *et al.*, 2005;Simons and Ikonen, 1997), commonly called rafts, that act as platforms creating membrane heterogeneities with many proposed functions. There are two basic tenets of the raft hypothesis; one that sterols and sphingolipids interact specifically in biological membranes and second, that their interaction causes an increase in membrane order that affects protein function, diffusion, and/or localisation.

There is clear biophysical evidence that sterols and sphingolipids can segregate from other lipids in simple artificial membrane systems to form liquid ordered domains (Ahmed *et al.*, 1997). Sterol partitioning experiments between membranes *in vitro* also

suggest that they have affinity for membranes with a high content of sphingolipids (Wattenberg and Silbert, 1983). Sterols have been shown to have a condensing affect on artificial membranes (Radhakrishnan and McConnell, 2005) and sterol sphingomyelin condensed complexes have been characterised (Radhakrishnan *et al.*, 2001). Some evidence exists in yeast suggesting a genetic interaction between mutants in sterol and sphingolipid biosynthesis (Baudry *et al.*, 2001;Eisenkolb *et al.*, 2002;Jin *et al.*, 2008), however, little, if any, convincing evidence exists to show that these two lipid species function together in complex biological membranes. Sterols and sphingolipids are concomitantly affected in certain diseases. In Niemann Pick disease, although the primary defect is not yet completely certain, defects in sphingolipid and cholesterol trafficking seemed to be interdependent (Pagano *et al.*, 2000;Puri *et al.*, 1999;Vance, 2006). One of the proposed functions of amyloid beta and presenilin is in control of sphingomyelin and cholesterol amounts in the brain (Grimm *et al.*, 2005), which could affect the ontology of Alzheimer's disease. Sphingolipid depletion has also been shown to influence the sterol response element binding protein (SREBP) pathway, controlling cholesterol and lipid biosynthesis (Scheek *et al.*, 1997).

In Chapter 3, a mass spectrometry-based approach to profile lipids from minimally processed organic extracts of *S. cerevisiae* was described. In this study, I extend the application of the methodology, in combination with genetics to study yeast mutants in sterol biosynthesis. This systematic analysis provides evidence that yeast cells have a mechanism to respond to the presence of specific sterol structures in their membranes and adjust their sphingolipid composition accordingly. The genetic analysis

provides convincing evidence that sterols and sphingolipids function together in cells to carry out multiple functions. Furthermore, the results suggest that sterol and sphingolipid structures have co-evolved to provide optimal interaction properties between the two lipid species.

4.2 Materials and Methods

4.2.1 Strain construction

All mutants used in this study were obtained from Howard Riezman (University of Geneva, Switzerland), which were created using standard gene disruption procedures, with complete removal of open reading frames, in their strain background. Double mutants were obtained by genetic crosses. Strains are listed in Table 4.1.

Table 4.1 List of *S. cerevisiae* strains used in this study.

Name	Genotype
RH448	MATa *his4 ura3 lys2 leu2 bar1*
RH5812	MATa *erg2::LEU2 his4 ura3 lys2 leu2 bar1*
RH4213	MATa *erg3::LEU2 his4 ura3 lys2 leu2 bar1*
RH4217	MATa *erg4::URA3 his4 ura3 lys2 leu2 bar1*
RH6969	MATa *erg4::ura3 his4 ura3 lys2 leu2 bar1*
RH6774	MATa *erg5::KanMx his4 ura3 lys2 leu2 bar1*
RH5684	MATa *erg6::KanMx his4 ura3 lys2 leu2 bar1*
RH5912	MATa *isc1::KanMx his4 ura3 lys2 leu2 bar1*
RH4348	MATa *sur2::LEU2 his4 ura3 leu2 bar1*
RH4524	MATa *scs7::LEU2 his4 ura3 leu2 bar1*
RH5913	MATa *erg2::LEU2 isc1 ::KanMx his4 ura3 lys2 leu2 bar1*
RH5935	MATa *erg3::LEU2 isc1 ::KanMx his4 ura3 lys2 leu2 bar1*
RH5916	MATa *erg4::LEU2 isc1 ::KanMx his4 ura3 lys2 leu2 bar1*
RH5917	MATa *erg5::LEU2 isc1 ::KanMx his4 ura3 lys2 leu2 bar1*
RH6787	MATa *erg6::LEU2 isc1 ::KanMx his4 ura3 lys2 leu2 bar1*
RH5818	MATa *erg3::LEU2 erg6::LEU2 isc1::KanMx his4 ura3 lys2 leu2 bar1*
RH6711	MATa *erg2::LEU2 sur2::LEU2 his4 ura3 lys2 leu2 bar1*
RH6749	MATa *erg3::LEU2 sur2::LEU2 his4 ura3 lys2 leu2 bar1*
RH6718	MATa *erg4::URA3 sur2::LEU2 his4 ura3 lys2 leu2 bar1*
RH6915	MATa *erg4::ura3 sur2::LEU2 his4 ura3 lys2 leu2 bar1*
RH6732	MATa *erg5 ::KanMx sur2::LEU2 his4 ura3 lys2 leu2 bar1*
RH6744	MATa *erg6 ::KanMx sur2::LEU2 his4 ura3 lys2 leu2 bar1*
RH6709	MATa *erg2 ::LEU2 scs7 ::LEU2 his4 ura3 leu2 bar1*
RH6741	MATa *erg3::LEU2 scs7::LEU2 his4 ura3 lys2 leu2 bar1*
RH6714	MATa *erg4::URA3 scs7::LEU2 his4 ura3 lys2 leu2 bar1*
RH6916	MATa *erg4::ura3 scs7::LEU2 his4 ura3 lys2 leu2 bar1*
RH6734	MATa *erg5::KanMx scs7::LEU2 his4 ura3 lys2 leu2 bar1*
RH6752	MATa *erg6::KanMx scs7::LEU2 his4 ura3 lys2 leu2 bar1*
RH5928	MATa *erg2::LEU2 erg3::LEU2 his4 ura3 lys2 leu2 bar1*
RH5864	MATa *erg2::LEU2 erg4::LEU2 his4 ura3 lys2 leu2 bar1*
RH5866	MATa *erg2::LEU2 erg5::LEU2 his4 ura3 lys2 leu2 bar1*
RH3616	MATa *erg2::URA3 erg6∆ura3 leu2 bar1*
RH5868	MATa *erg3::LEU2 erg4::LEU2 his4 ura3 lys2 leu2 bar1*
RH5871	MATa *erg3::LEU2 erg5::LEU2 his4 ura3 lys2 leu2 bar1*
RH5930	MATa *erg3::LEU2 erg6::LEU2 his4 ura3 lys2 leu2 bar1*
RH5873	MATa *erg4::LEU2 erg5::LEU2 his4 ura3 lys2 leu2 bar1*
RH5874	MATa *erg5::LEU2 erg6::LEU2 his4 ura3 lys2 leu2 bar1*
RH6971	Matα *PDR12::CFP::HygB ura3 leu2 his4 lys2 bar1*
RH6926	Matα *sur2::LEU2 PDR12::CFP::HygB ura3 leu2 his4 lys2 bar1*
RH6919	Matα *erg4::URA3 PDR12::CFP::HygB ura3 leu2 his4 lys2 bar1*
RH6930	Matα *erg4::URA3 isc1::KanMx PDR12::CFP::HygB ura3 leu2 his4 lys2 bar1*
RH6925	Matα *erg4::URA3 sur2::LEU2 PDR12::CFP::HygB ura3 leu2 his4 lys2 bar1*
RH6922	Matα *erg4::URA3 scs7::LEU2 PDR12::CFP::HygB ura3 leu2 his4 lys2 bar1*

4.2.2 Lipid standards

All lipid standards were obtained from Avanti Polar Lipids (Alabaster, AL), with the exception of C19:0-Cer, which was obtained from Matreya Inc., (Pleasant Gap, PA) and diC8:0-GPIns, which was obtained from Echelon Biosciences (Salt Lake City, UT).

4.2.3 Cell culture for lipid analysis

Cells were kept on YPUAD plates (1% yeast extract, 2% peptone, 2% glucose, 40 mg/l uracil and adenine) and single colonies were cultured overnight in YPUAD medium. The cells were then diluted into fresh medium and cultured to mid-logarithmic (log) phase (OD600 1.0 – 1.5) for lipidomic analysis. 40 OD600 units of cells were harvested by centrifugation, washed with twice with water and frozen.

4.2.4 Lipid extraction and analysis by ESI-MS and MS/MS

Lipids were extracted from 40 OD600 units of cells as described in Chapter 3, but with the following modifications. 5μg of dimyristoyl GPCho (di14:0-GPCho), 20μg of dimyristoyl GPEtn (di14:0-GPEtn), 4μg of dioctyl GPIns (di8:0-GPIns), 15μg of didocosahexaenoyl GPSer (di22:6-GPSer) and 3μg of C19:0-Cer were added as internal standards.

The two methods of targeted and non-targeted analysis by mass spectrometry as described in Chapter 3 were employed, with the following modifications. (i) Instead of using manual direct injection, a high performance liquid chromatography system (Agilent Technologies, Santa Clara, CA) was coupled to the mass spectrometer and samples were introduced into the mass spectrometer by loop injections with chloroform-methanol (1:1, v/v) as a mobile phase at a flow rate of 200μL/min. (ii) For targeted lipid quantification, in addition to the transitions for sphingolipids described in Chapter 3 (Fig. 3.5), additional transitions were set up for glycerophospholipids, based on the parent → headgroup fragment transitions. Lipid levels were calculated relative to relevant internal

standards as described in Section 3.2.4. Comparison of the means of wild type and individual genotypes from three independent experiments were performed. The quantities of lipids are expressed as ion intensities relative to wild type levels, converted to a log10 scale, and represented as a heat plot.

4.2.5 Growth and plating assays

For the plating assays, yeast were grown to stationary phase, diluted to 10^7 cells per ml in water and 10 fold serial dilutions were pinned onto agar plates containing rich medium with additives adjusted to pH 5.5 (40 mM MES) unless indicated (in collaboration with Howard Riezman). Sorbic acid sensitivity was tested on agar plates containing rich medium adjusted to pH 4.5 and supplemented with 1mM of sorbic acid. Control plates contain rich medium adjusted to pH 4.5 without any supplements.

4.2.6 Polymerase chain reaction (PCR)-based generation of yeast expressing cerulean fluorescent protein (CFP)-tagged Pdr12p

4.2.6.1 PCR generation of CFP-tagged PDR12 cassette

Our collaborator, Howard Riezman, had previously used cerulean (Rizzo *et al.*, 2004) (CFP) to fluorescently tag Pdr12p at the N-terminus, with hygromycin B (HygB) as a selection marker, in the genome of yeast using the plasmid pBS10 (YRC, Univ. Wash) and had generously provided genomic DNA isolated from cells tagged with *PDR12::CFP::HygB*. The cassette for genomic tagging of *PDR12::CFP::HygB* was prepared by PCR, using the Expand High Fidelity PCR kit (Roche Applied Science, Germany), the forward primer - GCTTCAATATTGCCGCTATGTTGATTTG, the reverse primer - GATTCTATACATAAAACATTAGTGTG, and the genomic DNA as

the template. The thermocycling profile was as follows: initial denaturation at 94°C for 2 minutes, followed by 9 cycles of denaturation at 92°C for 30s, annealing at 55°C for 45 minutes, and primer extension at 68°C for 3 minutes. This was followed by another 18 cycles of denaturation at 92°C for 30 seconds, annealing at 50°C for 30s, and primer extension at 68°C for 4 minutes and 20s. Final extension was then performed at 68°C for 7 minutes. The PCR product was analysed using agarose gel eletrophoresis.

4.2.6.2 Transformation of yeast

Transformation of *S. cerevisiae* was performed using lithium acetate. Briefly, cells were grown to mid-log phase in YPUAD in a 10mL culture. Cells were harvested by centrifugation at 5000*g* at 4°C for 5 minutes and the cell pellet was subsequently washed twice with 5mL of sterile deionised water. The cells were resuspended in 100µL of 100mM lithium acetate and transferred into two Eppendorf tubes. The cells were pelleted in a microfuge for 15s and the supernatant was decanted. While preparing the cells, sheared salmon sperm carrier deoxyribonucleic acid (DNA) (10mg/mL stock) was boiled for 5 minutes and placed on ice for at least 2 minutes. To one tube of cells, the following reagents were added according to the order they are listed – 240µL of 50% polyethylene glycol, 36µL of 1.0M lithium acetate, 25µL of sheared salmon sperm DNA and 45µL of cassette (from PCR product obtained in Section 4.2.6.1). A control tube contains everything except the cassette. The samples were mixed and placed in a 30°C rotator for 45 minutes. Heat shock was then performed in a 42°C water bath for 25 minutes. Cells were pelleted at 6000*g* for one minute and resuspended in 400µL of YPUAD media. The cells were then plated on two YPUAD plates and incubated at 30°C overnight. Replica

plating was performed the next day to the selective medium, YPUAD + 200μg/mL hygromycin (Hygromycin B from *Streptomyces hygroscopicus*, Roche) and incubated at 30°C for two days. No cells from the control experiment should grow and for cells transformed with the DNA cassette, a few single colonies were picked and streaked on selective medium.

4.2.6.3 Colony PCR

Colony PCR was performed to check for proper integration of *PDR12::CFP::HygB* into the genome. Hygromycin B-resistant colonies were selected and added to separate tubes containing 50μL of 5mg/mL 20T zymolyase. The samples were incubated at 35^{o}C for 30 minutes, followed by centrifugation for 5 minutes at 5000rpm. The supernatant was removed and the pellets were allowed to dry by incubating at 92°C for 5 minutes with caps open. PCR was carried out using ThermoPol polymerase (New England Biolabs Inc., USA), the same set of forward primers and reverse primers for the cassette, in a 25μL reaction. The thermocycling profile was as follows: initial denaturation at 94°C for 2 minutes, followed by 9 cycles of denaturation at 92°C for 30 seconds, annealing at 50°C for 30 minutes, and primer extension at 70°C for 3 minutes and 30s. This was followed by another 18 cycles of denaturation at 92°C for 30 seconds, annealing at 50°C for 30s, and primer extension at 68°C for 3 minutes and 20s. Final extension was then performed at 68°C for 7 minutes. The PCR product was analysed using agarose gel eletrophoresis. Sorbic acid sensitivity was reassessed for the strains successfully tagged with *PDR12::CFP::HygB* (Fig. 4.5A).

4.2.7 Sorbic acid treatment and localization of Pdr12p in cells

Pdr12p-CFP expressing cells were kept on YPUAD plates and single colonies were cultured overnight in YPUAD medium. The cells were inoculated in fresh YPUAD medium and cultured till they reach log phase (OD600~0.5-0.8).Cells were washed with deionised water and resuspended in YPUAD, pH 4.5 containing 0.25mM of sorbic acid (in ethanol). A control set was resuspended in YPUAD, pH 4.5 with ethanol. The cells were incubated at 30°C for three hours to induce Pdr12p expression and localisation to the plasma membrane. Cells were washed with synthetic defined (SD) media and resuspended in 30 to 50 μL of synthetic defined media containing 10mM HEPES and viewed under an Axio Imager Z1 fluorescence microscope.

4.2.8 Assay of Pdr12p activity by efflux of fluorescein diacetate (FDA)

Pdr12p activity was assayed by monitoring the efflux of FDA as described by Holyoak and co-workers (Holyoak *et al.*, 1999), with some modifications. Cells were grown in YPUAD media to early log phase and incubated with 0.25mM sorbic acid, pH 4.5, for 3 hours to induce Pdr12p. After washing 3 times with water, 10^7 cells per time point were resuspended in 1mL of 50 mM HEPES-NaOH, pH 7.0 containing 5mM 2-deoxyglucose and 50μM FDA and were shaken at 30°C for 1 hour. Starved cells were washed twice with HEPES-NaOH, pH 7.0, resuspended in the same buffer, split into equal aliquots and incubated for 5 minutes at 30°C before the addition of glucose to one of the samples. Aliquots were harvested over a time course of 2.5, 5, 10 and 15 minutes and cells were pelleted. The supernatant was collected and FDA fluorescence was measured with a spectrofluorometer (SpectraMax Gemini EM, Molecular Devices,

Sunnyvale, CA) using an excitation wavelength of 435nm and an emission wavelength of 525nm. The difference in fluorescence between the samples containing glucose and the starved cells represents the energy-dependent efflux of FDA.

4.2.9 Statistical Analysis

For the lipid analysis, the difference in levels of individual lipid species between wild type and individual genotypes was determined statistically using the Kruskal Wallis test, which is indicated by an asterisk for p-value less than 0.05 (*).

For FDA efflux assay, comparison of the wild type and mutant strains was performed using the mean of at least 4 independent samples ± standard error of the mean (SEM) from individual samples. Statistical significance between wild type and mutant yeast strains was determined using Student's t-test and indicated by ** for p-value less than 0.05.

4.3 Results

4.3.1 Mutants of sterol biosynthesis display altered lipids profiles

Although the last five steps of ergosterol synthesis is non-essential in *S. cerevisiae* (Fig. 4.1 and Table 4.1), deletion of the genes lead to a wide variety of phenotypes. The Riezman laboratory has previously created an isogenic set of single and double mutants in ergosterol biosynthesis and have characterised them for their sterol compositions and endocytic phenotypes (Munn *et al.*, 1999;Heese-Peck *et al.*, 2002). In addition, it was observed that one of the double deletion mutants, *erg3*Δ*erg6*Δ, which has a substantial growth defect, showed changes in its sphingolipid metabolism (Supplementary material

4.2) and that this change could be reversed by mutation of the yeast sphingomyelinase homolog (Sawai *et al.*, 2000) encoded by *ISC1* (Fig. 4.1). The mutation in *ISC1* aggravated the growth defect of the *erg3*Δ*erg6*Δ double mutant at 37°C (Supplementary material 4.2). Swain and co-workers isolated a single mutant, *erg26-1* and further characterised sphingolipid metabolism in this mutant (Baudry *et al.*, 2001;Swain *et al.*, 2002). Together, these suggest an interaction between sterols and sphingolipids, but these particular cases might not be representative. Therefore, the lipid composition of all the *erg* deletion mutants were systematically analyzed using electrospray ionisation-mass spectrometry (ESI-MS), based primarily on the method described in Chapter 3. In addition to major yeast sphingolipids, the targeted analysis by MRM was extended to include both the quantification of the major glycerophospholipids (except for cardiolipin). Quantification was carried out and is expressed relative to wild type cells, as presented in Figure 4.2. Results on mannosyl diinositolphosphorylceramide (M(IP)2C) was not presented because the data were not easily interpretable due to the presence of singly and doubly charged species (Guan and Wenk, 2008), together with the fact that no good internal standard was available. By steady state phosphate labelling and TLC analysis, M(IP)2C represents less than 20% of the total sphingolipids in *S. cerevisiae* (Schorling *et al.*, 2001).

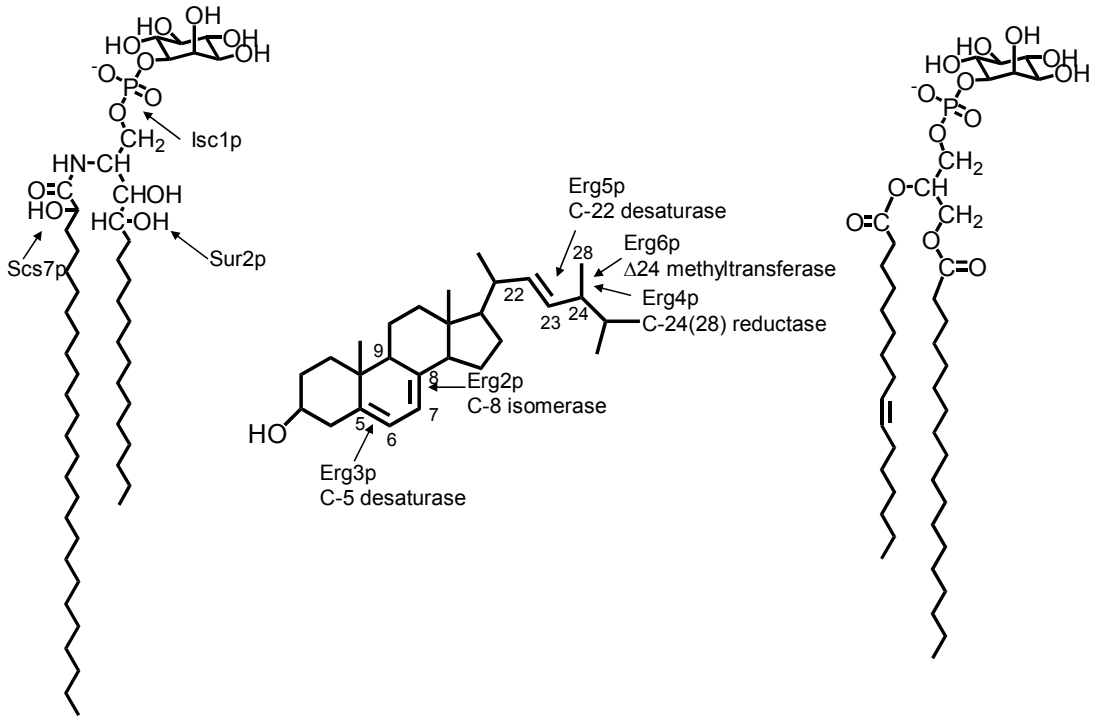

Figure 4.1 Structures of some abundant sphingolipid, sterol and glycerophospholipid species in *Saccharomyces cerevisiae.*
Isc1p is an inositolphosphorylceramide (IPC) hydrolase that converts IPC to ceramide and inositol phosphate. Sur2p and Scs7p are enzymes responsible for hydroxylation of the sphingoid base and fatty acid, respectively, of sphingolipids. The last five steps of ergosterol biosynthesis are shown. The order of events is not implied here. For comparison, one of the most abundant yeast glycerophospholipids, 34:1 glycerophosphoinositol (GPIns) is shown. For details, see Supplementary material 4.1.

The single *erg* deletion mutants showed substantial changes (>30%) in less than 10% of their glycerophospholipid species, but showed substantial changes in over 45% of their sphingolipid species. Consistent trends were obtained based on unbiased profiling (data not shown). Remarkably, the sphingolipid pattern found in each single *erg* deletion mutant was different. Therefore, the changes cannot be due to a lack of ergosterol because none of the mutant strains have ergosterol, but to the presence of the abnormal sterols, for which the composition is different between the different mutants. This astounding result implies that the yeast cells have the capacity to modify their

sphingolipid composition in response to changes in sterol structures in their membranes. Double deletion mutants in ergosterol biosynthesis have substantial changes in their sphingolipid pattern, but also have substantially more changes in their glycerophospholipids (Fig. 4.2). The single *erg6*Δ mutant appears somewhat intermediate in its lipid pattern between the single and double *erg* mutants. This is probably due to the fact that the *ERG2* gene product works very inefficiently in the *erg6*Δ mutant strain as noted by the accumulation of sterols with a double bond at position 8 (Heese-Peck *et al.*, 2002) (H. Riezman, Supplementary Table 4.1E) explaining why the *erg6*Δ mutant has partial properties of a double *erg2*Δ*erg6*Δ mutant. Consistent with the radioactive labelling experiments, most of the double deletion mutants as well as the *erg2*Δ and *erg6*Δ single deletion mutant strains have less of the major IPC species, IPC-C. Otherwise, the patterns of sphingolipid prevalence vary considerably. Interestingly, when mutations in sphingolipid hydroxylation or head group turnover are introduced, there are no major changes in sterol compositions or quantities (H. Riezman, Supplementary Table 4.1A). Most double *erg* deletion mutants show more substantial changes in their sphingolipid patterns than either of the corresponding single *erg* deletion mutants. There is one notable exception to this, the *erg5*Δ*erg6*Δ mutant, whose sphingolipid pattern is closer to wild type than either of the two single mutants. This might have evolutionary significance (see discussion in Section 4.4.5).

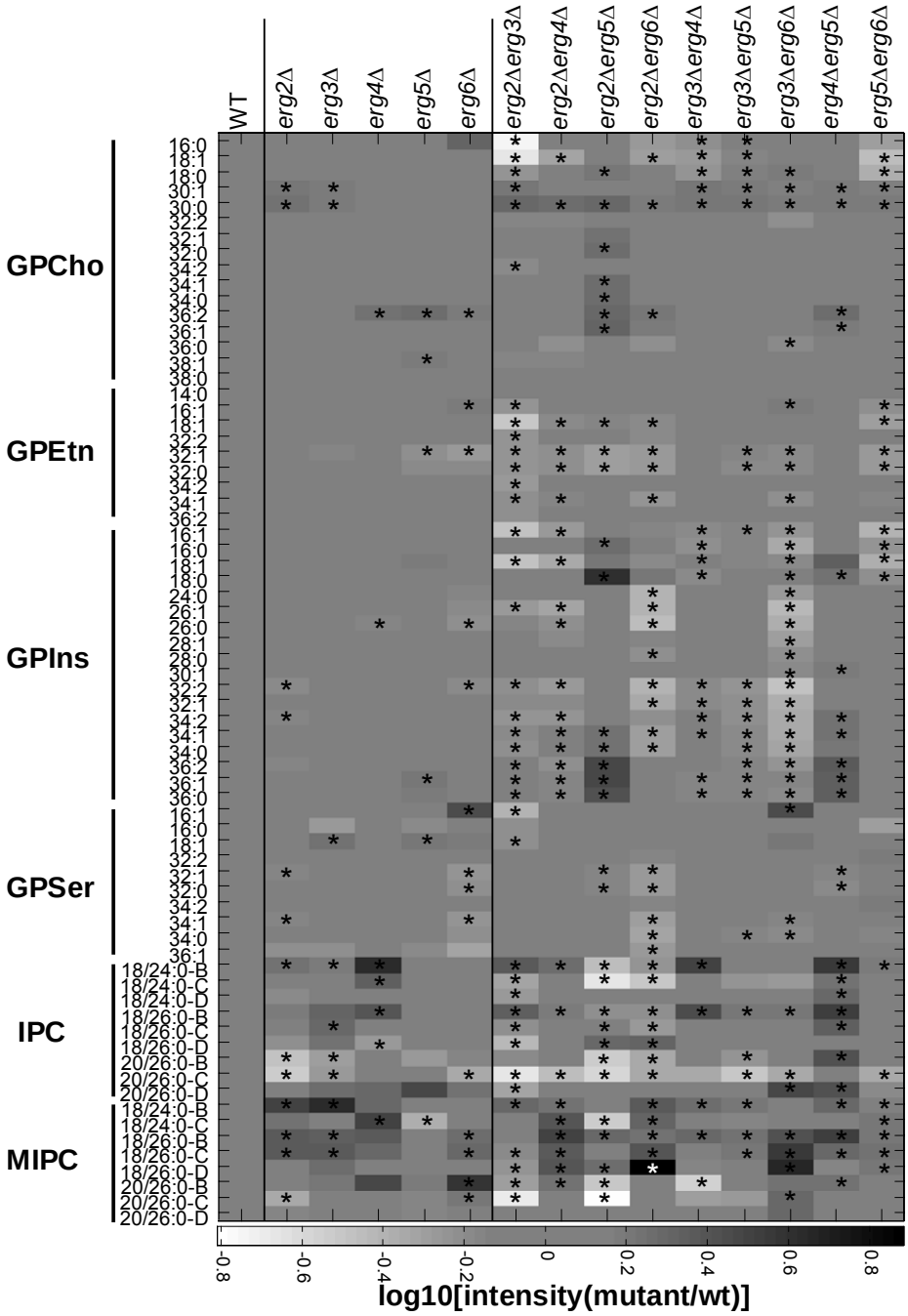

Figure 4.2 Glycerophospholipidome and sphingolipidome of deletion mutants in ergosterol biosynthesis.

Isogenic wild type and ergosterol mutant strains were grown as indicated. Lipid standards were added to 40 OD600-equivalents of cells and lipids were extracted and measured using ESI-MS (Guan and Wenk, 2006). The quantities of lipids are expressed as ion intensities relative to wild type levels, converted to a log10 scale. Glycerophospholipids: GPCho, glycerophosphocholine; GPEtn, glycerophosphoethanolamine; GPIns, glycerophosphoinositol; GPSer, glycerophosphoserine. Sphingolipids: IPC, inositolphosphorylceramide; MIPC, mannosyl inositolphosphorylceramide. The suffixes -B, -C, and -D on IPC and MIPC denote hydroxylation states, having two, three, or four hydroxyl groups respectively. Data are presented as means of 3 independent biological samples. Statistical significance between wild type and individual genotypes was determined using the Kruskal Wallis test. * denotes significance $P<0.05$.

4.3.2 Sterol and sphingolipid biosynthesis pathways interact genetically

The specificity of the sphingolipid patterns in the different single *erg* deletion mutants suggests that these changes may be an adaptive response and led to the hypothesis that sterols and sphingolipids functionally interact in yeast cells. To test this hypothesis, isogenic double deletion mutants in sterol and sphingolipid biosynthesis were generated. The prediction is that simultaneous defects in both pathways should lead to synthetic phenotypes. Most of the changes seen in sphingolipid patterns (Fig. 4.2) are changes in sphingolipid hydroxylation or in head group composition. Therefore, a mutant that affects sphingolipid head group turnover, *isc1*Δ, and mutants affecting sphingolipid hydroxylation were chosen. The *sur2*Δ mutant is unable to hydroxylate the sphingoid base and the *scs7*Δ mutant is defective in hydroxylation of the fatty acid on sphingolipids (See Fig. 4.1 and Supplementary material 4.1) (Haak *et al.*, 1997). All 15 possible double mutant combinations of the 5 single *erg* mutants with the 3 mutants affecting sphingolipid metabolism were constructed and analysed for their ability to grow under a number of conditions. All of the single *erg* deletion mutants, with or without sphingolipid defects, grew well at 30°C on rich medium, as do all of the double *erg* deletion mutants except *erg2*Δ*erg6*Δ (Fig. 4.3). At 37°C or on plates with non-fermentable carbon sources, several double mutants showed reduced growth when compared to the corresponding single mutants (marked with arrows). It was observed that the double *erg* deletion mutants often had more severe phenotypes than the single *erg* deletion mutants from which they were derived.

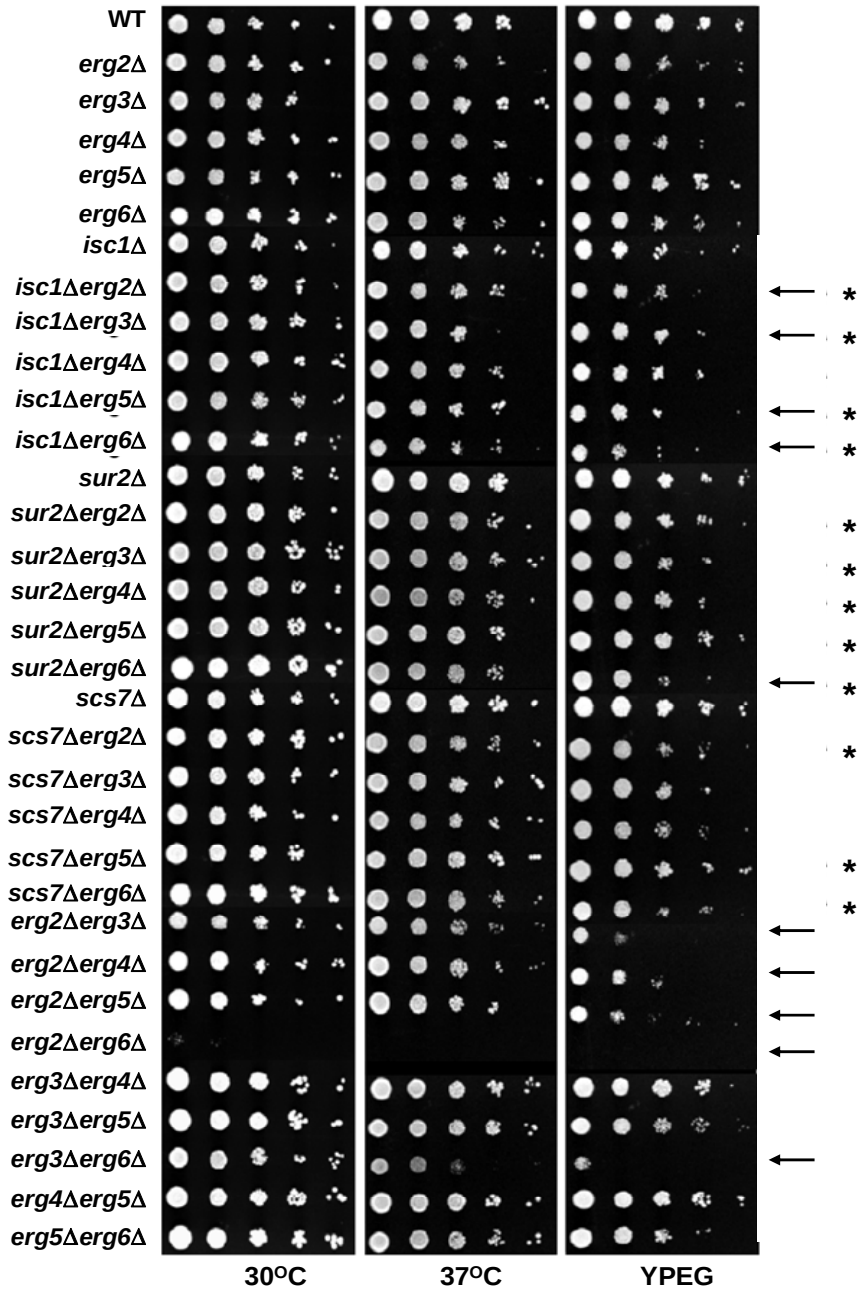

Figure 4.3 Systematic phenotype analysis.
The indicated strains were grown and pinned onto YPUAD or YPEG (1% Yeast Extract, 2% Peptone, 3% ethanol, 3% glycerol, 40mM MES, pH 5.5) plates and grown at 30°C except when indicated. Plates were photographed after 2 (30°C and 37°C) or 4 days (YPEG). Arrows denote conditions where sterol-sphingolipid double deletion mutants showed different growth than the single *erg* deletion mutants under the conditions shown. Each asterisk represents where the double mutant shows a change in growth properties (synthetic growth defect or suppression) when compared to the single *erg* deletion mutant (Supplementary material 4.3). Of the 15 double deletion mutants constructed, 13 showed synthetic phenotypes (CM Souza and H Riezman).

Growth under a wide variety of conditions was assayed in order to uncover new phenotypes (Supplementary material 4.3). Some particularly illustrative examples from these assays are shown (Fig. 4.4). Blocking hydroxylation of either the sphingoid base or the fatty acid of sphingolipids is able to suppress the slow growth phenotype of the *erg2*Δ mutant at 16°C (Fig. 4.4A). The results found at 16°C are quite atypical, because changes in hydroxylation usually have much more specific effects on strains with aberrant sterols (Fig. 4.4B). Combination of a mutation in sphingolipid fatty acid hydroxylation (*scs7*) with the *erg2*Δ mutation completely abrogates growth on plates with low amounts of caffeine, an inhibitor of the Target of Rapamycin Complex (TORC) 1 signalling pathway (Reinke *et al.*, 2006), whereas both corresponding single mutants grow well on caffeine plates. A similar result was found for sensitivity to rapamycin. Combination of *sur2* deletion with *erg3* or *erg6* deletion led to synthetic growth phenotypes on plates with a low concentration of a glycosylphosphatidylinositol synthesis inhibitor, YW3548 (Sutterlin *et al.*, 1997) or a low concentration of sodium dodecyl sulfate (SDS) (Fig. 4.4C), respectively, both expected to induce cell wall defects. The specificity of the site of hydroxylation in combination with particular sterol biosynthesis mutations suggests that it is the combination of the structures that leads to the synthetic phenotype. The simplest way to interpret this would be to postulate that sphingolipids and sterols interact physically in membranes to carry out some of their required functions. At the very least, it can be concluded that sterols and sphingolipids work in common pathways.

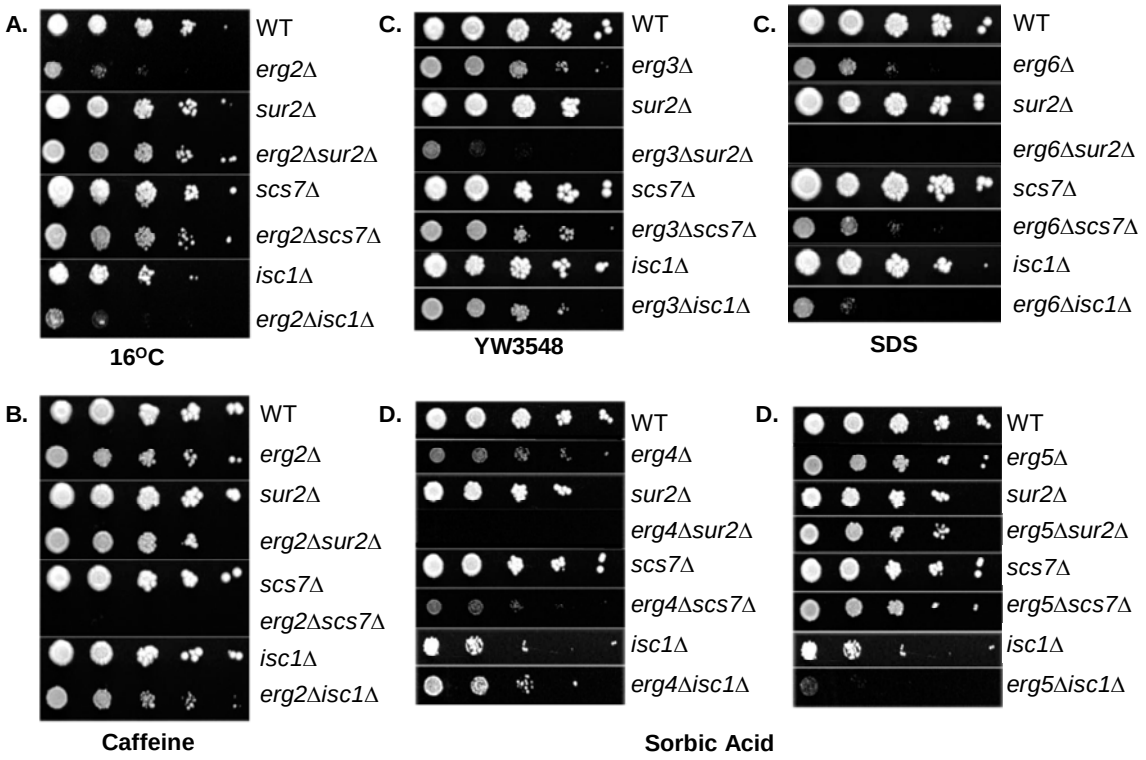

Figure 4.4 Examples of suppression and synthetic phenotypes.
Dilutions of indicated strains were spotted onto plates (A) containing the following additions; 1mM sorbic acid (C), 2mM caffeine (B), 1μg/mL YW3548 (B), or 0.01% sodium dodecyl sulfate (SDS) (B). The sorbic acid plates were adjusted to pH 4.5 (CM Souza and H Riezman).

Sorbic acid resistance is conferred by an adenosine trisphosphate (ATP) binding cassette (ABC) transporter, Pdr12p (Piper *et al.*, 1998), which exports weak acids like sorbic and benzoic acids. This process is most affected by the *erg3* and *erg6* mutations (Supplementary material 4.3), suggesting that a Δ5 double bond in the B-ring and methylation of the side chain of ergosterol are the most important features for Pdr12p function. The *erg4*Δ mutant strain grows weakly on 1mM sorbic acid plates, but combination with the *sur2* mutation completely abrogates growth (Fig. 4.4D). Introduction of the *isc1* mutation improves growth slightly under the same conditions. The effects of sphingolipid changes on the *erg5*Δ mutant are quite different. The *sur2* and *scs7* mutations have almost no effect on growth of *erg5* mutant cells on sorbic acid

plates, whereas introduction of the *isc1* mutation completely blocks growth under the same conditions. These data show that the *isc1* mutation is not having a simple positive or negative effect that is added to the effect of the sterol mutant. These results further confirm that it is the specific combinations of sphingolipid and sterol structures that lead to the synthetic phenotypes.

By using very simple tests, synthetic phenotypes in 13 of the 15 possible double mutants in ergosterol and sphingolipid biosynthesis was found (Fig. 4.3), providing genetic proof that these two pathways work together in multiple cellular functions. A possible explanation for the genetic interaction could be that creation of the double mutants causes additional changes in glycerophospholipids and/or sterols. To examine this, the glycerophospholipids and sphingolipids in the double mutant strains were analyzed by ESI-MS (Supplementary material 4.4) and the sterol composition measured by gas chromatography mass spectrometry (in collaboration with H. Riezman, Supplementary Table 4.1). As expected from the introduction of mutations in sphingolipid modification, dramatic changes in the sphingolipid pattern, but relatively minor changes in the glycerophospholipids or sterols (Supplementary material 4.4 and Supplementary Table 4.1) were observed, lending additional support to the conclusion that it is the structural interactions between the aberrant sterols and sphingolipids that cause the synthetic phenotypes and not further changes in glycerophospholipids or sterols.

4.3.3 Cellular sterol and sphingolipid compositions affect the activity of membrane transporter, Pdr12p

Based on our phenotypic assay, it was observed that *erg4* mutant grows weakly on 1mM sorbic acid. Interestingly combination of *erg4* with the *sur2* mutation, but not *scs7* mutation, completely abrogates growth while combination of either *sur2* or *scs7* mutation has no effect on the *erg5*Δ mutant (Fig. 4.4). Sorbic acid is a commonly used food preservative that diffuses into cells when protonated at low pH and is trapped internally when it becomes deprotonated. It can be detoxified by yeast cells via the ABC transporter, Pdr12p (Piper *et al.*, 1998) in an ATP-dependent manner. A likely molecular explanation for the lack of growth under these conditions is a defect in detoxification of sorbic acid. It is hypothesised that PDR12p function is altered by specific combinations of defects in sphingolipid and sterol structures. Therefore, the function of PDR12p, in terms of its localisation and activity, in the various ergosterol and sphingolipid mutants was analysed.

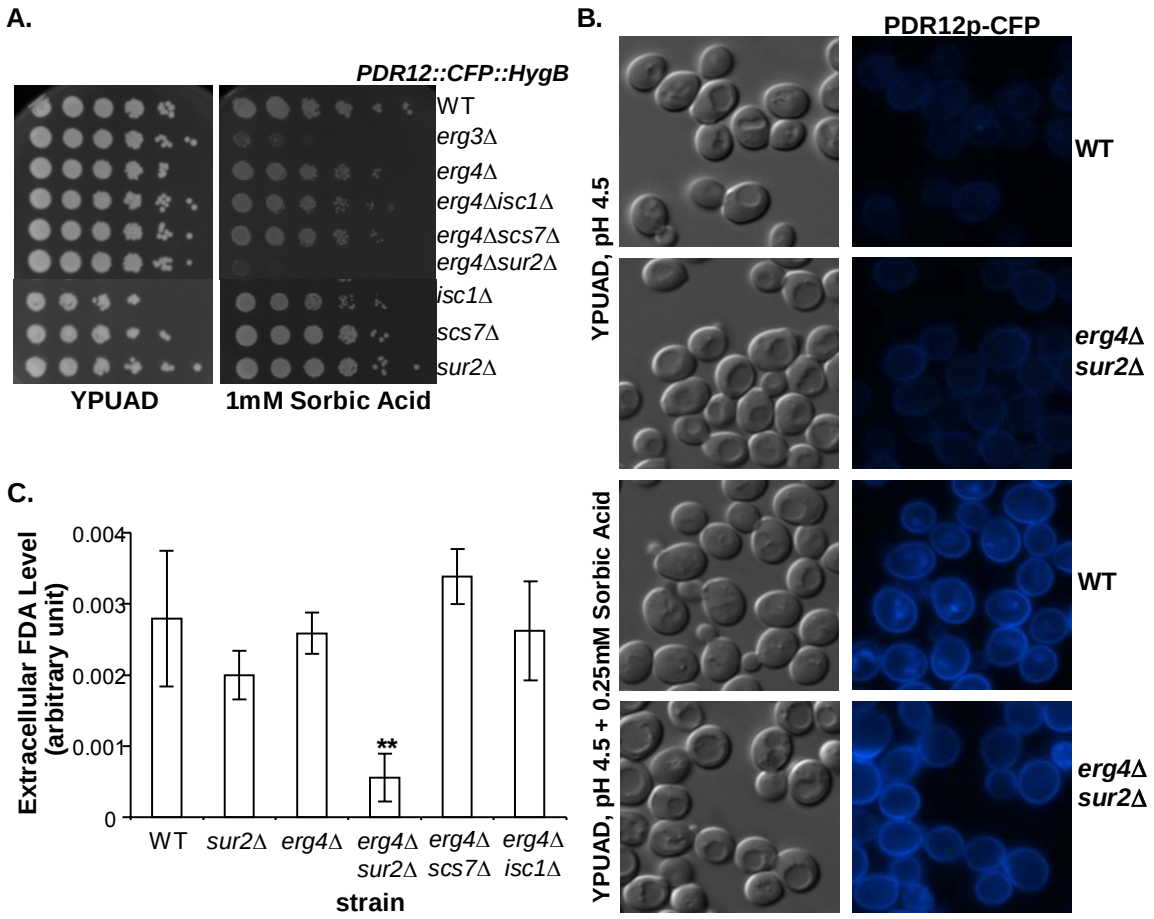

Figure 4.5 Sorbic acid sensitivity in *erg4Δsur2Δ* is due to defective export by Pdr12p.
(A) Assessment of sorbic acid sensitivity of *PDR12::CFP::HygB*-integrated strains. (B) Pdr12p-CFP induction and localisation in the absence and presence of sorbic acid were visualized in the indicated strains. (C) Strains without genomic integration of *PDR12::CFP::HygB* were loaded with fluorescein diacetate (FDA) in the presence of 2-deoxygluose to deplete ATP. The cells were harvested and resuspended in glucose containing medium and extracellular fluorescein was quantified after 15 and 30 seconds. Relative rates of FDA export per minute are shown. Statistical significance between wild type and mutant strains was determined using Student's t-test. **p<0.05.

In order to examine Pdr12p induction and localisation, a functional, fluorescently labeled Pdr12p was constructed using C-terminal genomic fusion of *PDR12* with cerulean fluorescent protein (CFP). Sorbic acid induces Pdr12p expression and the protein is delivered to the cell surface (Piper *et al.*, 1998) where it exports weak organic acids, including sorbic and benzoic acids as well as fluorescein (Holyoak *et al.*, 1999). In wild type, *erg4*Δ, *sur2*Δ and *erg4*Δ *sur2*Δ mutants, expression of Pdr12p-CFP was induced and the protein is transported to the cell surface normally (Fig. 4.5B). Indeed, the

induction and localisation of Pdr12p in other sorbic acid sensitive strains, such as *erg3*Δ mutant, was also normal. Pdr12p activity was measured based on the export of fluorescein. Fluorescein diacetate (FDA) was loaded into yeast in the absence of glucose. Glucose was added to allow fluorescein export. The double *erg4*Δ*sur2*Δ mutant showed drastically reduced fluorescein export (Fig. 4.5C). No observed difference in the transcript levels of *PDR12* in the double mutant was observed (H. Riezman, Supplementary material 4.5B). These results show that the Pdr12p is properly expressed and transported to the cell surface, but is not active if membranes lack functional sterol/sphingolipid structures.

4.4 Discussion

4.4.1 Dependence of sphingolipid metabolism on sterol composition

One of the major new findings emanating from this study is that cells have a mechanism to sense and react to changes in their membrane sterol composition by modifying their membrane lipid compositions affecting mainly sphingolipids. The mechanism of the adaptation of sphingolipid levels is not clear, but is most likely not uniquely due to differences in transcript levels of the different genes involved in the pathway as most of the genes were unchanged (H. Riezman, data not shown). The mechanism used to detect the changes in sterol composition is currently under study and genetic approaches are possible. It is not the absence of ergosterol that is sensed, because each *erg* deletion mutant shows a different pattern of sphingolipids. This pathway is most likely fundamentally different than previously described sterol sensing mechanisms where different amounts of cholesterol are sensed by the SREBP pathway or other sterol

sensors and then control gene expression (Goldstein *et al.*, 2006), because sterol intermediates, rather than the total quantity of sterols, seem to affect sphingolipid composition in different ways. Recently, an SREBP dependent pathway has been described in *Schizosaccharomyces pombe*, which has several features in common with what is observed in this study, because there is a coordinate regulation of anaerobically expressed genes with ergosterol biosynthesis genes (Todd *et al.*, 2006) (Supplementary material 4.5) and because sterol biosynthesis intermediates seem to be important (Hughes *et al.*, 2007), but no specific effects on sphingolipids have been described. The pathway cannot be identical in *S. cerevisiae* because this yeast does not have an SREBP homolog, although they do have oxysterol binding proteins that have been proposed to be involved in intracellular sterol transport (Raychaudhuri *et al.*, 2006).

The control of sphingolipid species is unlikely to be solely the result of transcriptional changes as few differences in sphingolipid metabolic enzymes were seen. In some strains, some changes in sphingolipid content are likely to be due to head group turnover via Isc1p (Supplementary material 4.2). The mode of activation of Isc1p in this case is unknown, but one possibility is regulation by localisation because its localisation has been shown to change due to changes in culture conditions in yeast (Vaena de *et al.*, 2004).

The specific and major changes in sphingolipid species when sterol intermediates are present in the membrane show a dependence of sphingolipid metabolism on sterol composition, but also suggest that sterols and sphingolipids function together. In this

work, the genetic analysis of double deletion mutants in sterol and sphingolipid metabolism, which uncovered a large number of synthetic and suppression phenotypes, provides proof for this concept. Synthetic phenotypes can occur for different reasons; when there are two parallel pathways and one mutation is in each pathway or when two mutations affect the same pathway, quite often at the same step. Each mutation would affect the step partially, but the double mutant would have a much stronger phenotype. Classically, this can result when two proteins work together as a complex. In a similar manner it is possible to interpret our data by suggesting that sterols and sphingolipids might function in a variety of pathways as a sterol-sphingolipid complex.

4.4.2 Functional interactions between sterols and sphingolipids is required for cellular physiology

Many different phenotypes, including growth in presence of cell wall disturbances, weak organic acid sensitivity, different carbon sources, temperatures, various classes of inhibitors affecting a number of different pathways were tested (in collaboration with H. Riezman, Fig. 4.3, 4.4 and Supplementary material 4.3). In addition, a systematic analysis of transcript levels was performed (H. Riezman, Supplementary material 4.5A). It is virtually impossible that sterols and sphingolipids happen to act in parallel pathways to carry out each of these functions where synthetic phenotypes have been uncovered. Therefore, it can be concluded that sterols and sphingolipids function together to carry out a wide variety of cellular functions. The conclusion that sterols and sphingolipids function together fulfils one of the tenets of the (lipid) raft hypothesis. The other main tenet of the raft hypothesis is that the increased order produced by sterol-sphingolipid interactions is important for function. To begin to

test this, plasma membrane anisotropy, an indicator of membrane order, was measured (H. Riezman, Supplementary Table 4.2). Even though there were substantial and significant differences in anisotropy indicating a decrease in membrane order in several of the mutants, there was a lack of correlation between the measurements of membrane anisotropy with any of the phenotypes assayed. Therefore it is concluded that membrane order is not likely to have a great influence on the functions that were examined. Therefore, while these results strongly support one tenet of the raft hypothesis, the overall hypothesis does not seem useful to interpret our data.

4.4.3 Sterol and sphingolipid dependence for protein localisation

The raft hypothesis has been invoked to explain a large number of membrane trafficking events, which prompted the examination of the localisation of two plasma membrane proteins that have been shown to be localised in microdomains of the plasma membrane. One of the best established systems where proteins have been localized to specific plasma membrane microdomains is in *Saccharomyces cerevisiae*, where two distinct types of domains have been seen. One of these is patches of approximately 300 nm on the cell surface that contain the various permeases, including the tryptophan transporter Tat2p and the arginine transporter, Can1p. Both transporters have been reported to be resistant to cold-detergent extraction, a technique that is often correlated with presence in rafts (Malinska *et al.*, 2004;Malinska *et al.*, 2003;Mayor and Riezman, 2004;Umebayashi and Nakano, 2003). The permease-containing plasma membrane patches also stain for filipin indicating the presence of ergosterol (Malinska *et al.*, 2004;Malinska *et al.*, 2003). The permease-containing patches are surrounded by membrane domains containing the plasma membrane ATPase, Pma1p, a protein that has

also been claimed to be functionally associated with rafts for biosynthetic delivery to the cell surface (Bagnat *et al.*, 2000;Bagnat and Simons, 2002). To test further phenotypes of our single and double mutants, the localisation of green fluorescent protein- (GFP-) tagged Tat2p and Can1p, proteins found in the same domains at the cell surface, was analysed (H. Riezman, Supplementary material 4.6). In wild type cells under the conditions tested, Tat2p is found in approximately equal amounts in the plasma membrane and in the vacuole. The vacuolar Tat2p may be generated by direct targeting from the biosynthetic pathway or via delivery to the cell surface and subsequent endocytosis.

To compare the mutants, cell surface and vacuolar Tat2-GFP were quantified. The single *erg* deletion mutants as well as *isc1*Δ and *sur2*Δ increased the amount of Tat2-GFP in the vacuole and several strains showed slight ER accumulation (Supplementary material 4.6 and Supplementary Table 4.3). The increase in vacuole localisation in the *erg3*Δ mutant is partially suppressed by the *scs7* mutation, whereas the increase in vacuolar localisation in the *erg6*Δ mutant is enhanced by *isc1* and *sur2* mutations. This demonstrates suppression and synthetic effects also for protein localisation. On the other hand, the effects on Can1-GFP localisation are only minor. In all mutants, the majority of Can1-GFP was detected at the plasma membrane (Supplementary material 4.6). In the *erg2*Δ and *erg3*Δ series, a small amount of vacuole staining was observed, but no synthetic phenotypes (Supplementary Table 4.3). The Can1-GFP construct was active in all strains because it conferred canavanine sensitivity. Here again, the raft hypothesis does not easily help to explain the results of steady state localisation of Tat2p and Can1p

in the various single and double mutants. Although the two transporters colocalise to the same plasma membrane patches, they show completely different dependence on sterols and sphingolipids for their localisation. Localisation of Tat2p, which was affected by sphingolipid and sterol mutations, did not correlate with anisotropy measurements. It could be that anisotropy measurements of the plasma membrane do not reflect fluidity of the compartment where Tat2p sorting occurs (Golgi or endosomal compartment) or that measuring the overall fluidity of the membrane does not indicate the fluidity in rafts.

4.4.4 Complexity of sterols and sphingolipids interactions

In what ways could sterol-sphingolipid interactions influence function in such a complex way? A trivial explanation would be that addition of sterol mutations with sphingolipid mutations cause an indirect effect by generally increasing the stress to the cells, which affects many functions. This is not the case for the observed hypersensitivities to caffeine or sorbic acid, which do not correlate with stress gene induction. Indirect effects, while certainly occurring in some cases, are unlikely to be a common explanation for the synthetic effects observed because of the specificity of the position of hydroxylation of the sphingolipid. Moreover, different combinations of specific sterol and sphingolipid mutations affect only specific cellular pathways rather than having highly pleiotropic effects.

Biophysical (Ahmed *et al.*, 1997;Feigenson, 2007) and molecular dynamics (Aittoniemi *et al.*, 2007) experiments have clearly demonstrated that sterols and sphingolipids can interact preferentially in artificial membranes. This means that these lipids exist in at least two forms in the membrane, free sterol and sphingolipid, as well as

sterol-sphingolipid complexes. The results in this work suggest that this interaction will also be seen *in vivo* if suitable techniques become available. It is hypothesized that most of the phenotypes seen here are results of defects in direct protein-lipid interactions and not changes in the fluidity properties of the membrane or membrane domains. Any integral or peripheral membrane protein could interact with either a sterol, a sphingolipid, or a sphingolipid-sterol complex, helping to explain the complexity of the phenotypic analysis. There are various ways to interpret the enhancement of phenotypes that was observed. For example, in *erg4*Δ and *sur2*Δ single mutant cells Pdr12p shows substantial activity, but in *erg4*Δ*sur2*Δ double mutants, activity is lost. Pdr12p might require interaction with sterol-sphingolipid complexes for full activity. The interaction could be reduced because of a stronger change in shape of the complex due to the combination. The complex might adapt a different tilt in the membrane due to the two mutations. Molecular dynamics studies suggest that sphingomyelin binding to cholesterol controls its tilt in the lipid bilayer (Aittoniemi *et al.*, 2006). Alternatively, the combination of the *erg4* and *sur2* mutations could affect the equilibrium between the free lipids with sterol-sphingolipid complexes any component affecting Pdr12p activity.

4.4.5 Structural compatibility of sterols and sphingolipids and evolution

In order for sterols and sphingolipids to function together, their structural compatibility had to be maintained through evolution? Strikingly, there was one outlier from the lipid analysis of the double *erg* deletion mutants (Fig. 4.2). The sphingolipid pattern in the *erg5*Δ*erg6*Δ double mutant was more similar to wild type than the corresponding single mutants. The double mutation is "sphingolipid neutral". The *ERG5*

and *ERG6* genes are responsible for changes in the sterol side chain, the principle difference in the biosynthetic pathways of cholesterol and ergosterol. The two genes are linked in *S. cerevisiae*. This suggests that the *ERG5* and *ERG6* genes could have been inherited or lost together during evolution without causing major sphingolipid changes, allowing a co-evolution of sphingolipids and sterols.

Some organisms do not synthesize sterols, but receive them from their diet. Two particularly well studied systems are *D. melanogaster* and *C. elegans* (Matyash *et al.*, 2001;Silberkang *et al.*, 1983). Experiments with *Drosophila* did not detect any major changes in glycerophospholipid head groups or acyl group composition when grown with different amounts of cholesterol (Silberkang *et al.*, 1983). Sphingolipids were not examined in this study. No information is available yet from either system about the lipid composition of these organisms when they are grown using different sterols. It is possible that a similar mechanism as seen here for yeast could be used to adjust membrane composition in response to sterol content.

4.4.6 Lipids and sensitivity to drugs

This study also shows that sterol and sphingolipid composition can affect how a cell responds to a drug or inhibitor. Several examples are shown here (Supplementary material 4.3), most prominently, the hypersensitivity of the *erg2*Δ*scs7*Δ double mutant to caffeine and rapamycin, and the *erg4*Δ*sur2*Δ double mutant to sorbic acid (Fig. 4.4D), the latter explained by changes in the activity of the weak acid transporter Pdr12p. Pdr12p belongs to the superfamily of ABC-transporter and interest in this class of proteins is

enormous due to their prominent ability to confer multidrug resistance (MDR) in cancer cells in humans, as well as drug resistance in major microbial pathogens. Various lines of evidence have indicated the multiple interfaces between lipid homeostasis and drug resistance. In addition to alterations in membrane permeability as a consequence of changes in lipid composition, PDR transporters and drug resistance may be functionally affected by specific lipids (Gulshan and Moye-Rowley, 2007). Using inhibitors to selectively block sphingolipid biosynthesis in various *erg*-null mutants in *Candida albicans*, Mukhopadhyay and co-workers demonstrated that membrane sphingolipid-ergosterol interactions are important determinants of multidrug resistance conferred by Cdr1p (Mukhopadhyay *et al.*, 2004). This study corroborated these previous findings. In addition, this work provides fine details of the molecular species of sterols and sphingolipids and how their unique interactions affect the function of an ABC-transporter, as well as further mechanistic insights on how exquisite sterol-sphingolipid interactions affect other proteins and/or signalling pathways (H. Riezman, Guan *et al.*, under revision).

The extent to which this paradigm can be extended to higher eukaryotes, particularly humans is not presently clear, but it is evident that genetic factors, such as polymorphisms of multidrug resistance transporters, and diet affect sensitivity and effects of certain drugs. It is highly intriguing that "polymorphism" of sterols and sphingolipids could play an important role in these variations in the population and the implications of pharmacolipidomics, which is defined the application of functional lipidomics to diagnosis, treatment, and monitoring of pathophysiological errors in lipid metabolism and

signalling (Prestwich, 2005), are rather provocative. Furthermore, the findings in this work provide evidence of an exquisite specificity of interactions between sterols and sphingolipids in living cells that is critical for cellular functions. Specifically, it was demonstrated that functions of different proteins are altered by changes in specific changes in sterols and sphingolipids species of the cells, corroborating the role of lipids in modulating protein functions. The highly unique nature of lipid-protein relationship supports the possibility of modulation of membrane lipid as a potential therapeutic approach (Escriba *et al.*, 2008).

Prior to the emergence of lipidomics, most studies had focused on bulk membrane lipids, and commonly examined lipids in a highly targeted class-specific fashion (e.g. sphingolipids) without considering structural variants (e.g. hydroxylation or headgroup modifications). In this work, the genetic study is supported by the lipidomic and transcript data (Fig. 4.2 and Supplementary material 4.5), providing the first insights on a systems level scale on the intimate interaction of membrane lipids, which appear to be highly specific and are crucial for proper function of a cell.

Chapter 5. High Resolution and Targeted Profiling of Glycerophospholipids and Sphingolipids in Extracts from *Drosophila melanogaster*[4]

[4] The results described in this Chapter is included in the following manuscript:
Kohler K, Brunner E, **Guan XL,** Boucke K, Greber UF, Mohanty S, Barth J, Wenk MR and Hafen E. A combined proteomic and genetic analysis identifies a role for the lipid desaturase Desat1 in starvation induced autophagy in Drosophila. **Autophagy** (Under Revision).

5.1 Introduction

In *Drosophila melanogaster*, many molecular genetic studies have been carried out, particularly in embryogenesis, development, differentiation, signalling, cell cycle and in recent times in cancer and metastases studies (Busser *et al.*, 2008;Crozatier *et al.*, 2007;Edgar and Lehner, 1996;Hardie and Raghu, 2001;Jacob and Lum, 2007;Nusslein-Volhard and Wieschaus, 1980;O'Farrell *et al.*, 1989;Tapon, 2003;Tenenbaum, 2003;Weaver and Krasnow, 2008). Indeed, many studies in *Drosophila* have contributed to our current understanding of lipid signalling and functions in these diverse biological functions (Acharya *et al.*, 2004;Brill *et al.*, 2000;Chen *et al.*, 2007;chi-Yamada *et al.*, 1999;Herr *et al.*, 2004;Milligan *et al.*, 1997;Phan *et al.*, 2007;Rohrbough *et al.*, 2004;Stocker *et al.*, 2002), and will continue to further improve our knowledge on lipid biology, and provide new insights on the functional significance of lipid diversity and differential regulation between organisms.

Despite the effort to provide high quality genome annotation after the complete sequencing of the fly genome (Drysdale, 2003), many lipid enzymes and regulators are yet to be biochemically and functionally characterised. Nonetheless, the relative ease of genetic manipulation and the increasing availability of mutant libraries, as well as many previously established models for diverse biology makes *Drosophila* an important model organism to study enzymes and regulators involved in lipid biosynthesis and lipid functions (Rohrbough *et al.*, 2004;Cherry *et al.*, 2006). The development of sensitive techniques, such as mass spectrometry, therefore makes reverse genetics an attractive approach for systematic *in vivo* analysis of lipid biology.

Few reports are available on the measurements of fly lipids and these are rather fragmented (Table 1.5). Furthermore, they fail to provide a global view on the lipidome of the fly (Fyrst *et al.*, 2004;Gamo *et al.*, 1999;Rao *et al.*, 2007;Rietveld *et al.*, 1999;Seppo *et al.*, 2000;Stark *et al.*, 1993a;Stark *et al.*, 1993b;Fyrst *et al.*, 2008). In this Chapter, lipids from *Drosophila* was isolated and the workflow described in Chapters 2 and 3 (Guan *et al.*, 2006;Guan and Wenk, 2006;Guan and Wenk, 2008) was adopted to profile and quantify major glycerophospholipids and sphingolipids (Fig. 3.1) in wild type larvae and a mutant deficient in a desaturase encoded by the gene *DESAT1* (*desat1*-/-). Interest in this mutant stems from its isolation in a screen for fat body proteome associated with starvation-induced autophagy. Work is currently in progress to provide further biochemical and molecular insights into the function of *DESAT1*, which have not been characterised previously (Kohler *et al.,* in preparation).

5.2 Materials and Methods

5.2.1 Fly stock

All fly materials described in this Chapter were kindly provided by Irena Jevtov and Katja Kohler from the laboratory of Ernst Hafen at ETH, Zurich, Switzerland. The analysis of imaginal discs, kindly provided by Marcos Gonzalez from the University of Geneva, Switzerland, was mentioned but not described.

5.2.2 Lipid extraction

10mg (dry weight) of fly material (head or larvae) were homogenized in 100μL of ice-cold phosphate buffered saline using a motorised hand-held pestle. 400μL of methanol was added and the homogenisation was repeated, followed by the addition of

200µL of chloroform. 0.5µg of C19-Cer, 15µg of di24:0-GPCho, 15µg of di14:0-GPEtn, 0.75µg of di14:0-GPSer, 0.75µg of di14:0-GPGro and 2µg of di8:0-GPIns were added as internal standards. The mixture was vortexed hard for one minute and incubated on a thermomixer at 4°C, at 1000rpm for 2 hours, with intermittent vortexing. Debris was pelleted by centrifugation and the supernatant was transferred to a fresh tube. The pellet was re-extracted once more with 300µL of chloroform-methanol (1:2, v/v) with 30 minute incubation. The supernatants were pooled and 450µL of chloroform and 300µL of water were added. The mixture was vortexed hard for one minute, followed by centrifugation at 9000rpm for two minutes at 4°C. The organic phase was collected and the aqueous phase was re-extracted with 750µL of chloroform and the organic phase was pooled to the first extract and dried under liquid nitrogen. The dried lipid film was resuspended in 800µL of chloroform-methanol (1:1, v/v) and a 400µL aliquot was placed in a separate tube for alkaline hydrolysis treatment, while the remainder was used for subsequent mass spectrometry analysis.

A fraction enriched in sphingolipids was obtained by mild alkaline hydrolysis which degrades ester linkages found in many glycerophospholipids (Brockerhoff, 1963). To achieve this, the extract was adjusted to chloroform-methanol-water, (16:16:5, v/v/v). Glycerophospholipids were deacylated by 400µL of 0.2N NaOH and incubation at 30°C for 90 minutes. 400µL of 0.5M EDTA was added and the samples were neutralized with 1N acetic acid. 400µL of chloroform was added and the mixture was vortexed for one minute, followed by centrifugation at 9000rpm for two minutes at 4°C. The lower organic phase was collected and dried under nitrogen.

5.2.3 Lipid analysis by ESI-MS

ESI-MS was performed using a Waters Micromass Q-Tof micro (Waters Corp., Milford, MA) mass spectrometer as described in Chapters 2 and 3, except that the scan range was limited to m/z 400 – 1000. Lipid extracts were reconstituted in 800μL of chloroform-methanol (1:1, v/v), and further diluted two-fold before analysis. For differential profiling of WT and mutant MS spectra, plain text files obtained from MassLynx were loaded into Matlab (The MathWorks Inc., Natick, MA) for processing (Guan *et al.*, 2006, See Chapters 2 and 3).

Tandem mass spectrometry for characterisation/identification as well as quantification of lipid molecular species was performed using precursor ion scanning (PREIS), neutral loss scanning (NL) and multiple-reaction monitoring (MRM) respectively with an Applied Biosystems 4000 Q-Trap mass spectrometer (Applied Biosystems, Foster City, CA), as described in Section 2.2.6. Results are expressed as normalized intensities based on relevant internal standards, with the exception, for transitions based on parent → fatty acyl fragments, the normalized value is derived by the signal of each lipid transition divided by the sum of all transitions.

5.2.4 Statistical analysis

Comparison of the wild type and *desat1*-/- mutant was performed using the mean of at least 3 independent samples ± standard error of the mean (SEM) from individual samples. Statistical significance between wild type and mutant flies was determined using Student's t-test.

5.3 Results

5.3.1 A simple and rapid method to isolate and profile polar lipids from *D. melanogaster*

Chloroform-methanol extracts of lipids were obtained from various fly parts, including whole flies, heads and larvae. Figure 5.1A shows a typical negative ion mode ESI-MS profile of wild type fly heads. The most prominent ions represent major glycerophospholipid species which ionize efficiently in negative mode. The inset shows a fatty acyl profile, derived by intra-source fragmentation of the lipids. A wide range of chain length for the fatty acids are present in the mixture, including odd chain fatty acids, which are in low abundance. Major fatty acyls are C16 and C18, with zero to three double bonds, consistent with previous reports based on gas chromatography mass spectrometry and fast atom bombardment mass spectrometry (Gamo *et al.*, 1999;Stark *et al.*, 1993a;Stark *et al.*, 1993b;Yoshioka *et al.*, 1985).

Figure 5.1B shows a MS profile of a sphingolipid enriched fraction after mild alkaline hydrolysis. It should be noted that sphingolipids ionise efficiently in both ESI negative and positive modes. Although the measurement of phosphorylethanolamine ceramide (PE-ceramide) has been previously reported (Rao *et al.*, 2007), limited information is available on the spectra of molecular species that exist and the detailed fragmentation patterns. Nonetheless, based on the simple nitrogen rule (McLafferty and Turecek, 1993;Han and Gross, 2005a;Guan and Wenk, 2008) since deprotonated molecular ions of ethanolamine sphingolipids have odd nominal masses due to the presence of two nitrogen atoms, while ions of ethanolamine glycerophospholipids have even nominal masses, it is predicted that the signals at m/z 631 and 659 in Figure 5.1A

are PE-ceramides, which is consistent with the fact that these signals are retained after alkaline hydrolysis (Figure 5.1B).

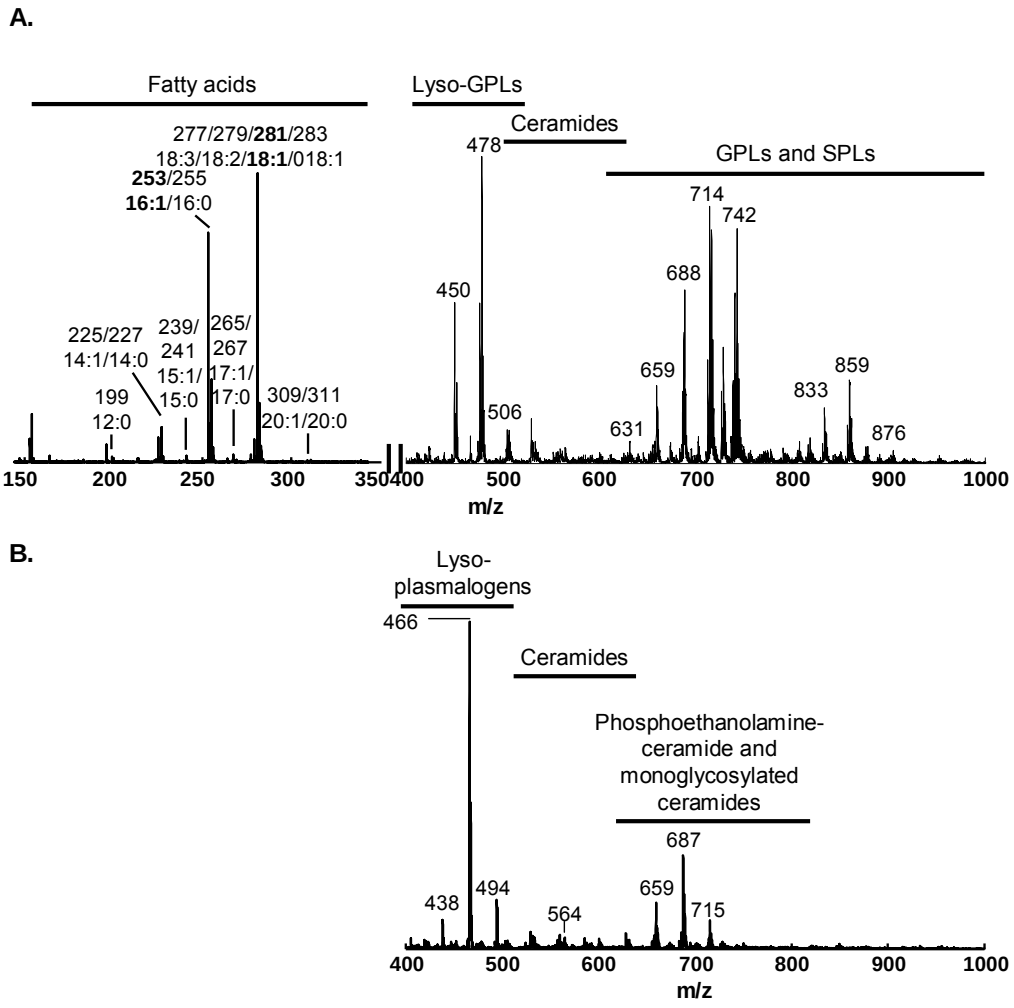

Figure 5.1 Glycerophospho- and sphingo- lipid profiles of heads of *D. melanogaster*.
Typical fatty acyl (A, left) glycerophospholipid (A, right) and sphingolipid (B) profiles of wild type (WT) *Drosophila* heads. Fatty acyl profile (A, left) is obtained from ESI-MS intra-source fragmentation of a total lipid extract.

5.3.2 Comparative lipidomics of WT and *desat1*-/- *Drosophila* larvae by non-targeted profiling

Kohler and co-workers isolated *desat1* in a screen for fat body proteome that is associated with starvation-induced autophagy. Figure 5.2A and B shows the single stage profiles of total lipid extracts from wild type and mutant larvae with homozygote deletion

of *desat1* (*desat1*-/-). *DESAT1* encodes for a fatty acyl CoA desaturase, which catalyzes the desaturation of saturated fatty acyls to monounsaturated fatty acyls (Fig. 5.2), some of which are precursors in the production of unsaturated hydrocarbons in position 7 that play an important role in mating behaviour (Labeur *et al.*, 2002). In mouse, four isoforms of steaoryl CoA desaturase (*scd1-4*) has been reported (Miyazaki *et al.*, 2006;Ntambi *et al.*, 2004;Parimoo *et al.*, 1999), while in *Drosophila melanogaster*, two isoforms, *desat1* and *desat2*, have been annotated.

A differential profile which displays differences in ion response between the *desat1*-/- and wild type conditions is shown in Figure 5.2C. Overall, the differences in profiles are dramatic. Although the substrates for Desat1 are hydrocarbons, these are precursors for more complex lipids, such as glycerophospholipids and sphingolipids, as well as glycerolipids. Furthermore, in mice knockout models of *scd1* and *scd2*, alterations in lipid metabolism and levels have been reported (Miyazaki *et al.*, 2005;Miyazaki and Ntambi, 2003;Miyazaki *et al.*, 2000;Xu *et al.*, 2007).

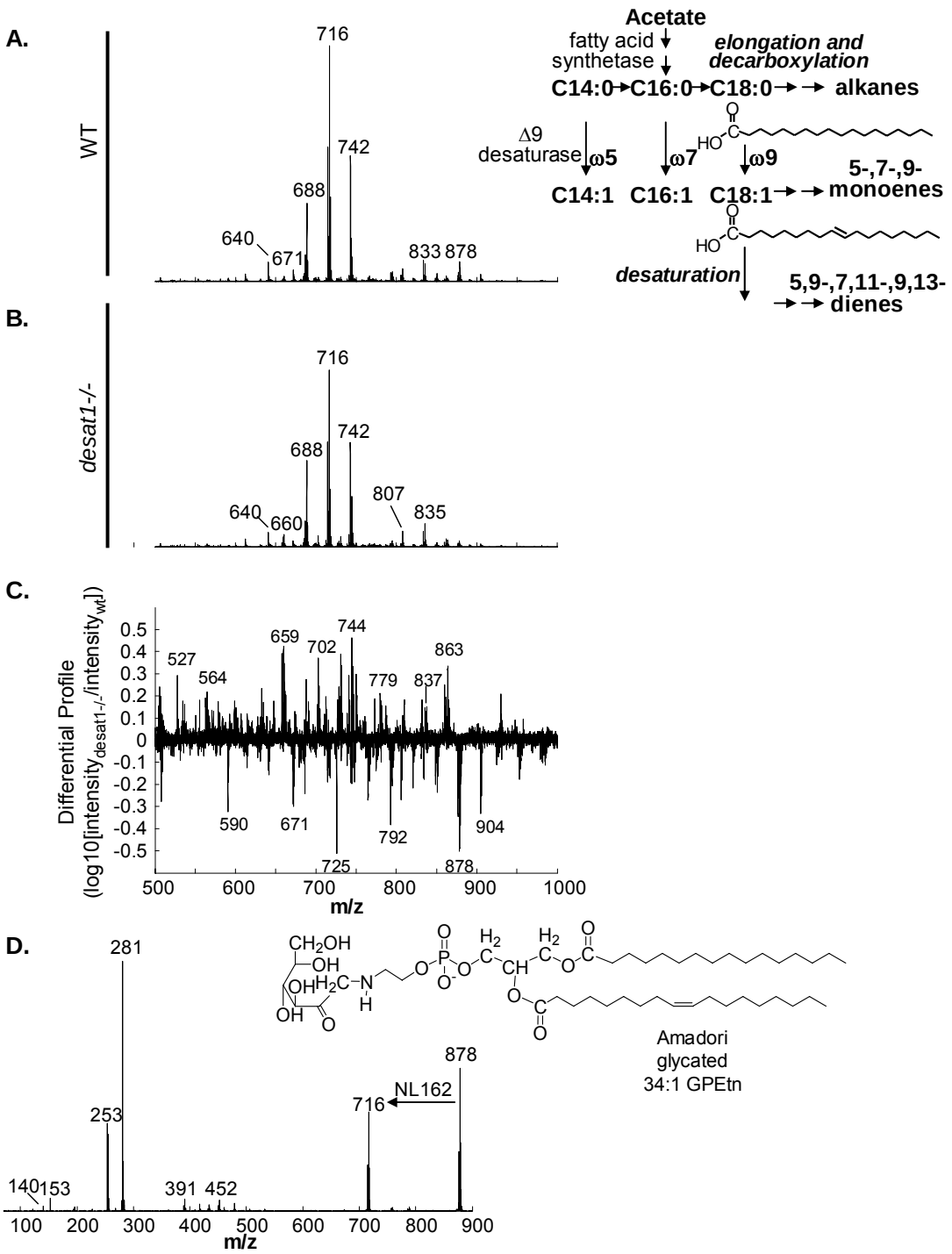

Figure 5.2 Changes in lipid profiles in *desat1* deficient fly larvae and identification by ESI-MS/MS. Fly larvae were extracted using chloroform-methanol and analysed using negative ion mode ESI-MS. (A) Averaged normalized spectra from wild type (WT) larvae. (B) Averaged normalized spectra from *desat1* deficient larvae (n=3). Inset represents the desaturation pathway in *D. melanogaster* (Dallerac *et al.*, 2000). (C) Differential lipid profile to compare differences in lipid composition between *desat1*-deficient and WT larvae. (D) MS/MS of m/z 878 and chemical structure of Amadori-glycated 34:1 GPEtn. It was noted that two batches of samples were analysed in triplicates, and some variations were noted. Therefore, we only characterised and report lipids that were consistently altered and further validation is required to determine the source of variations for the other ions.

Some ions can be tentatively assigned – upregulation of glycerophospholipids with higher degree of saturation for instance, GPIns (m/z 809, 837 for 32:0 and 34:0 GPIns respectively), as well as ceramides (m/z 536 and 564) and PE-ceramides (m/z 659) – consistent with the function of Desat1 as a fatty acid desaturase. To unambiguously identify the ions that were differentially regulated, further characterisation and identification was carried out using tandem mass spectrometry and collision-induced dissociation (CID) (Fig. 1.3).

5.3.3 Characterisation of lipids in WT and *desat1*-/- larvae

Two significant observations were made. Firstly, a strong downregulation of ions at m/z 878 and 904 was observed. Figure 5.2D shows the product ion spectra of the negative ion m/z 878. The distinct fragments are m/z 140, 153, 253 and 281 are diagnostic of phosphoethanolamine, glycerophosphate and the fatty acyls, 16:1 and 18:1, respectively. Strikingly, the daughter ion with m/z 716 corresponds to the m/z of 34:1 GPEtn and it is equivalent to a loss of 162 mass units from the parent ion, suggesting a loss of a sugar group. This would suggest that a glycerophosphoethanolamine is glycosylated and indeed, such glycated lipids of amine containing lipids do exist due to the formation of a Schiff base with sugars, although they are not frequently reported. Nakagawa *et al.* reported the structural characterisation of glycated GPEtn in the positive ion mode (Nakagawa *et al.*, 2005a), consistent with our data (not shown), which corroborate our findings that m/z 878 is a glycated GPEtn, or more commonly denoted Amadori-glycated GPEtn.

Ions corresponding to ceramides (m/z 536 and 564) and PE-ceramides (m/z 659, 687) accumulated in *desat1*-/- larvae. Product ion spectra in the negative ion mode of m/z 564 and 687 are represented in Figure 5.3B and C. Although descriptions of *Drosophila* sphingolipids had been previously reported (Acharya and Acharya, 2005;Acharya *et al.*, 2003;Fyrst *et al.*, 2004;Rao *et al.*, 2007;Seppo *et al.*, 2000), this work reports for the first time the characterisation of some of these lipids. Figure 5.3A shows the fragmentation pattern of a synthetic d18:1/18:0 ceramide (m/z 564), which is commonly found in mammalian cells. The ion, m/z 564, in the *Drosophila* extract, yields a completely different pattern as compared to the standard. However, annotation to the structure can be made and it is derived that this ion corresponds to a mixture of d14:1/22:0 ceramide (major) and d16:1/20:0 ceramide (minor). The fragmentation of m/z 687 yields a major fragment ion of m/z 140 in the negative ion mode, which potentially corresponds to the dehydrated ion of phosphoethanolamine headgroup. A similar pattern is observed with a qualitative PE-ceramide (d17:1/12:0) standard (data not shown). The structural information from a negative ion mode analysis is limited. Thus, the lipids were analyzed in the positive ion mode. The gain of proton would yield an ion at m/z 689 for the major PE-ceramide. The fragments ions of m/z 548, 208 and 236 are from the neutral loss of phosphoethanolamine, and the d14:1 and d16:1 sphingoid bases respectively (Figure 5.3D).

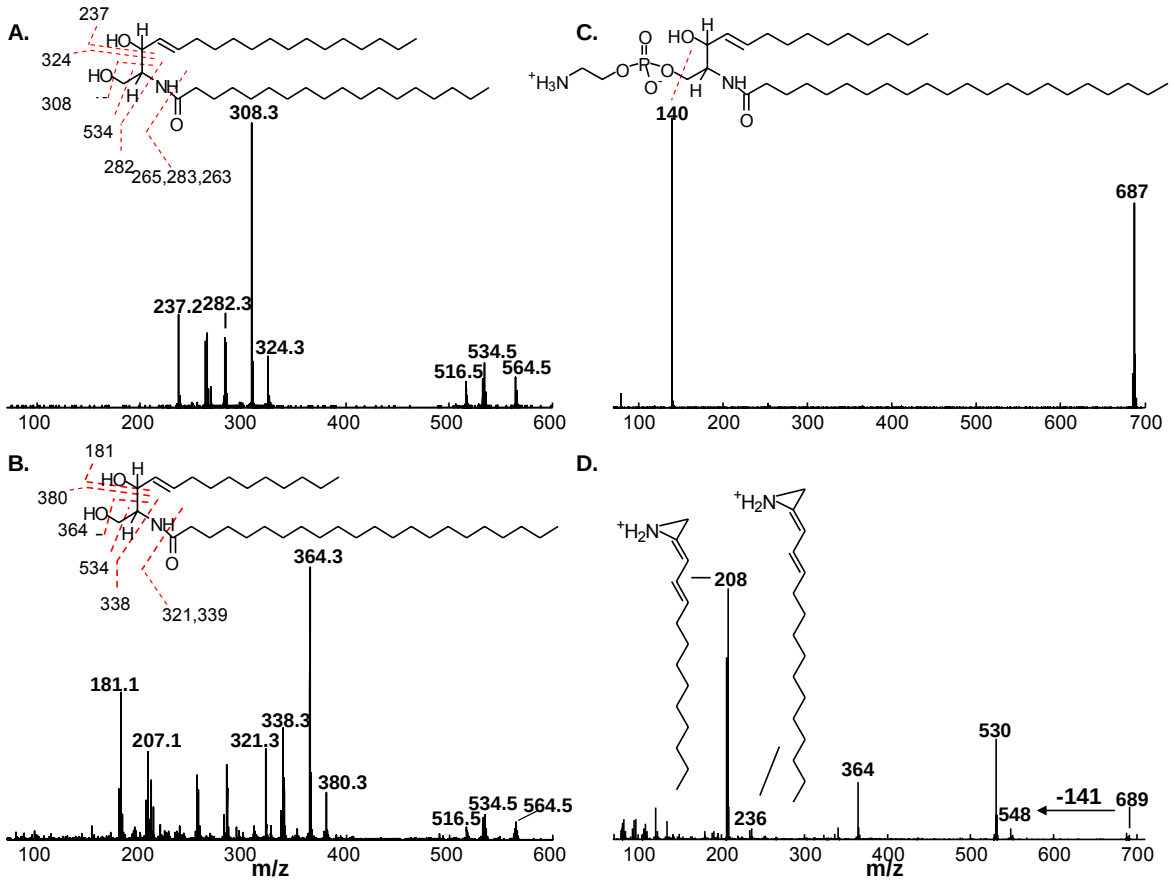

Figure 5.3. Characterisation of *Drosophila* sphingolipids by tandem MS.
Tandem mass spectrometry and collision-induced dissociation (CID) of (A) d18:1/18:0 ceramide standard; (B) m/z 564 and (C) m/z 687 in *Drosophila* larvae lipid extraction in the negative ion mode; and (D) m/z 689 in the positive ion mode. Structures in (A)-(C) represents possible fragmentation pathways for the various lipids.

In summary, these results indicate that disruption of the *DESAT1* gene leads to dramatic changes in glycerophospholipids as well as sphingolipids, most notably accumulation of glycerophospholipids containing saturated fatty acids, increase in both ceramides and PE-ceramides and decreased levels of glycated GPEtn. Note however that further detailed characterisation is required for some of the ions that were misregulated in the *desat1* deficient mutant.

5.3.4 Targeted quantification of glycerophospholipids and sphingolipids of WT and desat1-/- Drosophila larvae

Multiple-reaction monitoring (MRM) is a highly selective and sensitive (though biased) way for quantification of small molecules in complex mixtures and has the advantage of differentiating isobaric compounds.

5.3.4.1 Glycerophospholipids

Dallerac and co-workers previously demonstrated the substrate specificity of Desat1 for palmitoyl- and stearoyl- CoA (Dallerac *et al.*, 2000). Glycerophospholipids with combinations of acyl chains of either 16 and/or 18 carbons in WT and *desat1*-/- larvae were selectively measured by MRM and Figure 5.4A and B show the analysis of GPIns and GPEtn. For all classes of glycerophospholipids analysed (Fig. 5.4A and B, and data not shown), a change in the saturation profile of the fatty acyl composition of glycerophospholipids was observed. Levels of all molecular species with no double bonds in both acyl chains (e.g. 16:0/16:0) are elevated in the mutant and levels of all molecular species with both acyl chains containing monounsaturated fatty acids (e.g. 16:1/16:1) are decreased, consistent with the function of *DESAT1* (Fig. 5.2). However, levels of glycerophospholipids with a fatty acyl containing two double bonds (e.g. 16:0/18:2, 18:0/18:2) were found to be elevated, which may be compensatory effect by other desaturases.

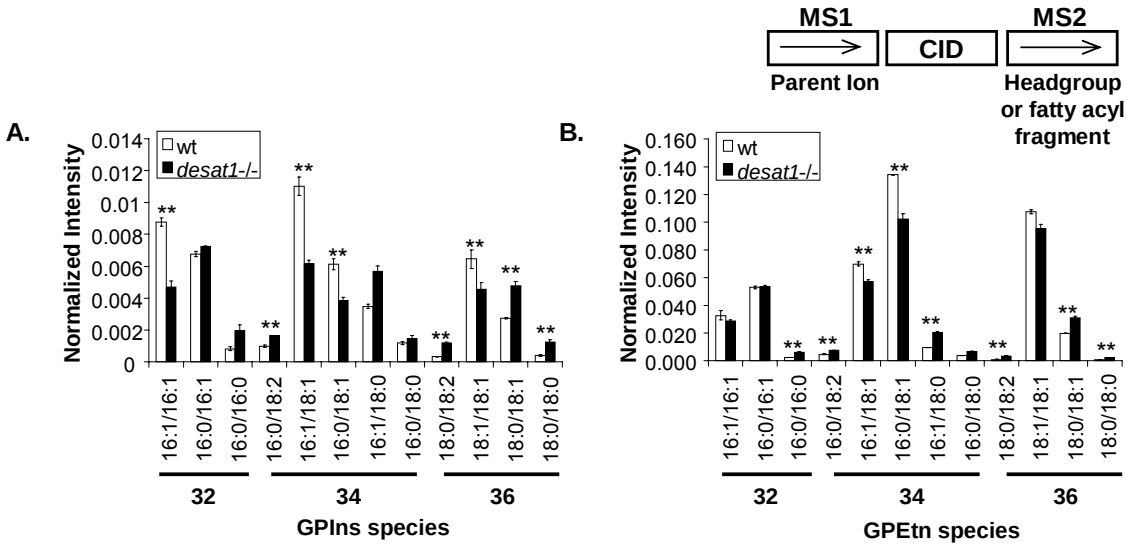

Figure 5.4 Quantification of glycerophospholipids in WT and *desat1*-/- larvae.
Multiple-reaction monitoring was used to quantify major glycerophospholipids in WT and *desat1*-/- larvae (n=3). Relative abundance of major GPIns (A) and GPEtn (B) are presented. Statistical significance between wild type and mutant strains was determined using Student's t-test. **p<0.05.

5.3.4.2 Sphingolipids

Quantitative analysis of *Drosophila* ceramides and PE-ceramides by ESI-MS has been described previously. However, these studies have been limited to sphingolipid containing the major sphingoid base d14:1. Furthermore, in the case of PE-ceramide, a transition based on the neutral loss of phosphoethanolamine in the positive ion mode was employed, and information on the sphingoid and fatty acyl compositions is lost. In this work, ceramides and PE-ceramides were extensively characterized and data for quantification of d14:1, d15:1 and d16:1-sphingoid base (sphingosine) containing sphingolipids is presented. This is however not an exhaustive list as sphingolipids with sphingoid bases containing no double bond or two double bonds (dihydrosphingosine and sphingadiene) are also found in *Drosophila* (Fyrst *et al.*, 2004;Fyrst *et al.*, 2008).

Figure 5.5A and B show the relative levels of the ceramide and PE-ceramide levels measured. Overall, there is a general increase across all the major sphingolipid species.

The degree of change is noted to be more pronounced for d14:1 sphingoid containing sphingolipids. A technical issue to note is, due to the lack of PE-ceramide standards, normalisation was made relative to a d18:1/19:0 ceramide standard.

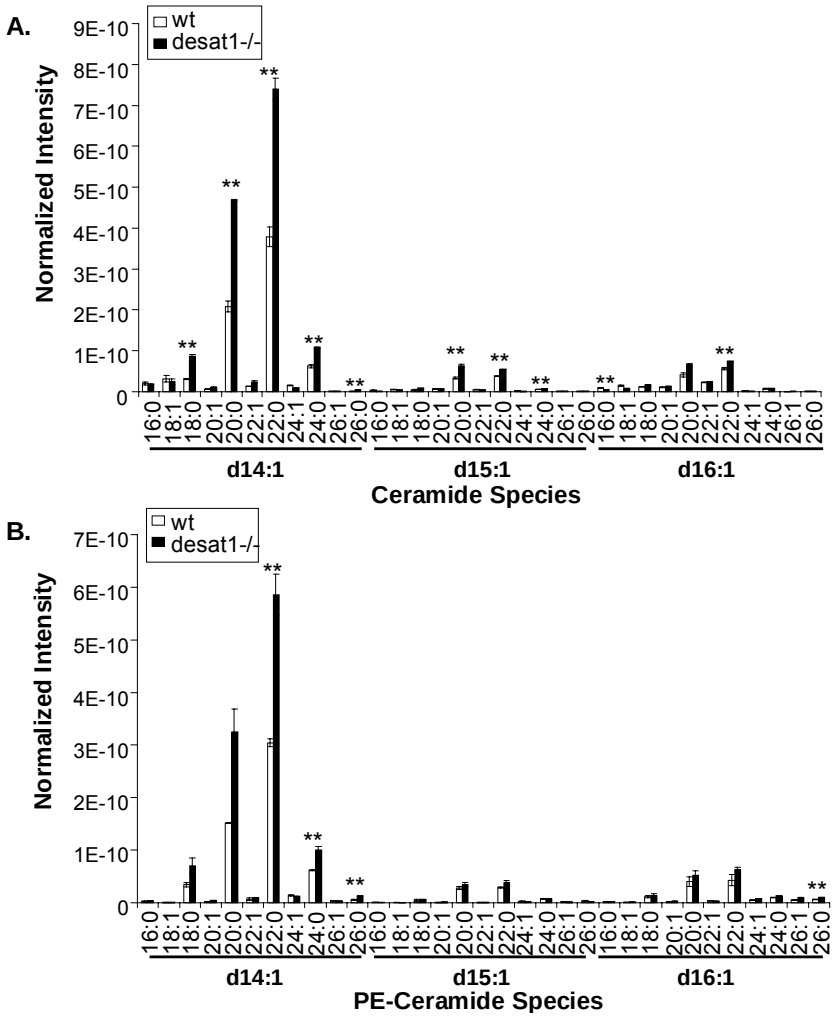

Figure 5.5 Quantification of membrane sphingolipids in wild type and *desat1* deficient larvae.
Data represent sphingosine-containing- (A) Ceramides and (B) PE Ceramides (n=3). Statistical significance between wild type and mutant strains was determined using Student's t-test. **p<0.05.

5.4 Discussion

A non-targeted profiling and targeted quantification approach described in Chapters 2 and 3 was adopted for lipidomic analysis of *Drosophila* lipids, with a focus on glycerophospholipids and sphingolipids. Using a rather simple extraction protocol it is

possible to obtain semi-quantitative information of overall changes in lipid levels (Fig. 5.2) as well as fully quantitative levels of a large number of lipids, including PE-ceramides (Fig. 5.5A).

It is not in the context of the present work to correlate the changes in lipid composition to the function of *DESAT1* in *Drosophila* without any further functional studies. However, the preliminary results from this study have demonstrated the powerful nature of the non-targeted profiling approach developed in this work, as illustrated by the detection of changes in ions which can be attributed to Amadori-glycated GPEtn. The presence of Amadori-glycated GPEtn is reported for the first time in *Drosophila*, the levels of which is lower in *desat1* deficient larvae. It was proposed that its formation is due to the exposure of GPEtn to glycation under hyperglycemic conditions *in vivo* (Lertsiri *et al.*, 1998;Pamplona *et al.*, 1995). While studies on Amadori-glycated GPEtn is currently limited and its precise function is not known, Amadori-glycated GPEtn has been associated with angiogenesis, lipid peroxidation, and lipoprotein uptake, and its level is found to be elevated in red blood cells and plasma of diabetic animals (Miyazawa *et al.*, 2008;Miyazawa *et al.*, 2005;Nakagawa *et al.*, 2005b;Oak *et al.*, 2000;Oak *et al.*, 2003). Manipulation of the levels of this lipid to reveal functions may be technically challenging since it may be formed from the non-enzymatic Maillard reaction. An attractive tool to probe to function of Amadori-glycated GPEtn was described Higuchi and co-workers, who demonstrated the *in vivo* inhibition of lipid glycation by pyridoxal 5'-phosphate (Higuchi *et al.*, 2006).

The comparative lipidomics approach provides evidence that deficiency in *desat1* in *Drosophila* larvae is distinct from *scd1* and *scd2* deficiency in mice (Dobrzyn *et al.*, 2005;Miyazaki *et al.*, 2005). In both *Drosophila* and mice, deficiency of the fatty acid desaturase resulted in reduction of monounsaturated C16 and C18 acyl chains of glycerophospholipids. However, the effect sphingolipid biosynthesis between the organisms was different. In *desat1*-/- larvae, a dramatic increase in ceramide and PE-ceramide levels was noted, and levels of these lipids (in the case of mice, the phosphosphingolipid is sphingomyelin instead of PE-ceramide), were similar, if not slightly lowered, in the epidermis of *scd2*-/-. Nonetheless, clearly, alterations in fatty acid desaturation resulted in pleiotropic effects at the level of lipid aberrations, as well as phenotypic changes. Notably, homozygote larvae of *desat1* deletion arrest in development at a very early larval stage (Kohler *et al.,* in preparation). A possible explanation is that Desat1 is involved in regulation of ceramide synthesis and ceramide is known to induce cell death and growth arrest (Obeid and Hannun, 1995;Low *et al.*, 2008). Furthermore, fatty acids and/or their derivatives are potent signalling molecules (Duplus *et al.*, 2000;Farrell and Merkler, 2008;Mansilla *et al.*, 2008;Serhan, 2005;Brock and Peters-Golden, 2007) and Desat1 functions to produce and maintain the balance of unsaturated and saturated fatty acids, which may be critical for cellular physiology.

In addition to discovery of novel metabolites by unbiased profiling, the partial characterisation of the *Drosophila* lipidome, using whole organism (whole adult fly and larvae) (Fig. 5.2 and data not shown), body parts (head and body) (Fig. 5.1 and data not shown) and organs (imaginal discs) (data not shown) was carried out in this study. In

addition, as opposed to previous work (Acharya *et al.*, 2003), the analysis described in this work allowed the discrimination of isobaric species of PE-ceramides based on their sphingoid base composition. However, the coverage of the fly lipidome is not exhaustive. For instance, glycosylated ceramides have not been included as these require separation by liquid chromatography due to isobaric complications. Nonetheless, the characterisation of major Drosophila glycerophospholipids and sphingolipids offers the possibility of targeted quantification using as little as two larvae for comprehensive profiling of these two major classes of membrane lipids. Together with non-targeted differential profiling, these methods offer a highly sensitive tool for discovery lipidomics.

The motivation for the establishment of the measurement of mammalian and yeast glycerophospholipids and sphingolipids applies to fly lipids – it is hoped that such a tool will allow us to characterise many annotated but biochemically uncharacterised lipid enzymes as well as a discovery tool for many applications. Imperative applications of the tool developed include (i) analysis of mutants of the sphingolipid pathway to 'isolate' sphingolipids which have not been characterised, such as ceramide ciliatine and (ii) extending the studies on functional interactions between membrane lipids to a fly model. In Chapter 4, it was demonstrated that in *S. cerevisiae*, cells sense alterations in sterols composition by altering their sphingolipid composition and levels. *Drosophila* is a sterol auxotroph and acquires this lipid from their diet. Manipulation of sterol levels, and composition, can be achieved through the feed, for instance using the ergosterol mutants described in Chapter 4, or by providing different sterol derivatives, which can be obtained commercially.

Chapter 6. Discussion and Conclusion

In the preceding chapters, I have described the development of a novel MS-based approach for non-targeted differential profiling of lipids and the advantage of the tool is the non-essential requirement for the prior knowledge of the chemistry of the lipids under investigation and is well-suited for surveying poor characterised or uncharacterised lipidomes (Fig. 1.4). The method is therefore generally applicable to analyze complex mixtures obtained from various biological sources, including mammalian cells/ tissues (Chapter 2), the budding yeast *S. cerevisiae* (Chapters 3 and 4) and the fruit fly *D. melanogaster* (Chapter 5). The lipid fingerprint of each organism is clearly unique (Fig. 6.1) and with a focus on glycerophospholipids and sphingolipids, the selective measurement of each unique chemical entity, based on the fine chemical details (for instance headgroup modifications, hydroxylations and fatty acyl heterogeneity), was developed. As discussed in Chapter 1, the diversity of membrane lipids is enormous and the number of lipids is estimated to be in the range of hundreds of thousand (Yetukuri *et al.*, 2008). The diversity of glycerophospholipids stems from the various headgroups and heterogeneity in the hydrophobic tails derived from different fatty acyls, alkyls and alkenyls and the permutations of their positions on the glycerol backbone (Fig. 1.1). Overall, the biosynthetic pathways of glycerophospholipids are well understood and generally well-conserved among species ranging from prokaryotes to eukaryotes (Lykidis, 2007;Dowhan *et al.*, 2004;Dowhan, 1997). The analysis of this class of lipids was in fact facilitated by the prior knowledge on the chemistry and biology of glycerophospholipids in different organisms as well as the availability of well-established methods (Brugger *et al.*, 1997;Han and Gross, 2005b;Taguchi *et al.*, 2005).

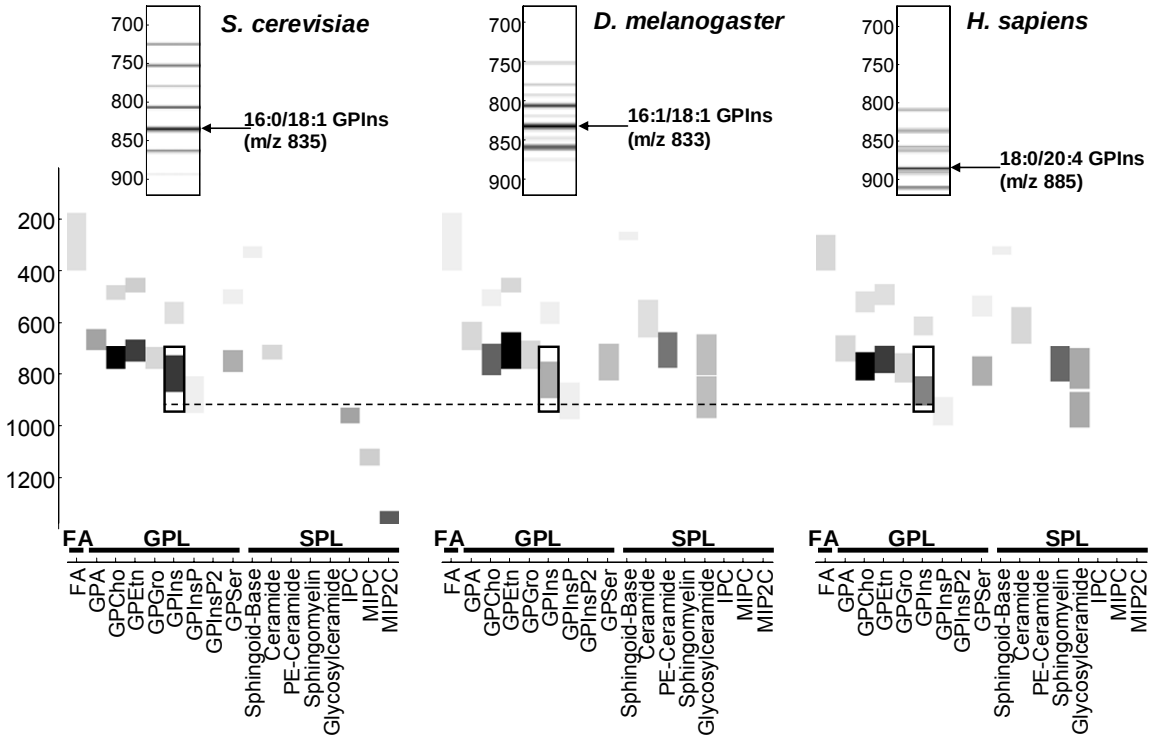

Figure 6.1 Theoretical portion of glycerophospholipids (GPL) and sphingolipids (SPL) inventory of various eukaryotic organisms.
The grey bars denote the typical range of fatty acyl compositions (varying chain length and degree of unsaturation) for a number of prominent GPL and SPL. The relative levels are represented by the intensity of the symbols (the darker the more abundant the respective lipid). The inset is an enlarged region which provides information of the various molecular species of GPIns lipids present in the yeast *S. cerevisiae*, the fruit fly *D. melanogaster* and mammalian cells, in this case human, *H. sapiens*. Different organisms have strikingly different lipid inventories. In the case of the yeast these are more saturated and shorter fatty acyls (dotted lines and ceramides with unique phosphoryl mannoside headgroups (IPC, MIPC, M(IP)2C). While in the fly, the fatty acyls are slightly longer (but shorter than in mammals) and the ceramides contain the unique phosphoryl ethanolamine headgroup. Abbreviations: FA, fatty acyl; GPL, glycerophospholipids; SPL, sphingolipids; GPA, phosphatidic acid; GPCho, glycerophosphocholine; GPEtn, glycerophosphoethanolamine; GPGro, glycerophosphoglycerol; GPIns, glycerophosphoinositol; GPInsP, glycerophosphoinositol-phosphate; GPInsP2, glycerophosphoinositol-bisphosphate; GPSer, glycerophosphoserine; PE-Ceramide, phosphorylethanolamine ceramide; IPC, inositolphosphorylceramide; MIPC, mannosyl inositolphosphorylceramide; M(IP)2C, mannosyl diinositolphosphorylceramide. This graphical representation is modified from (Wenk, 2006).

Sphingolipids, on the other hand, are found with few exceptions only in eukaryotic cells. While numerous reports are available for targeted analysis of sphingolipids (Han, 2002;Pettus *et al.*, 2004;Sullards and Merrill, Jr., 2001;Sullards *et al.*, 2007), these are typically restricted to mammalian tissues/ cells and not entirely

applicable to other organisms due to the distinct structural variants between different eukaryotes (see Section 6.1 onwards for a discussion on sphingolipid diversity and function). In this work, a subset of the sphingolipidome of the model organisms, *S. cerevisiae* and *D. melanogaster*, was characterised and a method for the relative quantification of each unique entity was established.

Model organisms are an invaluable biological reagent to study lipid function and with the development of a tool for system scale analysis of lipids, it is now possible to combine genetic-biochemical and functional investigations to extend and complement our knowledge of lipid functions at a very high resolution. In addition to their function in regulating membrane properties such as thickness and fluidity, the work in this thesis demonstrated for the first time an exquisite specificity of interactions between sterols and sphingolipids in living cells, specifically in *S. cerevisiae*, which is critical for cellular functions.

With the rapid advances in lipid biology and analytics, our knowledge of how distinct lipid and its interacting partners function in a systems context is crystallising and the field is one step closer to the endeavour of unveiling Nature's intention for the creation such enormous diversity among lipids. The next section of this Chapter is intended to discuss the diversity of sphingolipids structures and how they affect cellular functions because although their structures are distinct between organisms, this enigmatic class of lipids seems to be ubiquitous in many cellular processes and peculiarly, inference from model organisms such as *S. cerevisiae* has proven especially useful in our

understanding of sphingolipid metabolism and function in higher eukaryotes (Dickson, 1998).

6.1 Diversity of Sphingolipids

6.1.1 Biosynthesis of sphingolipids

The general structure of a sphingolipid comprise of a long-chain amino alcohol backbone (also known as a sphingoid base) to which a fatty acid can be covalently linked to form ceramide (Refer to section 1.1.1, Fig. 1.1B). Structural variants arise from head group substitutions as well as chain length differences and hydroxylation in the sphingoid base and fatty acyl chains (Fig. 1.1D and Fig. 1.2). Interestingly, these structural variations seem to serve as 'molecular signatures' of the three organisms we've discussed in this thesis, namely, mammals, the yeast, *S. cerevisiae* and the fruit fly, *D. melanogaster*. *S. cerevisiae* has the simplest sphingolipid inventory, with only three headgroup modifications reported, while in mammals and fly, more than a hundred different modifications exist (Merrill, Jr. *et al.*, 2007). In addition to the obvious headgroup differences of the sphingolipids, the biosynthesis of sphingolipids in fact diverge at steps upstream of headgroup modifications and structural variations in terms of degree of hydroxylation and desaturation of the ceramide backbone are found between the three eukaryotic organisms. Despite several differences, the overall biosynthetic machinery as well as the functions of sphingolipids is nonetheless considered highly conserved in eukaryotes (Dickson, 1998;Cowart *et al.*, 2007;Acharya and Acharya, 2005).

The first and rate-limiting early step in sphingolipid synthesis is similar and involves condensation of L-serine and acyl-coenzyme A (acyl-CoA) (Figure 6.2) by the enzyme complex, serine palmitoyltransferase, forming the sphingoid base, 3-ketodihydrosphingosine (3-KDS). 3-KDS is reduced into dihydrosphingosine (DHS) by a 3-KDS reductase. In yeast, DHS can be phosphorylated or hydroxylated to form DHS-1-phosphate and phytosphingosine (PHS) respectively, and the latter is the primary sphingoid base. The enzyme responsible for sphingoid base hydroxylation is Sur2p (Haak *et al.*, 1997). Both DHS and PHS are condensed with a very long chain fatty acid (typically C24 and C26) to make dihydroceramide and phytoceramide. In yeast, hydroxylation of the fatty acyl chain is common and is catalyzed by the hydroxylase, Scs7p (Haak *et al.*, 1997). Phosphoinositol is transferred to yeast ceramide catalyzed by the inositol phosphotransferase, AUR1, forming the first complex sphingolipid in the series, inositolphosphorylceramide (Nagiec *et al.*, 1997), which can be further modified with additional mannosyl and phosphoinositol moieties to form mannosyl inositolphosphorylceramide (MIPC) and mannosyl diinositolphosphorylceramide (M(IP)2C) respectively (details of the sphingolipid biosynthesis pathway in yeast can be found in Supplementary material 4.1).

In mammals and *Drosophila*, instead of forming phytoceramide, a double bond is introduced in dihydroceramide to form ceramide (Michel *et al.*, 1997). Furthermore, the primary sphingoid base in mammals and fly is formed from the deacylation of ceramide. In mammals, hydroxylation of sphingoid base and fatty acyl hydroxylation has been reported but is less common compared to yeast and tend to be organ and lipid specific.

For instance, phytoceramide is abundant in various organs including skin, kidney and brain and hydroxylated sphingolipids are uniquely abundant in myelin galactosylceramide and sulfatide, but not in free ceramides or other sphingolipids (Alderson *et al.*, 2006). However, in *Drosophila*, the presence of hydroxylated sphingolipids and the enzymes have not been reported to date, and in fact, many sphingolipids enzymes have been annotated in the fly based on homology, but not biochemically.

In addition to the difference in the hydroxylation and desaturation profiles, the acyl groups in yeast typically have long carbon chains (C24 and C26) while in mammals and fly, the N-acyl group range from 16 to 26 carbons. Another point of divergence of sphingolipid biosynthesis between the various organisms is at the level of headgroup modifications (Fig. 1.1 and 6.2). In fly and mammals, the major phosphosphingolipids are phosphoethanolamine and phosphocholine respectively. The enzyme that is responsible for the transfer of these headgroups is known as sphingomyelin synthase (SMS) or SMS-related protein (Tafesse *et al.*, 2006). Furthermore, in mammals and fly, in contrast to *S. cerevisiae*, sugar groups are directly linked to ceramide, giving rise to a sub-class of sphingolipids, known as glycosphingolipids (Merrill, Jr. *et al.*, 2007).With these differences in headgroup modifications and in mammals and fly, phospho- and glyco- sphingolipids are functionally distinct, a fundamental question is which category does yeast complex sphingolipids functionally belong to, since they comprise of both phospho- as well as sugar groups which are not found as separate moieties.

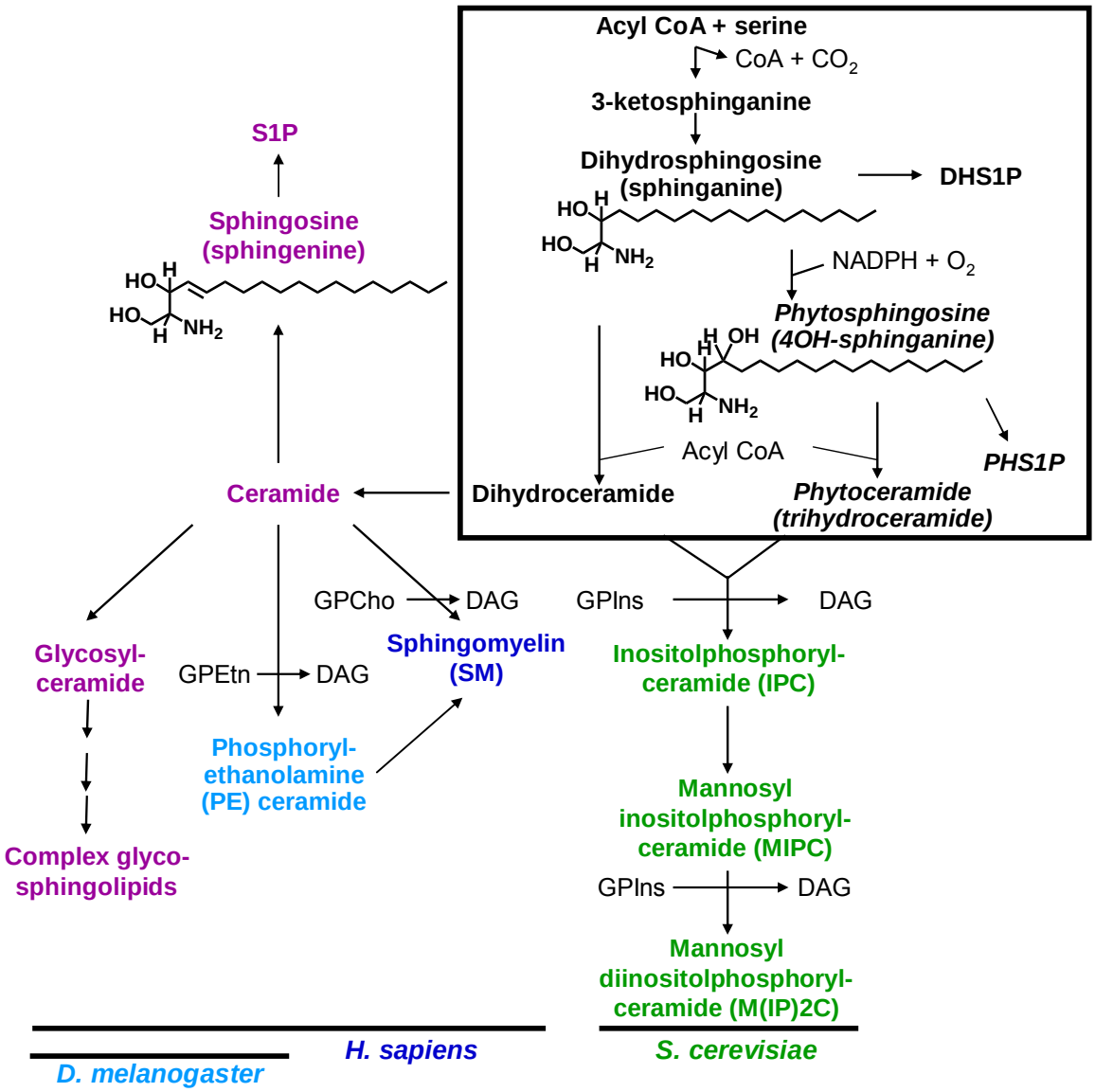

Figure 6.2 Simplified sphingolipid metabolic pathways of various eukaryotic organisms.
Metabolites in black have been reported in all three organisms, yeast, fly and humans, with the exception of those in italics, which have not been reported in fly and were not measured in this work. The colored fonts represent the unique sphingolipids found in distinct organism. It should be noted that although PE-ceramide biosynthesis may be a minor pathway for sphingomyelin synthesis, its presence has not been reported in mammals. In purple are the sphingolipid metabolites common in both the fly and mammals. Abbreviations: CoA, Coenzyme A; DAG, diacylglycerol; DHS1P, dihydrosphingosine-1-phosphate; GPCho, glycerophosphocholine; GPEtn, glycerophosphoethanolamine; GPIns, glycerophosphoinositol; NADPH, nicotinamide adenine dinucleotide phosphate; PHS1P, phytosphingosine-1-phosphate; S1P, sphingosine-1-phosphate.

6.1.2 Sphingolipid Structure and Functions

Clearly, unique structure of individual species of sphingolipids has distinct function, either by itself or through interaction with other lipids. For instance, in Chapter 4, it was demonstrated that the hydroxylation of either the sphingoid base or fatty acyl, and headgroup turnover affect interactions with sterols and have an impact on cellular functions in *S. cerevisiae*. Structural variations in lipids affect functions via various possible mechanisms, including changes in membrane biophysical properties and permeability, alterations in signalling processes, as well as direct and indirect effects on protein functions (Figure 6.3). In this section, I will review how hydroxylation and desaturation status and headgroup differences affect these processes and attempt to compare existing reports that support similar functions for sphingolipids that are found in the three eukaryotic organisms described in this thesis.

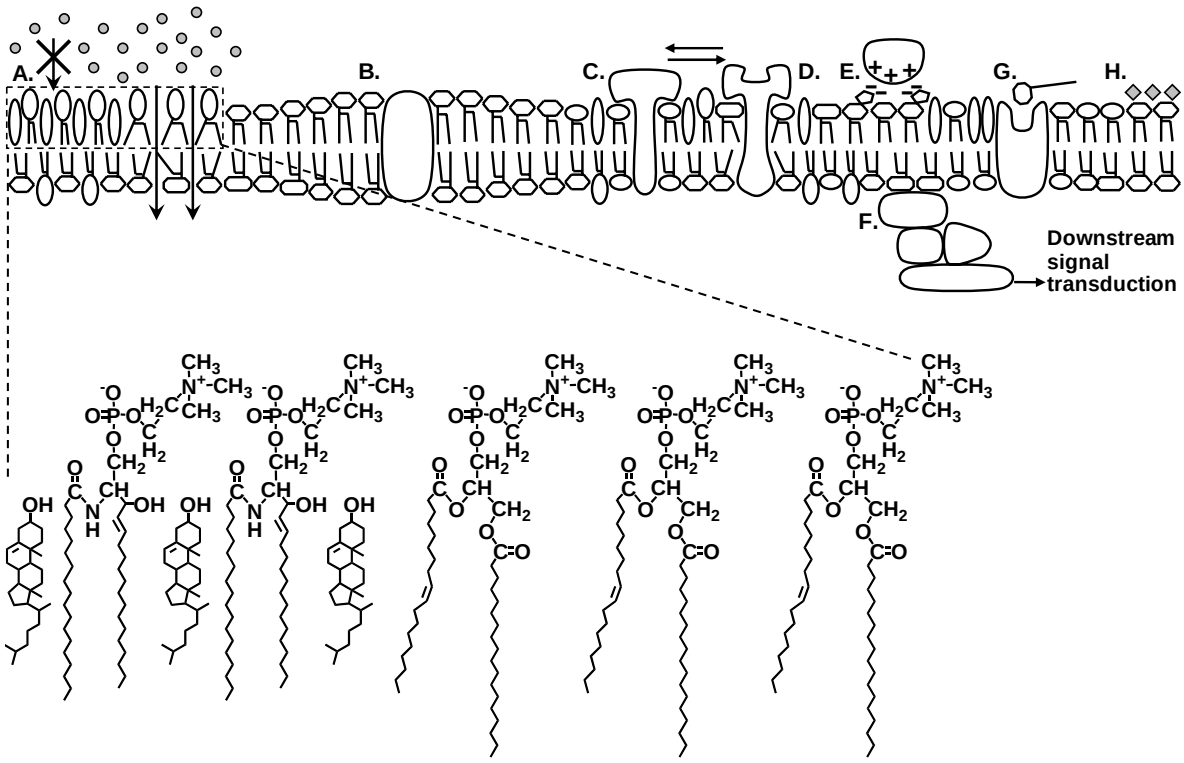

Figure 6.3 Membrane lipids, organisation and function.
Structural variations in membrane lipids affect their propensity to interact with each other and with other components including proteins and small molecules. The packing density and therefore membrane permeability is affected by the conformation of specific lipids. In addition, certain lipids, for instance sterols and sphingolipids exhibit a preference for partitioning into distinct domains, and are segregated from phospholipids (A). Inset shows the organisation of the three major classes of membrane lipids, sterols, sphingolipids and glycerophospholipids as reviewed by Harder and Simons (Harder and Simons, 1997). It was proposed that sphingolipids and intercalating cholesterol form a tightly packed microdomain in a glycerophosphocholine (GPCho)-rich environment. The GPCho regions are less densely packed and more fluid than are the sphingolipid-sterol-rich domains. Variations in lipid structures may affect protein functions through as they influence membrane thickness, which is important for the hydrophobic matching of integral membrane proteins (B). In addition, a lateral pressure profile is exerted by lipids on the two layers of biological membrane, which affects the conformational changes of proteins (C). The function of a protein may be regulated by its lipid microenvironment (D). Lipids may also function as cellular receptors. For instance, glycosylated sphingolipids, particularly gangliosides, serve as recognition sites through their highly decorated sugar headgroup and their charge (E). In addition, lipids affect cellular functions through their signalling roles, either by recruiting and regulating signalling complexes (F) or acting as a signalling molecule themselves (G). Membrane lipids affect drug action since interactions of certain drugs (or small molecules) with the cellular protective barrier are lipid-structure dependent (H).

6.1.2.1. Membrane organization and integrity

Lipid-lipid and lipid-protein interactions are thought to provide the underlying basis for membrane domain formation, with sterols and sphingolipids being particularly prominent components of these domains (Simons and Ikonen, 1997;Ramstedt and Slotte,

2006). Like compartmentalisation of cellular components by organelles to bring about localized effects, domain formation in membranes is also thought to segregate (and concentrate) biological activities. The association of specific proteins to distinct domains further suggest specific lipid requirement for protein functions. Although lipid domains have been a subject of debate and remain a challenging topic (Jacobson *et al.*, 2007;Munro, 2003;Pike, 2008), they nonetheless contributed to our knowledge and rekindled our interest in the interactions between sterols and sphingolipids in membranes and their effects on cellular functions . It should be noted that the propensity to form clusters/domains in biological membranes is not restricted solely to sterols and sphingolipids, for instance, polyunsaturated fatty acids (PUFA) and sterols possess a natural aversion that drives the lateral segregation of PUFA-containing glycerophospholipids into highly disordered domains away from cholesterol (Wassall *et al.*, 2004). Numerous biophysical analyses have been carried out to determine the structural determinants for sterol-sphingolipids interactions in the context of lipid domain formation and provide a starting point to understand how structural differences in sphingolipids affect membrane organisation and function.

Sphingolipids in general exhibit a preference for partitioning into domains in membranes which are proposed to be critical in the control of cellular functions (Goni and Alonso, 2006;Maggio *et al.*, 2006;Zhang *et al.*, 2008). The distinction between sphingolipids and glycerophospholipids is that the latter carries only fatty acyl carbonyl groups which act as hydrogen bond acceptors, while sphingolipids have both hydrogen bond donating and accepting capacities conferred by the hydroxyl and amide group

respectively. This property of sphingolipids has often been associated with their propensity for lateral organisation in membranes. Structural variations including headgroups (single hydroxyl for ceramide versus phospho- headgroup versus large assemblies of carbohydrates), hydroxylation of sphingoid base and fatty acyl chain as well as chain length asymmetry affect the partitioning of these lipids. With respect to hydroxylation and desaturation, like ceramide, dihydroceramide show similar membrane modulation properties in terms of stabilizing effect on domains and sterol displacing propensity (Alanko *et al.*, 2005). Phytoceramide, with an additional hydroxyl group on the sphingoid base, has additional hydrogen-bonding capability, which is associated with its effect of increased domain stability (Megha *et al.*, 2007). Indeed, early structural analyses revealed distinct conformational differences between the hydroxylated forms of ceramides which affect their packing and their hydrogen bonding network (Dahlen and Pascher, 1972;Pascher and Sundell, 1992).

Interestingly, the lipid envelope of the human immunodeficiency virus is selectively enriched in dihydrosphingomyelin, instead of the usual sphingomyelin (Brugger *et al.*, 2006). Dihydrosphingomyelin is proposed to form a more ordered domain with a higher melting temperature and confers resistance to oxidation, probably serving as a protective shield for the virus and its persistence. The effect of lipid composition and ordering in membranes on the stability and transmission of viruses further extend to other viruses including influenza virus (Polozov *et al.*, 2008). In fact, Pascher proposed in an early work on the apparent relation of ceramide hydroxylation to membrane stability against environment (Pascher, 1976). Notably, erythrocytes

occupying a stable environment has only one free hydroxyl group, while epithelial of small intestine, kidney and skin have three hydroxyl groups; and yeast cells, which have a non-regulated environment for cell growth, typically have three, if not four hydroxyl groups. These suggest that hydroxylation and desaturation of sphingolipids are important determinants of membrane integrity and may be a mechanism cells adopt to survive in their respective environments. Changes in the permeability of the barrier is often associated with alterations in solute and compound movement across membranes and partly attribute to cellular sensitivity or resistance to drugs, although other possible mechanisms may exist (See section 6.1.2.3). In addition to regulating membrane stability/ permeability, changes in membrane lipid composition may influence the curvature propensity of membranes, which is related to endocytic and fusogenic processes, as well as the lateral pressure profiles of the lipid bilayer (Cantor, 1999), thereby affecting protein functions (See section 6.1.2.3).

Clearly, the preferential segregation of specific lipids into distinct domains has been extensively reported, primarily based on biophysical analysis of artificial membranes and the functional relevance of these interactions is beginning to be revealed in biological systems. Studies on the phospho- headgroup size on intermolecular association and on sphingomyelin-cholesterol interactions and ordered domain formation demonstrated that phosphoethanolamine containing ceramide has a markedly lower affinity for cholesterol than sphingomyelin (Terova *et al.*, 2005). Sphingolipids concentrate into domains in plasma membrane which play a role as receptors and uptake of toxins and viruses (Fantini *et al.*, 2000;Pelkmans, 2005) (Section 6.1.2.3). The

individual interactions of sugar headgroups of glycosphingolipids may affect the efficiency of close lateral packing and form lateral domains which are spatially and functionally separated from sphingomyelin-cholesterol domains (Ramstedt and Slotte, 2006). On the other hand, the ordering effects of modifications of sterol structures in model membrane have been addressed and ergosterol tends to have a greater ordering effect (Urbina *et al.*, 1995;Xu *et al.*, 2001). While a significant part of our knowledge on sphingolipid metabolism is attributed to studies in yeast, most of our understanding on the biophysical interactions between lipids has been derived from model membrane systems employing the mammalian sterol and sphingolipid counterparts. In *Drosophila* and yeast, the major phosphosphingolipids contain phosphoethanolamine and phosphoinositol respectively, and the major sterol tends to be ergosterol (depending on the diet in the case of fly) and it would be of great relevance to incorporate these variants in biophysical investigations to represent the interactions between lipids from these model organisms. Probing for such interactions in cells will provide invaluable insight into the functional relevance. An attractive potential of capitalizing on the differences in lipid structures between organisms is the possibility to engineer the lipid structures by introducing enzymes that produces non-endogenous structural variants, especially since many of these enzymes have been cloned. Nonetheless, the existing studies that propose the segregation of distinct lipids into different domains support the specific interactions between cholesterol and unique variants of sphingolipids and while a neutral stand is taken with regards to the actual existence of lipid domains in biological membranes, it is proposed that the exquisite interactions is physiologically relevant, supported by the study described in Chapter 4. Moreover, the differential affinity between sterol and

sphingolipid variants may in part account for the coexistence of structural variations between different organisms which may contribute to conservation of functions.

6.1.2.2. Bioeffector functions of sphingolipids

Sphingolipids are well known for their functions as second messenger in signalling pathways for vital cellular processes including apoptosis, cell survival and aging. The yeast has provided numerous opportunities for understanding the functions of sphingolipids, particularly sphingoid bases, their phosphorylated products, and ceramides on diverse cellular processes, which appeared to be conserved in humans (Dickson, 1998). On the contrary, the signalling functions of complex sphingolipids have been largely derived from mammalian studies and our knowledge of the functions of complex sphingolipids in yeast is only beginning to be unravelled. The chemical structure of sphingolipids and their biological functions have been previously discussed (Dyatlovitskaya, 1998;Dyatlovitskaya, 2000). I will limit the discussion on the correlation between structure and bioeffector function of sphingolipid to growth inhibition and/or apoptosis induction, with emphasis on the structural variants between organisms, as one of the recurrent observations in this thesis and our published work based on metabolite profiling is ceramide accumulation in degenerating rat hippocampal neurons (Guan *et al.*, 2006) and mutant fly larvae that ceased growth (Chapter 5, Kohler *et al.,* in preparation). However, it should be noted that various stimuli induce the formation of these signalling lipids, which may mediate attenuation of cell growth and induction of apoptosis through several potential signalling pathways and though important, the function of sphingolipids as signalling molecules has not been adequately investigated in this work.

Enzymes of sphingolipid metabolism are intimately linked in an interconnected network that serves to regulate the levels of individual bioactive lipids and their metabolic conversion, serving as a rheostat that allows a rapid switch between functions (Maceyka *et al.*, 2002;Taha *et al.*, 2006). For example, ceramide (i.e. acylated sphingosine) and sphingosine are associated with cell growth arrest and are important regulatory components of stress responses and apoptosis. In contrast, phosphorylated products of sphingosine have been implicated in cellular proliferation and survival, illustrating how metabolic conversion result in structurally distinct lipids which act as a molecular switch between life and death (Fig. 6.4A). While ceramide induces apoptosis in cells (Bielawska *et al.*, 1993) the equivalent dihydroceramide species which lacks the double bond is inactive, or very weakly active (Karasavvas *et al.*, 1996). Dihydroceramide in this case is considered an inert compound which serves as an intermediate of ceramide metabolism, for instance, in the generation of the bioactive dihydrosphingosine-1-phosphate and ceramide (Fig. 6.2). Nonetheless, it should be acknowledged that dihydroceramide and ceramide differs in biophysical properties, which may attribute to the biological function of dihydroceramide in other aspects (See section 6.1.2.1). Although the double bond in ceramide appears to be important for its apoptotic activity, phytoceramide, which has no double bond but has an additional hydroxyl group compared to dihydroceramide, exhibit a greater potency in the induction of apoptosis than ceramide (Hwang *et al.*, 2001;Kyogashima *et al.*, 2008). These suggest that functionally, the major yeast ceramide, which is phytoceramide, is similar to mammalian and fly ceramide.

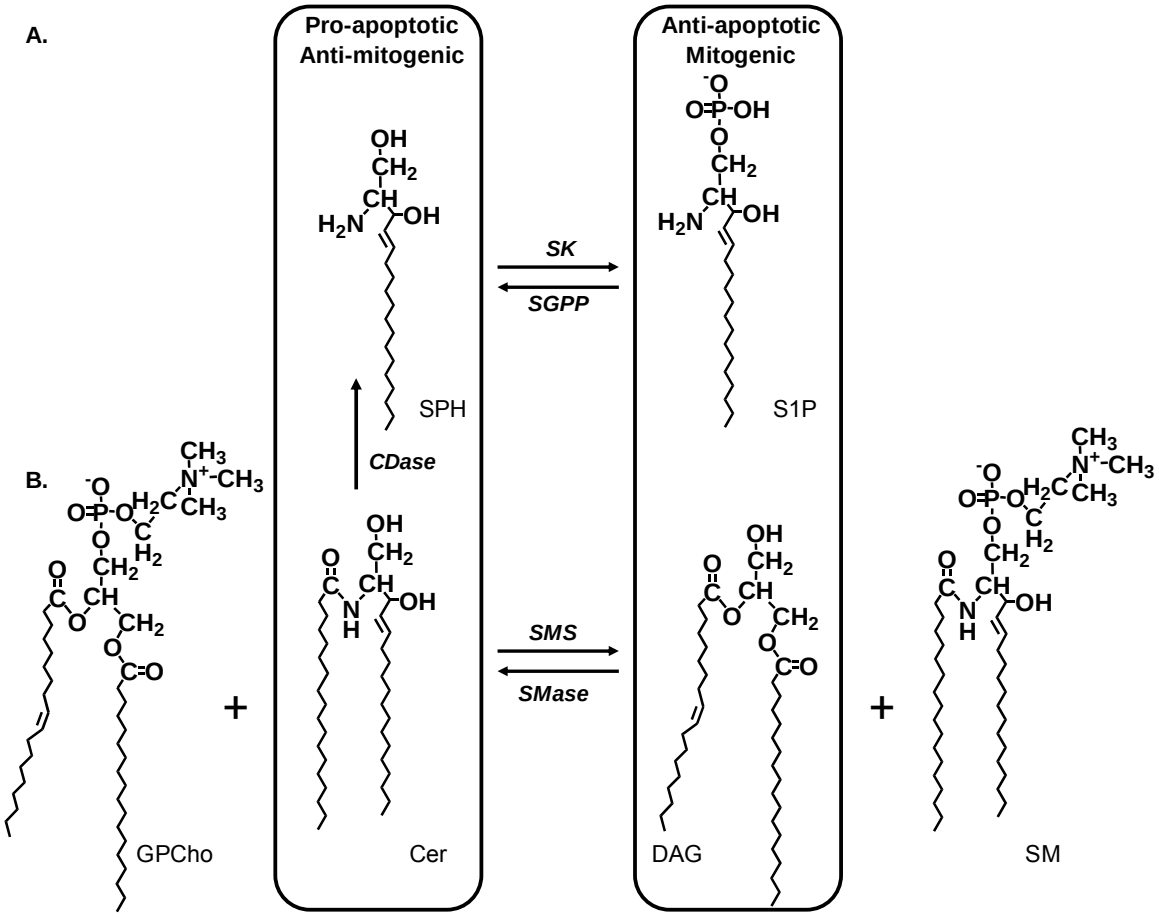

Figure 6.4 The sphingolipid rheostat in mammalian cells.
The metabolic conversion of sphingolipids generates metabolites with antagonistic functions, forming a rheostat system that controls the balance of life and death. Ceramide (Cer) is deacylated by ceramidase (CDase) to form sphingosine (SPH). Both Cer and SPH are pro-apoptotic mediators. SPH is phosphorylated by sphingosine kinase (SK) to form the anti-apoptotic and mitogenic sphingosine-1-phosphate (S1P) and the reaction can be reversed by sphingosine phosphate phosphatise (SGPP) (A). Sphingomyelin (SM) is formed by the transfer of the phosphocholine headgroup from glycerophosphocholine (GPCho) to Cer, catalysed by the enzyme, sphingomyelin synthase (SMS). The other product, diacylglycerol (DAG), formed from this reaction is mitogenic. The reverse reaction is catalysed by the enzyme, sphingomyelinase (SMase) (B).

The sphingomyelin cycle represents yet another molecular and cellular rheostat in the sphingolipid pathway with a role in the control of cellular proliferation and apoptosis (Fig. 6.4B). While ceramide is associated with attenuation of cell growth (Obeid and Hannun, 1995), diacylglycerol, a physiological agonist of protein kinase C, is associated

with mitogenesis (Rozengurt *et al.*, 1984). The formation of sphingomyelin is derived from the transfer of the phospho- headgroup, in this case, phosphocholine, from the glycerophospholipid, glycerophosphocholine, to ceramide, generating diacylglycerol (Fig. 6.2 and 6.4B). Therefore, in producing sphingomyelin, the reaction results in consumption of ceramide and production of diacylglycerol, possibly shifting the balance of growth-attenuation to growth promotion. Despite the differences in the phospho-headgroup, this signalling function is conserved between yeast and mammals (Cerbon *et al.*, 2005). However, although the deacylated form of sphingomyelin (lysosphingomyelin or sphingosine-1-phosphocholine) is known for its bioeffector function, for instance as a potent mitogen, neither the ethanolamine nor the inositol containing variants have been reported in *Drosophila* and yeast and if present, their functions are currently unknown. With the increasing availability of synthetic lipids, which includes sphingosine-1-phosphocholine, sphingosine-1-phosphoethanolamine, and sphingosine-1-phosphoinositol, a comparison of their *in vitro* functions is technically feasible.

6.1.2.3. Lipid-protein and lipid-small molecule interactions

In a general context, lipids regulate cellular functions through interactions with their interacting partners. The organisation of lipids biological membranes is likely to affect the functions of integral and peripheral membrane proteins at the very least. Apart from being one of the topological determinants of membrane proteins, the structures of lipids are critical for modulating membrane thickness. Based on the hydrophobic matching theory, it is suggested that the hydrophobic part of intergral membrane proteins has to be matched to the hydrophobic thickness of the lipid bilayer membrane in which they are embedded in and the degree of match affects protein function (Jensen and

Mouritsen, 2004). Furthermore, lipid molecules contribute to the lateral stress profile of the membrane layer, which is structure-dependent, and between the two lipid layers of a membrane bilayer, the catalogue of lipids is distinct, and this in turn leads to conformational changes in protein. Therefore, the mechanic coupling between lipids and proteins plays a regulatory role in protein functions.

In Section 6.1.2.1, I've discussed several aspects of lipid interactions and their organisation in biological membranes, and while it is still a subject of controversy if lipids are the driving forces for clustering of proteins into specific domains, or vice versa, early studies in T-cell signalling postulated such segregation function to concentrate certain proteins within domains which define zones for signal transduction, for instance. The specificity of this interaction between lipids and proteins can be illustrated by the preferential partitioning of CD40 into ceramide-enriched platforms while a CD40/45 chimera does not cluster in these regions, similar to CD45 (Bock and Gulbins, 2003). In Chapter 4, the localisation of two plasma membrane proteins, Tat2p and Can1p was examined. Although both proteins have been shown to be localized in microdomains of the plasma membrane in yeast (Umebayashi and Nakano, 2003;Malinska *et al.*, 2004), they exhibited completely different dependence on sterols and sphingolipids for their localisation (Supplementary material 4.6). In addition, numerous lines of evidence have implicated the direct association and potent regulation of proteins by specific lipids (Osenkowski *et al.*, 2008;Ledeen and Wu, 2006). This highlights the complexity and specificity of protein-lipid interactions in regulating protein localisation and functions.

Membrane lipids also serve as receptors and the structural signature of sphingolipids play a crucial role in their binding properties. Interactions between cell surface glycosphingolipids with lipids, proteins and/or glycans mediate cell-cell and cell-matrix interactions in multi-cellular organisms (Regina and Hakomori, 2008). Although yeast is a unicellular eukaryote, it does not necessarily mean that it lives as an isolated individual independent of other cells. In fact, yeast colonies are organised, multi-cellular structures which display dynamic cell-cell communication (Palkova *et al.*, 1997). However, direct cell-cell contact between yeast and a role of yeast (complex) sphingolipids in cell-cell communication has yet to be reported. The interactions of membrane lipids with the cell's surrounding environment can be further demonstrated by the entry of viruses, which have been reported to depend on the binding of envelope proteins on the surface of the pathogens to glycolipids with specific structural determinants on the host cells' surface (Aoki *et al.*, 2006;Neu *et al.*, 2008;Suzuki *et al.*, 1985). In addition, the glycosylated sphingolipid, globotriaosyl ceramide is a verotoxin receptor, and toxin binding is increased with hydroxylation of fatty acid, which is probably a determinant of cellular specificity of the toxin since hydroxylated sphingolipids are more abundant in the kidney (Binnington *et al.*, 2002). When pathogens and toxins bind to membrane sphingolipids, the hydrogen bond-based stability of membrane conferred by these lipids is compromised and serve as a potential invasion mechanism.

While many drugs are known to target lipid enzymes directly, and structural analogues of lipids have been designed for therapeutic purposes, an important aspect of

structural variations in membrane lipids is the effects on drug responses. In Chapter 4, it was demonstrated that cellular sensitivity to sorbic acid is affected by a mere difference in the position of hydroxylation of sphingolipids, which resulted in alteration in function of a membrane transporter that exports the weak acid (Fig. 4.5) and the role of lipids in regulation of multidrug resistance transporter was further discussed (Section 4.4.6). In fact, numerous studies in yeast have demonstrated distinct mechanisms for drug sensitivity/resistance which is associated with variation in sphingolipid structures. For instance, the antifungal action of DmAMP1, a peptide defensin produced by the plant, dahlia, involves interaction with sterols and sphingolipids, specifically M(IP)2C in yeast (Thevissen *et al.*, 2003). Other drugs which demonstrated sphingolipid-dependence for their action include the antifungal syringomycin E, and the antitumor drug, PM02734. Yeast mutants deficient in phosphoinositol transferase, Ipt1p, fatty acid elongases, Fen1p and Sur4p, as well as sphingolipid hydroxylases, Sur2p and Scs7p, are resistant to syringomycin, suggesting that the complex M(IP)2C with a very long chain fatty acid and phytosphingosine but not dihydrosphingosine is essential for interactions of the drug with the plasma membrane and its antifungal activity (Grilley *et al.*, 1998;Stock *et al.*, 2000;Hama *et al.*, 2000). In contrast, while the yeast mutant lacking the fatty acid hydroxylase, *scs7*Δ, is resistant to the antitumor drug, PM02734, deletion of other genes in sphingolipid biosynthesis, including *CSG2* and *SUR2* renders the cells sensitive to PM02734 (Herrero *et al.*, 2008). The striking contrast of the sphingolipid dependence on drug sensitivity/resistance of cyclic compounds demonstrates the exquisite interactions between small molecules with specific membrane proteins. In addition, in the case of PM02734, mammalian cells lacking FA2H, the homologue for fatty acid hydroxylase, are

reported to be resistant to the compound, suggesting the similarity in the function of hydroxylated sphingolipids the action of the drug in both yeast and mammals.

An interesting observation based on our genetic analysis of yeast deficient in various steps of sterol and sphingolipid pathways is the effects on the components of the Target of Rapamycin (TOR) signalling network (Guan *et al.*, under revision). TOR is a nutrient-regulated protein kinase that assembles into two distinct protein complexes, TOR complex 1 and 2 (TORC1 and TORC2). TORC1 is the target of caffeine and rapamycin in yeast both *in vivo* and *in vitro* (Wanke *et al.*, 2008), whereas TORC2 is not significantly inhibited by either drug. However, one of the double mutants, *erg2*Δ*scs7*Δ, which exhibits extreme sensitivity to these two drugs (Fig. 4.4B and Supplementary material 4.6), possesses normal TORC1 activity and expression of effector genes. Surprisingly, TORC2 activity and its effector genes are compromised in the mutant (Guan *et al.*, under revision). It is highly intriguing how the combination of sterols and sphingolipids results in a switch in the signalling complex targeted by a drug or inhibitor and affect how a cell responds to the compound. As inhibitors of mammalian TOR are currently in use to treat graft rejection and restenosis and are also tested in clinical trials for several human pathologies including cancers (Tsang *et al.*, 2007), it would be of great interest to determine how this observation translates to other organisms and these information on drug-membrane lipid interactions will provide additional insights to how lipids affect drug activities and help in drug target or even patient selection.

6.2 Conclusion and Future Perspectives

Lipids are a critically important class of metabolites, yet many of their functions remain poorly understood. The incremental advances in analytics, particularly mass spectrometry, are instrumental to lipid research. A novel analytical approach, based on mass spectrometry, for comparative lipidomics was developed. Specifically, the methodology encompasses non-targeted differential profiling of high resolution mass spectra, as well as targeted quantification of glycerophospholipids and sphingolipids from mammals, yeast and fly. The method is generally applicable to any biological system of interest and prior knowledge on the chemistry of the lipids is not required. However, the coverage of lipids analysed in this study is limited and requires alternative MS methods to probe other lipid classes such as sphingoid bases and sterol variants, although the latter was measured in this work by gas capillary mass spectrometry. Mass spectrometry-based analysis yields an extensive dataset on how much of a particular lipid species is present under a given condition, and allows the monitoring of the changes in the levels upon perturbation and identification of the associated biochemical pathways. However, this is a highly static view of the cellular lipidome and a wider perspective of the biological network that lipids are involved in should take into consideration of their relative organisation and their interacting partners. This would require integration of other tools such as optical imaging, genetics and biophysical methods. Indeed, genetics analysis, in combination of lipidomics, has provided evidence for the complex interactions between sphingolipids and sterols in cells. Further investigations are now required to provide mechanistic insights on this functional partnership. Since sterol structures and the most prevalent sphingolipid species differ between the organisms, an ongoing work is in progress (in collaboration with H. Riezman) to address how yeast cells respond when

they are genetically engineered to produce structurally distinct "non-self" sterols or sphingolipids, in terms of changes in their lipid composition as well as the effects on cellular function. Furthermore, the functional interaction between lipids can be addressed by manipulation of lipid enzymes, and therefore lipid levels, based on gene silencing in *Drosophila* or mammalian cell cultures. Through these series of investigations, it is hoped not only to address the structure-dependence of lipid interactions in biological membranes, but also the evolutionary and functional consequences of lipid diversity between organisms. Finally, this work described differences in lipids between various organisms, which to a certain degree, may be functionally conserved. It is envisioned that via the use of model systems including yeast and fly, and through the integration of extensive datasets from different fields, including lipidomics, genomics and proteomics, interaction networks can be constructed for which the complex biological processes in mammals, especially human, can be inferred.

Chapter 7. Bibliography

1. Acharya, U. and J.K.Acharya. 2005. Enzymes of sphingolipid metabolism in Drosophila melanogaster. *Cell Mol. Life Sci* 62:128-142.

2. Acharya, U., M.B.Mowen, K.Nagashima, and J.K.Acharya. 2004. Ceramidase expression facilitates membrane turnover and endocytosis of rhodopsin in photoreceptors. *Proc. Natl. Acad. Sci. U. S. A* 101:1922-1926.

3. Acharya, U., S.Patel, E.Koundakjian, K.Nagashima, X.Han, and J.K.Acharya. 2003. Modulating sphingolipid biosynthetic pathway rescues photoreceptor degeneration. *Science* 299:1740-1743.

4. Ahmed, S.N., D.A.Brown, and E.London. 1997. On the origin of sphingolipid/cholesterol-rich detergent-insoluble cell membranes: physiological concentrations of cholesterol and sphingolipid induce formation of a detergent-insoluble, liquid-ordered lipid phase in model membranes. *Biochemistry* 36:10944-10953.

5. Aittoniemi, J., P.S.Niemela, M.T.Hyvonen, M.Karttunen, and I.Vattulainen. 2007. Insight into the putative specific interactions between cholesterol, sphingomyelin, and palmitoyl-oleoyl phosphatidylcholine. *Biophys. J* 92:1125-1137.

6. Aittoniemi, J., T.Rog, P.Niemela, M.Pasenkiewicz-Gierula, M.Karttunen, and I.Vattulainen. 2006. Tilt: major factor in sterols' ordering capability in membranes. *J Phys. Chem. B* 110:25562-25564.

7. Akiyama, M. 2006. Pathomechanisms of Harlequin Ichthyosis and ABCA Transporters in Human Diseases. *Arch Dermatol* 142:914-918.

8. Alanko, S.M., K.K.Halling, S.Maunula, J.P.Slotte, and B.Ramstedt. 2005. Displacement of sterols from sterol/sphingomyelin domains in fluid bilayer membranes by competing molecules. *Biochim. Biophys. Acta* 1715:111-121.

9. Alderson, N.L., E.N.Maldonado, M.J.Kern, N.R.Bhat, and H.Hama. 2006. FA2H-dependent fatty acid 2-hydroxylation in postnatal mouse brain. *J Lipid Res* 47:2772-2780.

10. Allikmets, R., N.F.Shroyer, N.Singh, J.M.Seddon, R.A.Lewis, P.S.Bernstein, A.Peiffer, N.A.Zabriskie, Y.Li, A.Hutchinson, M.Dean, J.R.Lupski, and M.Leppert. 1997. Mutation of the Stargardt disease gene (ABCR) in age-related macular degeneration. *Science* 277:1805-1807.

11. Altelaar, A.F., S.L.Luxembourg, L.A.McDonnell, S.R.Piersma, and R.M.Heeren. 2007. Imaging mass spectrometry at cellular length scales. *Nat Protoc.* 2:1185-1196.

12. Angus, W.W. and R.L.Lester. 1972. Turnover of inositol and phosphorus containing lipids in Saccharomyces cerevisiae; extracellular accumulation of

glycerophosphorylinositol derived from phosphatidylinositol. *Arch. Biochem. Biophys.* 151:483-495.

13. Aoki, C., K.I.Hidari, S.Itonori, A.Yamada, N.Takahashi, T.Kasama, F.Hasebe, M.A.Islam, K.Hatano, K.Matsuoka, T.Taki, C.T.Guo, T.Takahashi, Y.Sakano, T.Suzuki, D.Miyamoto, M.Sugita, D.Terunuma, K.Morita, and Y.Suzuki. 2006. Identification and characterization of carbohydrate molecules in mammalian cells recognized by Dengue virus type 2. *J Biochem (Tokyo)* 139:607-614.

14. Aronova, S., K.Wedaman, P.A.Aronov, K.Fontes, K.Ramos, B.D.Hammock, and T.Powers. 2008. Regulation of ceramide biosynthesis by TOR complex 2. *Cell Metab* 7:148-158.

15. Athenstaedt, K. and G.Daum. 1997. Biosynthesis of phosphatidic acid in lipid particles and endoplasmic reticulum of Saccharomyces cerevisiae. *J. Bacteriol.* 179:7611-7616.

16. Azad, A.K., T.D.Sirakova, N.D.Fernandes, and P.E.Kolattukudy. 1997. Gene Knockout Reveals a Novel Gene Cluster for the Synthesis of a Class of Cell Wall Lipids Unique to Pathogenic Mycobacteria. *J. Biol. Chem.* 272:16741-16745.

17. Bagnat, M., S.Keranen, A.Shevchenko, A.Shevchenko, and K.Simons. 2000. Lipid rafts function in biosynthetic delivery of proteins to the cell surface in yeast. *Proc. Natl. Acad. Sci U. S. A* 97:3254-3259.

18. Bagnat, M. and K.Simons. 2002. Lipid rafts in protein sorting and cell polarity in budding yeast Saccharomyces cerevisiae. *Biol. Chem.* 383:1475-1480.

19. Baker, C.J., R.Kanagasabai, W.T.Ang, A.Veeramani, H.S.Low, and M.R.Wenk. 2008. Towards ontology-driven navigation of the lipid bibliosphere. *BMC. Bioinformatics.* 9 Suppl 1:S5.

20. Balazy, M. 2004. Eicosanomics: targeted lipidomics of eicosanoids in biological systems. *Prostaglandins Other Lipid Mediat.* 73:173-180.

21. Baudry, K., E.Swain, A.Rahier, M.Germann, A.Batta, S.Rondet, S.Mandala, K.Henry, G.S.Tint, T.Edlind, M.Kurtz, and J.T.Nickels, Jr. 2001. The effect of the erg26-1 mutation on the regulation of lipid metabolism in Saccharomyces cerevisiae. *J Biol Chem* 276:12702-12711.

22. Beeler, T., D.Bacikova, K.Gable, L.Hopkins, C.Johnson, H.Slife, and T.Dunn. 1998. The Saccharomyces cerevisiae TSC10/YBR265w gene encoding 3-ketosphinganine reductase is identified in a screen for temperature-sensitive suppressors of the Ca2+-sensitive csg2Delta mutant. *J. Biol. Chem.* 273:30688-30694.

23. Benghezal, M., C.Roubaty, V.Veepuri, J.Knudsen, and A.Conzelmann. 2007. SLC1 and SLC4 encode partially redundant acyl-coenzyme A 1-acylglycerol-3-phosphate O-acyltransferases of budding yeast. *J Biol. Chem.* 282:30845-30855.

24. Benveniste, J., J.P.Le Couedic, J.Polonsky, and M.Tence. 1977. Structural analysis of purified platelet-activating factor by lipases. *Nature* 269:170-171.

25. Bhattathiry, M. 1971. Lipid synthesis in rats during cold acclimatization. *J Biochem.* 69:415-420.

26. Bielawska, A., H.M.Crane, D.Liotta, L.M.Obeid, and Y.A.Hannun. 1993. Selectivity of ceramide-mediated biology. Lack of activity of erythro-dihydroceramide. *J Biol Chem.* 268:26226-26232.

27. Binnington, B., D.Lingwood, A.Nutikka, and C.A.Lingwood. 2002. Effect of globotriaosyl ceramide fatty acid alpha-hydroxylation on the binding by verotoxin 1 and verotoxin 2. *Neurochem. Res* 27:807-813.

28. Blagovic, B., J.Rupcic, M.Mesaric, K.Georgia, and V.Maric. 2001. Lipid composition of Brewer's Yeast. *Food Technology and Biotechnology* 39:175-181.

29. Blagovic, B., J.Rupcic, M.Mesaric, and V.Maric. 2005. Lipid analysis of the plasma membrane and mitochondria of brewer's yeast. *Folia Microbiol. (Praha)* 50:24-30.

30. Bligh, E.G. and W.J.Dyer. 1959. A rapid method of total lipid extraction and purification. *Can. J. Biochem. Physiol* 37:911-917.

31. Bock, J. and E.Gulbins. 2003. The transmembranous domain of CD40 determines CD40 partitioning into lipid rafts. *FEBS Lett.* 534:169-174.

32. Boumann, H.A., P.T.Chin, A.J.Heck, K.B.De, and A.I.De Kroon. 2004a. The yeast phospholipid N-methyltransferases catalyzing the synthesis of phosphatidylcholine preferentially convert di-C16:1 substrates both in vivo and in vitro. *J Biol. Chem.* 279:40314-40319.

33. Boumann, H.A., K.B.De, A.J.Heck, and A.I.De Kroon. 2004b. The selective utilization of substrates in vivo by the phosphatidylethanolamine and phosphatidylcholine biosynthetic enzymes Ept1p and Cpt1p in yeast. *FEBS Lett.* 569:173-177.

34. Boumann, H.A., J.Gubbens, M.C.Koorengevel, C.S.Oh, C.E.Martin, A.J.Heck, J.Patton-Vogt, S.A.Henry, K.B.De, and A.I.De Kroon. 2006. Depletion of phosphatidylcholine in yeast induces shortening and increased saturation of the lipid acyl chains: evidence for regulation of intrinsic membrane curvature in a eukaryote. *Mol. Biol. Cell* 17:1006-1017.

35. Bretscher, M.S. and S.Munro. 1993. Cholesterol and the Golgi apparatus. *Science* 261:1280-1281.

36. Brill, J.A., G.R.Hime, M.Scharer-Schuksz, and M.T.Fuller. 2000. A phospholipid kinase regulates actin organization and intercellular bridge formation during germline cytokinesis. *Development* 127:3855-3864.

37. Brock, T.G. and M.Peters-Golden. 2007. Activation and regulation of cellular eicosanoid biosynthesis. *ScientificWorldJournal.* 7:1273-1284.

38. Brockerhoff, H. 1963. Breakdown of phospholipids in mild alkaline hydrolysis. *J. Lipid Res.* 35:96-99.

39. Brugger, B., G.Erben, R.Sandhoff, F.T.Wieland, and W.D.Lehmann. 1997. Quantitative analysis of biological membrane lipids at the low picomole level by nano-electrospray ionization tandem mass spectrometry. *Proc. Natl. Acad. Sci U. S. A* 94:2339-2344.

40. Brugger, B., B.Glass, P.Haberkant, I.Leibrecht, F.T.Wieland, and H.G.Krausslich. 2006. The HIV lipidome: A raft with an unusual composition. *PNAS* 103:2641-2646.

41. Brunelle, A. and O.Laprevote. 2008. Lipid imaging with cluster time-of-flight secondary ion mass spectrometry. *Anal. Bioanal. Chem.*

42. Busser, B.W., M.L.Bulyk, and A.M.Michelson. 2008. Toward a systems-level understanding of developmental regulatory networks. *Curr. Opin. Genet. Dev.*

43. Caffrey, M. and J.Hogan. 1992. LIPIDAT: a database of lipid phase transition temperatures and enthalpy changes. DMPC data subset analysis. *Chem. Phys. Lipids* 61:1-109.

44. Campbell, S.M., S.M.Crowe, and J.Mak. 2002. Virion-associated cholesterol is critical for the maintenance of HIV-1 structure and infectivity. *AIDS* 16:2253-2261.

45. Cantor, R.S. 1999. Lipid composition and the lateral pressure profile in bilayers. *Biophys. J* 76:2625-2639.

46. Carlson, E.E. and B.F.Cravatt. 2007. Chemoselective probes for metabolite enrichment and profiling. *Nat Meth* 4:429-435.

47. Carman, G.M. and S.A.Henry. 1989. Phospholipid biosynthesis in yeast. *Annu. Rev. Biochem.* 58:635-669.

48. Cerantola, V., C.Vionnet, O.F.Aebischer, T.Jenny, J.Knudsen, and A.Conzelmann. 2007. Yeast sphingolipids do not need to contain very long chain fatty acids. *Biochem. J* 401:205-216.

49. Cerbon, J., A.Falcon, C.Hernandez-Luna, and D.Segura-Cobos. 2005. Inositol phosphoceramide synthase is a regulator of intracellular levels of diacylglycerol and ceramide during the G1 to S transition in Saccharomyces cerevisiae. *Biochem. J.* 388:169-176.

50. Chan, R., P.D.Uchil, J.Jin, G.Shui, D.E.Ott, W.Mothes, and M.R.Wenk. 2008. Retroviruses human immunodeficiency virus and murine leukemia virus are enriched in phosphoinositides. *J Virol.* 82:11228-11238.

51. Chen, Y.W., J.W.Pedersen, H.H.Wandall, S.B.Levery, S.Pizette, H.Clausen, and S.M.Cohen. 2007. Glycosphingolipids with extended sugar chain have specialized functions in development and behavior of Drosophila. *Dev. Biol.* 306:736-749.

52. Cherry, S., A.Kunte, H.Wang, C.Coyne, R.B.Rawson, and N.Perrimon. 2006. COPI activity coupled with fatty acid biosynthesis is required for viral replication. *PLoS. Pathog.* 2:e102.

53. chi-Yamada, T., T.Gotoh, I.Sugimura, M.Tateno, Y.Nishida, T.Onuki, and H.Date. 1999. De novo synthesis of sphingolipids is required for cell survival by down-regulating c-Jun N-terminal kinase in Drosophila imaginal discs. *Mol. Cell Biol.* 19:7276-7286.

54. Choi, J.Y., W.E.Martin, R.C.Murphy, and D.R.Voelker. 2004. Phosphatidylcholine and N-methylated phospholipids are nonessential in Saccharomyces cerevisiae. *J. Biol. Chem.* 279:42321-42330.

55. Cowart, L.A., Y.A.Hannun, and L.M.Obeid. 2007. Metabolism and function of sphingolipids in *Saccharomyces cerevisiae*: relevance to cancer research. *In* Yeast as tools in cancer research. J.L.Nitiss and J.Heitman, editors. Springer-Verlag, New York, LLC. 191-210.

56. Crozatier, M., J.Krzemien, and A.Vincent. 2007. The hematopoietic niche: a Drosophila model, at last. *Cell Cycle* 6:1443-1444.

57. Cui, Y., B.Colsch, C.Afonso, N.Baumann, J.C.Tabet, J.M.Mallet, and Y.Zhang. 2008. Synthetic sulfogalactosylceramide (sulfatide) and its use for the mass spectrometric quantitative urinary determination in metachromatic leukodystrophies. *Glycoconj. J* 25:147-155.

58. D'Hondt, K., A.Heese-Peck, and H.Riezman. 2000. Protein and lipid requirements for endocytosis. *Annu. Rev. Genet.* 34:255-295.

59. Dahlen, B. and I.Pascher. 1972. Molecular arrangements in sphingolipids - Crystal-structure of N-tetracosanoylphytosphingosine. *Acta Crystallographica Section B* 28:2396-2404.

60. Dallerac, R., C.Labeur, J.M.Jallon, D.C.Knipple, W.L.Roelofs, and C.Wicker-Thomas. 2000. A delta9 desaturase gene with a different substrate specificity is

responsible for the cuticular diene hydrocarbon polymorphism in Drosophila melanogaster. *Proceedings of the National Academy of Sciences of the United States of America* 97:9449-9454.

61. Daum, G., N.D.Lees, M.Bard, and R.Dickson. 1998. Biochemistry, cell biology and molecular biology of lipids of Saccharomyces cerevisiae. *Yeast* 14:1471-1510.

62. Daum, G., G.Tuller, T.Nemec, C.Hrastnik, G.Balliano, L.Cattel, P.Milla, F.Rocco, A.Conzelmann, C.Vionnet, D.E.Kelly, S.Kelly, E.Schweizer, H.J.Schuller, U.Hojad, E.Greiner, and K.Finger. 1999. Systematic analysis of yeast strains with possible defects in lipid metabolism. *Yeast* 15:601-614.

63. DeLong, C.J., P.R.Baker, M.Samuel, Z.Cui, and M.J.Thomas. 2001. Molecular species composition of rat liver phospholipids by ESI-MS/MS: the effect of chromatography. *J Lipid Res* 42:1959-1968.

64. Devane, W.A., L.Hanus, A.Breuer, R.G.Pertwee, L.A.Stevenson, G.Griffin, D.Gibson, A.Mandelbaum, A.Etinger, and R.Mechoulam. 1992. Isolation and structure of a brain constituent that binds to the cannabinoid receptor. *Science* 258:1946-1949.

65. Di Paolo, G. and P.De Camilli. 2006. Phosphoinositides in cell regulation and membrane dynamics. *Nature* 443:651-657.

66. Dickson, R.C. 1998. Sphingolipid functions in Saccharomyces cerevisiae: comparison to mammals. *Annu. Rev Biochem* 67:27-48.

67. Dickson, R.C., G.B.Wells, A.Schmidt, and R.L.Lester. 1990. Isolation of mutant Saccharomyces cerevisiae strains that survive without sphingolipids. *Mol. Cell Biol.* 10:2176-2181.

68. Ding, J., C.M.Sorensen, N.Jaitly, H.Jiang, D.J.Orton, M.E.Monroe, R.J.Moore, R.D.Smith, and T.O.Metz. 2008. Application of the accurate mass and time tag approach in studies of the human blood lipidome. *Journal of Chromatography B* 871:243-252.

69. Dobrzyn, A., P.Dobrzyn, S.H.Lee, M.Miyazaki, P.Cohen, E.Asilmaz, D.G.Hardie, J.M.Friedman, and J.M.Ntambi. 2005. Stearoyl-CoA desaturase-1 deficiency reduces ceramide synthesis by downregulating serine palmitoyltransferase and increasing beta-oxidation in skeletal muscle. *Am J Physiol Endocrinol Metab* 288:E599-E607.

70. Dowhan, W. 1997. Molecular basis for membrane phospholipid diversity: why are there so many lipids? *Annu. Rev Biochem* 66:199-232.

71. Dowhan, W., E.Mileykovskaya, and M.Bogdanov. 2004. Diversity and versatility of lipid-protein interactions revealed by molecular genetic approaches. *Biochim. Biophys. Acta* 1666:19-39.

72. Drysdale, R. 2003. The Drosophila melanogaster genome sequencing and annotation projects: A status report. *Brief Funct Genomic Proteomic* 2:128-134.

73. Dunn, T.M., D.Haak, E.Monaghan, and T.J.Beeler. 1998. Synthesis of monohydroxylated inositolphosphorylceramide (IPC-C) in Saccharomyces cerevisiae requires Scs7p, a protein with both a cytochrome b5-like domain and a hydroxylase/desaturase domain. *Yeast* 14:311-321.

74. Duplus, E., M.Glorian, and C.Forest. 2000. Fatty acid regulation of gene transcription. *J Biol. Chem.* 275:30749-30752.

75. Dyatlovitskaya, E.V. 1998. Correlation between bioeffector characteristics of sphingolipids and the structure of their hydrophobic fragment. *Biochemistry (Mosc.)* 63:55-61.

76. Dyatlovitskaya, E.V. 2000. The interrelation between the biological functios of sphingolipids and their chemical structure. *Russian Journal of Bioorganic Chemistry* 26:12-18.

77. Edgar, B.A. and C.F.Lehner. 1996. Developmental control of cell cycle regulators: a fly's perspective. *Science* 274:1646-1652.

78. Eisenkolb, M., C.Zenzmaier, E.Leitner, and R.Schneiter. 2002. A specific structural requirement for ergosterol in long-chain fatty acid synthesis mutants important for maintaining raft domains in yeast. *Mol. Biol Cell* 13:4414-4428.

79. Ejsing, C.S., E.Duchoslav, J.Sampaio, K.Simons, R.Bonner, C.Thiele, K.Ekroos, and A.Shevchenko. 2006a. Automated identification and quantification of glycerophospholipid molecular species by multiple precursor ion scanning. *Anal. Chem.* 78:6202-6214.

80. Ejsing, C.S., T.Moehring, U.Bahr, E.Duchoslav, M.Karas, K.Simons, and A.Shevchenko. 2006b. Collision-induced dissociation pathways of yeast sphingolipids and their molecular profiling in total lipid extracts: a study by quadrupole TOF and linear ion trap-orbitrap mass spectrometry. *J Mass Spectrom.* 41:372-389.

81. Ekroos, K., I.V.Chernushevich, K.Simons, and A.Shevchenko. 2002. Quantitative profiling of phospholipids by multiple precursor ion scanning on a hybrid quadrupole time-of-flight mass spectrometer. *Anal. Chem.* 74:941-949.

82. Escriba, P.V. 2006. Membrane-lipid therapy: a new approach in molecular medicine. *Trends Mol Med.* 12:34-43.

83. Escriba, P.V., J.M.Gonzalez-Ros, F.M.Goni, P.K.Kinnunen, L.Vigh, L.Sanchez-Magraner, A.M.Fernandez, X.Busquets, I.Horvath, and G.Barcelo-Coblijn. 2008. Membranes: a meeting point for lipids, proteins and therapies. *J Cell Mol Med.* 12:829-875.

84. Fadok, V.A., D.R.Voelker, P.A.Campbell, J.J.Cohen, D.L.Bratton, and P.M.Henson. 1992. Exposure of phosphatidylserine on the surface of apoptotic lymphocytes triggers specific recognition and removal by macrophages. *J Immunol* 148:2207-2216.

85. Faergeman, N.J., S.Feddersen, J.K.Christiansen, M.K.Larsen, R.Schneiter, C.Ungermann, K.Mutenda, P.Roepstorff, and J.Knudsen. 2004. Acyl-CoA-binding protein, Acb1p, is required for normal vacuole function and ceramide synthesis in Saccharomyces cerevisiae. *Biochem. J* 380:907-918.

86. Fahy, E., S.Subramaniam, H.A.Brown, C.K.Glass, A.H.Merrill, Jr., R.C.Murphy, C.R.Raetz, D.W.Russell, Y.Seyama, W.Shaw, T.Shimizu, F.Spener, M.G.van, M.S.VanNieuwenhze, S.H.White, J.L.Witztum, and E.A.Dennis. 2005. A comprehensive classification system for lipids. *J. Lipid Res.* 46:839-862.

87. Fahy, E., M.Sud, D.Cotter, and S.Subramaniam. 2007. LIPID MAPS online tools for lipid research. *Nucleic Acids Res* 35:W606-W612.

88. Fantini, J., M.Maresca, D.Hammache, N.Yahi, and O.Delezay. 2000. Glycosphingolipid (GSL) microdomains as attachment platforms for host pathogens and their toxins on intestinal epithelial cells: activation of signal transduction pathways and perturbations of intestinal absorption and secretion. *Glycoconj. J* 17:173-179.

89. Farrell, E.K. and D.J.Merkler. 2008. Biosynthesis, degradation and pharmacological importance of the fatty acid amides. *Drug Discov. Today* 13:558-568.

90. Feddersen, S., T.B.Neergaard, J.Knudsen, and N.J.Faergeman. 2007. Transcriptional regulation of phospholipid biosynthesis is linked to fatty acid metabolism by an acyl-CoA-binding-protein-dependent mechanism in Saccharomyces cerevisiae. *Biochem. J* 407:219-230.

91. Fei, W., G.Shui, B.Gaeta, X.Du, L.Kuerschner, P.Li, A.J.Brown, M.R.Wenk, R.G.Parton, and H.Yang. 2008. Fld1p, a functional homologue of human seipin, regulates the size of lipid droplets in yeast. *J Cell Biol.* 180:473-482.

92. Feigenson, G.W. 2007. Phase boundaries and biological membranes. *Annu. Rev. Biophys. Biomol. Struct.* 36:63-77.

93. Ferguson-Yankey, S.R., M.S.Skrzypek, R.L.Lester, and R.C.Dickson. 2002. Mutant analysis reveals complex regulation of sphingolipid long chain base phosphates and long chain bases during heat stress in yeast. *Yeast* 19:573-586.

94. Folch, J., M.Lees, and G.H.S.Stanley. 1957. A simple method for the isolation and purificatio of total lipides from animal tissues. *J. Biol. Chem.* 226:497-509.

95. Forrester, J.S., S.B.Milne, P.T.Ivanova, and H.A.Brown. 2004. Computational lipidomics: a multiplexed analysis of dynamic changes in membrane lipid composition during signal transduction. *Mol Pharmacol.* 65:813-821.

96. Fyrst, H., D.R.Herr, G.L.Harris, and J.D.Saba. 2004. Characterization of free endogenous C14 and C16 sphingoid bases from Drosophila melanogaster. *J Lipid Res* 45:54-62.

97. Fyrst, H., X.Zhang, D.R.Herr, H.S.Byun, R.Bittman, V.H.Phan, G.L.Harris, and J.D.Saba. 2008. Identification and characterization by electrospray mass spectrometry of endogenous Drosophila sphingadienes. *J Lipid Res* 49:597-606.

98. Gaigg, B., T.B.Neergaard, R.Schneiter, J.K.Hansen, N.J.Faergeman, N.A.Jensen, J.R.Andersen, J.Friis, R.Sandhoff, H.D.Schroder, and J.Knudsen. 2001. Depletion of acyl-coenzyme A-binding protein affects sphingolipid synthesis and causes vesicle accumulation and membrane defects in Saccharomyces cerevisiae. *Mol Biol Cell* 12:1147-1160.

99. Gaigg, B., A.Toulmay, and R.Schneiter. 2006. Very long-chain fatty acid-containing lipids rather than sphingolipids per se are required for raft association and stable surface transport of newly synthesized plasma membrane ATPase in yeast. *J Biol Chem.* 281:34135-34145.

100. Gamo, S., A.Kawabe, H.Kohara, H.Yamaguchi, Y.Tanaka, and S.Yagi. 1999. Fast atom bombardment tandem mass spectrometric analysis of phospholipids in Drosophila melanogaster. *J Mass Spectrom.* 34:590-600.

101. Garton, S., L.V.Michaelson, F.Beaudoin, M.H.Beale, and J.A.Napier. 2003. The dihydroceramide desaturase is not essential for cell viability in Schizosaccharomyces pombe. *FEBS Lett.* 538:192-196.

102. Ghosh, T.K., J.Bian, and D.L.Gill. 1990. Intracellular calcium release mediated by sphingosine derivatives generated in cells. *Science* 248:1653-1656.

103. Goker-Alpan, O., G.Lopez, J.Vithayathil, J.Davis, M.Hallett, and E.Sidransky. 2008. The spectrum of parkinsonian manifestations associated with glucocerebrosidase mutations. *Arch Neurol.* 65:1353-1357.

104. Goldman, S.S. 1975. Cold resistance of the brain during hibernation. III. Evidence of a lipid adaptation. *Am J Physiol* 228:834-838.

105. Goldstein, J.L., R.A.Bose-Boyd, and M.S.Brown. 2006. Protein sensors for membrane sterols. *Cell* 124:35-46.

106. Goni, F.M. and A.Alonso. 2006. Biophysics of sphingolipids I. Membrane properties of sphingosine, ceramides and other simple sphingolipids. *Biochim. Biophys. Acta* 1758:1902-1921.

107. Gray, A., H.Olsson, I.H.Batty, L.Priganica, and D.C.Peter. 2003. Nonradioactive methods for the assay of phosphoinositide 3-kinases and phosphoinositide phosphatases and selective detection of signaling lipids in cell and tissue extracts. *Anal. Biochem.* 313:234-245.

108. Grilley, M.M., S.D.Stock, R.C.Dickson, R.L.Lester, and J.Y.Takemoto. 1998. Syringomycin action gene SYR2 is essential for sphingolipid 4-hydroxylation in Saccharomyces cerevisiae. *J. Biol. Chem.* 273:11062-11068.

109. Grimm, M.O., H.S.Grimm, A.J.Patzold, E.G.Zinser, R.Halonen, M.Duering, J.A.Tschape, S.B.De, U.Muller, J.Shen, and T.Hartmann. 2005. Regulation of cholesterol and sphingomyelin metabolism by amyloid-beta and presenilin. *Nat. Cell Biol.* 7:1118-1123.

110. Gu, Z., F.Valianpour, S.Chen, F.M.Vaz, G.A.Hakkaart, R.J.Wanders, and M.L.Greenberg. 2004. Aberrant cardiolipin metabolism in the yeast taz1 mutant: a model for Barth syndrome. *Mol. Microbiol.* 51:149-158.

111. Guan, X. and M.R.Wenk. 2008. Biochemistry of inositol lipids. *Front Biosci.* 13:3239-3251.

112. Guan, X.L., X.He, W.Y.Ong, W.K.Yeo, G.Shui, and M.R.Wenk. 2006. Non-targeted profiling of lipids during kainate-induced neuronal injury. *FASEB J.* 20:1152-1161.

113. Guan, X.L. and M.R.Wenk. 2006. Mass spectrometry-based profiling of phospholipids and sphingolipids in extracts from Saccharomyces cerevisiae. *Yeast* 23:465-477.

114. Guldberg, P., P.thor Straten, A.Birck, V.Ahrenkiel, A.F.Kirkin, and J.Zeuthen. 1997. Disruption of the MMAC1/PTEN Gene by Deletion or Mutation Is a Frequent Event in Malignant Melanoma. *Cancer Res* 57:3660-3663.

115. Gulshan, K. and W.S.Moye-Rowley. 2007. Multidrug resistance in fungi. *Eukaryot. Cell* 6:1933-1942.

116. Haak, D., K.Gable, T.Beeler, and T.Dunn. 1997. Hydroxylation of Saccharomyces cerevisiae ceramides requires Sur2p and Scs7p. *J. Biol. Chem.* 272:29704-29710.

117. Haimi, P., A.Uphoff, M.Hermansson, and P.Somerharju. 2006. Software tools for analysis of mass spectrometric lipidome data. *Anal. Chem.* 78:8324-8331.

118. Hama, H., D.A.Young, J.A.Radding, D.Ma, J.Tang, S.D.Stock, and J.Y.Takemoto. 2000. Requirement of sphingolipid alpha-hydroxylation for fungicidal action of syringomycin E. *FEBS Lett.* 478:26-28.

119. Hamasur, B., J.Bruchfeld, M.Haile, A.Pawlowski, B.Bjorvatn, G.Kallenius, and S.B.Svenson. 2001. Rapid diagnosis of tuberculosis by detection of mycobacterial lipoarabinomannan in urine. *J Microbiol. Methods* 45:41-52.

120. Han, X. 2002. Characterization and direct quantitation of ceramide molecular species from lipid extracts of biological samples by electrospray ionization tandem mass spectrometry. *Anal. Biochem.* 302:199-212.

121. Han, X. and R.W.Gross. 2003. Global analyses of cellular lipidomes directly from crude extracts of biological samples by ESI mass spectrometry: a bridge to lipidomics. *J. Lipid Res.* 44:1071-1079.

122. Han, X. and R.W.Gross. 2005a. Shotgun lipidomics: electrospray ionization mass spectrometric analysis and quantitation of cellular lipidomes directly from crude extracts of biological samples. *Mass Spectrom. Rev* 24:367-412.

123. Han, X. and R.W.Gross. 2005b. Shotgun lipidomics: multidimensional MS analysis of cellular lipidomes. *Expert. Rev. Proteomics.* 2:253-264.

124. Han, X., J.Yang, H.Cheng, H.Ye, and R.W.Gross. 2004. Toward fingerprinting cellular lipidomes directly from biological samples by two-dimensional electrospray ionization mass spectrometry. *Anal. Biochem.* 330:317-331.

125. Han, X., K.Yang, and R.W.Gross. 2008. Microfluidics-based electrospray ionization enhances the intrasource separation of lipid classes and extends identification of individual molecular species through multi-dimensional mass spectrometry: development of an automated high-throughput platform for shotgun lipidomics. *Rapid Commun. Mass Spectrom.* 22:2115-2124.

126. Hanada, K., K.Kumagai, S.Yasuda, Y.Miura, M.Kawano, M.Fukasawa, and M.Nishijima. 2003. Molecular machinery for non-vesicular trafficking of ceramide. *Nature* 426:803-809.

127. Harder, T. and K.Simons. 1997. Caveolae, DIGs, and the dynamics of sphingolipid-cholesterol microdomains. *Curr. Opin. Cell Biol* 9:534-542.

128. Hardie, R.C. and P.Raghu. 2001. Visual transduction in Drosophila. *Nature* 413:186-193.

129. He, X., X.L.Guan, W.Y.Ong, A.A.Farooqui, and M.R.Wenk. 2006. Expression, activity, and role of serine palmitoyltransferase in the rat hippocampus after kainate injury. *J. Neurosci. Res.*

130. Hechtberger, P., E.Zinser, R.Saf, K.Hummel, F.Paltauf, and G.Daum. 1994. Characterization, quantification and subcellular localization of inositol-containing sphingolipids of the yeast, Saccharomyces cerevisiae. *Eur. J. Biochem.* 225:641-649.

131. Heese-Peck, A., H.Pichler, B.Zanolari, R.Watanabe, G.Daum, and H.Riezman. 2002. Multiple functions of sterols in yeast endocytosis. *Mol. Biol. Cell* 13:2664-2680.

132. Herr, D.R., H.Fyrst, M.B.Creason, V.H.Phan, J.D.Saba, and G.L.Harris. 2004. Characterization of the Drosophila sphingosine kinases and requirement for Sk2 in normal reproductive function. *J Biol. Chem.* 279:12685-12694.

133. Herrero, A.B., A.M.Astudillo, M.A.Balboa, C.Cuevas, J.Balsinde, and S.Moreno. 2008. Levels of SCS7/FA2H-Mediated Fatty Acid 2-Hydroxylation Determine the Sensitivity of Cells to Antitumor PM02734. *Cancer Res* 68:9779-9787.

134. Higuchi, O., K.Nakagawa, T.Tsuzuki, T.Suzuki, S.Oikawa, and T.Miyazawa. 2006. Aminophospholipid glycation and its inhibitor screening system: a new role of pyridoxal 5'-phosphate as the inhibitor. *J Lipid Res* 47:964-974.

135. Hokin, L.E. and M.R.Hokin. 1955. Effects of acetylcholine on the turnover of phosphoryl units in individual phospholipids of pancreas slices and brain cortex slices. *Biochim. Biophys. Acta* 18:102-110.

136. Holyoak, C.D., D.Bracey, P.W.Piper, K.Kuchler, and P.J.Coote. 1999. The Saccharomyces cerevisiae weak-acid-inducible ABC transporter Pdr12 transports fluorescein and preservative anions from the cytosol by an energy-dependent mechanism. *J Bacteriol.* 181:4644-4652.

137. Homann, M.J., A.M.Bailis, S.A.Henry, and G.M.Carman. 1987. Coordinate regulation of phospholipid biosynthesis by serine in Saccharomyces cerevisiae. *J Bacteriol.* 169:3276-3280.

138. Hou, W., H.Zhou, F.Elisma, S.A.Bennett, and D.Figeys. 2008. Technological developments in lipidomics. *Brief. Funct. Genomic. Proteomic.*

139. Hsu, F.F., A.Bohrer, and J.Turk. 1998. Electrospray ionization tandem mass spectrometric analysis of sulfatide. Determination of fragmentation patterns and characterization of molecular species expressed in brain and in pancreatic islets. *Biochim. Biophys. Acta* 1392:202-216.

140. Hsu, F.F. and J.Turk. 2002. Characterization of ceramides by low energy collisional-activated dissociation tandem mass spectrometry with negative-ion electrospray ionization. *J Am Soc. Mass Spectrom.* 13:558-570.

141. Hughes, A.L., C.Y.Lee, C.M.Bien, and P.J.Espenshade. 2007. 4-Methyl sterols regulate fission yeast SREBP-Scap under low oxygen and cell stress. *J Biol Chem.* 282:24388-24396.

142. Hughey, C.A., R.P.Rodgers, and A.G.Marshall. 2002. Resolution of 11,000 compositionally distinct components in a single electrospray ionization Fourier transform ion cyclotron resonance mass spectrum of crude oil. *Anal. Chem.* 74:4145-4149.

143. Huijbregts, R.P., L.Topalof, and V.A.Bankaitis. 2000. Lipid metabolism and regulation of membrane trafficking. *Traffic.* 1:195-202.

144. Hutchins, P.M., R.M.Barkley, and R.C.Murphy. 2008. Separation of cellular nonpolar neutral lipids by normal-phase chromatography and analysis by electrospray ionization mass spectrometry. *J Lipid Res* 49:804-813.

145. Hwang, O., G.Kim, Y.J.Jang, S.W.Kim, G.Choi, H.J.Choi, S.Y.Jeon, D.G.Lee, and J.D.Lee. 2001. Synthetic Phytoceramides Induce Apoptosis with Higher Potency than Ceramides. *Mol Pharmacol* 59:1249-1255.

146. Isaac, G., R.Jeannotte, S.W.Esch, and R.Welti. 2007. New mass-spectrometry-based strategies for lipids. *Genet. Eng (N. Y.)* 28:129-157.

147. Ito, S., T.Nabetani, Y.Shinoda, Y.Nagatsuka, and Y.Hirabayashi. 2008. Quantitative analysis of a novel glucosylated phospholipid by liquid chromatography-mass spectrometry. *Analytical Biochemistry* 376:252-257.

148. Iverson, S.L., M.Enoksson, V.Gogvadze, M.Ott, and S.Orrenius. 2004. Cardiolipin is not required for Bax-mediated cytochrome c release from yeast mitochondria. *J Biol. Chem.* 279:1100-1107.

149. Jacob, L. and L.Lum. 2007. Hedgehog signaling pathway in Drosophila. *Sci. STKE.* 2007:cm7.

150. Jacobson, K., O.G.Mouritsen, and R.G.Anderson. 2007. Lipid rafts: at a crossroad between cell biology and physics. *Nat Cell Biol* 9:7-14.

151. Jemal, M., D.Teitz, Z.Ouyang, and S.Khan. 1999. Comparison of plasma sample purification by manual liquid-liquid extraction, automated 96-well liquid-liquid extraction and automated 96-well solid-phase extraction for analysis by high-performance liquid chromatography with tandem mass spectrometry. *J Chromatogr. B Biomed. Sci. Appl.* 732:501-508.

152. Jenkins, G.M., A.Richards, T.Wahl, C.Mao, L.Obeid, and Y.Hannun. 1997. Involvement of yeast sphingolipids in the heat stress response of Saccharomyces cerevisiae. *J. Biol. Chem.* 272:32566-32572.

153. Jensen, M.O. and O.G.Mouritsen. 2004. Lipids do influence protein function-the hydrophobic matching hypothesis revisited. *Biochim. Biophys. Acta* 1666:205-226.

154. Jiang, X., H.Cheng, K.Yang, R.W.Gross, and X.Han. 2007. Alkaline methanolysis of lipid extracts extends shotgun lipidomics analyses to the low-abundance regime of cellular sphingolipids. *Analytical Biochemistry* 371:135-145.

155. Jin, H., J.M.McCaffery, and E.Grote. 2008. Ergosterol promotes pheromone signaling and plasma membrane fusion in mating yeast. *J Cell Biol.* 180:813-826.

156. Jungnickel, H., E.A.Jones, N.P.Lockyer, S.G.Oliver, G.M.Stephens, and J.C.Vickerman. 2005. Application of TOF-SIMS with chemometrics to discriminate between four different yeast strains from the species Candida glabrata and Saccharomyces cerevisiae. *Anal. Chem.* 77:1740-1745.

157. Karasavvas, N., R.K.Erukulla, R.Bittman, R.Lockshin, and Z.Zakeri. 1996. Stereospecific induction of apoptosis in U937 cells by N-octanoyl-sphingosine stereoisomers and N-octyl-sphingosine. The ceramide amide group is not required for apoptosis. *Eur. J Biochem* 236:729-737.

158. Kawai, H., K.Sango, K.A.Mullin, and R.L.Proia. 1998. Embryonic stem cells with a disrupted GD3 synthase gene undergo neuronal differentiation in the absence of b-series gangliosides. *J Biol Chem.* 273:19634-19638.

159. Kearns, B.G., J.G.Alb, Jr., and V.Bankaitis. 1998. Phosphatidylinositol transfer proteins: the long and winding road to physiological function. *Trends Cell Biol.* 8:276-282.

160. Kitagaki, H., L.A.Cowart, N.Matmati, A.S.Vaena de, S.A.Novgorodov, Y.H.Zeidan, J.Bielawski, L.M.Obeid, and Y.A.Hannun. 2007. Isc1 regulates sphingolipid metabolism in yeast mitochondria. *Biochim. Biophys. Acta* 1768:2849-2861.

161. Kitagawa, T., N.Ishige, K.Suzuki, M.Owada, T.Ohashi, M.Kobayashi, Y.Eto, A.Tanaka, K.Mills, B.Winchester, and J.Keutzer. 2005. Non-invasive screening method for Fabry disease by measuring globotriaosylceramide in whole urine samples using tandem mass spectrometry. *Mol. Genet Metab* 85:196-202.

162. Kobayashi, T., H.Takematsu, T.Yamaji, S.Hiramoto, and Y.Kozutsumi. 2005. Disturbance of sphingolipid biosynthesis abrogates the signaling of Mss4, phosphatidylinositol-4-phosphate 5-kinase, in yeast. *J. Biol. Chem.* 280:18087-18094.

163. Kohlwein, S.D., G.Daum, R.Schneiter, and F.Paltauf. 1996. Phospholipids: synthesis, sorting, subcellular traffic - the yeast approach. *Trends Cell Biol.* 6:260-266.

164. Korekane, H., S.Tsuji, S.Noura, M.Ohue, Y.Sasaki, S.Imaoka, and Y.Miyamoto. 2007. Novel fucogangliosides found in human colon adenocarcinoma tissues by means of glycomic analysis. *Analytical Biochemistry* 364:37-50.

165. Kulik, W., L.H.van, F.S.Stet, R.H.Houtkooper, H.Kemp, J.E.Stone, C.G.Steward, R.J.Wanders, and F.M.Vaz. 2008. Bloodspot assay using HPLC-tandem mass spectrometry for detection of Barth syndrome. *Clin. Chem.* 54:371-378.

166. Kunz, J., R.Henriquez, U.Schneider, M.uter-Reinhard, N.R.Movva, and M.N.Hall. 1993. Target of rapamycin in yeast, TOR2, is an essential phosphatidylinositol kinase homolog required for G1 progression. *Cell* 73:585-596.

167. Kusumi, A., C.Nakada, K.Ritchie, K.Murase, K.Suzuki, H.Murakoshi, R.S.Kasai, J.Kondo, and T.Fujiwara. 2005. Paradigm shift of the plasma membrane concept from the two-dimensional continuum fluid to the partitioned fluid: high-speed single-molecule tracking of membrane molecules. *Annu. Rev Biophys. Biomol. Struct.* 34:351-378.

168. Kyogashima, M., K.Tadano-Aritomi, T.Aoyama, A.Yusa, Y.Goto, K.Tamiya-Koizumi, H.Ito, T.Murate, R.Kannagi, and A.Hara. 2008. Chemical and Apoptotic Properties of Hydroxy-Ceramides Containing Long-Chain Bases with Unusual Alkyl Chain Lengths. *J Biochem* 144:95-106.

169. Labeur, C., R.Dallerac, and C.Wicker-Thomas. 2002. Involvement of desat1 gene in the control of Drosophila melanogaster pheromone biosynthesis. *Genetica* 114:269-274.

170. Leavell, M.D. and J.A.Leary. 2006. Fatty acid analysis tool (FAAT): An FT-ICR MS lipid analysis algorithm. *Anal. Chem.* 78:5497-5503.

171. Leber, A., P.Fischer, R.Schneiter, S.D.Kohlwein, and G.Daum. 1997. The yeast mic2 mutant is defective in the formation of mannosyl-diinositolphosphorylceramide. *FEBS Lett.* 411:211-214.

172. Ledeen, R.W. and G.Wu. 2006. Gangliosides of the nuclear membrane: a crucial locus of cytoprotective modulation. *J Cell Biochem* 97:893-903.

173. Lemmon, M.A. 2003. Phosphoinositide recognition domains. *Traffic.* 4:201-213.

174. Lertsiri, S., M.Shiraishi, and T.Miyazawa. 1998. Identification of deoxy-D-fructosyl phosphatidylethanolamine as a non-enzymic glycation product of phosphatidylethanolamine and its occurrence in human blood plasma and red blood cells. *Biosci. Biotechnol. Biochem.* 62:893-901.

175. Lester, R.L., G.B.Wells, G.Oxford, and R.C.Dickson. 1993. Mutant strains of Saccharomyces cerevisiae lacking sphingolipids synthesize novel inositol

glycerophospholipids that mimic sphingolipid structures. *J. Biol. Chem.* 268:845-856.

176. Li, F. and G.D.Prestwich. 2005. Functional Lipidomics. Dekker-CRC, New York.

177. Liebisch, G., W.Drobnik, M.Reil, B.Trumbach, R.Arnecke, B.Olgemoller, A.Roscher, and G.Schmitz. 1999. Quantitative measurement of different ceramide species from crude cellular extracts by electrospray ionization tandem mass spectrometry (ESI-MS/MS). *J Lipid Res* 40:1539-1546.

178. Liebisch, G., M.Binder, R.Schifferer, T.Langmann, B.Schulz, and G.Schmitz. 2006. High throughput quantification of cholesterol and cholesteryl ester by electrospray ionization tandem mass spectrometry (ESI-MS/MS). *Biochimica et Biophysica Acta (BBA) - Molecular and Cell Biology of Lipids* 1761:121-128.

179. Liscovitch, M. and L.C.Cantley. 1994. Lipid second messengers. *Cell* 77:329-334.

180. Low, C.P., G.Shui, L.P.Liew, S.Buttner, F.Madeo, I.W.Dawes, M.R.Wenk, and H.Yang. 2008. Caspase-dependent and -independent lipotoxic cell-death pathways in fission yeast. *J Cell Sci.* 121:2671-2684.

181. Lykidis, A. 2007. Comparative genomics and evolution of eukaryotic phospholipid biosynthesis. *Prog. Lipid Res* 46:171-199.

182. Maceyka, M., S.G.Payne, S.Milstien, and S.Spiegel. 2002. Sphingosine kinase, sphingosine-1-phosphate, and apoptosis. *Biochim. Biophys. Acta* 1585:193-201.

183. Maggio, B., M.L.Fanani, C.M.Rosetti, and N.Wilke. 2006. Biophysics of sphingolipids II. Glycosphingolipids: an assortment of multiple structural information transducers at the membrane surface. *Biochim. Biophys. Acta* 1758:1922-1944.

184. Malinska, K., J.Malinsky, M.Opekarova, and W.Tanner. 2003. Visualization of protein compartmentation within the plasma membrane of living yeast cells. *Mol. Biol. Cell* 14:4427-4436.

185. Malinska, K., J.Malinsky, M.Opekarova, and W.Tanner. 2004. Distribution of Can1p into stable domains reflects lateral protein segregation within the plasma membrane of living S. cerevisiae cells. *J Cell Sci.* 117:6031-6041.

186. Mansilla, M.C., C.E.Banchio, and M.D.de. 2008. Signalling Pathways Controlling Fatty Acid Desaturation. *Subcell. Biochem.* 49:71-99.

187. Marsh, D. 1990. Handbook of lipid bilayers. CRC Press, Boca Raton.

188. Matyash, V., E.V.Entchev, F.Mende, M.Wilsch-Brauninger, C.Thiele, A.W.Schmidt, H.J.Knolker, S.Ward, and T.V.Kurzchalia. 2004. Sterol-derived

hormone(s) controls entry into diapause in Caenorhabditis elegans by consecutive activation of DAF-12 and DAF-16. *PLoS. Biol* 2:e280.

189. Matyash, V., C.Geier, A.Henske, S.Mukherjee, D.Hirsh, C.Thiele, B.Grant, F.R.Maxfield, and T.V.Kurzchalia. 2001. Distribution and transport of cholesterol in Caenorhabditis elegans. *Mol. Biol. Cell* 12:1725-1736.

190. Matyash, V., G.Liebisch, T.V.Kurzchalia, A.Shevchenko, and D.Schwudke. 2008. Lipid extraction by methyl-tert-butyl ether for high-throughput lipidomics. *J Lipid Res* 49:1137-1146.

191. Maurice, A. and M.Malgat. 1990. Evidence for the biosynthesis of ceramide-phosphoethanolamine in brain synaptic plasma membrane vesicles and in sciatic nerve microsomes from normal and Trembler mice. *Neurosci. Lett.* 118:177-180.

192. Maxfield, F.R. and I.Tabas. 2005. Role of cholesterol and lipid organization in disease. *Nature* 438:612-621.

193. Mayor, S. and H.Riezman. 2004. Sorting GPI-anchored proteins. *Nat Rev Mol Cell Biol* 5:110-120.

194. McLafferty, R.H. and F.Turecek. 1993. Interpretation of mass spectra. University Science Books, Sausalito, CA.

195. McQuaw, C.M., L.Zheng, A.G.Ewing, and N.Winograd. 2007. Localization of sphingomyelin in cholesterol domains by imaging mass spectrometry. *Langmuir* 23:5645-5650.

196. Megha, P.Sawatzki, T.Kolter, R.Bittman, and E.London. 2007. Effect of ceramide N-acyl chain and polar headgroup structure on the properties of ordered lipid domains (lipid rafts). *Biochim. Biophys. Acta* 1768:2205-2212.

197. Mercer, J. and A.Helenius. 2008. Vaccinia virus uses macropinocytosis and apoptotic mimicry to enter host cells. *Science* 320:531-535.

198. Merrill, A.H., E.M.Schmelz, D.L.Dillehay, S.Spiegel, J.A.Shayman, J.J.Schroeder, R.T.Riley, K.A.Voss, and E.Wang. 1997. Sphingolipids--The Enigmatic Lipid Class: Biochemistry, Physiology, and Pathophysiology. *Toxicology and Applied Pharmacology* 142:208-225.

199. Merrill, A.H., Jr., M.C.Sullards, J.C.Allegood, S.Kelly, and E.Wang. 2005. Sphingolipidomics: high-throughput, structure-specific, and quantitative analysis of sphingolipids by liquid chromatography tandem mass spectrometry. *Methods* 36:207-224.

200. Merrill, A.H., Jr., M.D.Wang, M.Park, and M.C.Sullards. 2007. (Glyco)sphingolipidology: an amazing challenge and opportunity for systems biology. *Trends Biochem. Sci.* 32:457-468.

201. Michel, C., G.van Echten-Deckert, J.Rother, K.Sandhoff, E.Wang, and A.H.Merrill, Jr. 1997. Characterization of ceramide synthesis. A dihydroceramide desaturase introduces the 4,5-trans-double bond of sphingosine at the level of dihydroceramide. *J Biol Chem.* 272:22432-22437.

202. Milligan, S.C., J.G.Alb, Jr., R.B.Elagina, V.A.Bankaitis, and D.R.Hyde. 1997. The phosphatidylinositol transfer protein domain of Drosophila retinal degeneration B protein is essential for photoreceptor cell survival and recovery from light stimulation. *J Cell Biol.* 139:351-363.

203. Milne, S.B., P.T.Ivanova, D.DeCamp, R.C.Hsueh, and H.A.Brown. 2005. A targeted mass spectrometric analysis of phosphatidylinositol phosphate species. *J. Lipid Res.* 46:1796-1802.

204. Mitra, K., I.Ubarretxena-Belandia, T.Taguchi, G.Warren, and D.M.Engelman. 2004. Modulation of the bilayer thickness of exocytic pathway membranes by membrane proteins rather than cholesterol. *Proc. Natl. Acad. Sci. U. S. A* 101:4083-4088.

205. Miyazaki, M., S.M.Bruggink, and J.M.Ntambi. 2006. Identification of mouse palmitoyl-coenzyme A Delta9-desaturase. *J Lipid Res* 47:700-704.

206. Miyazaki, M., A.Dobrzyn, P.M.Elias, and J.M.Ntambi. 2005. Stearoyl-CoA desaturase-2 gene expression is required for lipid synthesis during early skin and liver development. *Proc. Natl. Acad. Sci. U. S. A* 102:12501-12506.

207. Miyazaki, M., Y.C.Kim, M.P.Gray-Keller, A.D.Attie, and J.M.Ntambi. 2000. The biosynthesis of hepatic cholesterol esters and triglycerides is impaired in mice with a disruption of the gene for stearoyl-CoA desaturase 1. *J Biol. Chem.* 275:30132-30138.

208. Miyazaki, M. and J.M.Ntambi. 2003. Role of stearoyl-coenzyme A desaturase in lipid metabolism. *Prostaglandins Leukot. Essent. Fatty Acids* 68:113-121.

209. Miyazawa, T., D.Ibusuki, S.Yamashita, and K.Nakagawa. 2008. Analysis of amadori-glycated phosphatidylethanolamine in the plasma of healthy subjects and diabetic patients by liquid chromatography-tandem mass spectrometry. *Ann. N. Y. Acad. Sci.* 1126:291-294.

210. Miyazawa, T., J.H.Oak, and K.Nakagawa. 2005. A convenient method for preparation of high-purity, Amadori-glycated phosphatidylethanolamine and its prooxidant effect. *Ann. N. Y. Acad. Sci.* 1043:276-279.

211. Mougous, J.D., M.D.Leavell, R.H.Senaratne, C.D.Leigh, S.J.Williams, L.W.Riley, J.A.Leary, and C.R.Bertozzi. 2002. Discovery of sulfated metabolites in mycobacteria with a genetic and mass spectrometric approach. *Proc. Natl. Acad. Sci. U. S. A* 99:17037-17042.

212. Mousley, C.J., K.Tyeryar, K.E.Ile, G.Schaaf, R.L.Brost, C.Boone, X.Guan, M.R.Wenk, and V.A.Bankaitis. 2008. Trans-Golgi Network and Endosome Dynamics Connect Ceramide Homeostasis with Regulation of the Unfolded Protein Response and TOR Signaling in Yeast. *Mol. Biol. Cell*.

213. Mukhopadhyay, D., K.S.Howell, H.Riezman, and G.Capitani. 2008. Identifying key residues of sphinganine-1-phosphate lyase for function in vivo and in vitro. *J Biol. Chem.* 283:20159-20169.

214. Mukhopadhyay, K., T.Prasad, P.Saini, T.J.Pucadyil, A.Chattopadhyay, and R.Prasad. 2004. Membrane sphingolipid-ergosterol interactions are important determinants of multidrug resistance in Candida albicans. *Antimicrob. Agents Chemother.* 48:1778-1787.

215. Mullner, H. and G.Daum. 2004. Dynamics of neutral lipid storage in yeast. *Acta Biochim. Pol.* 51:323-347.

216. Munn, A.L., A.Heese-Peck, B.J.Stevenson, H.Pichler, and H.Riezman. 1999. Specific sterols required for the internalization step of endocytosis in yeast. *Mol. Biol. Cell* 10:3943-3957.

217. Munro, S. 2003. Lipid rafts: elusive or illusive? *Cell* 115:377-388.

218. Murphy, R.C. 2002. Mass spectrometry of phospholipids: Table of molecular and product ions. Illuminati Press, Denver Colorado, US.

219. Nagiec, M.M., E.E.Nagiec, J.A.Baltisberger, G.B.Wells, R.L.Lester, and R.C.Dickson. 1997. Sphingolipid synthesis as a target for antifungal drugs. Complementation of the inositol phosphorylceramide synthase defect in a mutant strain of Saccharomyces cerevisiae by the AUR1 gene. *J Biol Chem.* 272:9809-9817.

220. Nagiec, M.M., G.B.Wells, R.L.Lester, and R.C.Dickson. 1993. A suppressor gene that enables Saccharomyces cerevisiae to grow without making sphingolipids encodes a protein that resembles an Escherichia coli fatty acyltransferase. *J Biol Chem.* 268:22156-22163.

221. Nagiec, M.M., C.L.Young, P.G.Zaworski, and S.D.Kobayashi. 2003. Yeast sphingolipid bypass mutants as indicators of antifungal agents selectively targeting sphingolipid synthesis. *Biochem. Biophys. Res. Commun.* 307:369-374.

222. Nakagawa, K., J.H.Oak, O.Higuchi, T.Tsuzuki, S.Oikawa, H.Otani, M.Mune, H.Cai, and T.Miyazawa. 2005a. Ion-trap tandem mass spectrometric analysis of Amadori-glycated phosphatidylethanolamine in human plasma with or without diabetes. *J Lipid Res* 46:2514-2524.

223. Nakagawa, K., J.H.Oak, and T.Miyazawa. 2005b. Angiogenic potency of Amadori-glycated phosphatidylethanolamine. *Ann. N. Y. Acad. Sci.* 1043:413-416.

224. Neu, U., K.Woellner, G.Gauglitz, and T.Stehle. 2008. Structural basis of GM1 ganglioside recognition by simian virus 40. *PNAS* 105:5219-5224.

225. Nielsen, N.V., J.M.Carstensen, and J.Smedsgaard. 1998. Alignment of single and multiple wavelength chromatographic profiles for chemometric data analysis using correlation optimised warping. *Journal of Chromatography A* 805:17-35.

226. Nikolova-Karakashian, M. 2000. Assays for the biosynthesis of sphingomyelin and ceramide phosphoethanolamine. *In* Methods in Enzymology Sphingolipid Metabolism and Cell Signaling Part A. H.M.Alfred, editor. Academic Press, 31-42.

227. Ntambi, J.M., M.Miyazaki, and A.Dobrzyn. 2004. Regulation of stearoyl-CoA desaturase expression. *Lipids* 39:1061-1065.

228. Nusslein-Volhard, C. and E.Wieschaus. 1980. Mutations affecting segment number and polarity in Drosophila. *Nature* 287:795-801.

229. O'Farrell, P.H., B.A.Edgar, D.Lakich, and C.F.Lehner. 1989. Directing cell division during development. *Science* 246:635-640.

230. Oak, J., K.Nakagawa, and T.Miyazawa. 2000. Synthetically prepared Aamadori-glycated phosphatidylethanolaminecan trigger lipid peroxidation via free radical reactions. *FEBS Lett.* 481:26-30.

231. Oak, J.H., K.Nakagawa, S.Oikawa, and T.Miyazawa. 2003. Amadori-glycated phosphatidylethanolamine induces angiogenic differentiations in cultured human umbilical vein endothelial cells. *FEBS Lett.* 555:419-423.

232. Obeid, L.M. and Y.A.Hannun. 1995. Ceramide: a stress signal and mediator of growth suppression and apoptosis. *J Cell Biochem.* 58:191-198.

233. Odorizzi, G., M.Babst, and S.D.Emr. 2000. Phosphoinositide signaling and the regulation of membrane trafficking in yeast. *Trends Biochem. Sci.* 25:229-235.

234. Ohya, Y., Y.Ohsumi, and Y.Anraku. 1986. Isolation and characterization of Ca2+-sensitive mutants of Saccharomyces cerevisiae. *J. Gen. Microbiol.* 132:979-988.

235. Osenkowski, P., W.Ye, R.Wang, M.S.Wolfe, and D.J.Selkoe. 2008. Direct and Potent Regulation of {gamma}-Secretase by Its Lipid Microenvironment. *J. Biol. Chem.* 283:22529-22540.

236. Overgaard, J., A.Tomcala, J.G.Sorensen, M.Holmstrup, P.H.Krogh, P.Simek, and V.Kostal. 2008. Effects of acclimation temperature on thermal tolerance and membrane phospholipid composition in the fruit fly Drosophila melanogaster. *J Insect Physiol* 54:619-629.

237. Pagano, R.E., V.Puri, M.Dominguez, and D.L.Marks. 2000. Membrane traffic in sphingolipid storage diseases. *Traffic.* 1:807-815.

238. Palkova, Z., B.Janderova, J.Gabriel, B.Zikanova, M.Pospisek, and J.Forstova. 1997. Ammonia mediates communication between yeast colonies. *Nature* 390:532-536.

239. Pamplona, R., M.J.Bellmunt, M.Portero, D.Riba, and J.Prat. 1995. Chromatographic evidence for Amadori product formation in rat liver aminophospholipids. *Life Sci.* 57:873-879.

240. Parimoo, S., Y.Zheng, K.Eilertsen, L.Ge, S.Prouty, J.Sundberg, and K.Stenn. 1999. Identification of a novel SCD gene and expression of the SCD gene family in mouse skin. *J Investig. Dermatol Symp. Proc.* 4:320-322.

241. Pascher, I. 1976. Molecular arrangements in sphingolipids. Conformation and hydrogen bonding of ceramide and their implication on membrane stability and permeability. *Biochim. Biophys. Acta* 455:433-451.

242. Pascher, I. and S.Sundell. 1992. Molecular arrangements in sphingolipids - Crystal-structure of the ceramide N-(2D,3D-dihydroxyoctadecanoyl)-phytosphingosine. *Chem. Phys. Lipids* 62:79-86.

243. Pelkmans, L. 2005. Secrets of caveolae- and lipid raft-mediated endocytosis revealed by mammalian viruses. *Biochimica et Biophysica Acta (BBA) - Molecular Cell Research* 1746:295-304.

244. Perry, R.J. and N.D.Ridgway. 2006. Oxysterol-binding protein and vesicle-associated membrane protein-associated protein are required for sterol-dependent activation of the ceramide transport protein. *Mol Biol Cell* 17:2604-2616.

245. Pettitt, T.R., S.K.Dove, A.Lubben, S.D.J.Calaminus, and M.J.O.Wakelam. 2006. Analysis of intact phosphoinositides in biological samples. *J. Lipid Res.* 47:1588-1596.

246. Pettus, B.J., B.J.Kroesen, Z.M.Szulc, A.Bielawska, J.Bielawski, Y.A.Hannun, and M.Busman. 2004. Quantitative measurement of different ceramide species from crude cellular extracts by normal-phase high-performance liquid chromatography coupled to atmospheric pressure ionization mass spectrometry. *Rapid Commun. Mass Spectrom.* 18:577-583.

247. Phan, V.H., D.R.Herr, D.Panton, H.Fyrst, J.D.Saba, and G.L.Harris. 2007. Disruption of sphingolipid metabolism elicits apoptosis-associated reproductive defects in Drosophila. *Dev. Biol.* 309:329-341.

248. Pietilainen, K.H., M.Sysi-Aho, A.Rissanen, T.Seppanen-Laakso, H.Yki-Jarvinen, J.Kaprio, and M.Oresic. 2007. Acquired obesity is associated with changes in the serum lipidomic profile independent of genetic effects - a monozygotic twin study. *PLoS. ONE.* 2:e218.

249. Pike, L.J. 2008. The challenge of lipid rafts. *J Lipid Res.*

250. Piper, P., Y.Mahe, S.Thompson, R.Pandjaitan, C.Holyoak, R.Egner, M.Muhlbauer, P.Coote, and K.Kuchler. 1998. The pdr12 ABC transporter is required for the development of weak organic acid resistance in yeast. *EMBO J* 17:4257-4265.

251. Polozov, I.V., L.Bezrukov, K.Gawrisch, and J.Zimmerberg. 2008. Progressive ordering with decreasing temperature of the phospholipids of influenza virus. *Nat Chem. Biol* 4:248-255.

252. Prestwich, G.D. 2005. Visualization and perturbation of phosphoinositide and phospholipid signaling. *Prostaglandins Other Lipid Mediat.* 77:168-178.

253. Proszynski, T.J., R.W.Klemm, M.Gravert, P.P.Hsu, Y.Gloor, J.Wagner, K.Kozak, H.Grabner, K.Walzer, M.Bagnat, K.Simons, and C.Walch-Solimena. 2005. A genome-wide visual screen reveals a role for sphingolipids and ergosterol in cell surface delivery in yeast. *Proc. Natl. Acad. Sci. U. S. A* 102:17981-17986.

254. Pruett, S.T., A.Bushnev, K.Hagedorn, M.Adiga, C.A.Haynes, M.C.Sullards, D.C.Liotta, and A.H.Merrill, Jr. 2008. Biodiversity of sphingoid bases ("sphingosines") and related amino alcohols. *J Lipid Res* 49:1621-1639.

255. Pulfer, M. and R.C.Murphy. 2003. Electrospray mass spectrometry of phospholipids. *Mass Spectrom. Rev* 22:332-364.

256. Puri, V., R.Watanabe, M.Dominguez, X.Sun, C.L.Wheatley, D.L.Marks, and R.E.Pagano. 1999. Cholesterol modulates membrane traffic along the endocytic pathway in sphingolipid-storage diseases. *Nat. Cell Biol.* 1:386-388.

257. Radhakrishnan, A., X.M.Li, R.E.Brown, and H.M.McConnell. 2001. Stoichiometry of cholesterol-sphingomyelin condensed complexes in monolayers. *Biochim. Biophys. Acta* 1511:1-6.

258. Radhakrishnan, A. and H.McConnell. 2005. Condensed complexes in vesicles containing cholesterol and phospholipids. *Proc. Natl. Acad. Sci. U. S. A* 102:12662-12666.

259. Ramstedt, B. and J.P.Slotte. 2006. Sphingolipids and the formation of sterol-enriched ordered membrane domains. *Biochim. Biophys. Acta* 1758:1945-1956.

260. Rao, R.P., C.Yuan, J.C.Allegood, S.S.Rawat, M.B.Edwards, X.Wang, A.H.Merrill, Jr., U.Acharya, and J.K.Acharya. 2007. Ceramide transfer protein function is essential for normal oxidative stress response and lifespan. *Proc. Natl. Acad. Sci. U. S. A* 104:11364-11369.

261. Rapaka, R.S., D.Piomelli, S.Spiegel, N.Bazan, and E.A.Dennis. 2005. Targeted lipidomics: signaling lipids and drugs of abuse. *Prostaglandins Other Lipid Mediat.* 77:223-234.

262. Raychaudhuri, S., Y.J.Im, J.H.Hurley, and W.A.Prinz. 2006. Nonvesicular sterol movement from plasma membrane to ER requires oxysterol-binding protein-related proteins and phosphoinositides. *J Cell Biol* 173:107-119.

263. Regina, T.A. and S.I.Hakomori. 2008. Functional role of glycosphingolipids and gangliosides in control of cell adhesion, motility, and growth, through glycosynaptic microdomains. *Biochim. Biophys. Acta* 1780:421-433.

264. Reinke, A., J.C.Chen, S.Aronova, and T.Powers. 2006. Caffeine targets TOR complex I and provides evidence for a regulatory link between the FRB and kinase domains of Tor1p. *J Biol. Chem.* 281:31616-31626.

265. Rietveld, A., S.Neutz, K.Simons, and S.Eaton. 1999. Association of sterol- and glycosylphosphatidylinositol-linked proteins with Drosophila raft lipid microdomains. *J Biol. Chem.* 274:12049-12054.

266. Rilfors, L. and G.Lindblom. 2002. Regulation of lipid composition in biological membranes - biophysical studies of lipids and lipid synthesizing enzymes. *Colloids and Surfaces B: Biointerfaces* 26:112-124.

267. Rizzo, M.A., G.H.Springer, B.Granada, and D.W.Piston. 2004. An improved cyan fluorescent protein variant useful for FRET. *Nat Biotechnol.* 22:445-449.

268. Robinson, N., M.Wolke, K.Ernestus, and G.Plum. 2007. A Mycobacterial Gene Involved in Synthesis of an Outer Cell Envelope Lipid Is a Key Factor in Prevention of Phagosome Maturation. *Infect. Immun.* 75:581-591.

269. Rohrbough, J., E.Rushton, L.Palanker, E.Woodruff, H.J.Matthies, U.Acharya, J.K.Acharya, and K.Broadie. 2004. Ceramidase regulates synaptic vesicle exocytosis and trafficking. *J Neurosci.* 24:7789-7803.

270. Rozengurt, E., A.Rodriguez-Pena, M.Coombs, and J.Sinnett-Smith. 1984. Diacylglycerol stimulates DNA synthesis and cell division in mouse 3T3 cells: role of Ca2+-sensitive phospholipid-dependent protein kinase. *Proceedings of the National Academy of Sciences of the United States of America* 81:5748-5752.

271. Sawai, H., Y.Okamoto, C.Luberto, C.Mao, A.Bielawska, N.Domae, and Y.A.Hannun. 2000. Identification of ISC1 (YER019w) as inositol phosphosphingolipid phospholipase C in Saccharomyces cerevisiae. *J Biol. Chem.* 275:39793-39798.

272. Schaub, T.M., C.L.Hendrickson, K.Qian, J.P.Quinn, and A.G.Marshall. 2003. High-resolution field desorption/ionization fourier transform ion cyclotron resonance mass analysis of nonpolar molecules. *Anal Chem.* 75:2172-2176.

273. Scheek, S., M.S.Brown, and J.L.Goldstein. 1997. Sphingomyelin depletion in cultured cells blocks proteolysis of sterol regulatory element binding proteins at site 1. *Proc. Natl. Acad. Sci. U. S. A* 94:11179-11183.

274. Schiller, J., R.Suss, B.Fuchs, M.Muller, O.Zschornig, and K.Arnold. 2007. MALDI-TOF MS in lipidomics. *Front Biosci.* 12:2568-2579.

275. Schneiter, R., B.Brugger, C.M.Amann, G.D.Prestwich, R.F.Epand, G.Zellnig, F.T.Wieland, and R.M.Epand. 2004. Identification and biophysical characterization of a very-long-chain-fatty-acid-substituted phosphatidylinositol in yeast subcellular membranes. *Biochem. J* 381:941-949.

276. Schneiter, R., B.Brugger, R.Sandhoff, G.Zellnig, A.Leber, M.Lampl, K.Athenstaedt, C.Hrastnik, S.Eder, G.Daum, F.Paltauf, F.T.Wieland, and S.D.Kohlwein. 1999. Electrospray ionization tandem mass spectrometry (ESI-MS/MS) analysis of the lipid molecular species composition of yeast subcellular membranes reveals acyl chain-based sorting/remodeling of distinct molecular species en route to the plasma membrane. *J Cell Biol.* 146:741-754.

277. Schorling, S., B.Vallee, W.P.Barz, H.Riezman, and D.Oesterhelt. 2001. Lag1p and Lac1p are essential for the Acyl-CoA-dependent ceramide synthase reaction in Saccharomyces cerevisae. *Mol. Biol Cell* 12:3417-3427.

278. Schwudke, D., J.T.Hannich, V.Surendranath, V.Grimard, T.Moehring, L.Burton, T.Kurzchalia, and A.Shevchenko. 2007. Top-down lipidomic screens by multivariate analysis of high-resolution survey mass spectra. *Anal. Chem.* 79:4083-4093.

279. Schwudke, D., J.Oegema, L.Burton, E.Entchev, J.T.Hannich, C.S.Ejsing, T.Kurzchalia, and A.Shevchenko. 2006. Lipid profiling by multiple precursor and neutral loss scanning driven by the data-dependent acquisition. *Anal. Chem.* 78:585-595.

280. Seppo, A., M.Moreland, H.Schweingruber, and M.Tiemeyer. 2000. Zwitterionic and acidic glycosphingolipids of the Drosophila melanogaster embryo. *Eur. J Biochem.* 267:3549-3558.

281. Serhan, C.N. 2005. Mediator lipidomics. *Prostaglandins Other Lipid Mediat.* 77:4-14.

282. Serhan, C.N., N.Chiang, and T.E.Van Dyke. 2008. Resolving inflammation: dual anti-inflammatory and pro-resolution lipid mediators. *Nat Rev Immunol* 8:349-361.

283. Shui, G., A.K.Bendt, K.Pethe, T.Dick, and M.R.Wenk. 2007. Sensitive profiling of chemically diverse bioactive lipids. *J Lipid Res.* 48:1976-1984.

284. Silberkang, M., C.M.Havel, D.S.Friend, B.J.McCarthy, and J.A.Watson. 1983. Isoprene synthesis in isolated embryonic Drosophila cells. I. Sterol-deficient eukaryotic cells. *J Biol. Chem.* 258:8503-8511.

285. Simons, K. and E.Ikonen. 1997. Functional rafts in cell membranes. *Nature* 387:569-572.

286. Simonsen, A., A.E.Wurmser, S.D.Emr, and H.Stenmark. 2001. The role of phosphoinositides in membrane transport. *Curr. Opin. Cell Biol.* 13:485-492.

287. Song, H., F.F.Hsu, J.Ladenson, and J.Turk. 2007. Algorithm for processing raw mass spectrometric data to identify and quantitate complex lipid molecular species in mixtures by data-dependent scanning and fragment ion database searching. *J Am Soc. Mass Spectrom.* 18:1848-1858.

288. Stark, W.S., T.N.Lin, D.Brackhahn, J.S.Christianson, and G.Y.Sun. 1993a. Fatty acids in the lipids of Drosophila heads: effects of visual mutants, carotenoid deprivation and dietary fatty acids. *Lipids* 28:345-350.

289. Stark, W.S., T.N.Lin, D.Brackhahn, J.S.Christianson, and G.Y.Sun. 1993b. Phospholipids in Drosophila heads: effects of visual mutants and phototransduction manipulations. *Lipids* 28:23-28.

290. Stock, S.D., H.Hama, D.B.DeWald, and J.Y.Takemoto. 1999. SEC14-dependent secretion in Saccharomyces cerevisiae. Nondependence on sphingolipid synthesis-coupled diacylglycerol production. *J Biol Chem.* 274:12979-12983.

291. Stock, S.D., H.Hama, J.A.Radding, D.A.Young, and J.Y.Takemoto. 2000. Syringomycin E inhibition of Saccharomyces cerevisiae: requirement for biosynthesis of sphingolipids with very-long-chain fatty acids and mannose- and phosphoinositol-containing head groups. *Antimicrob. Agents Chemother.* 44:1174-1180.

292. Stocker, H., M.Andjelkovic, S.Oldham, M.Laffargue, M.P.Wymann, B.A.Hemmings, and E.Hafen. 2002. Living with lethal PIP3 levels: viability of flies lacking PTEN restored by a PH domain mutation in Akt/PKB. *Science* 295:2088-2091.

293. Storey, M.K., K.L.Clay, T.Kutateladze, R.C.Murphy, M.Overduin, and D.R.Voelker. 2001. Phosphatidylethanolamine has an essential role in

Saccharomyces cerevisiae that is independent of its ability to form hexagonal phase structures. *J Biol. Chem.* 276:48539-48548.

294. Subbanagounder, G., N.Leitinger, D.C.Schwenke, J.W.Wong, H.Lee, C.Rizza, A.D.Watson, K.F.Faull, A.M.Fogelman, and J.A.Berliner. 2000. Determinants of bioactivity of oxidized phospholipids. Specific oxidized fatty acyl groups at the sn-2 position. *Arterioscler. Thromb. Vasc. Biol* 20:2248-2254.

295. Sud, M., E.Fahy, D.Cotter, A.Brown, E.A.Dennis, C.K.Glass, A.H.Merrill, Jr., R.C.Murphy, C.R.Raetz, D.W.Russell, and S.Subramaniam. 2007. LMSD: LIPID MAPS structure database. *Nucleic Acids Res* 35:D527-D532.

296. Sullards, M.C., J.C.Allegood, S.Kelly, E.Wang, C.A.Haynes, H.Park, Y.Chen, and A.H.Merrill, Jr. 2007. Structure-specific, quantitative methods for analysis of sphingolipids by liquid chromatography-tandem mass spectrometry: "inside-out" sphingolipidomics. *Methods Enzymol.* 432:83-115.

297. Sullards, M.C. and A.H.Merrill, Jr. 2001. Analysis of sphingosine 1-phosphate, ceramides, and other bioactive sphingolipids by high-performance liquid chromatography-tandem mass spectrometry. *Sci STKE.* 2001:L1.

298. Sutphen, R., Y.Xu, G.D.Wilbanks, J.Fiorica, E.C.Grendys, Jr., J.P.LaPolla, H.Arango, M.S.Hoffman, M.Martino, K.Wakeley, D.Griffin, R.W.Blanco, A.B.Cantor, Y.J.Xiao, and J.P.Krischer. 2004. Lysophospholipids are potential biomarkers of ovarian cancer. *Cancer Epidemiol. Biomarkers Prev.* 13:1185-1191.

299. Sutterlin, C., A.Horvath, P.Gerold, R.T.Schwarz, Y.Wang, M.Dreyfuss, and H.Riezman. 1997. Identification of a species-specific inhibitor of glycosylphosphatidylinositol synthesis. *EMBO J* 16:6374-6383.

300. Suzuki, Y., M.Matsunaga, and M.Matsumoto. 1985. N-Acetylneuraminyllactosylceramide, GM3-NeuAc, a new influenza A virus receptor which mediates the adsorption-fusion process of viral infection. Binding specificity of influenza virus A/Aichi/2/68 (H3N2) to membrane-associated GM3 with different molecular species of sialic acid. *J. Biol. Chem.* 260:1362-1365.

301. Swain, E., K.Baudry, J.Stukey, V.McDonough, M.Germann, and J.T.Nickels, Jr. 2002. Sterol-dependent regulation of sphingolipid metabolism in Saccharomyces cerevisiae. *J. Biol. Chem.* 277:26177-26184.

302. Tabuchi, M., A.Audhya, A.B.Parsons, C.Boone, and S.D.Emr. 2006. The phosphatidylinositol 4,5-biphosphate and TORC2 binding proteins Slm1 and Slm2 function in sphingolipid regulation. *Mol. Cell Biol.* 26:5861-5875.

303. Tafesse, F.G., P.Ternes, and J.C.Holthuis. 2006. The multigenic sphingomyelin synthase family. *J Biol Chem.* 281:29421-29425.

304. Taguchi, R., T.Houjou, H.Nakanishi, T.Yamazaki, M.Ishida, M.Imagawa, and T.Shimizu. 2005. Focused lipidomics by tandem mass spectrometry. *J Chromatogr. B Analyt. Technol. Biomed. Life Sci.* 823:26-36.

305. Taguchi, R., M.Nishijima, and T.Shimizu. 2007. Basic analytical systems for lipidomics by mass spectrometry in Japan. *Methods Enzymol.* 432:185-211.

306. Taha, T.A., T.D.Mullen, and L.M.Obeid. 2006. A house divided: Ceramide, sphingosine, and sphingosine-1-phosphate in programmed cell death. *Biochimica et Biophysica Acta (BBA) - Biomembranes* 1758:2027-2036.

307. Takamiya, K., A.Yamamoto, K.Furukawa, S.Yamashiro, M.Shin, M.Okada, S.Fukumoto, M.Haraguchi, N.Takeda, K.Fujimura, M.Sakae, M.Kishikawa, H.Shiku, K.Furukawa, and S.Aizawa. 1996. Mice with disrupted GM2/GD2 synthase gene lack complex gangliosides but exhibit only subtle defects in their nervous system. *Proc. Natl. Acad. Sci. U. S. A* 93:10662-10667.

308. Tamaki, H., A.Shimada, Y.Ito, M.Ohya, J.Takase, M.Miyashita, H.Miyagawa, H.Nozaki, R.Nakayama, and H.Kumagai. 2007. LPT1 encodes a membrane-bound O-acyltransferase involved in the acylation of lysophospholipids in the yeast Saccharomyces cerevisiae. *J Biol. Chem.* 282:34288-34298.

309. Tapon, N. 2003. Modeling transformation and metastasis in Drosophila. *Cancer Cell* 4:333-335.

310. Tenenbaum, D. 2003. What's All the Buzz? Fruit Flies Provide Unique Model for Cancer Research. *J Natl. Cancer Inst.* 95:1742-1744.

311. Terova, B., R.Heczko, and J.P.Slotte. 2005. On the importance of the phosphocholine methyl groups for sphingomyelin/cholesterol interactions in membranes: a study with ceramide phosphoethanolamine. *Biophys. J* 88:2661-2669.

312. Thevissen, K., I.E.Francois, J.Y.Takemoto, K.K.Ferket, E.M.Meert, and B.P.Cammue. 2003. DmAMP1, an antifungal plant defensin from dahlia (Dahlia merckii), interacts with sphingolipids from Saccharomyces cerevisiae. *FEMS Microbiol. Lett.* 226:169-173.

313. Todd, B.L., E.V.Stewart, J.S.Burg, A.L.Hughes, and P.J.Espenshade. 2006. Sterol regulatory element binding protein is a principal regulator of anaerobic gene expression in fission yeast. *Mol Cell Biol* 26:2817-2831.

314. Tsang, C.K., H.Qi, L.F.Liu, and X.F.Zheng. 2007. Targeting mammalian target of rapamycin (mTOR) for health and diseases. *Drug Discov. Today* 12:112-124.

315. Tsui, Z.C., Q.R.Chen, M.J.Thomas, M.Samuel, and Z.Cui. 2005. A method for profiling gangliosides in animal tissues using electrospray ionization-tandem mass spectrometry. *Analytical Biochemistry* 341:251-258.

316. Umebayashi, K. and A.Nakano. 2003. Ergosterol is required for targeting of tryptophan permease to the yeast plasma membrane. *J Cell Biol* 161:1117-1131.

317. Urbina, J.A., S.Pekerar, H.B.Le, J.Patterson, B.Montez, and E.Oldfield. 1995. Molecular order and dynamics of phosphatidylcholine bilayer membranes in the presence of cholesterol, ergosterol and lanosterol: a comparative study using 2H-, 13C- and 31P-NMR spectroscopy. *Biochim. Biophys. Acta* 1238:163-176.

318. Vaena de, A.S., Y.Okamoto, and Y.A.Hannun. 2004. Activation and localization of inositol phosphosphingolipid phospholipase C, Isc1p, to the mitochondria during growth of Saccharomyces cerevisiae. *J Biol Chem.* 279:11537-11545.

319. van Meer, G., D.R.Voelker, and G.W.Feigenson. 2008. Membrane lipids: where they are and how they behave. *Nat Rev Mol Cell Biol* 9:112-124.

320. van, M.G. 2005. Cellular lipidomics. *EMBO J.* 24:3159-3165.

321. Vance, J.E. 2003. Molecular and cell biology of phosphatidylserine and phosphatidylethanolamine metabolism. *Prog. Nucleic Acid Res. Mol. Biol.* 75:69-111.

322. Vance, J.E. 2006. Lipid imbalance in the neurological disorder, Niemann-Pick C disease. *FEBS Lett.* 580:5518-5524.

323. Vance, J.E. 2008. Thematic Review Series: Glycerolipids. Phosphatidylserine and phosphatidylethanolamine in mammalian cells: two metabolically related aminophospholipids. *J. Lipid Res.* 49:1377-1387.

324. Vanhaesebroeck, B., S.J.Leevers, K.Ahmadi, J.Timms, R.Katso, P.C.Driscoll, R.Woscholski, P.J.Parker, and M.D.Waterfield. 2001. Synthesis and function of 3-phosphorylated inositol lipids. *Annu. Rev. Biochem.* 70:535-602.

325. Vaz, F.M., R.H.Houtkooper, F.Valianpour, P.G.Barth, and R.J.Wanders. 2003. Only one splice variant of the human TAZ gene encodes a functional protein with a role in cardiolipin metabolism. *J Biol. Chem.* 278:43089-43094.

326. Wanke, V., E.Cameroni, A.Uotila, M.Piccolis, J.Urban, R.Loewith, and V.C.De. 2008. Caffeine extends yeast lifespan by targeting TORC1. *Mol Microbiol.* 69:277-285.

327. Wassall, S.R., M.R.Brzustowicz, S.R.Shaikh, V.Cherezov, M.Caffrey, and W.Stillwell. 2004. Order from disorder, corralling cholesterol with chaotic lipids: The role of polyunsaturated lipids in membrane raft formation. *Chemistry and Physics of Lipids* 132:79-88.

328. Wattenberg, B.W. and D.F.Silbert. 1983. Sterol partitioning among intracellular membranes. Testing a model for cellular sterol distribution. *J Biol. Chem.* 258:2284-2289.

329. Weaver, M. and M.A.Krasnow. 2008. Dual origin of tissue-specific progenitor cells in Drosophila tracheal remodeling. *Science* 321:1496-1499.

330. Wells, G.B., R.C.Dickson, and R.L.Lester. 1998. Heat-induced elevation of ceramide in Saccharomyces cerevisiae via de novo synthesis. *J Biol. Chem.* 273:7235-7243.

331. Wenk, M.R. 2005. The emerging field of lipidomics. *Nat. Rev. Drug Discov.* 4:594-610.

332. Wenk, M.R. 2006. Lipidomics in drug and biomarker development. *Expert Opinion on Drug Discovery* 1:723-736.

333. Wenk, M.R. and P.De Camilli. 2005. Phosphoinositide profiling in complex lipid mixtures. *In* Functional Lipidomics. F.Li and G.Pretswich, editors. CRC Press, Boca Raton. 243-262.

334. Wenk, M.R., L.Lucast, P.G.Di, A.J.Romanelli, S.F.Suchy, R.L.Nussbaum, G.W.Cline, G.I.Shulman, W.McMurray, and C.P.De. 2003. Phosphoinositide profiling in complex lipid mixtures using electrospray ionization mass spectrometry. *Nat. Biotechnol.* 21:813-817.

335. Whitfield, P.D., P.C.Sharp, D.W.Johnson, P.Nelson, and P.J.Meikle. 2001. Characterization of urinary sulfatides in metachromatic leukodystrophy using electrospray ionization-tandem mass spectrometry. *Mol Genet. Metab* 73:30-37.

336. Xiao, Y., Y.Chen, A.W.Kennedy, J.Belinson, and Y.Xu. 2000. Evaluation of plasma lysophospholipids for diagnostic significance using electrospray ionization mass spectrometry (ESI-MS) analyses. *Ann. N. Y. Acad. Sci.* 905:242-259.

337. Xu, H., D.Wilcox, P.Nguyen, M.Voorbach, H.Smith, S.Brodjian, T.Suhar, R.M.Reilly, P.B.Jacobson, C.A.Collins, K.Landschulz, and T.K.Surowy. 2007. Hepatic knockdown of stearoyl-CoA desaturase 1 via RNA interference in obese mice decreases lipid content and changes fatty acid composition. *Front Biosci.* 12:3781-3794.

338. Xu, X., R.Bittman, G.Duportail, D.Heissler, C.Vilcheze, and E.London. 2001. Effect of the Structure of Natural Sterols and Sphingolipids on the Formation of Ordered Sphingolipid/Sterol Domains (Rafts). Comparison of Cholesterol to Plant, Fungal, and Disease-associate Sterols and Comparison of Sphingomyelin, Cerebrosides, and Ceramide. *J. Biol. Chem.* 276:33540-33546.

339. Ye, J. 2007. Reliance of host cholesterol metabolic pathways for the life cycle of hepatitis C virus. *PLoS. Pathog.* 3:e108.

340. Yetukuri, L., K.Ekroos, A.Vidal-Puig, and M.Oresic. 2008. Informatics and computational strategies for the study of lipids. *Mol Biosyst.* 4:121-127.

341. Yetukuri, L., M.Katajamaa, G.Medina-Gomez, T.Seppanen-Laakso, A.Vidal-Puig, and M.Oresic. 2007. Bioinformatics strategies for lipidomics analysis: characterization of obesity related hepatic steatosis. *BMC. Syst. Biol* 1:12.

342. Yoshinaga, N., T.Aboshi, C.Ishikawa, M.Fukui, M.Shimoda, R.Nishida, C.G.Lait, J.H.Tumlinson, and N.Mori. 2007. Fatty acid amides, previously identified in caterpillars, found in the cricket Teleogryllus taiwanemma and fruit fly Drosophila melanogaster larvae. *J Chem. Ecol.* 33:1376-1381.

343. Yoshioka, T., H.Inoue, T.Kasama, Y.Seyama, S.Nakashima, Y.Nozawa, and Y.Hotta. 1985. Evidence that arachidonic acid is deficient in phosphatidylinositol of Drosophila heads. *J Biochem.* 98:657-662.

344. Zacarias, A., D.Bolanowski, and A.Bhatnagar. 2002. Comparative measurements of multicomponent phospholipid mixtures by electrospray mass spectroscopy: relating ion intensity to concentration. *Analytical Biochemistry* 308:152-159.

345. Zehethofer, N. and D.M.Pinto. 2008. Recent developments in tandem mass spectrometry for lipidomic analysis. *Anal. Chim. Acta* 627:62-70.

346. Zemski Berry, K.A. and R.C.Murphy. 2006. Analysis of polyunsaturated aminophospholipid molecular species using isotope-tagged derivatives and tandem mass spectrometry/mass spectrometry/mass spectrometry. *Anal. Biochem.* 349:118-128.

347. Zewail, A., M.W.Xie, Y.Xing, L.Lin, P.F.Zhang, W.Zou, J.P.Saxe, and J.Huang. 2003. Novel functions of the phosphatidylinositol metabolic pathway discovered by a chemical genomics screen with wortmannin. *Proc. Natl. Acad. Sci. U. S. A* 100:3345-3350.

348. Zhang, Y., X.Li, K.A.Becker, and E.Gulbins. 2008. Ceramide-enriched membrane domains-Structure and function. *Biochim. Biophys. Acta*.

349. Zhao, Z., Y.Xiao, P.Elson, H.Tan, S.J.Plummer, M.Berk, P.P.Aung, I.C.Lavery, J.P.Achkar, L.Li, G.Casey, and Y.Xu. 2007. Plasma lysophosphatidylcholine levels: potential biomarkers for colorectal cancer. *J Clin. Oncol.* 25:2696-2701.

350. Zinser, E., F.Paltauf, and G.Daum. 1993. Sterol composition of yeast organelle membranes and subcellular distribution of enzymes involved in sterol metabolism. *J. Bacteriol.* 175:2853-2858.

351. Zweytick, D., K.Athenstaedt, and G.Daum. 2000. Intracellular lipid particles of eukaryotic cells. *Biochim. Biophys. Acta* 1469:101-120.

Appendix

Supplementary Material 2.1 – Matlab algorithm for Q-ToF mass spectrometry data analysis.

Mass spectra were aligned using COW and relative differences in lipid levels between conditions were computed based on the ratio of the peak intensity of treated samples relative to that of control samples.

```
% read spectrum lists obtained from MassLynx
control1 = dlmread('RAT_HC1.txt');
control2 = dlmread('RAT_HC2.txt');
control3 = dlmread('RAT_HC3.txt');
spiked1 = dlmread('DMPG1.txt');
spiked2 = dlmread('DMPG2.txt');
spiked3 = dlmread('DMPG3.txt');
%detect minimum number of rows
num_of_rows = [length(control1) length(control2) length(control3) length(spiked1) length(spiked2) length(spiked3)];
minimum_rows = min(num_of_rows);
% Normalisation of individual ion intensity to the total ion intensities
control1_mass = control1(1:minimum_rows,1);
control1_intensity = control1(1:minimum_rows,2)/sum(control1(1:minimum_rows,2));
control2_mass = control2(1:minimum_rows,1);
control2_intensity = control2(1:minimum_rows,2)/sum(control2(1:minimum_rows,2));
control3_mass = control3(1:minimum_rows,1);
control3_intensity = control3(1:minimum_rows,2)/sum(control3(1:minimum_rows,2));
spiked1_mass = spiked1(1:minimum_rows,1);
spiked1_intensity = spiked1(1:minimum_rows,2)/sum(spiked1(1:minimum_rows,2));
spiked2_mass = spiked2(1:minimum_rows,1);
spiked2_intensity = spiked2(1:minimum_rows,2)/sum(spiked2(1:minimum_rows,2));
spiked3_mass = spiked3(1:minimum_rows,1);
spiked3_intensity = spiked3(1:minimum_rows,2)/sum(spiked3(1:minimum_rows,2));
%warp control spectra
[xW,warping,diagnos] = cow(control1_intensity',control2_intensity',1000,[],[0 1 1]);
control2_warped_intensity = xW';
[xW,warping,diagnos] = cow(control1_intensity',control3_intensity',1000,[],[0 1 1]);
control3_warped_intensity = xW';
% average control spectra
WARPED_control_intensity = [control1_intensity control2_warped_intensity control3_warped_intensity];
Mean_WARPED_control_intensity = mean(WARPED_control_intensity,2);
% warp spiked spectra
[xW,warping,diagnos] = cow(spiked1_intensity',spiked2_intensity',1000,[],[0 1 1]);
spiked2_warped_intensity = xW';
[xW,warping,diagnos] = cow(spiked1_intensity',spiked3_intensity',1000,[],[0 1 1]);
spiked3_warped_intensity = xW';
% average spiked spectra
WARPED_spiked_intensity = [spiked1_intensity spiked2_warped_intensity spiked3_warped_intensity];
Mean_WARPED_spiked_intensity = mean(WARPED_spiked_intensity,2);
%Warp averaged spiked spectrum towards averaged control spectrum
[xW,warping,diagnos]= cow(Mean_WARPED_control_intensity',Mean_WARPED_spiked_intensity',1000,[],[0 1 1]);
spiked_warped_intensity = xW';
%Noise reduction
added_denom = Mean_WARPED_control_intensity+0.000005;
added_num = spiked_warped_intensity + 0.000005
%Computation of differential profile
log10ratio = log10(added_num./added_denom)

figure,
plot(control1_mass,Mean_WARPED_control_intensity,'b')
hold on
plot(control1_mass,spiked_warped_intensity,'g')
hold on
plot(control1_mass,log10ratio,'k')
legend('mean Rat HC','mean DMPG','log10ratio')
```

Supplementary Material 2.2 – List of transitions for quantification of mammalian glycerophospholipids and sphingolipids in brain tissue and blood by multiple-reaction monitoring (MRM).

No.	Precursor Ion (Q1)	Daughter Ion (Q3)	Lipid Species
1	409.4	255.2	409.4/255.3>GPA:Lyso 16:0
2	423.4	269.2	**423.4/269.3>GPA:Lyso 17:0**
3	433.4	279.2	433.4/279.3>GPA:Lyso 18:2
4	435.4	281.2	435.4/281.3>GPA:Lyso 18:1
5	437.4	283.2	437.4/283.3>GPA:Lyso 18:0
6	457.4	303.2	**457.4/303.3>GPA:Lyso 20:4**
7	459.6	305.2	459.6/305.5>GPA:Lyso 20:3
8	461.6	307.2	461.6/307.5>GPA:Lyso 20:2
9	463.7	309.2	463.7/309.5>GPA:Lyso 20:1
10	465.7	311.2	465.7/311.5>GPA:Lyso 20:0
11	481.4	327.3	481.4/327.3>GPA:Lyso 22:6
12	483.4	329.3	483.4/329.3>GPA:Lyso 22:5
13	494.4	407.4	494.4/407.4>GPSer:Lyso 16:1
14	496.4	409.4	496.4/409.4>GPSer:Lyso 16:0
15	522.4	435.4	522.4/435.4>GPSer:Lyso 18:1
16	524.4	437.4	524.4/437.4>GPSer:Lyso 18:0
17	544.4	457.4	544.4/457.4>GPSer:Lyso 20:4
18	568.4	481.4	568.4/481.4>GPSer:Lyso 22:6
19	570.4	483.4	570.4/483.4>GPSer:Lyso 22:5
20	732.6	645.6	732.6/645.6>GPSer:32:1
21	734.6	647.6	734.6/647.6>GPSer:32:0
22	758.6	671.6	758.6/671.6>GPSer:34:2
23	760.8	673.8	760.8/673.8>GPSer:34:1
24	762.8	675.7	762.8/675.7>GPSer:34:0
25	782.6	695.7	782.6/695.7>GPSer:36:4
26	784.8	697.8	784.8/697.8>GPSer:36:3
27	786.8	699.8	786.8/699.8>GPSer:36:2
28	788.8	701.8	788.8/701.8>GPSer:36:1
29	790.8	703.8	790.8/703.8>GPSer:36:0
30	796.6	699.6	796.6/699.6>GPSer:37:4
31	808.6	721.6	808.6/721.6>GPSer:38:6
32	810.8	723.8	810.8/723.8>GPSer:38:5
33	812.8	725.8	812.8/725.8>GPSer:38:4
34	814.6	727.6	814.6/727.6>GPSer:38:3
35	816.8	729.8	816.8/729.8>GPSer:38:2
36	818.8	731.8	818.8/731.8>GPSer:38:1
37	834.8	747.8	834.8/747.8>GPSer:40:6
38	836.8	749.8	836.8/749.8>GPSer:40:5
39	838.8	751.8	838.8/751.8>GPSer:40:4
40	840.6	753.7	840.6/753.7>GPSer:40:3
41	878.6	791.6	**878.6/327.3>GPSer:44:12**
42	764.9	97	764.9/97>Sulfatide:17:0
43	778.9	97	778.9/97>Sulfatide:16:0
44	806.9	97	806.9/97>Sulfatide:18:0
45	822.9	97	822.9/97>Sulfatide:18:0 (OH)
46	834.9	97	834.9/97>Sulfatide:20:0

47	850.9	97	850.9/97>Sulfatide:20:0 (OH)
48	862.9	97	862.9/97>Sulfatide:22:1
49	876.9	97	876.9/97>Sulfatide:23:0
50	878.9	97	878.9/97>Sulfatide:22:1 (OH)
51	888.9	97	888.9/97>Sulfatide:24:1
52	890.9	97	890.9/97>Sulfatide:24:0
53	904.9	97	904.9/97>Sulfatide:25:0
54	906.7	97	906.7/97>Sulfatide:24:0 (OH)
55	424.6	196.1	**424.6/196.1>GPEtn:Lyso 14:0**
56	436.6	196.1	436.6/196.1>GPEtn:Lyso 16:1e, 16:0p
57	450.4	196.1	450.4/196.1>GPEtn:Lyso 16:1
58	452.4	196.1	452.4/196.1>GPEtn:Lyso 16:0
59	462.4	196.1	462.4/196.1>GPEtn:Lyso 18:2e, 18:1p
60	464.5	196.1	464.5/196.1>GPEtn:Lyso 18:1e, 18:0p
61	476.6	196.1	476.6/196.1>GPEtn:Lyso 18:2a
62	478.4	196.1	478.4/196.1>GPEtn:Lyso 18:1
63	480.4	196.1	480.4/196.1>GPEtn:Lyso 18:0
64	492.5	196.1	492.5/196.1>GPEtn:Lyso 20:1e, 20:0p
65	500.4	196.1	500.4/196.1>GPEtn:Lyso 20:4
66	524.4	196.1	524.4/196.1>GPEtn:Lyso 22:6
67	688.6	196.1	688.6/196.1>GPEtn:32:1
68	690.7	196.1	690.7/196.1>GPEtn:32:0
69	698.6	196.1	698.6/196.1>GPEtn:34:2p, 34:3e
70	700.6	196.1	700.6/196.1>GPEtn:34:1p, 34:2e
71	702.6	196.1	702.6/196.1>GPEtn:34:0p, 34:1e
72	710.8	196.1	710.8/196.1>GPEtn:34:4
73	712.8	196.1	712.8/196.1>GPEtn:34:3
74	714.7	196.1	714.7/196.1>GPEtn:34:2
75	716.7	196.1	716.7/196.1>GPEtn:34:1
76	718.6	196.1	718.6/196.1>GPEtn:34:0
77	722.6	196.1	722.6/196.1>GPEtn:36:4p, 35:5e
78	724.6	196.1	724.6/196.1>GPEtn:36:3p, 36:4e
79	726.6	196.1	726.6/196.1>GPEtn:36:2p, 36:3e
80	728.6	196.1	728.6/196.1>GPEtn:36:1p, 36:2e
81	730.7	196.1	730.7/196.1>GPEtn:35:1
82	732.8	196.1	732.8/196.1>GPEtn:16:0/19:0
83	738.8	196.1	738.8/196.1>GPEtn:36:4
84	740.8	196.1	740.8/196.1>GPEtn:36:3
85	742.8	196.1	742.8/196.1>GPEtn:36:2
86	744.6	196.1	744.6/196.1>GPEtn:36:1
87	746.8	196.1	746.8/196.1>GPEtn:36:0
88	748.6	196.1	748.6/196.1>GPEtn:38:5p, 38:6e
89	750.6	196.1	750.6/196.1>GPEtn:38:4p, 38:5e
90	752.6	196.1	752.6/196.1>GPEtn:38:3p, 38:4e
91	754.6	196.1	754.6/196.1>GPEtn:38:2p, 38:3e
92	756.6	196.1	756.6/196.1>GPEtn:38:1p, 38:2e
93	758.7	196.1	758.7/196.1>GPEtn:37:1, 38:1e
94	762.8	196.1	762.8/196.1>GPEtn:38:6
95	764.8	196.1	764.8/196.1>GPEtn:38:5
96	766.8	196.1	766.8/196.1>GPEtn:38:4

97	768.8	196.1	768.8/196.1>GPEtn:38:3
98	770.6	196.1	770.6/196.1>GPEtn:38:2
99	772.6	196.1	772.6/196.1>GPEtn:38:1
100	776.6	196.1	776.6/196.1>GPEtn:40:5p, 40:6e
101	778.6	196.1	778.6/196.1>GPEtn:40:4p, 40:5e
102	780.6	196.1	780.6/196.1>GPEtn:40:3p, 40:4e
103	784.6	196.1	784.6/196.1>GPEtn:40:1p, 40:2e
104	788.8	196.1	788.8/196.1>GPEtn:40:7
105	790.8	196.1	790.8/196.1>GPEtn:40:6
106	792.6	196.1	792.6/196.1>GPEtn:40:5
107	794.6	196.1	794.6/196.1>GPEtn:40:4
108	796.8	196.1	796.8/196.1>GPEtn:40:3
109	798.6	196.1	798.6/196.1>GPEtn:40:2
110	569.4	241.1	569.4/241.1>GPIns:Lyso 16:1
111	571.3	241.1	571.3/241.1>GPIns:Lyso 16:0
112	585.7	241.1	**585.7/241.1>GPIns:8:0/8:0**
113	595.4	241.1	595.4/241.1>GPIns:Lyso 18:2
114	597.4	241.1	597.4/241.1>GPIns:Lyso 18:1
115	599.4	241.1	599.4/241.1>GPIns:Lyso 18:0
116	619.5	241.1	619.5/241.1>GPIns:Lyso 20:4
117	621.5	241.1	621.5/241.1>GPIns:Lyso 20:3
118	623.5	241.1	623.5/241.1>GPIns:Lyso 20:2
119	625.5	241.1	625.5/241.1>GPIns:Lyso 20:1
120	627.5	241.1	627.5/241.1>GPIns:Lyso 20:0
121	679.5	241.1	679.5/241.1>GPIns:Lyso 24:2
122	821.8	241.1	821.8/241.1>GPIns:34:1
123	833.7	241.1	833.7/241.1>GPIns:34:2
124	835.7	241.1	835.7/241.1>GPIns:34:1
125	835.7	281.1	835.7/281.1>GPIns:34:1
126	857.7	241.1	857.7/241.1>GPIns:36:4
127	859.8	241.1	859.8/241.1>GPIns:36:3
128	861.8	241.1	861.8/241.1>GPIns:36:2
129	863.7	241.1	863.7/241.1>GPIns:36:1
130	865.8	241.1	865.8/241.1>GPIns:36:0
131	873.8	241.1	873.8/241.1>GPIns:37:3
132	883.8	241.1	883.8/241.1>GPIns:38:5
133	885.8	241.1	885.8/241.1>GPIns:38:4
134	887.8	241.1	887.8/241.1>GPIns:38:3
135	889.8	241.1	889.8/241.1>GPIns:38:2
136	891.8	241.1	891.8/241.1>GPIns:38:1
137	893.8	241.1	893.8/241.1>GPIns:38:0
138	909.8	241.1	909.8/241.1>GPIns:40:6
139	911.8	241.1	911.8/241.1>GPIns:40:5
140	913.8	241.1	913.8/241.1>GPIns:40:4
141	915.8	241.1	915.8/241.1>GPIns:40:3
142	917.8	241.1	917.8/241.1>GPIns:40:2
143	919.8	241.1	919.8/241.1>GPIns:40:1
144	963.9	241.1	963.9/241.1>GPInsP:38:5
145	963.9	321.1	963.9/321.1>GPInsP:38:5
146	965.9	241.1	965.9/241.1>GPInsP:38:4

147	965.9	321.1	965.9/321.1>GPInsP:38:4
148	967.9	241.1	967.9/241.1>GPInsP:38:3
149	967.9	321.1	967.9/321.1>GPInsP:38:3
150	1045.9	241.1	1045.9/241.1>GPInsP2:38:4
151	1045.9	321.1	1045.9/321.1>GPInsP2:38:4
152	1045.9	401.1	1045.9/401.1>GPInsP2:38:4
153	1047.9	241.1	1047.9/241.1>GPInsP2:38:3
154	1047.9	321.1	1047.9/321.1>GPInsP2:38:3
155	1047.9	401.1	1047.9/401.1>GPInsP2:38:3
156	1125.9	241.1	1125.9/241.1>GPInsP3:38:4
157	1125.9	321.1	1125.9/321.1>GPInsP3:38:4
158	1125.9	401.1	1125.9/401.1>GPInsP3:38:4
159	1125.9	481.1	1125.9/481.1>GPInsP3:38:4
160	494.4	184.1	494.4/184.1>GPCho:Lyso 16:1
161	496.4	184.1	496.4/184.1>GPCho:Lyso 16:0
162	520.4	184.1	520.4/184.1>GPCho:Lyso 18:2
163	522.4	184.1	522.4/184.1>GPCho:Lyso 18:1
164	524.4	184.1	524.4/184.1>GPCho:Lyso 18:0
165	544.4	184.1	544.4/184.1>GPCho:Lyso 20:4
166	568.4	184.1	568.4/184.1>GPCho:Lyso 22:6
167	570.4	184.1	570.4/184.1>GPCho:Lyso 22:5
168	678.5	184.1	678.5/184.1>GPCho:28:0
169	704.6	184.1	704.6/184.1>GPCho:30:1a
170	706.6	184.1	706.6/184.1>GPCho:30:0a
171	718.6	184.1	718.6/184.1>GPCho:32:0p, 32:1e
172	730.8	184.1	730.8/184.1>GPCho:32:2
173	732.6	184.1	732.6/184.1>GPCho:32:1a
174	734.6	184.1	734.6/184.1>GPCho:32:0a
175	742.6	184.1	742.6/184.1>GPCho:34:2p, 34:3e
176	744.6	184.1	744.6/184.1>GPCho:34:1p, 34:2e
177	746.6	184.1	746.6/184.1>GPCho:34:0p, 34:1e
178	748.6	184.1	748.6/184.1>GPCho:34:0e
179	756.6	184.1	756.6/184.1>GPCho:34:3a
180	758.7	184.1	758.7/184.1>GPCho:34:2a
181	760.6	184.1	760.6/184.1>GPCho:34:1a
182	762.6	184.1	762.6/184.1>GPCho:34:0a
183	768.6	184.1	768.6/184.1>GPCho:36:3p, 36:4e
184	770.6	184.1	770.6/184.1>GPCho:36:2p, 36:3e
185	772.6	184.1	772.6/184.1>GPCho:36:1p, 36:2e
186	774.6	184.1	774.6/184.1>GPCho:36:0p, 36:1e
187	782.6	184.1	782.6/184.1>GPCho:36:4a
188	784.6	184.1	784.6/184.1>GPCho:36:3a
189	786.6	184.1	786.6/184.1>GPCho:36:2a
190	788.6	184.1	788.6/184.1>GPCho:36:1a
191	790.8	184.1	790.8/184.1>GPCho:36:0
192	792.6	184.1	792.6/184.1>GPCho:38:5p, 38:6e
193	794.6	184.1	794.6/184.1>GPCho:38:4p, 38:5e
194	796.6	184.1	796.6/184.1>GPCho:38:3p, 38:4e
195	798.6	184.1	798.6/184.1>GPCho:38:2p, 38:3e
196	800.6	184.1	800.6/184.1>GPCho:38:1p, 38:2e

197	808.6	184.1	808.6/184.1>GPCho:38:5a
198	810.6	184.1	810.6/184.1>GPCho:38:4a
199	812.6	184.1	812.6/184.1>GPCho:38:3a
200	814.6	184.1	814.6/184.1>GPCho:38:2a
201	816.6	184.1	816.6/184.1>GPCho:38:1a
202	820.6	184.1	820.6/184.1>GPCho:40:5p, 40:6e
203	822.6	184.1	822.6/184.1>GPCho:40:4p, 40:5e
204	824.6	184.1	824.6/184.1>GPCho:40:3p, 40:4e
205	826.6	184.1	826.6/184.1>GPCho:40:2p, 40:3e
206	828.6	184.1	828.6/184.1>GPCho:40:1p, 40:2e
207	834.6	184.1	834.6/184.1>GPCho:40:6a
208	836.6	184.1	836.6/184.1>GPCho:40:5a
209	838.6	184.1	838.6/184.1>GPCho:40:4a
210	647.7	184.1	**647.7/184.1>SM:d18:1/12:0**
211	701.8	184.1	701.8/184.1>SM:d18:1/16:1
212	703.8	184.1	703.8/184.1>SM:d18:1/16:0
213	705.8	184.1	705.8/184.1>SM:d18:0/16:0
214	727.8	184.1	727.8/184.1>SM:d18:1/18:2
215	729.8	184.1	729.8/184.1>SM:d18:118:1
216	731.8	184.1	731.8/184.1>SM:d18:1/18:0
217	733.8	184.1	733.8/184.1>SM:d18:0/18:0
218	757.8	184.1	757.8/184.1>SM:d18:1/20:1
219	759.8	184.1	759.8/184.1>SM:d18:1/20:0
220	761.8	184.1	761.8/184.1>SM:d18:0/20:0
221	787.8	184.1	787.8/184.1>SM:d18:1/22:0;d18:0/22:1
222	789.8	184.1	789.8/184.1>SM:d18:0/22:0
223	813.8	184.1	813.8/184.1>SM:d18:1/24:1
224	815.8	184.1	815.8/184.1>SM:d18:1/24:0;d18:0/24:1
225	817.9	184.1	817.9/184.4>SM:d18:0/24:0
226	841.9	184.1	841.9/184.1>SM:d18:1/26:1
227	843.9	184.1	843.9/184.1>SM:d18:1/26:0;d18:0/26:1
228	845.9	184.4	845.9/184.1>SM:d18:0/26:0
229	538.7	264.4	538.7/264.4>Cer:d18:1/16:0
230	540.7	266.4	540.7/266.4>Cer:d18:0/16:0
231	580.9	264.4	**580.9/264.4>Cer:d18:1/19:0**
232	566.7	264.4	566.7/264.4>Cer:d18:1/18:0
233	568.7	266.4	568.7/266.4>Cer:d18:0/18:0
234	594.7	264.4	594.7/264.4>Cer:d18:1/20:0
235	596.7	266.4	596.7/266.4>Cer:d18:0/20:0
236	622.8	264.4	622.8/264.4>Cer:d18:1/22:0
237	624.8	266.4	624.8/266.4>Cer:d18:0/22:0
238	648.9	264.4	648.9/264.4>Cer:d18:1/24:1
239	650.9	264.4	650.9/264.4>Cer:d18:1/24:0
240	650.9	266.4	650.9/266.4>Cer:d18:0/24:1
241	652.9	266.4	652.9/266.4>Cer:d18:0/24:0
242	676.9	264.4	676.9/264.4>Cer:d18:1/26:1
243	678.9	264.4	678.9/264.4>Cer:d18:1/26:0
244	678.9	266.4	678.9/266.4>Cer:d18:0/26:1
245	680.9	266.4	680.9/266.4>Cer:d18:0/26:0
246	588.8	264.4	**588.8/264.4>MonoGluCer:d18:1/8:0**

247	700.7	264.4	700.7/264.4>MonoHexCer:d18:1/16:0
248	702.7	266.4	702.7/266.4>MonoHexCer:d18:0/16:0
249	728.7	264.4	728.7/264.4>MonoHexCer:d18:1/18:0
250	730.7	266.4	730.7/266.4>MonoHexCer:d18:0/18:0
251	756.7	264.4	756.7/264.4>MonoHexCer:d18:1/20:0
252	758.7	266.4	758.7/266.4>MonoHexCer:d18:0/20:0
253	784.8	264.4	784.8/264.4>MonoHexCer:d18:1/22:0
254	786.8	266.4	786.8/266.4>MonoHexCer:d18:0/22:0
255	810.9	264.4	810.9/264.4>MonoHexCer:d18:1/24:1
256	812.9	264.4	812.9/264.4>MonoHexCer:d18:1/24:0
257	812.9	266.4	812.9/266.4>MonoHexCer:d18:0/24:1
258	814.9	266.4	814.9/266.4>MonoHexCer:d18:0/24:0
259	838.9	264.4	838.9/264.4>MonoHexCer:d18:1/26:1
260	840.9	264.4	840.9/264.4>MonoHexCer:d18:1/26:0
261	840.9	266.4	840.9/266.4>MonoHexCer:d18:0/26:1
262	842.9	266.4	842.9/266.4>MonoHexCer:d18:0/26:0
263	862.7	264.4	862.7/264.4>DiHexCer:d18:1/16:0
264	864.7	266.4	864.7/266.4>DiHexCer:d18:0/16:0
265	890.7	264.4	890.7/264.4>DiHexCer:d18:1/18:0
266	892.7	266.4	892.7/266.4>DiHexCer:d18:0/18:0
267	918.7	264.4	918.7/264.4>DiHexCer:d18:1/20:0
268	920.7	266.4	920.7/266.4>DiHexCer:d18:0/20:0
269	946.8	264.4	946.8/264.4>DiHexCer:d18:1/22:0
270	948.8	266.4	948.8/266.4>DiHexCer:d18:0/22:0
271	972.9	264.4	972.9/264.4>DiHexCer:d18:1/24:1
272	974.9	264.4	974.9/264.4>DiHexCer:d18:1/24:0
273	974.9	266.4	974.9/266.4>DiHexCer:d18:0/24:1
274	976.9	266.4	976.9/266.4>DiHexCer:d18:0/24:0
275	1000.9	264.4	1000.9/264.4>DiHexCer:d18:1/26:1
276	1002.9	264.4	1002.9/264.4>DiHexCer:d18:1/26:0
277	1002.9	266.4	1002.9/266.4>DiHexCer:d18:0/26:1
278	1004.9	266.4	1004.9/266.4>DiHexCer:d18:0/26:0

Lipids in bold are synthetic standards that are spiked into the lipid mixture for relative quantification. Each transition requires optimisation of several parameters such as declustering potential and collision energy, as these are compound-dependent parameters, but are also dependent on instrument settings. Abbreviations: Cer, ceramide; GPA, phosphatidic acid; GPCho, glycerophosphocholine; GPEtn, glycerophosphoethanolamine; GPIns, glycerophosphoinositol; GPInsP, glycerophosphoinositol monophosphate; GPInsP2, glycerophosphoinositol bisphosphate; GPInsP3, glycerophosphoinositol triphosphate; DiHexCer, dihexosylceramide; MonoGluCer, monoglucosylceramide; MonoHexCer, monohexosylceramide; SM, sphingomyelin. a, e and p on the fatty acyl groups refer to the diacyl, ether and plasmalogen species respectively.

Supplementary Material 3.1 – List of theoretically calculated mass for yeast glycerophospholipids and sphingolipids (see attached softcopy or www.lipidprofiles.com (Protocols)).

Supplementary Material 4.1 – Complete pathways of sterol and sphingolipid biosynthesis.

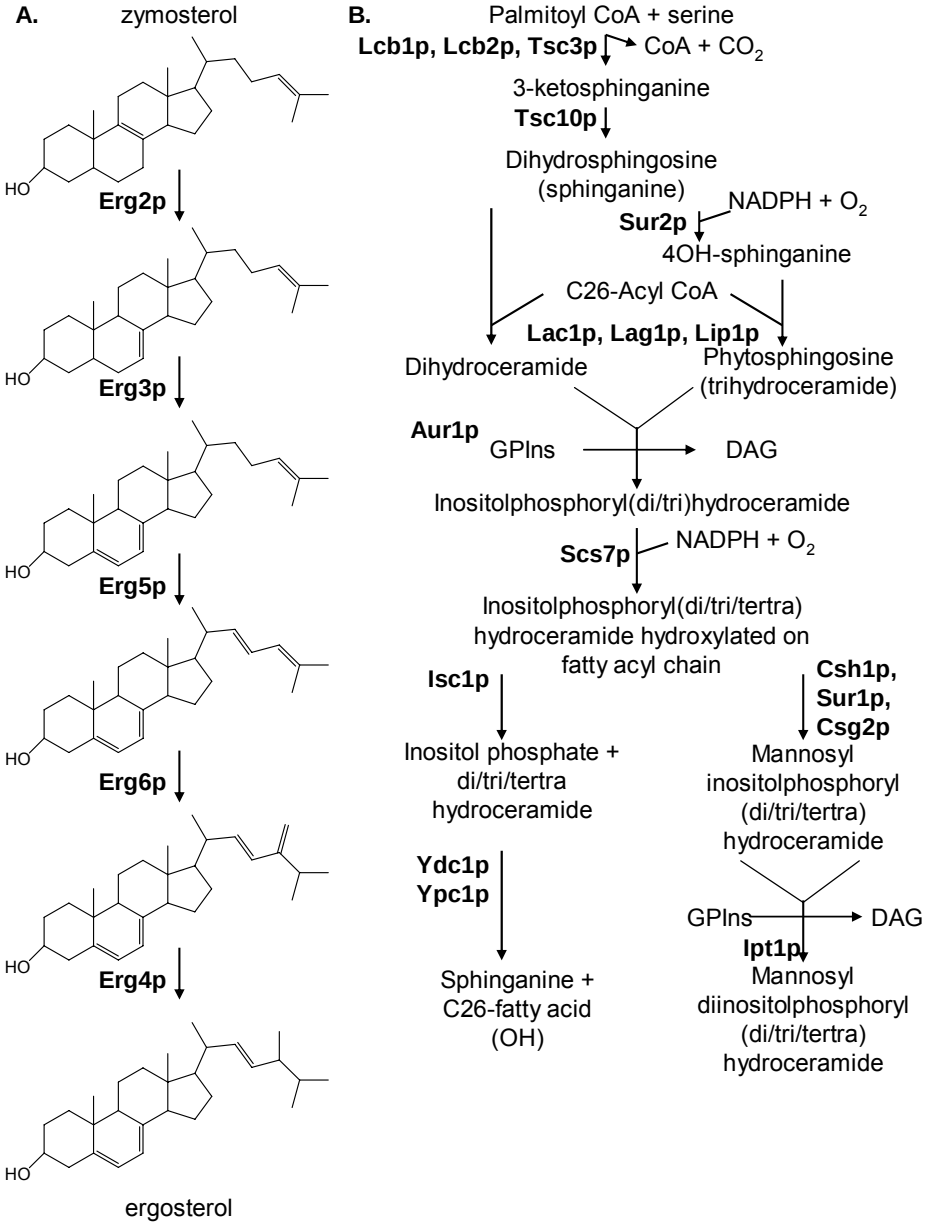

Supplementary Material 4.2 – Isc1p mediated turnover of IPC-C in *erg3 erg6* double mutant (H. Riezman).

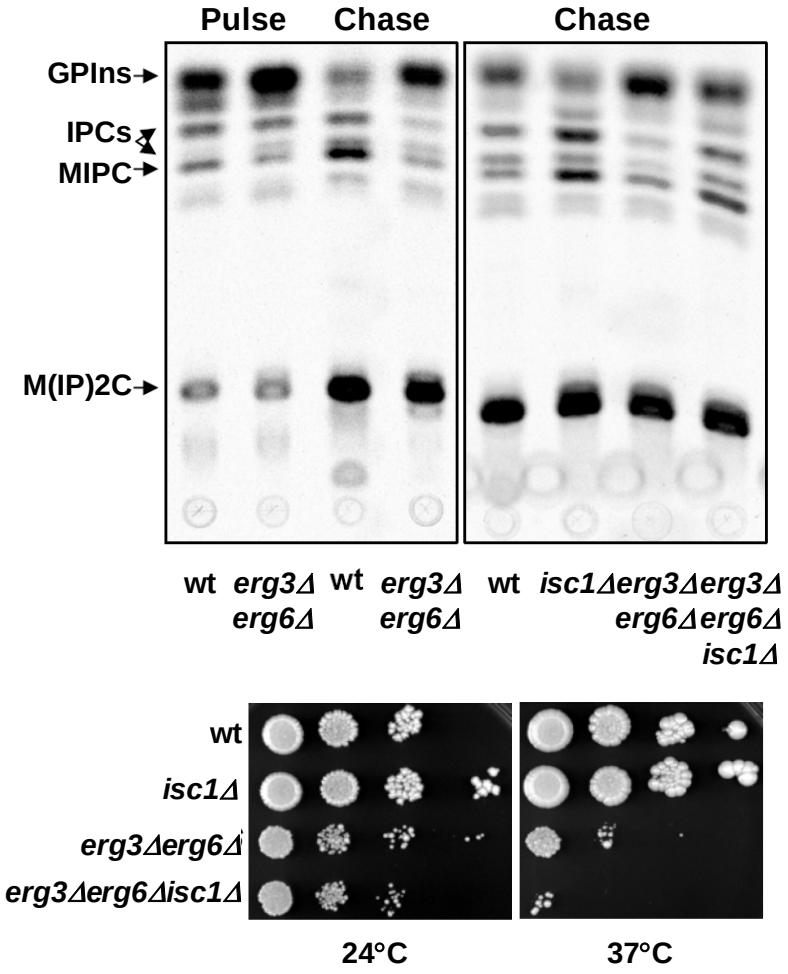

Supplementary Material 4.3 – Plating assays under all conditions (H. Riezman).

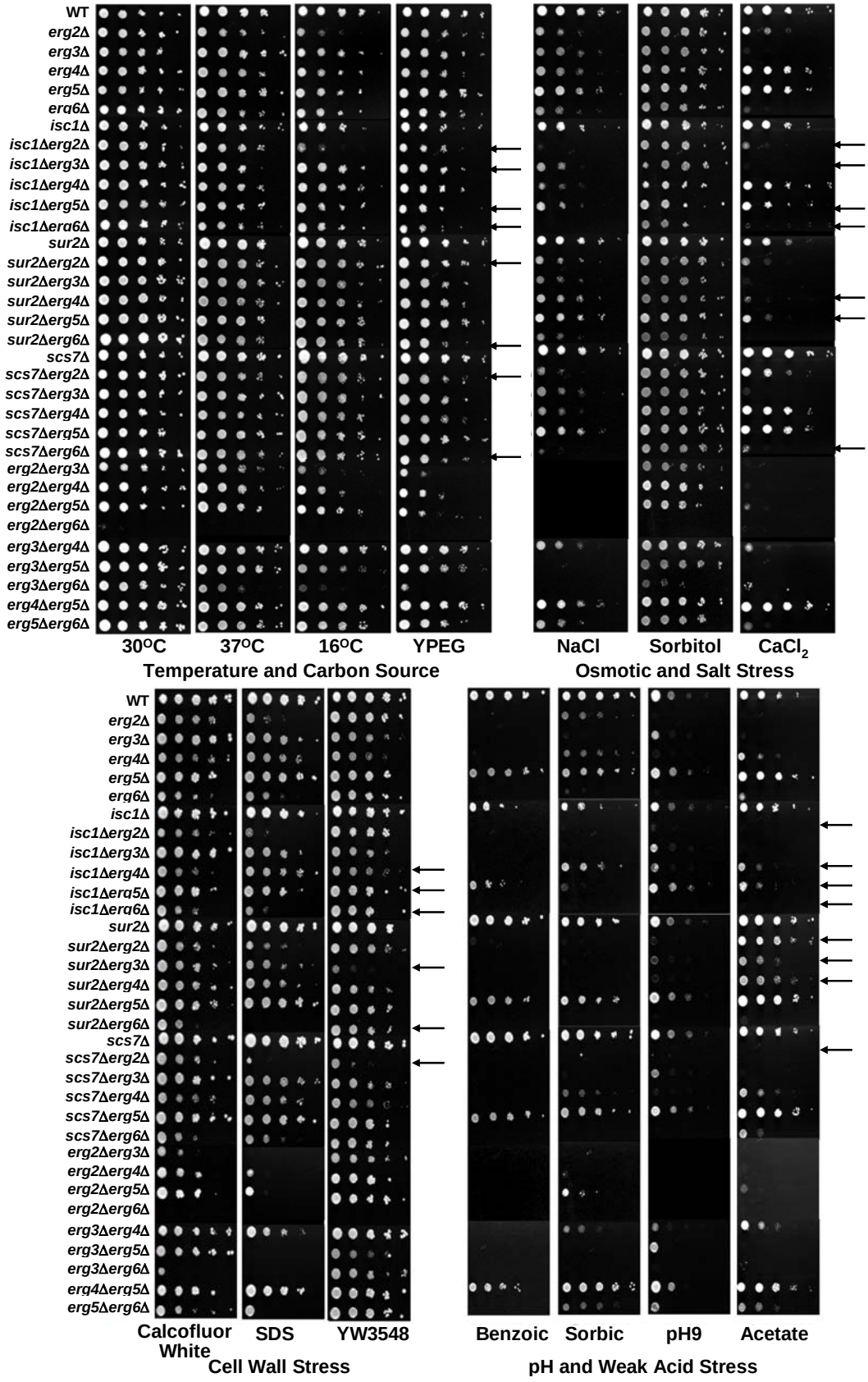

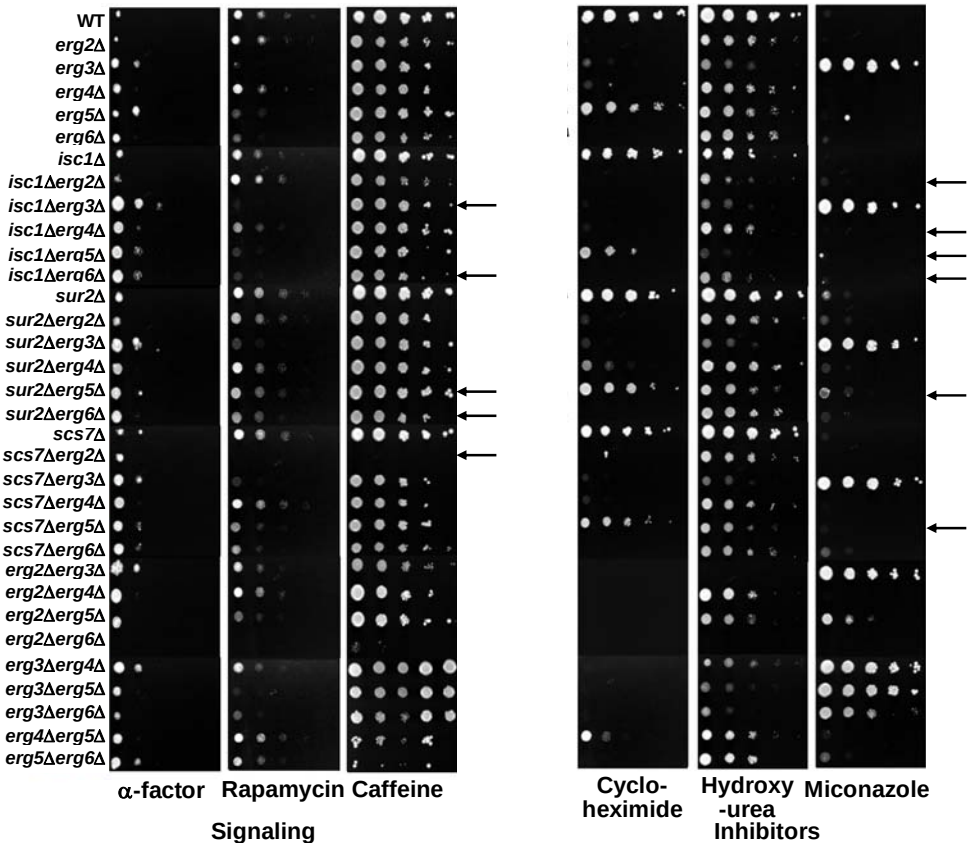

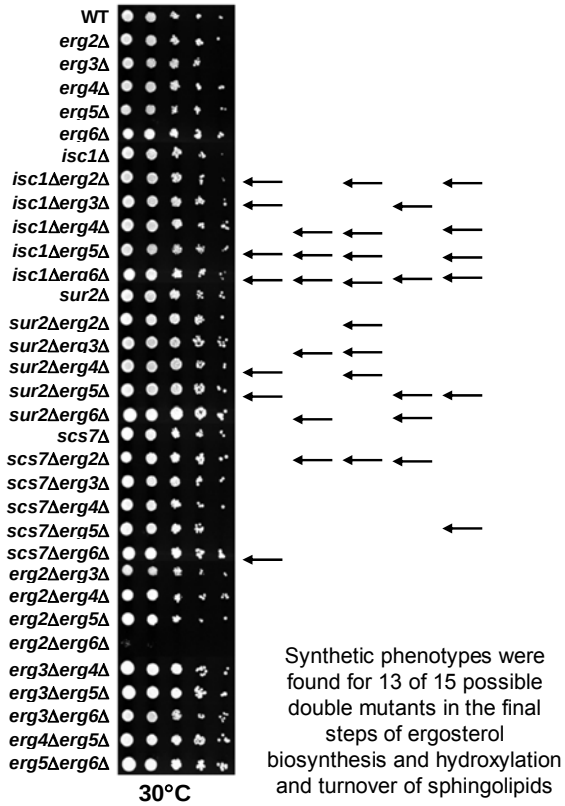

Synthetic phenotypes were found for 13 of 15 possible double mutants in the final steps of ergosterol biosynthesis and hydroxylation and turnover of sphingolipids

Supplementary Material 4.4 – Lipidomics analysis of sterol and sphingolipid double mutants

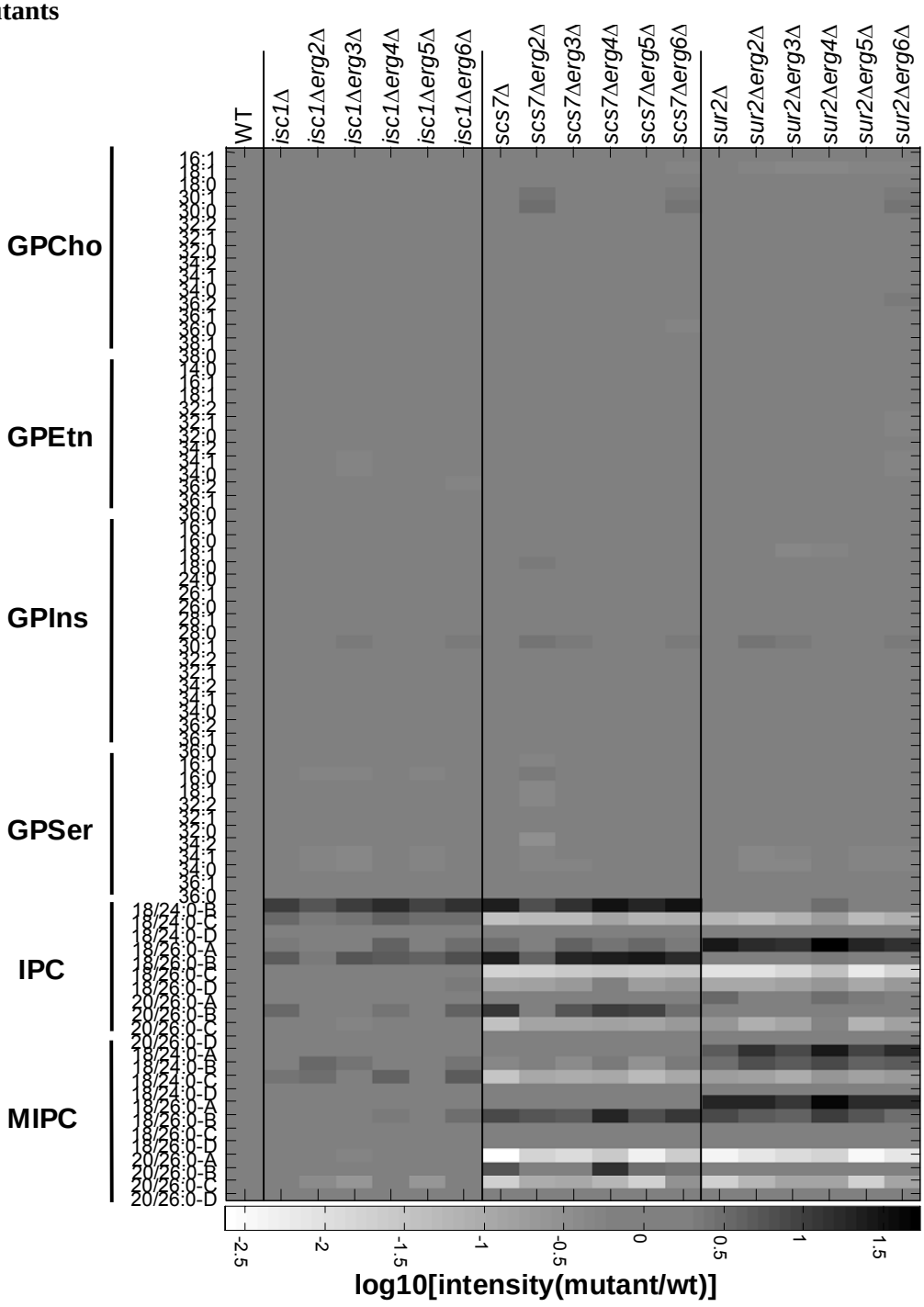

Supplementary Material 4.5 – Transcript levels in various mutants deficient in sterols and/ or sphingolipids (H. Riezman). (A) Cluster map of transcripts that change in the sterol and sphingolipid mutants. Transcript levels were determined in the indicated strains. Data for transcripts that changed at least two fold under one condition were clustered. Predominant characteristics of gene clusters are indicated on the right. The scale is a log transformed base 2. (B) Transcript levels *PDR12* in wild type cells and *erg4*Δ, *sur2*Δ, and *erg4*Δ*sur2*Δ mutants

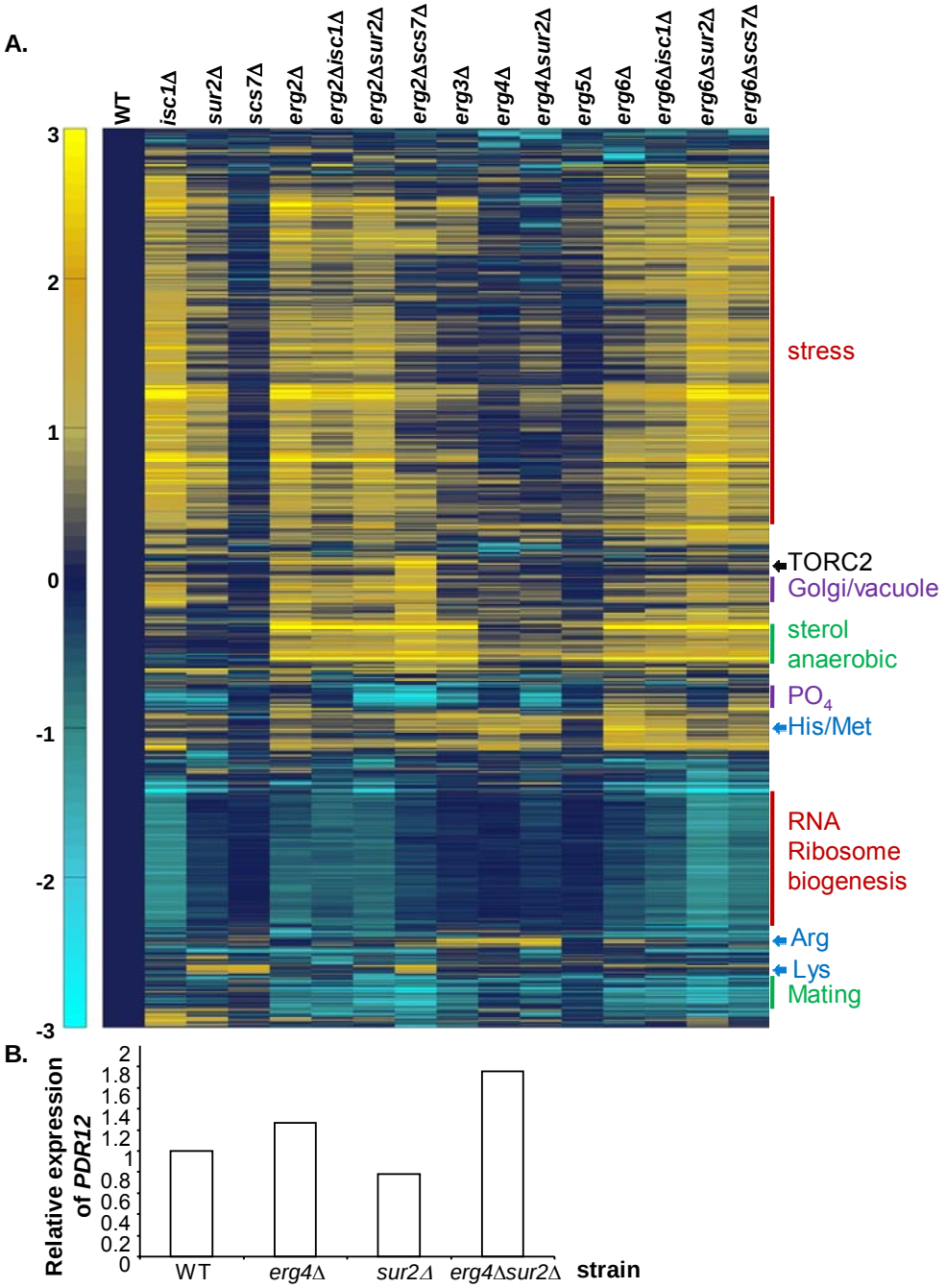

Supplementary Material 4.6 – Tat2p and Can1p localisation pictures (H. Riezman).

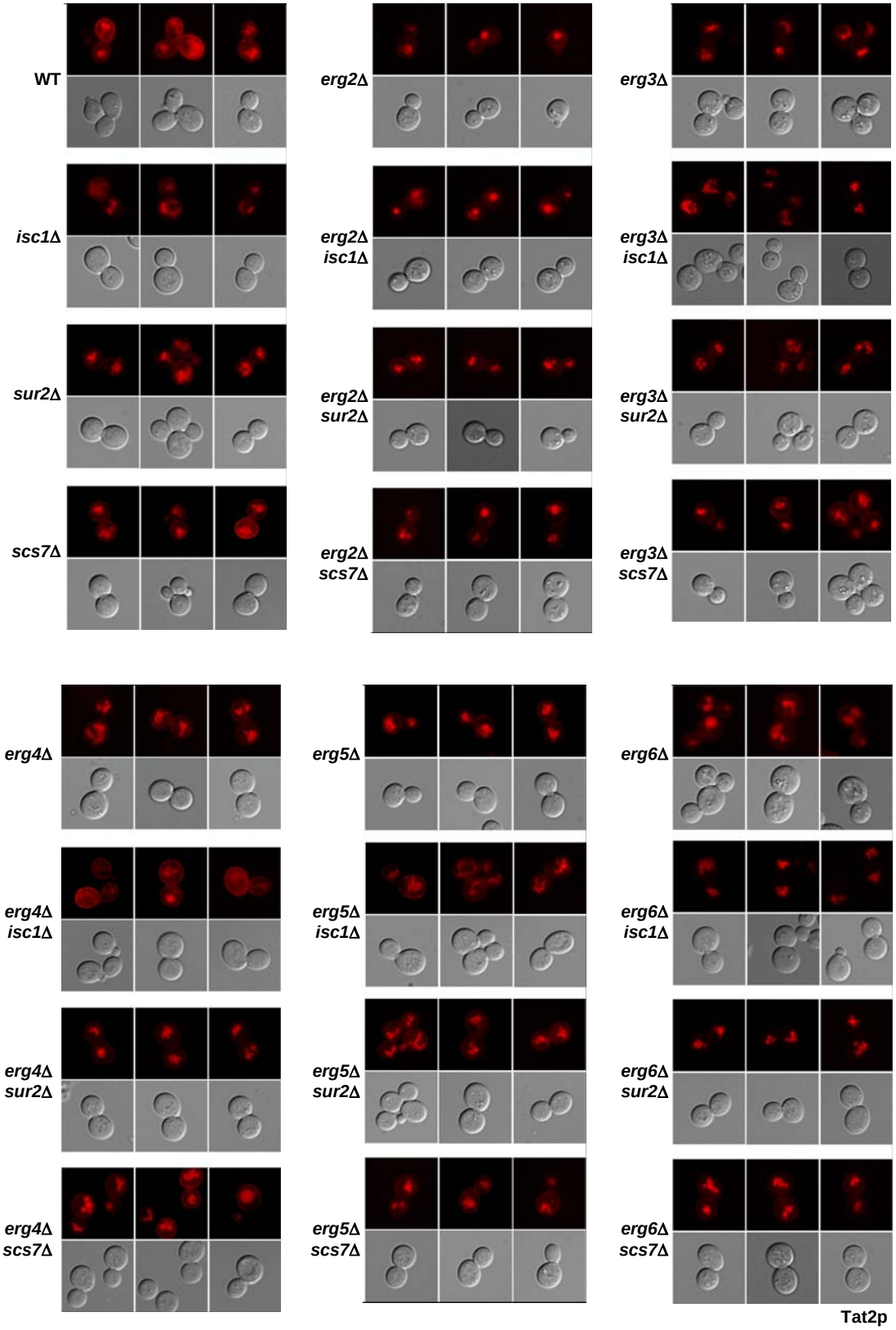

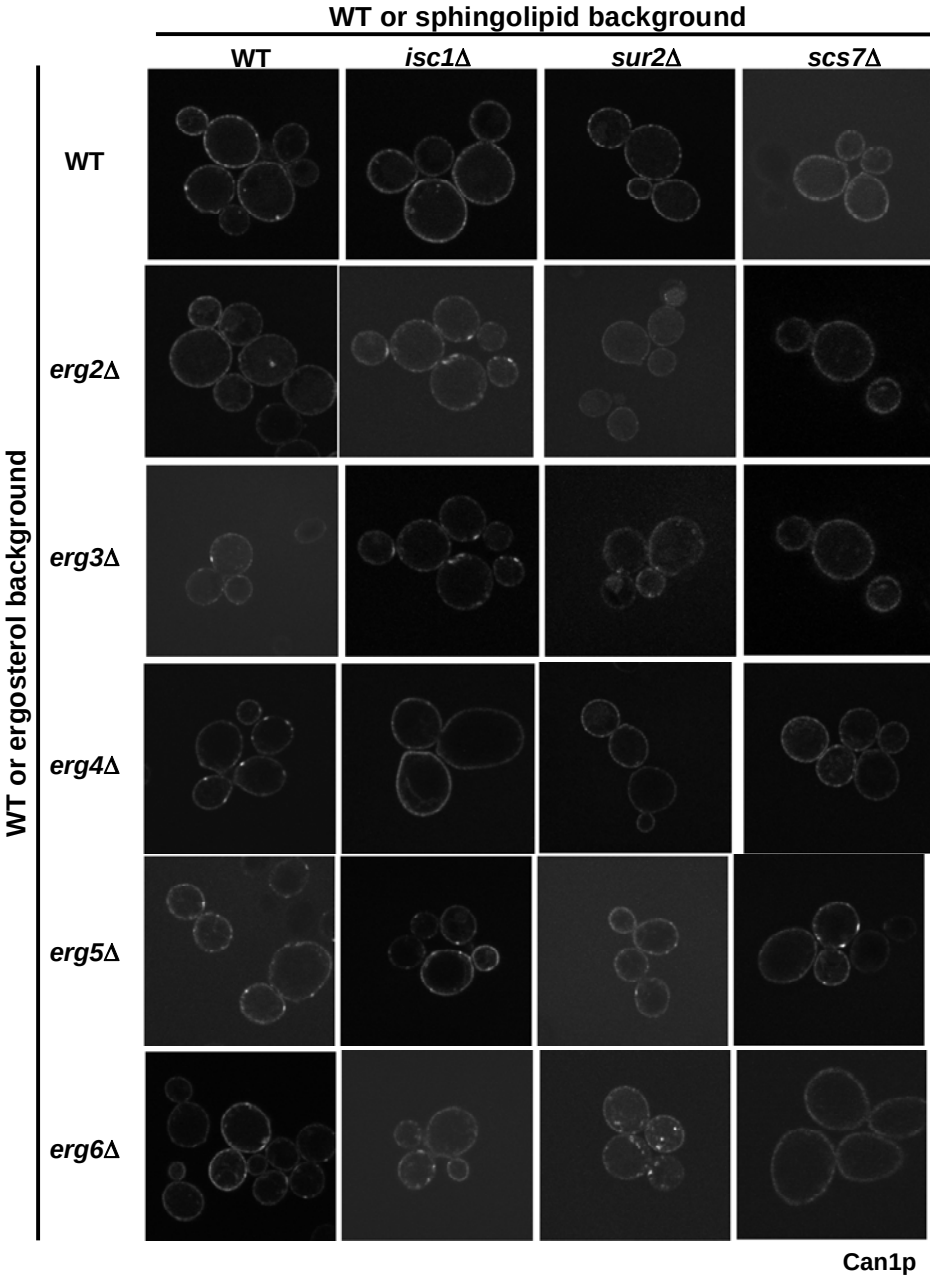
WT or sphingolipid background
WT
isc1Δ
sur2Δ
scs7Δ
WT or ergosterol background
WT
erg2Δ
erg3Δ
erg4Δ
erg5Δ
erg6Δ
Can1p

Supplementary Table 4.1 – Sterol compositions in the yeast strains used in this study (single determinations) (H. Riezman).

A. Wild type and sphingolipid mutant cells.

	Strain	**wt**	***isc1*Δ**	***sur2*Δ**	***scs7*Δ**
	µg sterols / 10^8 cells	26	33	30	31
Sterol	**Mass**				
Cholesta-5,8,24(25)-trienol	382	1.0 %	0.6 %	0.9 %	0.6 %
Cholesta-8,24(25)-dienol	384	9.6 %	7.9 %	8.6 %	9.3 %
Ergosta-5,8,14,22-tetraenol *	394	4.8 %	3.7 %	4.9 %	4.6 %
Ergosta-5,7,22,24(28)-tetraenol	394	2.8 %	2.9 %	3.3 %	3.0 %
Ergosta-5,7,22-trienol	396	58.5 %	59.1 %	61.4 %	64.7 %
Ergosta-5,8,14-trienol *	396	1.4 %	1.7 %	1.2 %	1.1 %
Ergosta-7,22,24(28)-trienol *	396	2.0 %	1.0 %	1.2 %	0.9 %
Ergosta-8,24(28)-dienol	398	1.0 %	1.5 %	2.6 %	2.1 %
Ergosta-5,7-dienol	398	16.5 %	17.2 %	12.2 %	11.7 %
Ergosta-7,24(28)-dienol	398	1.4 %	1.5 %	1.5 %	1.0 %
4,4,14-Trimethyl cholesta-8,24(25)-dienol	426	1.0 %	0.9 %	1.2 %	0.4 %

B. *erg2* mutant and *erg2*-derived strains.

	Strain	***erg2*Δ**	***isc1*Δ *erg2*Δ**	***sur2*Δ *erg2*Δ**	***scs7*Δ *erg2*Δ**
	µg sterols / 10^8 cells	62	52	51	59
Sterol	**Mass**				
Cholesta-5,8,14,24(25)-tetraenol *	380	9.3 %	8.5 %	8.9 %	6.2 %
Cholesta-8,24(25)-dienol	384	1.5 %	1.3 %	1.2 %	2.4 %
Ergosta-5,8,14,22-tetraenol *	394	2.9 %	2.5 %	2.3 %	1.6 %
Ergosta-5,8,22-trienol	396	23.1 %	22.6 %	27.1 %	20.7 %
Ergosta-5,8,24(28)-trienol *	396	2.7 %	1.8 %	1.5 %	1.9 %
??	396	2.0 %	1.2 %	1.1 %	1.5 %
Ergosta-8,22-dienol	398	1.7 %	2.0 %	1.6 %	1.2 %
Ergosta-5,8-dienol	398	3.8 %	5.4 %	5.0 %	3.0 %
Ergosta-8,24(28)-dienol	398	24.5 %	20.0 %	19.4 %	32.9 %
??	398	3.6 %	3.9 %	3.6 %	3.2 %
Ergosta-8-enol	400	23.8 %	29.9 %	27.6 %	24.5 %
4,4,14-Trimethyl cholesta-8,24(25)-dienol	426	0.4 %	0.3 %	0.2 %	0.5 %

C. *erg3* mutant and *erg3*-derived strains.

	Strain	*erg3*Δ	*isc1*Δ *erg3*Δ	*sur2*Δ *erg3*Δ	*scs7*Δ *erg3*Δ
	µg sterols / 10^8 cells	63	52	51	62
Sterol	**Mass**				
Cholesta-7,22,24(25)-trienol	382	0.2 %	0.2 %	0.2 %	0.3 %
Cholesta-8,24(25)-dienol	384	2.5 %	2.4 %	2.8 %	4.2 %
Ergosta-8,22,24(28)-trienol	396	0.5 %	0.7 %	0.5 %	0.4 %
Ergosta-8,14,24(28)-trienol *	396	1.0 %	1.0 %	0.8 %	0.7 %
Ergosta-7,22,24(28)-trienol	396	1.2 %	1.3 %	1.0 %	0.9 %
Ergosta-8,22-dienol	398	1.6 %	1.7 %	1.8 %	1.6 %
Ergosta-7,22-dienol	398	44.3 %	41.1 %	41.2 %	40.4 %
Ergosta-8,24(28)-dienol	398	6.4 %	6.5 %	7.5 %	7.5 %
Ergosta-7,24(28)-dienol	398	15.5 %	15.0 %	15.5 %	18.7 %
Ergosta-8-enol	400	4.2 %	4.5 %	4.7 %	4.3 %
Ergosta-7-enol	400	20.9 %	23.1 %	22.8 %	19.0 %
4,4,14-Trimethyl cholesta-8,24(25)-dienol	426	0.1 %	0.3 %	0.2 %	0.2 %

D. *erg4* mutant and *erg4*-derived strains.**

	Strain	*erg4*Δ	*isc1*Δ *erg4*Δ	*sur2*Δ *erg4*Δ
	µg sterols / 10^8 cells	43	57	43
Sterol	**Mass**			
Cholesta-8,24(25)-dienol	384	3.7 %	2.3 %	3.4%
Ergosta-5,8,14,22,24(28)-pentaenol *	392	3.3 %	2.8 %	2.7%
Ergosta-5,7,14,22,24(28)-pentaenol *	392	1.9 %	3.1 %	2.9 %
??	392	~ 6 %	~ 7 %	~6 %
Ergosta-5,8,22,24(28)-tetraenol	394	1.3 %	1.0 %	1.1 %
Ergosta-5,7,22,24(28)-tetraenol	394	79.2 %	79.1 %	80.5%
Ergosta-5,8,24(28)-trienol	396	~ 2 %	~ 2 %	~2 %
4-Methyl cholesta-8,24(25)-dienol	398	0.8 %	0.7 %	0.6 %
Ergosta-7,24(28)-dienol	398	0.7 %	0.9 %	0.7 %
4,4,14-Trimethyl cholesta-8,24(25)-dienol	426	0.4 %	0.5 %	0.4 %

	Strain	*erg4*Δ	*erg4*Δ *scs7*Δ
	µg sterols / 10^8 cells	39	38
Sterol	**Mass**		
Cholesta-8,24(25)-dienol	384	2.1 %	3.0 %
Ergosta-5,8,14,22,24(28)-pentaenol *	392	0.8 %	0.8 %
Ergosta-5,7,22,24(28)-tetraenol	394	86.8 %	85.5 %
Ergosta-5,8,22,24(28)-tetraenol *	394	1.0 %	1.0 %
Ergosta-5,8,24(28)-trienol	396	~6 %	~5 %
4-Methyl cholesta-8,24(25)-dienol	398	1.4 %	1.2 %
4,4-Dimethyl cholesta-8,24(25)-dienol	412	0.6 %	0.8 %
4,4,14-Trimethyl cholesta-8,24(25)-dienol	426	0.9 %	1.7 %

E. *erg5* mutant and *erg5*-derived strains.

	Strain	*erg5*Δ	*isc1*Δ *erg5*Δ	*sur2*Δ *erg5*Δ	*scs7*Δ *erg5*Δ
	µg sterols / 10^8 cells	54	32	43	35
Sterol	**Mass**				
Cholesta-8,24(25)-dienol	384	5.6 %	4.2 %	5.0%	6.1 %
Ergosta-5,8,14-trienol *	396	4.5 %	5.3 %	5.6 %	5.8 %
Ergosta-5,7,14-trienol *	396	5.3 %	5.6 %	5.6 %	5.3 %
Ergosta-5,7,24(28)-trienol	396	2.3 %	2.3 %	3.2 %	2.2 %
Ergosta-5,8-dienol	398	1.5 %	1.6 %	1.5 %	1.3 %
Ergosta-5,7-dienol	398	77.2 %	78.1 %	76.0 %	77.0 %
Ergosta-8,24(28)-dienol	398	0.8 %	0.6%	1.0 %	0.8 %
Ergosta-8-enol	400	0.1 %	-	0.2 %	-
4,4,14-Trimethyl cholesta-8,24(25)-dienol	426	1.4%	1.3 %	1.4 %	0.9 %

F. erg6 mutant and erg6-derived strains.**

	Strain	*erg6*Δ	*sur2*Δ *erg6*Δ	*scs7*Δ *erg6*Δ
	µg sterols / 10^8 cells	43	29	42
Sterol	**Mass**			
Cholesta-5,8,14,24(25)-tetraenol *	380	2.9 %	3.2 %	2.5 %
??	380	6.6 %	3.9 %	5.0 %
Cholesta-8,22,24(25)-trienol *	382	0.7 %	0.7 %	0.5 %
Cholesta-5,8,24(25)-trienol	382	5.8 %	7.8 %	6.3 %
Cholesta-7,22,24(25)-trienol *	382	2.1 %	2.5 %	~ 3 %
Cholesta-5,7,24(25)-trienol	382	34.5 %	27.4 %	30.1 %
Cholesta-8,24(25)-dienol	384	41.1 %	44.7 %	~ 46 %
Cholesta-7,24(25)-dienol	384	4.1 %	4.8 %	3.3 %
4-Methyl cholesta-8,24(25)-dienol	398	0.6 %	0.8 %	0.5 %
4,4-Dimethyl cholesta-8,24(25)-dienol	412	0.9 %	1.0 %	0.8 %
4,4,14-Trimethyl cholesta-8,24(25)-dienol	426	0.5 %	1.1 %	0.4 %

	Strain	*erg6*Δ	*erg6*Δ *isc1*Δ
	µg sterols / 10^8 cells	48	39
Sterol	**Mass**		
Cholesta-5,8,14,24(25)-tetraenol *	380	0.9 %	0.7 %
??	380	7.8 %	8.3 %
Cholesta-5,8,24(25)-trienol	382	7.1 %	6.9 %
Cholesta-5,7,24(25)-trienol	382	46.6 % %	50.2 %
Cholesta-8,24(25)-dienol	382	25.1 %	23.7 %
Cholesta-7,24(25)-dienol	382	5.8 %	5.9 %
4-Methyl cholesta-8,24(25)-dienol	384	1.5 %	1.1 %
4,4-Dimethyl cholesta-8,24(25)-dienol	384	1.9 %	1.1 %
4,4,14-Trimethyl cholesta-8,24(25)-dienol	398	2.0 %	1.2 %

* denotes sterols whose identity is not certain.

**Sterol determinations for some of the *erg4* and *erg6* deletion mutant strains were determined in two separate experiments. The data from each experiment is presented in a separate table.

Data on some minor sterols (less than 2% of total) whose identity was not certain is not shown.

Isogenic wild type and ergosterol mutant strains were grown overnight in 2% peptone, 1% yeast extract, 2% glucose, 20 mM MES, 40 mg/l each adenine, uracil, tryptophan at 30°C, harvested at 1-2 OD600/ml and washed three times with water. 4 µg of cholesterol was added as an internal standard to 5 x 10^8 cells and total sterols were extracted, derivatized and analysed as described previously (Heese-Peck *et al.*, 2002). One can see that there are some differences in sterols between experiments, however these differences sometimes exceed

those found between *erg* and *erg*-derived strains in a single experiment. Therefore, the differences in sterol composition in *erg* strains that are caused by introduction of the sphingolipid mutations is insignificant. In particular, in the wild type sterol background no substantial differences in sterol amounts or composition were detected (A). With the possible exception of the *sur2 erg6* strain all *erg* mutant strains show an increase in total sterols over wild type cells, although the sterol overproduction varies greatly between *erg* mutants. It should be noted that the analysis did not discriminate whether the increased sterol amount is due to an increase in free and/or esterified sterols, but it is likely that the increases are mainly reflected in esterified sterols.

Supplementary Table 4.2 – Summary of Tat2p and Can1p localisation data (H. Riezman).

Strain	Tat2 localisation			Can1p localisation			
	PM	Vacuole	SD	PM	Vacuole	small patches	large patches
WT	46	54	6	mostly	no	yes	yes
***isc1*Δ**	28	72	5	mostly	no	yes	no
***sur2*Δ**	35	65	6	mostly	no	yes	no
***scs7*Δ**	41	59	5	mostly	no	yes	no
***erg2*Δ**	35	65	6	mostly	no	yes	yes
***erg2*Δ*isc1*Δ**	36	64	8	mostly	yes	yes	no
***erg2*Δ*sur2*Δ**	34	66	6	mostly	yes	yes	no
***erg2*Δ*scs7*Δ**	34	66	6	mostly	yes	yes	yes
***erg3*Δ**	28	72	5	mostly	yes	yes	yes
***erg3*Δ*isc1*Δ**	24	76	5	mostly	yes	yes	yes
***erg3*Δ*sur2*Δ**	26	74	7	mostly	yes	nd	nd
***erg3*Δ*scs7*Δ**	37	63	7	mostly	yes	nd	nd
***erg4*Δ**	34	66	6	mostly	no	yes	yes
***erg4*Δ*isc1*Δ**	47	53	4	mostly	no	yes	yes
***erg4*Δ*sur2*Δ**	35	65	7	mostly	no	yes	no
***erg2*Δ*scs7*Δ**	38	62	6	mostly	no	yes	no
***erg5*Δ**	33	67	5	mostly	no	no	mainly
***erg5*Δ*isc1*Δ**	36	64	5	mostly	no	yes	yes
***erg5*Δ*sur2*Δ**	37	63	4	mostly	no	yes	yes
***erg5*Δ*scs7*Δ**	35	65	5	mostly	no	yes	yes
***erg6*Δ**	35	65	6	mostly	no	yes	yes
***erg6*Δ*isc1*Δ**	24	76	6	mostly	no	yes	yes
***erg6*Δ*sur2*Δ**	24	76	6	mostly	no	yes	yes
***erg6*Δ*scs7*Δ**	34	66	7	mostly	no	yes	reduced

Supplementary Table 4.3 – Anisotropy measurements using TMA-DPH, a cationic derivative of the membrane probe, 1,6-Diphenyl-1,3,5-hexatriene (DPH) (H. Riezman).

Strain	Mean	SD	Significance
WT	0.283	0.004	
***isc1*Δ**	0.278	0.005	P<0.2
***sur2*Δ**	0.284	0.011	
***scs7*Δ**	0.270	0.015	P<0.2
***erg2*Δ**	0.274	0.008	P<0.2
***erg2*Δ*isc1*Δ**	0.267	0.014	P<0.2
***erg2*Δ*sur2*Δ**	0.276	0.005	p>0.2
***erg2*Δ*scs7*Δ**	0.275	0.010	
***erg3*Δ**	0.276	0.009	
***erg3*Δ*isc1*Δ**	0.270	0.015	
***erg3*Δ*sur2*Δ**	0.273	0.006	P<0.1
***erg3*Δ*scs7*Δ**	0.291	0.010	
***erg4*Δ**	0.280	0.006	
***erg4*Δ*isc1*Δ**	0.268	0.006	P<0.05
***erg4*Δ*sur2*Δ**	0.291	0.012	
***erg2*Δ*scs7*Δ**	0.278	0.008	
***erg5*Δ**	0.276	0.004	P<0.2
***erg5*Δ*isc1*Δ**	0.285	0.005	
***erg5*Δ*sur2*Δ**	0.279	0.019	
***erg5*Δ*scs7*Δ**	0.277	0.005	P<0.2
***erg6*Δ**	0.249	0.015	P<0.05
***erg6*Δ*isc1*Δ**	0.265	0.008	P<0.05
***erg6*Δ*sur2*Δ**	0.270	0.008	P<0.1
***erg6*Δ*scs7*Δ**	0.268	0.009	P<0.1